มหาวิทยาลัยมหิดล

รายงานวิจัยฉบับสมบูรณ์

โครงการ การสังเคราะห์และศึกษาฤทธิ์ทางชีวภาพของสารโลหะเชิงซ้อนอนุพันธ์ 2-thiouracil-hydroxyquinolines และ sulfonamides

โดย ดร. อภิลักษณ์ วรชาติชีวัน
คณะเทคนิคการแพทย์ มหาวิทยาลัยมหิดล

30 มิถุนายน พ.ศ. 2560

สัญญาเลขที่ TRG5880143

รายงานวิจัยฉบับสมบูรณ์

โครงการ การสังเคราะห์และศึกษาฤทธิ์ทางชีวภาพของสารโลหะเชิงซ้อนอนุพันธ์ 2-thiouracil-hydroxyquinolines และ sulfonamides

ดร. อภิลักษณ์ วรชาติชีวัน
คณะเทคนิคการแพทย์ มหาวิทยาลัยมหิดล

สนับสนุนโดยสำนักงานกองทุนสนับสนุนการวิจัยและมหาวิทยาลัยมหิดล

ACKNOWLEDGEMENTS

I gratefully acknowledge the research grant supported by the Thailand Research Fund (Grant No. TRG5880143) and the Office of the Higher Education Commission, Mahidol University under the National Research Universities Initiative.

I would like to thank Prof. Dr. Virapong Prachayasittikul for supporting, suggestions, sharing knowledge and experiences in scientific research.

I would like to thank Prof. Dr. Supaluk Prachayasittkul and Assoc. Prof. Dr. Chanin Nantasenamat for suggestions and guidance in this research.

I would like to thank the Faculty of Medical Technology, Mahidol University for facilities and utilities.

Dr. Apilak Worachartcheewan

Abstract (บทคัดย่อ)

Project Code : TRG5880143

Project Title : การสังเคราะห์และศึกษาฤทธิ์ทางชีวภาพของสารโลหะเชิงซ้อนอนุพันธ์ 2-thiouracil-hydroxyquinolines และ sulfonamides (Synthesis and biological evaluation of transition metal complexes of 2-thiouracil-hydroxyquinoline derivatives and sulfonamide analogs)

Investigator : ดร. อภิลักษณ์ วรชาติชีวัน คณะเทคนิคการแพทย์ มหาวิทยาลัยมหิดล
ที่ปรึกษาโครงการ: ศ.ดร. วีระพงศ์ ปรัชชญาสิทธิกุล
คณะเทคนิคการแพทย์ มหาวิทยาลัยมหิดล

E-mail Address : apilak.woa@mahidol.ac.th

Project Period : 2 ปี (1 กรกฎาคม พ.ศ. 2558 - 30 มิถุนายน พ.ศ. 2560)

Abstract:

Based on superoxide dismutase (SOD) structure, it has metal ions as cofactors for catalyzing mechanism or function of the enzymes. Therefore, metal complexes as SOD mimic have been designed and synthesized to act as SOD-like activity. Transition metal complexes (i.e., Cu, Mn, Ni) of 2-thiouracil (2TU), and 2- and 8-hydroxyquinolines (8-HQ and 2-HQ) (**1**-**6**); and copper complexes of sulfonamide analogs (**7**-**16**) were synthesized and evaluated for their biological activities (i.e., antioxidant, antimicrobial and anticancer activities). The synthesis of metal complexes was carried out using chemical method. Biological activities were performed i.e., antioxidants using 2,2-diphenyl-1-picrylhydrazyl (DPPH) and superoxide dismutase (SOD) assays; antimicrobials using agar dilution method and anticancers using 3-(4,5-dimethylthiazol-2-yl)-2,5-diphenyltetrazolium bromide (MTT) and 2,3-bis-(2-methoxy-4-nitro-5-sulfophenyl)-2*H*-tetrazolium-5-carboxanilide salt (XTT) assays. The metal complexes **1**-**6** displayed SOD activity in ranges of IC_{50} of 1.81-516.56 μM. Interestingly, metal complex **5** (2TU-Cu-2HQ) has the highest SOD activity with IC_{50} of 1.81 μM. The complexes **1** (2TU-Ni-8HQ), **5** and **2** (2TU-Cu-8HQ) exhibited radical scavenging

activity (DPPH) with IC_{50} of 171.31, 194.25 and 388.56 μM, respectively, but the other complexes **3**, **4** and **6** were shown to be inactive compounds. The metal complex **3** (2TU-Mn-8HQ) showed good antimicrobial activity with the minimal inhibitory concentration (MIC) range of 11.07-708.64 μM against gram-positive and gram negative bacteria as well as diploid fungus, followed by metal complexes **2** (MIC of 23.68-757.70 μM) and **1** (MIC of 350.67-701.35 μM). In addition, copper (Cu) complexes (**7-16**) of 4-substituted (NO_2, OCH_3, CH_3 and Cl) benzenesulfonamide of anthranilic acid were synthesized and determined for antioxidant, antimicrobial and cytotoxic activities. The Cu complexes **7-16** elicited antioxidant activity (SOD) in range of IC_{50} of 0.062-0.152 μM, and cytotoxic activity with IC_{50} of 21.60-28.92 μM against MOLT-3 cell lines. The complex **10** (sulfonamides with NO_2 and Cl substituents) has the strongest SOD activity with IC_{50} of 0.062 μM and complex **16** (with Cl group) showed the best cytotoxicity against MOLT-3 cell lines with IC_{50} of 21.60 μM. Furthermore, insight into structure-activity relationship was investigated to elucidate molecular structures governing their biological activities. Therefore, a data set of 20 pyrazolopyridine derivatives with antioxidant activity was employed to construct a QSAR model. The obtained significant descriptors composed of 3D-MoRSE-signal 11/weighted by atomic masses (Mor11m), 3D-MoRSE-signal 25/weighted by atomic van der Waals volumes (Mor25v), mean topological charge index of order 5 (JGI5), H autocorrelation of lag 8/ weighted by atomic polarizabilities (H8p), Geary autocorrelation–lag 5/weighted by atomic polarizabilities (GATS5p), and Ghose-Viswanadhan-Wendoloski drug-like index at 50% (GVWAI-50) were used for generating the predictive model. The statistical qualities showed good predictive performance of Q^2 = 0.9370 and RMSE =4.7414 for internal validation (LOO-CV set). Moreover, the highest antioxidant activity required the compound with the highest JGI5 and GATS5p but with low Mor25v, that are well correlated to 3-aminopyrazole pharmacophore of the compounds. Furthermore, pyridine and pyrimidine derivatives as privileged scaffolds with anticancer activity have been reported. The body of knowledge is benefit for the design and development of novel bioactive pyridine and pyrimidine-based compounds. The findings afforded new potential candidate metal complexes (**1-16**), QSAR study for the rational design of new pyrazole analogs with potent antioxidant activity, and outlook of pyridines and pyrimidines for medicinal applications.

Keywords: metal complexes, hydroxyquinolines, sulfonamides, pyridines, pyrimidines, biological activities, QSAR, medicinal chemistry

บทคัดย่อ:

เนื่องจากภายในโครงสร้างของเอนไซม์ superoxide dismutase (SOD) ประกอบด้วยโลหะทรานซิชันซึ่งมีบทบาทเป็นโคแฟกเตอร์ที่สำคัญในการเกิดกลไกของปฏิกิริยาและการทำหน้าที่ของเอนไซม์ ดังนั้นการสังเคราะห์สารโลหะเชิงซ้อนจึงได้ทำการออกแบบเพื่อแสดงคุณสมบัติคล้ายเอนไซม์ SOD (SOD activity) โดยทำการสังเคราะห์สารโลหะเชิงซ้อนที่มีโลหะไอออนประเภท Cu, Mn, Ni ของอนุพันธ์ 2-thiouracil-hydroxyquinolines (**1-6**) และสังเคราะห์สารโลหะเชิงซ้อนที่มีโลหะไอออนประเภท Cu ของอนุพันธ์ sulfonamides (**7-16**) ด้วยกระบวนการทางเคมีสังเคราะห์ และสารสังเคราะห์ที่ได้นำไปศึกษาฤทธิ์ทางชีวภาพ ได้แก่ ฤทธิ์ต้านอนุมูลอิสระ ฤทธิ์ต้านเชื้อจุลชีพ และฤทธิ์ต้านเซลล์มะเร็ง วิธีการทดสอบฤทธิ์ต้านอนุมูลอิสระด้วยการใช้ 2 วิธีคือ วิธี 2,2-diphenyl-1-picrylhydrazyl (DPPH) และ superoxide dismutase (SOD); ฤทธิ์ต้านเชื้อจุลชีพใช้วิธี agar dilution และ ฤทธิ์ต้านเซลล์มะเร็งใช้วิธี 3-(4,5-dimethylthiazol-2-yl)-2,5-diphenyltetrazolium bromide (MTT) และ 2,3-bis-(2-methoxy-4-nitro-5-sulfophenyl)-2*H*-tetrazolium-5-carboxanilide salt (XTT) จากการศึกษาพบว่าสารโลหะเชิงซ้อน (**1-6**) แสดงฤทธิ์ต้านอนุมูลอิสระ (SOD activity) แสดงค่า IC_{50} ในช่วง 1.81-516.56 μM โดยสารโลหะเชิงซ้อน **5** (2TU-Cu-2HQ) แสดงฤทธิ์ต้านอนุมูลอิสระได้ดีที่สุด แสดงค่า IC_{50} เท่ากับ 1.81 μM นอกจากนี้แล้ว สารโลหะเชิงซ้อน **1** (2TU-Ni-8HQ), **5** และ **2** (2TU-Cu-8HQ) แสดงฤทธิ์ต้านอนุมูลอิสระชนิด radical scavenging activity (DPPH) แสดงค่า IC_{50} เป็น 171.31, 194.25 และ 388.56 μM ตามลำดับ ในขณะที่สารโลหะเชิงซ้อน **3**, **4** และ **6** ไม่แสดงฤทธิ์ดังกล่าว จากการทดสอบฤทธิ์ต้านเชื้อจุลชีพพบว่าสารโลหะเชิงซ้อน **3** (2TU-Mn-8HQ) แสดงฤทธิ์ในการต้านเชื้อจุลชีพได้ดี แสดงค่า minimal inhibitory concentration (MIC) ในช่วง 11.07-708.64 μM ในการต้านเชื้อแบคทีเรียแกรมบวก แบคทีเรียแกรมลบ และเชื้อรา สารโลหะเชิงซ้อน **2** (MIC เท่ากับ 23.68-757.70 μM) และ **1** (MIC เท่ากับ 350.67-701.35 μM) แสดงฤทธิ์ต้านเชื้อแบคทีเรียและเชื้อรา นอกจากนี้แล้วสารโลหะเชิงซ้อน copper sulfonamide (**7-16**) แสดงฤทธิ์ต้านอนุมูลอิสระ แสดงค่า IC_{50} เท่ากับ 0.062-0.152 μM และฤทธิ์ต้านเซลล์มะเร็งชนิด MOLT-3 แสดงค่า IC_{50} เท่ากับ 21.60-28.92 μM โดยสาร **10** (ที่มีหมู่ NO_2 และ Cl) แสดงฤทธิ์ต้านอนุมูลอิสระ (SOD activity) ได้ดีที่สุด แสดงค่า IC_{50} เท่ากับ 0.062 μM และสาร **16** (ที่มีหมู่ Cl) แสดงฤทธิ์ต้านเซลล์มะเร็งชนิด MOLT-3 ได้ดีที่สุด แสดงค่า IC_{50} เท่ากับ 21.60 μM นอกจากนี้ได้ศึกษาสารอนุพันธ์ pyrazolopyridine จำนวน 20 ชนิดที่มีฤทธิ์ต้านอนุมูลอิสระด้วยวิธีทางคอมพิวเตอร์ เพื่อหาความสัมพันธ์ระหว่างคุณสมบัติทางโครงสร้างและการออกฤทธิ์ต้านอนุมูลอิสระ (QSAR studies) พบว่าคุณสมบัติทางโครงสร้างประกอบด้วย 3D-MoRSE-signal 11/weighted by atomic masses (Mor11m), 3D-MoRSE-signal 25/weighted by atomic van der Waals volumes (Mor25v), mean topological charge index of order 5

(JGI5), H autocorrelation of lag 8/ weighted by atomic polarizabilities (H8p), Geary autocorrelation–lag 5/weighted by atomic polarizabilities (GATS5p) และ Ghose-Viswanadhan-Wendoloski drug-like index at 50% (GVWAI-50) มีความสัมพันธ์กับการออกฤทธิ์ต้านอนุมูลอิสระจึงได้นำไปใช้ในการสร้างรูปแบบการทำนาย โดยพบว่า ค่าความสัมพันธ์ (Q^2) แสดงค่า 0.9370 และค่าความผิดพลาดจากการทำนาย (RMSE) แสดงค่า 4.7414 ในชุดข้อมูลการทดสอบ (LOO-CV set) โดยสารที่แสดงฤทธิ์ต้านอนุมูลอิสระที่ดีจะมีค่า JGI5 และ GATS5p ที่สูง แต่จะมีค่า Mor25v ที่ต่ำ ซึ่งสอดคล้องกับ 3-aminopyrazole pharmacophore นอกจากนี้แล้วได้ทบทวนวรรณกรรมสารประเภท pyridine และ pyrimidine ซึ่งเป็นโครงสร้างหลัก (scaffolds) ที่มีความสำคัญต่อการออกฤทธิ์ต้านมะเร็ง จากการศึกษาในครั้งนี้แสดงให้เห็นถึงศักยภาพของสารโลหะเชิงซ้อนชนิดใหม่จำนวน 16 ชนิด (**1-16**) ที่มีฤทธิ์ทางชีวภาพและการประยุกต์ใช้เทคนิคทางคอมพิวเตอร์ในการศึกษา QSAR สำหรับใช้ในการออกแบบสารต้านอนุมูลอิสระชนิดใหม่ที่เป็นสารอนุพันธ์ pyrazole รวมถึงความสำคัญของสารประเภท pyridines และ pyrimidines ซึ่งจะเป็นประโยชน์ในการประยุกต์ใช้ในทางการแพทย์ต่อไป

คำสำคัญ : metal complexes, hydroxyquinolines, sulfonamides, pyridines, pyrimidines, biological activities, QSAR, medicinal chemistry

CONTENTS

Page

ACKNOWLEDGEMENTS **3**

ABSTRACT (ENGLISH)..... **4**

ABSTRACT (THAI)..... **6**

LIST OF TABLES..... **11**

LIST OF FIGURES..... **12**

LIST OF ABBREVIATIONS **13**

CHAPTER I: INTRODUCTION **14**

CHAPTER II: OBJECTIVES **16**

CHAPTER III: LITERATURE REVIEW **17**

3.1 Free radical and antioxidant systems 17

3.2 Enzymatic antioxidant system (Superoxide dismutase: SOD) 17

3.3 Non-enzymatic antioxidant system 18

3.3.1 Drug discovery and development process 18

3.3.2 Synthetic and natural antioxidant compounds..... 19

3.4 Computational approaches 22

CHAPTER IV: SYNTHESIS, ANTIOXIDANT AND ANTIMICROBIAL ACTIVITIES OF METAL COMPLEXES OF 2-THIOURACIL-HYDROXYQUINOLINE DERIVATIVES **23**

4.1 Abstract 23

4.2 Introduction 23

4.3 Materials and methods 25

4.3.1 General 25

4.3.2 Synthesis of 2-thiouracil and 8-hydroxyquinoline/ 2-hydroxyquinoline metal complexes 25

4.3.3 Antioxidant activity 26

4.3.4 Antimicrobial activity 27

4.4 Results and discussion 28

CONTENTS (cont.)

Page

4.4.1 Chemistry 28
4.4.2 Antioxidative activity 29
4.4.3 Antimicrobial activity 30

CHAPTER V: ANTIOXIDANT AND CYTOTOXIC ACTIVITIES OF COPPER COMPLEXES OF SULFONAMIDE ANALOGS 39

5.1 Abstract 39
5.2 Introduction 39
5.3 Materials and methods 40
5.3.1 General 40
5.3.2 Synthesis of copper-sulfonamide complexes (**1**-**10**) 41
5.3.3 Biological activities 42
5.3.3.1 Antioxidant activity 42
5.3.3.2 Antimicrobial activity 42
5.3.3.3 Cytotoxicity 43
5.4 Results and discussion 44
5.4.1 Chemistry 44
5.4.2 Antioxidant activity 44
5.4.3 Antimicrobial activity 45
5.4.4 Cytotoxic activity 45

CHAPTER VI: TOWARDS THE DESIGN OF 3-AMINOPYRAZOLE PHARMACOPHORE OF PYRAZOLOPYRIDINE DERIVATIVES AS A NEW ANTIOXIDANTS 51

6.1 Abstract 51
6.2 Introduction 51
6.3 Materials and methods 52
6.3.1 Data set 52
6.3.2 Descriptors calculation 52

CONTENTS (cont.)

Page

6.3.3 Data sampling 53
6.3.4 Multiple linear regression 53
6.3.5 Statistical analysis 54
6.4 Results and discussion 54
6.4.1 Descriptors calculation and feature selection 54
6.4.2 QSAR modeling of antioxidant activity 55
6.4.3 Structure-activity relationship 56
CHAPTER VII: CONCLUSION AND FUTURE PERSPECTIVE 63
REFERENCES……..... 64
APPENDIX……..... 74

LIST OF TABLES

Table		Page
4.1	IR spectra (cm^{-1}) and μ_{ef} (B.M) of 2-thiouracil-hydroxyquinolines metal complexes (**1-6**)	35
4.2	Antioxidant activities of 2-thiouracil-hydroxyquinolines metal complexes (**1-6**) and ligands	36
4.3	Antimicrobial activity of 2-thiouracil-hydroxyquinolines metal complexes (**1-6**) and ligands	37
5.1	IR spectra (cm^{-1}) and μ_{ef} (B.M) of copper complexes of sulfonamide analogs (**7-16**)	48
5.2	Characteristics of Cu-sulfonamide complexes (**7-16**)	49
5.3	Antioxidant activity (SOD) of Cu-sulfonamide complexes (**7-16**)	49
5.4	Cytotoxic activity of Cu-sulfonamide complexes (**7-16**)	50
6.1	Antioxidant activity and significant descriptors of pyrazolopyridine derivatives	61
6.2	Description of important descriptors for constructing the QSAR model	62
6.3	Intercorrelation matrix of significant descriptors	62

LIST OF FIGURES

Figure		Page
3.1	The mechanism of superoxide dismutase and catalase enzymes eliminated free radicals	18
3.2	General strategy used in preclinical drug discovery and development.	19
3.3	Chemical structures of substituted uracil analogs	20
3.4	Chemical structures of 2-thiouracil derivatives	20
3.5	Chemical structures of quinoline and its derivatives	21
3.6	Chemical structure of sulfonamide	21
4.1	Chemical structures of 2-thiouracil-hydroxyquinolines metal complexes **1**-**6** (a) and ligands (b)	34
5.1	Chemical structures of ligands (a) and Cu-sulfonamide complexes (**7**-**16**) (b)	47
6.1	Molecular structures of pyrazolopyridine derivatives **1**-**20**	59
6.2	Plot of the experimental and predicted activities for the training set (□; regression line is represented as solid line), and the leave-one-out cross-validated set (■; regression line is represented as dotted line)	60
6.3	Charge distribution of compound **1**	60
6.4	Possible structurally modified derivatives (**1A**-**1C**)	60

LIST OF ABBREVIATIONS

γ	Gamma parameter
η	Hardness; Learning rate
°C	Degree Celsius
2-TU	2-thiouracil
2-HQ	2-hydroxyquinoline
8-HQ	8-hydroxyquinoline
A549	Human lung carcinoma cell line
AM1	Austin model 1
B3LYP	Becke's three-parameter Lee-Yang-Parr
CADDD	Computer-aided drug discovery and development
DFT	Density functional theory
DMSO	Dimethyl sulfoxide
DPPH	2,2-diphenyl-1-picrylhydrazyl
EA	Electron affinity
E_{HOMO}	Energy of the highest occupied molecular orbital
E_{LUMO}	Energy of the lowest unoccupied molecular orbital
E_{total}	Total energy of the molecule
g	Gram
H69AR	Multidrug-resistance small cell lung cancer cell line
HepG2	Hepatocellular carcinoma cell line
HuCCA-1	cholangiocarcinoma cell line
IC_{50}	50% inhibition concentration
LOO-CV	Leave-one out cross validation
MIC	Minimum inhibitory concentration
MOLT-3	Acute lymphoblastic leukemia cell lines
QSAR	Quantitative structure-activity relationship
RSA	Radical scavenging activity
SOD	Superoxide dismutase

CHAPTER I

INTRODUCTION

Advancements in sciences and technology have been led to significant changes in environment, society, behavior and lifestyle. Finally, population may encourage to risk factors associated with diseases such as non-communicable diseases (i.e. diabetes mellitus, cardiovascular diseases and cancers). Free radicals have been documented as risk factors correlated with progression of diseases. In biological systems, superoxide dismutase (SOD) is an enzyme that converts superoxide anion, deriving from external and internal sources of the body, to oxygen and hydrogen peroxide. Interestingly, SOD occupies transition metal as a cofactor to be responsible for metabolism and function of enzyme. It has been found that manganese (Mn), copper (Cu) and zinc (Zn) are transition metals in SOD enzymes (1-3). However, an excessive of free radicals may cause imbalance between antioxidant enzyme (SOD) and free radicals leading to pathophysiological conditions and end with diseases. Therefore, drugs/compounds have been designed and synthesized to solve these problems. Considering the SOD enzymes have metal ion in the structure, consequently, syntheses of compounds as SOD-like activity have been developed using transition metal ion as a centered atom that coordinated with ligands i.e., compounds containing electron donor atoms (nitrogen (N), sulfur (S) and oxygen (O)), to form metal complexes. The metal complexes have been successfully synthesized and determined for their bioactivities. For example, metal complexes of uracil derivatives exhibited cytotoxic, antimicrobial and antioxidant activities (4, 5); metal complexes of cefdinir displayed antibacterial activity (6); metal complexes of pyridine derivatives showed antioxidant and antimicrobial activities (7, 8) and metal complexes of monomethyl succinate exhibited antimicrobial activity (9). Interestingly, 8-hydroxyquinoline (8-HQ) and its derivatives (i.e. 2-HQ) are ligands constituting O and N electron donor atoms that are capable of forming coordinated metal complexes with metal ions (10). In addition, sulfonamides containing O and N atoms that can form metal complexes with metal ions. These ligands (i.e., 8-HQ, uracils and sulfonamides) displayed diverse biological activities such as antioxidant, antimicrobial and anticancer activities. To search for new bioactive compounds, these known bioactivities of ligands (8-HQ, uracil and sulfonamide derivatives) are interested compounds to be used for the synthesis of metal complexes for value-added of compounds. This project aims to synthesize transition metal complexes as potential new

lead compounds for medicinal applications using 8-HQ (and its derivative; 2-HQ) and 2-thiouracil **(Appendix A)**, and sulfonamides ligands **(Appendix B)**; and evaluate for their biological activities including antioxidant, antimicrobial and cytotoxic activities, and to construct QSAR and insight into relationship between physicochemical properties and antioxidant activity of 3-aminopyrazole of pyrazolopyridine derivatives using computational analysis **(Appendix C)**. In addition, pyridine and pyrimidine as privileged scaffolds with attractive anticancer activities were described for the searching of new anticancer agents **(Appendix D)**.

CHAPTER II

OBJECTIVES

This research project aims:

1. To synthesize transition metal (Cu, Ni, Mn) complexes of 2-thiouracil and 8-hydroxyquinoline/2-hydroxyquinoline.
2. To synthesize transition metal (Cu) complexes of sulfonamide analogs
3. To determine antioxidant, antimicrobial and anticancer activities of transition metal complexes
4. To elucidate structure-activity relationship of the transition metal complexes with their bioactivities.
5. To construct QSAR model for 3-aminopyrazole scaffold of pyrazolopyridine derivatives with antioxidant activity using computational approaches

CHAPTER III
LITERATURE REVIEW

3.1 Free radical and antioxidant systems

Free radical is an unstable molecule containing unpaired valence electrons that can damage biomolecule in the body such as protein, lipid and deoxyribonucleic acid (DNA) (11-13). Free radical is divided into 2 types: reactive oxygen species (ROS) and reactive nitrogen species (RNS). The free radicals are produced from external (i.e. pollution, UV light and smoking) and internal (i.e. metabolism and inflammation) sources (11-13). Normally, free radical is eliminated by antioxidant systems that were categorized into 2 groups: i) enzymatic system such as superoxide dismutase (SOD), superoxide reductase and catalase and ii) non-enzymatic system such as vitamins C and E and flavonoids (14, 15). However, excessive of free radicals lead to imbalance between free radical and antioxidant systems, eventually, to develop diseases as pathological conditions such as neurodegenerative disease, atherosclerosis, cardiovascular disease and cancer (12, 13)

3.2 Enzymatic antioxidant system (Superoxide dismutase: SOD)

SOD is an important enzyme as found in living organisms that are divided into 3 classes depend on location and catalytic metal ions: manganese (Mn) in mitochondria, copper (Cu)/zinc (Zn) in cytoplasm and extracellular. Furthermore, nickel (Ni) SOD was found in prokaryotic organisms (1). The SODs are responsible for converting superoxide anion to oxygen and hydrogen peroxide which is a substrate of catalase and glutathione peroxidase enzymes as presented in Figure 3.1. It was found that SOD is an essential enzyme to remove free radical or chain reaction of free radicals serving as a substrate for other antioxidant enzymes.

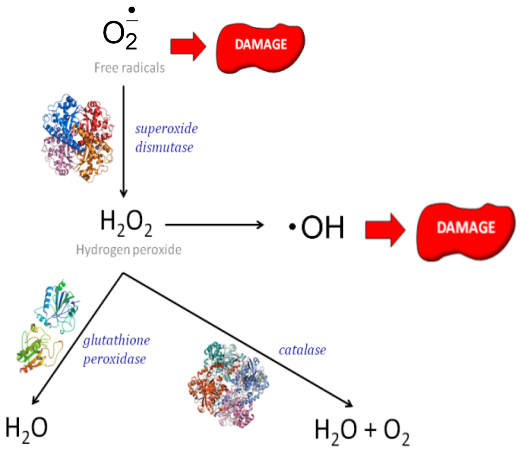

Figure 3.1. The mechanism of superoxide dismutase and catalase enzymes eliminated free radicals (16).

3.3 Non-enzymatic antioxidant system

Non-enzymatic antioxidant system such as vitamins (i.e. vitamins C and E) and carotenoids (i.e. lycopene and *β*-carotene) are nutrient antioxidants for detoxifying free radicals. Moreover, insufficiency of exogenous antioxidants lead to diseases derived from oxidative stress. Furthermore, discovery and development of compounds are considered as important process for exploring new candidate compounds (13).

3.3.1 Drug discovery and development process

Drug discovery and development have extensive historical evidences for the use of bioactive compounds from botanical sources in ameliorating conditions and treating diseases. There are started in the late 1800s and there are a few drugs available for treatment of diseases at the beginning of 1900s (17, 18). Based on early days, most drugs were obtained from herbs and extracted ingredients from plant, until 1900s, the synthetic compounds were achieved from chemical methods. Moreover, drug discovery is also focused on bioactive metabolites from natural products. After the advancements and breakthroughs in science and technology lead to the development of specific or broad spectrum of drugs in targeting of interested diseases or pathogenic organisms. The process of drug discovery are composed of target identification and validation, lead discovery and optimization, preclinical tests, clinical trials, manufacturing and marketing application (17, 18). The general strategy used in preclinical drug discovery and development (19) is shown in Figure 3.2. The main objective is to select drug candidates having efficacy in humans and avoid problems in clinical trials such as bioavailability and toxicity.

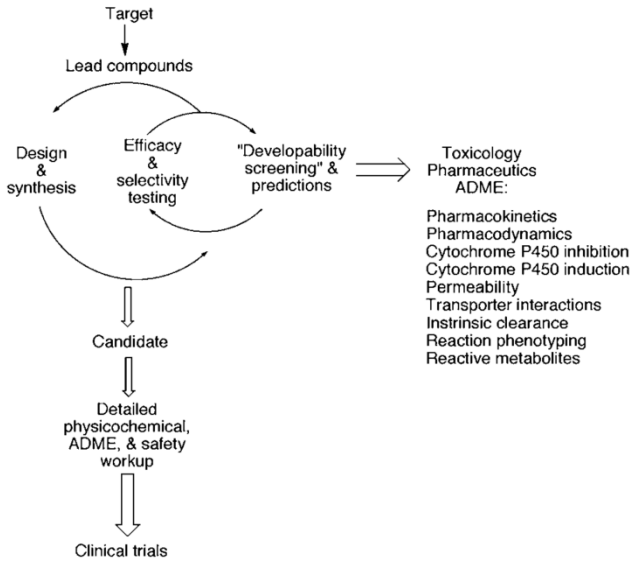

Figure 3.2. General strategy used in preclinical drug discovery and development (19).

3.3.2 Synthetic and natural antioxidant compounds

Synthetic and natural antioxidant compounds have been discovered and developed for new lead compounds. Natural compounds as bioactive metabolites with antioxidant, antimicrobial and anticancer activities have been identified in natural source such as *Spilanthes acmella* Murr. (20), *Hydnophytum formicarum* Jack. (21), *Saraca thaipingensis* (22), *Polyalthia cerasoides* (23) and *Pterocarpus indicus* (24). Furthermore, chemical synthesis is an important method for obtaining a variety of new bioactive compounds belonging to pyridine (25), pyrimidine (26), triazole (27), quinoline and isoquinoline (28) based compounds and metal complexes have been successfully synthesized as potent and promising bioactive compounds such as antioxidants, anticancers, antimicrobials and vasorelaxants. Interstingly, metal complexes have been synthesized as SOD mimetic. These metal complexes composed of a variety of transition metal ions such as Mn, Cu, Zn, Fe and Ni displaying pharmacological activities (4-7, 9, 29, 30). There are several ligands bearing N, S and O atoms that can bind to metal ions *via* coordination bond.

Uracil and its derivatives were found to be bioactive compounds displaying antioxidant (31), antimicrobial (32), anticancer (33)and antiviral (34) activities. For example, uracils (Figure 3.3) possessing halogen substituents at the 5- or 6-position (35) exhibited interesting bioactivities e.g. 5-fluorouracil as known anticancer drug (36), antimetabolites (37) and its N1-substituted derivative **1** (38), as well as nucleoside analogs **2** and **3** of 5-iodouracil and 5-trifluoromethyluracil, which are antivirals (39). Acyclic-nucleoside analogs were shown to be anti HIV-1 agents. Examples are acyclic

5,6-disubstituted uracils **4a-g** (Figure 3.3) (39, 40). Furthermore, a series of thiouracil (i.e., 2-thiouracil) derivatives (Figure 3.4) was reported to exhibit diverse bioactivities (26, 32, 41).

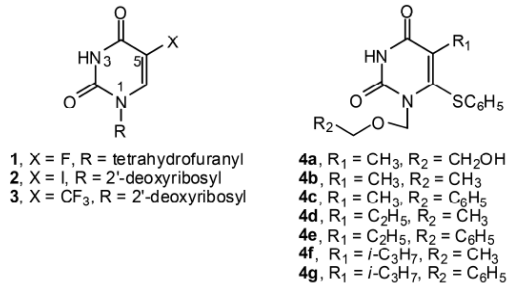

Figure 3.3. Chemical structures of substituted uracil analogs **1-4** (33).

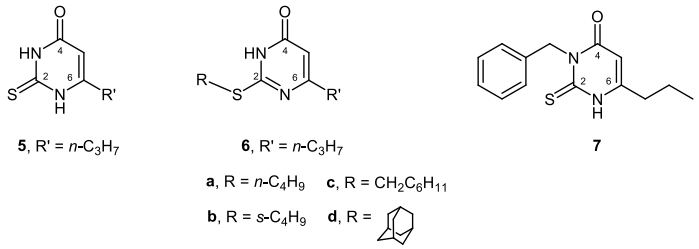

Figure 3.4. Chemical structures of 2-thiouracil derivatives (26).

It is known that substituted uracils play a vital role in many metabolic processes (42-44). Therefore, considerable interest has been drawn for using uracils as ligands for coordinated metal complexes with pharmacological activities (4, 5). Such ligands constitute O and N atoms that can form coordination complex with metal ions.

Quinolines are a chemical moiety that displayed a variety of pharmacological properties such as broad spectrum antibacterial (45), anticancer (46) and antiviral (47) activities. Quinoline is a used as scaffold for the synthesis of its derivatives, especially, 8-hydroxyquinoline (8-HQ) that exhibited bioactivities such as fungicidal and antibacterial activities (10). 8-HQ was considered as a ligand for metal complexes that it has O and N atoms in the molecule (10) atoms. The 8-HQ is a quinoline derivative found in natural products, therapeutic drug/compounds and chelating agents (10). It has been documented to show strong antioxidant and antimicrobial activities (5, 48). In addition, 2-hydroxyquinoline (2-HQ) is an isomeric from of 8-HQ that can form coordinated bond with metal ions. Chemical structures of quinoline and its derivatives are outlined in Figure 3.5.

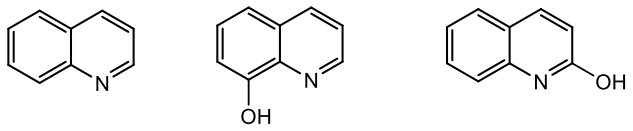

Quinoline 8-hydroxyquinoline 2-hydroxyquinoline

Figure 3.5. Chemical structures of quinoline and its derivatives.

In addition, synthesis and biological activities of metal complexes of quinolone derivatives have been documented, for example, fluoroquinolones analogs with mixed-ligand Cu (II) complexes displayed antimicrobial, antioxidant and DNA cleavage activities (49). Furthermore, metal complexes of 8HQ with 5-iodouracil/5-nitrouracil exhibited cytotoxic, antimicrobial, antioxidant and aromatase inhibitory activities (4, 5, 48).

Sulfonamide (Figure 3.6) is an important pharmacophore found in many drugs and bioactive compounds. sulfonamides exhibited a diverse biological activities such as antimicrobial (50), anticancer (51) and antiviral (52) activities. Considering the sulfonamide structure, it is interesting to use as the ligand to form metal complexes and evaluate for their bioactivities.

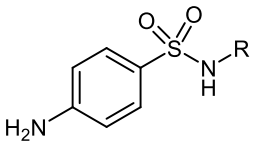

Figure 3.6. Chemical structure of sulfonamide.

Sulfonamide derivatives were used as a ligand to coordinate with metal ions (i.e., moononuclear complexes of 5-chloro-2-hydroxybenzylidene) aminobenzenesulfonamides with various metal ions, Cu complexes of *N*-substituted sulfonamides and Zn complexes of tosyl sulfonamide derivatives). It has found that metal complexes of sulfonamide derivatives exhibited biological activities such as anti-parasitic (53), DNA cleavage and cytotoxic activities (54).

Pyridine is a chemical moiety found in living organisms, it is a six-membered ring of five carbon atoms and one nitrogen atom (55). It has been used as a core structure for the synthesis of new compounds with pharmacological properties (25, 56-58). In addition, pyrazole is a five-membered ring of three carbon atoms and two nitrogen atoms, which has been considerable used as core structure for the drug design (59-61). Therefore, a fused ring of pyridine and pyrazole gave rise to the

pyrazolopyridine scaffold, which was shown to exert various biological activities such as antimicrobial (62); , anticancer (63) and kinase inhibitory (64) properties.

3.4 Computational approaches

Advanced computational technology, computer-aided drug discovery and development (CADDD), was applied for screening the interesting compounds with their biological or chemical properties *in silico* (65, 66). Particulary, quantitative structure-activity relationship (QSAR) was widely used to generate predictive models as well as insight into the correlation of chemical structural features that involved in governing their biological activities. The QSAR studies have been successfully demonstrated for developing the QSAR models such as antioxidant, anticancer, antimicrobial and anti-parasitic activities. The advantages of QSAR models are used as guideline for rational design of novel compounds with potential chemical/biological activities (65, 66).

CHAPTER IV

SYNTHESIS, ANTIOXIDANT AND ANTIMICROBIAL ACTIVITIES OF METAL COMPLEXES OF 2-THIOURACIL-HYDROXYQUINOLINE DERIVATIVES

4.1 Abstract

Metal ions are cofactors found in antioxidant enzymes such as superoxide dismutase (SOD), and are essential in catalytic mechanisms for scavenging the free radicals. Therefore, synthetic compounds containing metal ions coordination are designed for SOD mimic and other biological activities. The metal complexes **1**-**6** elicited SOD activity with IC_{50} of 1.81-516.56 μM, particularly, complex **5** (2TU-Cu-2HQ) showed the highest SOD activity with IC_{50} of 1.81 μM. In addition, complexes **1** (2TU-Ni-8HQ), **5** and **2** (2TU-Cu-8HQ) displayed radical scavenging activity (RSA) with IC_{50} of 171.31, 194.25 and 388.56 μM, respectively, whereas the complexes **3**, **4** and **6** were shown to be inactive. Furthermore, the metal complex **3** (2TU-Mn-8HQ) exhibited good antimicrobial activity with the minimal inhibitory concentration (MIC) range of 11.07-708.64 μM against gram-positive and gram negative bacteria as well as diploid fungus, followed by metal complexes 2 (MIC of 23.68-757.70 μM) and 1 (MIC of 350.67-701.35 μM). Interestingly, the similar mixed ligands with different metal ions of complexes **1** (Ni), **2** (Cu) and **3** (Mn), the complex **3** has the highest SOD (IC_{50} = 5.04 μM) and antimicrobial activities, but Cu complex (**5**) of 2TU and 2HQ showed the highest SOD, RSA and antimicrobial activities than Ni (**4**) and Mn (**6**) complexes. This finding reveals novel transition metal complexes with a potential for further development as medicinal compounds.

4.2 Introduction

Free radicals are a risk factor of various diseases such as diabetes mellitus, cancer as well as cardiovascular and neurodegenerative diseases (67, 68). Biological molecules in the body such as lipid, protein and deoxyribonucleic acid (DNA) can be damaged by the free radicals. The endogenous defense mechanisms against the free radicals can be overcomed by antioxidant enzymes i.e., superoxide dismutase (SOD), catalase and glutathione peroxidase. In addition, antioxidant compounds can be obtained from external sources i.e., supplement and dietary vitamins A, C and E (15,

69). However, an excess of the free radicals in the body can cause undesirable effects leading to physiological changes and eventually to clinical symptoms and diseases (67, 68)]. Therefore, antioxidant compounds can be recommended to reduce/neutralize the overload of free radicals for preventing a progression of the diseases. Interestingly, the SOD is an essential enzyme for catalyzing the dismutation of superoxide anion into oxygen and hydrogen peroxide. Considering the SOD structure, it composes of transition metal ions such as manganese (Mn) found in mitochondria, zinc (Zn) and copper (Cu) found in cytosol, iron (Fe) and nickel (Ni) found in bacteria (1-3). These metal ions are important cofactors for exerting the SOD activity, and are essential for catalytic mechanisms. Therefore, synthetic compounds containing metal ion coordination are attractive for designing SOD-like activity as well as other pharmacological activities.

Uracil is a heterocyclic compound acting as a nucleobase found in nucleic acid. The uracil and its derivatives were reported to display biological activities i.e., antioxidant (31), antimicrobial (32), anticancer (33) and antiviral (34) properties. Uracils possessing halogen substituents (70) were reported to exhibit interesting bioactivities i.e., 5-fluorouracil as anticancer drug (36) and antimetabolites (71) including N1-substituted derivatives of 5-iodouracil and 5-trifluoromethyluracil (72) are antivirals (73). Furthermore, a series of thiouracil derivatives have been shown to exhibit diverse bioactivities such as antioxidant, antimicrobial and anticancer activities (26, 41, 74). It is noted that substituted uracils play a vital role in many metabolic processes (75-77). Therefore, considerable interest has been drawn to use uracils (constitutes two oxygen (O) and two nitrogen (N) atoms) as ligands for the synthesis of various transition metal complexes (5, 29).

Quinoline is a bicyclic compound with a variety of pharmacological properties such as antibacterial (45), anticancer (46) and antiviral (47) activities. Quinoline derivatives, for example, 8-hydroxyquinoline (8HQ) exhibited various bioactivities such as fungicidal, antibacterial and anticancer activities (10, 78, 79). The 8HQ is a ligand bearing O and N electron donor atoms with metal chelating effect (10). It is found in natural products, therapeutics/compounds and chelating agents (65). It has been reported to display strong antioxidant, cytotoxic and antimicrobial activities (5, 48). In addition, 2-hydroxyquinoline (2HQ) is an isomeric from of 8HQ that can form coordinated bond with metal ions. Synthetic fluoroquinolones mixed-ligands Cu (II) complexes were reported to display antimicrobial, antioxidant and DNA cleavage activities (49). Furthermore, metal complexes of 8HQ with 5-iodouracil/5-nitrouracil exhibited cytotoxic, antimicrobial, antioxidant and aromatase inhibitory activities (5, 29, 48).

To search for novel uracil-quinoline metal complexes, therefore, 2-thiouracil (2TU) and hydroxyquinoline (HQ) including 8HQ and 2HQ were used as potential ligands for the synthesis of metal complexes. Herein, the synthesis of mixed ligands (2TU-8HQ/2HQ) transition metals (Ni, Cu, Mn) complexes as well as antimicrobial and antioxidant activities have been reported.

4.3 Materials and methods

4.3.1 General

Infrared (IR) spectra were obtained on a Perkin Elmer System 2000 FTIR. Mass spectra were recorded on a Finnigan INCOS50 and a Bruker Daltonics (Micro TOF). Magnetic moment was performed on a Magnetic Susceptibility Balance, Mark 1, Serial 15257, Sherwood Scientific, Cambridge, UK. Melting points were determined on an Electrothermal melting point apparatus and are uncorrected. Reagents for assays included HEPES (*N*-2-hydroxyethylpiperazine-*N*′-2-ethanesulfonic acid), vitamin E, DPPH (2,2-diphenyl-1-picrylhydrazyl), nitroblue tetrazolium (NBT) salt, L-methionine, riboflavin, Triton-100, superoxide dismutase (SOD) from bovine erythrocytes, DMSO (dimethyl sulfoxide, 99.9%) and ampicillin from Sigma, USA; Müeller Hinton Broth and Müeller Hinton Agar from Becton Dickinson, USA and sodium chloride from Merck, German. Solvents were analytical grades.

4.3.2 Synthesis of 2-thiouracil and 8-hydroxyquinoline/2- hydroxyquinoline metal complexes

A solution of metal salts (1 mmol) dissolved in methanol (2 mL) was added dropwise to the solution of 2-thiouracil (1 mmol) in 70°C methanol (30 mL) and then heated for 45 min. A solution of 8HQ/2HQ (1 mmol) in methanol (2 mL) was added dropwise to the reaction mixture and further heated for 1 h. The precipitated solid was collected by filtration, washed 4-5 times with cold methanol and dried *in vacuo* at room temperature.

Complexes **1**-**3** were separately synthesized from 1 mmol of 2TU (128.2 mg) and 8HQ (145.2 mg) and 1 mmol of metal salts; $Ni(OAc)_2 \cdot 4H_2O$ (248.9 mg) for **1**, $Cu(OAc)_2 \cdot H_2O$ (199.8 mg) for **2** and $MnCl_2 \cdot 4H_2O$ (198.1 mg) for **3**.

Complexes **4**-**6** were obtained from 1 mmol of 2TU (128.2 mg) and 2HQ (145.2 mg) and 1 mmol of $Ni(OAc)_2 \cdot 4H_2O$ for **4**, of $Cu(OAc)_2 \cdot H_2O$ for **5** and of $MnCl_2 \cdot 4H_2O$ for **6**. Yield and m.p. of the complexes are summarized: **1** as light yellow-green powder

($C_{13}H_{12}N_3NiO_4S$, MW 365.01 g/mol), 226.0 mg (61.9%), m.p. 282-284^{O}C, **2** as dark green powder ($C_{13}H_{12}CuN_3O_2S$, MW 337.86 g/mol), 123.2 mg (36.9%), m.p.> 350^{O}C, **3** as pale yellow powder ($C_{13}H_{12}MnN_3O_4S$, MW 361.25 g/mol), 120.4 mg (33.31%), m.p. 296-300^{O}C, **4** as light yellow-green powder ($C_{13}H_{12}N_3NiO_2S$, MW 333.01 g/mol), 251.8 mg (75.6%), m.p. 230-234^{O}C, **5** as light green powder ($C_{13}H_{12}CuN_3O_2S$, MW 337.86 g/mol), 181.8 mg (53.8%), m.p. 284-288^{O}C, **6** as pale yellow powder ($C_{13}H_{12}MnN_3O_2S$, MW 329.26 g/mol), 130.2 mg (39.5%), m.p. 286-290^{O}C.

4.3.3 Antioxidant activity

Antioxidant activities of metal complexes (**1**-**6**) and ligands were evaluated using 1,1-diphenyl-2-picrylhydrazyl (DPPH) and superoxide dismutase (SOD) assays.

DPPH is a stable purple color compound, which reacted with antioxidants to give light-yellow color product of 1,1-diphenyl-2-picrylhydrazine. Briefly, the reaction was performed by adding 1 mL solution of DPPH in methanol (0.1 mM) to the tested compounds (dissolved in DMSO) with the final concentration of 300 µg/mL. The reaction was incubated in a dark room for 30 min, and the absorbance was measured at 517 nm using UV-Visible spectrophotometer (UV-1610, Shimadzu). The percentage of antioxidant or radical scavenging activity (RSA) was calculated (80) using equation (1):

$$\text{RSA (\%)} = \left[1 - \frac{Abs._{sample}}{Abs._{control}}\right] \times 100 \quad (1)$$

where $Abs._{control}$ is the absorbance of the control reaction, and $Abs._{sample}$ is the absorbance of the tested compound. Vitamin E was used as a control and methanol was used as a blank reaction.

SOD activity was determined using SOD assay by measuring nitro blue tetrazolium (NBT) reduction (81). The stock solution (1 mL) containing 27 mL of HEPES buffer (50 mM, pH 7.8), 1.5 mL of L-methionine (30 mg/mL), 1 mL of NBT (1.41 mg/mL) and 750 µL of Triton X-100 (1 %wt) was added to the solution of metal complexes (**1**-**6**) dissolved in DMSO. The reaction was initially started by adding 10 µL of riboflavin (44 mg/mL) to the tested compounds with final concentration of 300 µg/mL, and followed by illumination under a Philips Classic Tone lamp (60 W) in a light box for 7 min. The absorbance of the reaction was measured at 550 nm using UV-Vis spectrophotometer that measured the inhibition of photoreduction of NBT. The percentage of SOD activity

was calculated using Eq. (1). The SOD enzyme from bovine erythrocytes was used as a control and DMSO solvent was used as a blank reaction.

The 50% inhibition concentration (IC_{50}) was calculated in case of compounds displayed antioxidant (RSA and SOD) activities greater than 50% at 300 µg/mL. It was calculated by plotting %RSA or %SOD activity against metal complexes concentrations.

4.3.4 Antimicrobial activity

Antimicrobial activity testing of metal complexes (**1**-**6**) and ligands was investigated by the agar dilution method (82). In parallel, Müeller Hinton Broth (MHB), DMSO and ampicillin drug were used as the control in this study. The solution of tested compounds was then transferred to the Müeller Hinton Agar (MHA) solution with final concentrations of 4-256 µg/mL. The microorganisms were cultured in MHB at 37^{o}C overnight, and then were diluted with 0.9% normal saline for adjusting the density of microorganism as 1×10^{8} cell/mL compared to 0.5 McFarland standards. The microorganisms were inoculated onto the agar plates containing various concentrations of the tested compounds, and incubated at 37^{o}C for 24-48 h. The minimum inhibitory concentration (MIC) of the compounds was determined as the lowest concentration to inhibit the growth of microorganisms. Twenty-seven microorganisms (reference strains and clinical isolates) were used for the assay including **Gram negative bacteria**; *Escherichia coli* ATCC 25922, *Klebsiella pneumoniae* ATCC 700603, *Serratia marcescens* ATCC 8100, *Salmonella typhimurium* ATCC 13311, *Salmonella choleraesuis* ATCC 10708, *Pseudomonas aeruginosa* ATCC 15442, *Pseudomonas stutzeri* ATCC 17587, *Shewanella putrefaciens* ATCC 8071, *Achromobacter xylosoxidans* ATCC 27061, and clinical strains: *Shigella dysenteriae*, *Salmonella enteritidis*, *Morganella morganii*, *Aeromonas hydrophila*, *Citrobacter freundii* and *Plesiomonas shigelloides*, **Gram positive bacteria**; *Staphylococcus aureus* ATCC 29213, *Staphylococcus aureus* ATCC 25923, *Staphylococcus epidermidis* ATCC 12228, *Enterococcus faecalis* ATCC 29212, *Enterococcus faecalis* ATCC 33186, *Micrococcus luteus* ATCC 10240, *Corynebacterium diphtheriae* NCTC 10356, *Bacillus subtilis* ATCC 6633, and clinical strains: *Bacillus cereus* and *Listeria monocytogenes*, and **diploid fungus** (yeast); *Candida albicans* ATCC 90028 and *Saccharomyces cerevisiae* ATCC 2601.

4.4 Results and discussion

4.4.1 Chemistry

Metal complexes **1**-**6** (Figure 4.1) were synthesized using 1:1:1 molar ratio of 2TU:M:8HQ (2HQ) in which M = Ni (**1** and **4**), Cu (**2** and **5**) and Mn (**3** and **6**). These complexes appeared as pale yellow-green to dark green powder.

IR spectra (Table 3.1) of 2TU-8HQ metal complexes **1** (Ni) and **3**(Mn) showed absorptions (cm^{-1}) of CO at 1701-1702 and 1686, of C=S at 1422-1424, of C=N at 1629 and 1572-1578, of C—N at 1388 and 1368-1374, of C—O at 1281-1285, 1213-1214 and 1108-1111. These absorptions of compounds **1** and **3** remained the same as the absorptions of 2TU free ligand, except for the stretchings of C-N and C-O at 1388 and 1281-1285 were shifted from 1381 and 1286 of 8HQ, respectively. This suggested that metal centered atoms (Ni and Mn) coordinated with C5,6 double bond π donor of 2TU, together with electron donor ring N atom and OH group of 8HQ. It was again confirmed by the absence of OH bending (δOH) at 1410 of 8HQ. However, NH bending of 2TU remained the same as the δNH of 2TU free ligand. Magnetic moments of metal complexes **1** and **3** were 2.70 and 3.40 B.M., respectively. It was suggested that metal complexes **1** and **3** were formed as octahedral geometry using bidentate ligands (2TU and 8HQ) and two water molecules as shown by broad OH stretchings at 3358 and 3400.

Such π electron donor coordination was reported for metal complexes of uracils such as 5-iodouracil-8HQ/8-aminoquinoline metal (Mn, Cu, Ni) complexes (4, 5) and Ru complexes of 5-substituted (X) uracils, X = F, Cl, Br, I and H (83).

Copper complex of 2TU-8HQ (**2**) showed the absorptions of CO at 1693, of C=N at 1625 and 1575, of C—N at 1386 and 1375, and of NH at 3178 as well as the weak bending δNH at 1527. These absorptions of Cu-complex (**2**) were shifted compared with the free ligands (2TU and 8HQ). Apparently, only one strong CO of 2TU moiety was noted at 1693. In addition, C=S of complex **2** was not observed. These suggested that Cu-complex **2** was resulted from the coordination of 2TU through N1, S2 (as thiol form), and 8HQ using ring N-atom and 8OH group. This N1, S2 coordination complex was described for 2-thiolumazine Cu-complex (84). The complex **2** had μ_{eff} value of 1.315 B.M., which was suggested as a square planar geometry.

Metal complexes (**4**-**6**) displayed the stretching absorptions of CO at 1701, 1962, 1682-1684 and 1654, of C=N at 1628, 1637-1638 and 1600-1601, of C=S at 1425-1428, of C—N at 1395-1396, and NH at 3122-3126. These absorptions were shifted from the free ligands (2TU and 2HQ), suggesting that metal complexes **4**-**6** were formed through

the coordinations of 2TU using thione (C=S) and NH electron donors, and of 2HQ using amino keto form of 2-quinolinol. Metal complex formation via amino thione electron donors was previously reported for 6-hydroxy-2-thiouracil (thiobarbituric acid) (85) and 6-amino-2-thiouracil (86). In addition, the amino keto form involved in metal complexation was previously described for 2-pyridinol metal complex (7). Magnetic moments of complexes **4**-**6** were 0.953, 0.807 and 0.794, respectively. The results suggested that Ni (**4**), Cu (**5**) and Mn (**6**) complexes were formed as a square planar geometry. Based on the literature, metal complexes **1**-**6** have not been reported. Antimicrobial and antioxidants activities of these compounds (**1**-**6**) were investigated.

4.4.2 Antioxidative activity

The metal complexes **1**-**6** and ligands (2TU, 2HQ and 8HQ) were investigated for their antioxidative activities using DPPH and SOD assays in term of radical-and superoxide-scavenging activities. The results (Table **3.2**) showed that compounds **1, 2**, **5** and 8HQ displayed the radical scavenging activity (RSA) with IC_{50} of 171.31, 388.56, 194.25 and 1113.75 µM, respectively, whereas compounds **3**, **4**, **6**, 2TU and 2HQ exhibited RSA <50% (24.56%, 34.92%, 21.68%, 33.00% and 10.10%, respectively) at 300 µg/mL. Compounds **1** (IC_{50} = 171.31 µM) and **5** (IC_{50} = 194.25 µM) showed stronger RSA than compound **2** (IC_{50} = 388.56 µM) and free ligands such as 8HQ (IC_{50} = 1113.75 µg/mL).

SOD activity of the metal complexes (**1**-**6**) was determined using NBT reduction. Most complexes (Table 4.2) exhibited good SOD activity with IC_{50} range of 1.81-69.07 µM, except for Mn complex (**6**, IC_{50} = 516.56 µM). Interestingly, Cu complex **5** afforded the strongest SOD activity with IC_{50} of 1.81µM followed by **3>2>1>4>6** with IC_{50} = 5.04, 10.06, 15.73, 69.07 and 516.56 µM, respectively. In a series of 2TU-8HQ metal complexes (**1**-**3**), Mn complex **3** (IC_{50} = 5.04 µM) displayed the strongest SOD activity. However, Cu complex (**5**, IC_{50} = 1.81 µM) of 2TU-2HQ was shown to be the most active antioxidant compared with the other tested compounds. In addition, 8HQ showed SOD activity with IC_{50} of 91.83 µM, but other ligands including 2TU (28.70%) and 2HQ (25.19%) displayed weak activity <50% at 300 µg/mL. The results indicated that types of ligands and metal ions for metal coordination played roles in antioxidant activities.

4.4.3 Antimicrobial activity

The antimicrobial activity of metal complexes (**1**-**6**) was performed using the agar dilution method against 27 strains of microorganisms. The results (Table 4.3) showed that compounds **1**-**3** exerted antimicrobial activity, whereas complexes **4**-**6** were inactive compounds. Complex **1** (Ni) displayed antimicrobial activity against gram positive bacteria: *S. aureus* ATCC 29213, *S. aureus* ATCC 25923, *E. faecalis* ATCC 29212, *E. faecalis* ATCC 33186, *M. luteus* ATCC 10240, *B. subtilis* ATCC 6633, *C. diphtheriae* NCTC 10356, and *B. cereus* as well as gram negative bacteria: *C. fluendii* with MIC of 701.35 μM. At lower MIC (350.67 μM), *S. epidermidis* ATCC 12228 and *P. shigelloides* were inhibited. Interestingly, complexes **2** (Cu) and **3** (Mn) showed better antimicrobial property with a range of MIC values 23.68-757.70 μM and 11.07-708.64 μM, respectively. Compound **2** showed antigrowth activity with MIC of 757.70 μM against gram negative bacteria: *S. putrefaciens* ATCC 8071 and *M. morganii*, with MIC of 378.85 μM against *E. coli* ATCC 25922, *S. macesens* ATCC 8100, *S. typhimurium* ATCC 13311, and *C. fluendii*, with MIC of 189.43 μM for *S. cerevisiae* ATCC 2601 and *A. hydrophila*, with MIC of 94.71 μM against *S. aureus* ATCC 25923, *E. faecalis* ATCC 29212, *E. faecalis* ATCC 33186, *M. luteus* ATCC 10240, *C. diphtheriae* NCTC 10356, *B. cereus* and *L. monocytogenes*, with MIC of 47.36 μM against *S. aureus* ATCC 29213 and *B. subtilis* ATCC 6633, and with MIC of 23.68 μM against *S. epidermidis* ATCC 12228 and *P. shigelloides*. Complex **3** (Mn) showed activity against *E. coli* ATCC 25922, *P. stutzeri* ATCC 17587, *S. putrefaciens* ATCC 8071, *A. xylosoxidans* ATCC 27061, *M. luteus* ATCC 10240 and *C. fluendii* with MIC of 708.64 μM, against *S. dysenteriae* with MIC of 354.32 μM, against *S. cerevisiae* ATCC 2601 with MIC of 88.56 μM, against *E. faecalis* ATCC 29212, *E. faecalis* ATCC 33186, *B. subtilis* ATCC 6633, *C. diphtheriae* NCTC 10356, *B. cereus* and *L. monocytogenes* with MIC of 44.29 μM, against *S. aureus* ATCC 29213, *S. aureus* ATCC 25923 and *S. epidermidis* ATCC 12228 with MIC of 22.15 μM, and against *P. shigelloides* with MIC of $\leq$11.07 μM. In addition, the free ligands (2TU, 8HQ and 2HQ) were also investigated for growth inhibition. It was shown that 2HQ had no activity against the tested microorganisms, but 2TU inhibited only *M. luteus* ATCC 10240 with MIC = 1997.62 μM. However, 8HQ showed antimicrobial activity (MIC = $\leq$27.56-1763.60 μM) against gram positive and gram negative bacteria as well as dipoid fungi (48, 87). Particularly, the resistant gram positive bacteria such as *S. aureus* ATCC 29213 and *S. aureus* ATCC 25923 displayed the activity with MIC $\leq$27.56 μM. At higher MIC value (220.45 μM), *E. coli* ATCC 25922, *S. typhimurium*

ATCC 13311, *P. stutzeri* ATCC 17587 and *C. fluendii* were inhibited by 8HQ. In addition, 8HQ also showed antigrowth activity against *K. pneumoniae* ATCC 700603 (MIC = 440.90 μM) and *P. aeruginosa* ATCC 15442 (MIC = 1763.60 μM). Moreover, *P. shigelloides* was inhibited by 8HQ with the lowest MIC ($\leq$27.56 μM). It should be noted that Cu complex **2** (MIC = 23.68 μM against *S. epidermidis* ATCC 12228 and *P. shigelloides*), and Mn complex **3** (MIC = 22.15 μM against *S. aureus* ATCC 29213, *S. aurues* ATCC 25923 and *S. epidermidis* ATCC 12228, MIC $\leq$11.07 μM against *P. shigelloides*) exerted better activity than the reference drug, ampicillin (MIC = 26.93 μM). Furthermore, all active compounds (**1**-**3** and 8HQ) expressed higher growth inhibition against gram positive bacteria than gram negative bacteria. Notably, it was found that 2TU-8HQ metal complexes (**1**-**3**) showed better antimicrobial activity than 2TU- 2HQ metal complexes (**4**-**6**). Particularly, compounds **2** (Cu) and **3** (Mn) displayed higher activity than compound **1** (Ni). In case of 2TU-2HQ metal complexes (**4**-**6**), all compounds exhibited no antimicrobial activity. In addition, the DMSO solvent was determined in parallel with the tested compounds, but no antimicrobial activity was observed.

An increase of antibiotic resistance in bacteria, causing either community-acquired infections or hospital-acquired infections, is a major health problem worldwide. Particularly, an attention has been focused on the multiple resistant pathogen i.e., *E. coli*, *K. pneumoniae* and methicillin-resistant *Staphylococcus aureus* (MRSA) (48, 88).

Currently, *P. aeruginosa* which is the common cause of nosocomial infection has been reported to generate multidrug resistance because of its biofilm synthesis (89). *K. pneumoniae* was found to be a causative agent of pneumonia, and a pathogen of septicemia in patients (90). The spread of *K. pneumoniae* carbapenemase (KPC) emerged in many countries has been reported (91).

There are many drug-resistant strains found in gram positive bacteria such as MRSA, vancomycin-resistant Enterococci (VRE) and penicillin-resistant *S. pneumoniae* (PRSP), and in gram negative bacteria i.e., extended spectrum β-lactamase (ESBL), AmpC β-lactamase and carbapenemase-producing Enterobacteriaceae (CPE) (87). ESBLs are enzymes capable of hydrolysing penicillins, broad spectrum cephalosporin and monobactams, and are generally derived from TEM and SHV-type enzymes (92). ESBL producing organisms are *K. pneumoniae*, *P. aeruginosa*, *E. coli*, *P. stutzeri*, *S. typhimurium* and *C. fruendii* (88, 92).

Interestingly, 2TU-8HQ metal complexes (**1**-**3**) exerted the activity against resistant gram positive (*S. aureus*) and gram negative ESBL (*E. coli*, *S. typhimurium*, *P.*

stutzeri and *C. fluendii*) bacteria. The higher activity against gram positive bacteria was noted for Mn (**3**) complex, and against gram negative bacteria was noted for Cu (**2**) complex. The results implied the potential of Cu (**2**) and Mn (**3**) complexes as antimicrobials for resistant *S. aureus* and ESBL producing organisms, respectively. On the other hand, the strongest antioxidant (SOD) activity was noted for 2TU-2HQ Cu complex (**5**) with IC_{50} of 1.81 μM.

The strongest SOD activity was noted for metal complex of 2TU-2HQ ligands compared with 2TU-8HQ metal complexes. It could be suggested that an inductive effect of both ligands, 2TU (4-oxo function) and 2HQ (2-oxo moiety), can withdraw electrons from the Cu centered atom (compound **5**) and facilitate the superoxide scavenging activity (5). In case of 2TU-8HQ, the inductive effect was resulted from one ligand (2TU) using 4-oxo group (compounds **1** and **3**), and using 2-thioimine moiety conjugated with α, β-unsaturated keto (compound **2**) as the superoxide scavenger. Metal complexes with the same ligands, but different metal ions would provide the compounds with different bioactivity (93) as seen for compounds **1**-**3** (**3>2>1**) and compounds **4**-**6** (**5>4>6**). In a series of 2TU-8HQ (**1**-**3**), Mn complex (**3**) afforded the strongest SOD activity (IC_{50} = 5.04 μM), whereas 2TU-2HQ Mn complex (**6**) displayed the lowest SOD activity (IC_{50} = 516.56 μM). Besides the property of ligands, metal centered atom also played important role in bioactivities of metal complexes [23]. Cu is essential for SOD activity (8), therefore, an incorporation of Cu into the ligand structures (2TU and 2HQ) increased the SOD activity as observed for Cu complex **5**. This is due to the change in oxidation state of Cu atom modulated through its coordination with metal chelating ligands (7).

However, dissociation of the metal complexes (**1**-**6**) could give rise to 1:1 charged complexes, $(8HQ\text{-}M)^+$ and $(2HQ\text{-}M)^+$, and free ligand (2TU) (94). The charged complexes ($(8HQ\text{-}M)^+$ and $(2HQ\text{-}M)^+$) became toxic entity by interacting and blocking the metal binding sites on enzymes that involved in the pteridine biosynthesis [50]. This can account for antimicrobial activity of complexes **1**-**3** compared with complexes **4**-**6**. It is possibly due to $(8HQ\text{-}M)^+$ of metal complexes **1**-**3** bearing 8HQ with the antimicrobial effect. Inversely, 2HQ was inactive compound, thus, metal complexes **4**-**6** exerted no antimicrobial activity.

In summary, novel metal (Ni, Cu, Mn) complexes of 2TU-8HQ (**1**-**3**) and 2TU-2HQ (**4**-**6**) were synthesized and investigated for antimicrobial and antioxidant (DPPH and SOD) activities. These metal complexes contanined 2TU as a common ligand, but different 8HQ or 2HQ ligands. These metal complexes exerted SOD activity, particularly, Cu complex **5** bearing 2HQ displayed the strongest SOD activity with IC_{50} of 1.81 μM. The Mn complex **3** bearing 8HQ exhibited good antimicrobial activity against gram-positive and gram negative bacteria as well as diploid fungus with MIC of 11.07-708.64 μM. This finding revealed the novel bioactive mixed ligand transition metal complexes with SOD-mimic and antimicrobial activities, and has a potential for further development as medicinal compounds.

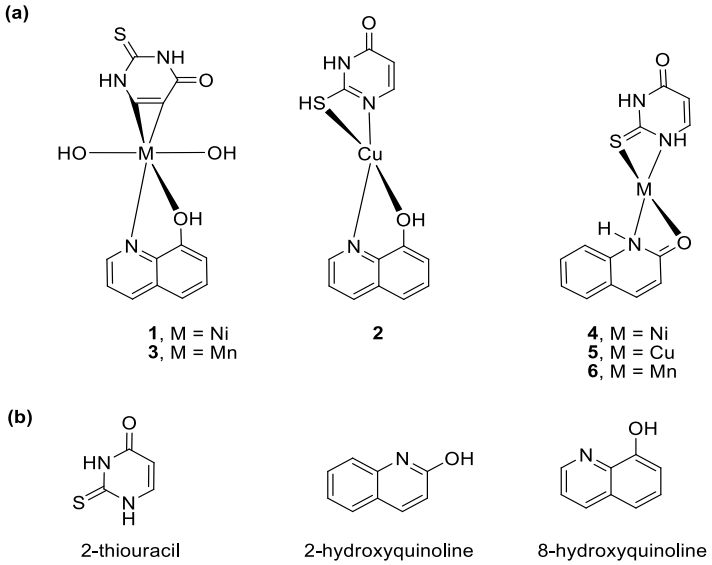

Figure 4.1. Chemical structures of 2-thiouracil-hydroxyquinolines metal complexes **1**-**6** (a) and ligands (b).

Table 4.1 IR spectra (cm^{-1}) and μ_{ef} (B.M) of 2-thiouracil-hydroxyquinolines metal complexes (**1-6**).

Compound	νC=O	νC=N	νC=S	νC-O	νC-N	νOH	νNH	δOH	δNH	μ_{eff}
2-TU-Ni-8HQ	1701s	1629vw	1424s	1285m	1388m	3358s,br	3196br	1470s	1560m, br	2.70
(**1**)	1686s	1578s		1214s	1374s		3087sh, br		745s	
				1111s						
2-TU-Cu-8HQ	1693s	1625m	——	1280m	1386s	——	3178w, br	1464s	1527w	1.315
(**2**)		1575m		1113s	1375s				741m	
2-TU-Mn-8HQ	1702s	1629w	1422s	1281w	1388s	3400br	3192sh, br	1466s	1562s	3.40
(**3**)	1686s	1572s		1213s	1368w		3135sh, br		743m	
				1108m						
2-TU-Ni-2HQ	1701s, br	1628s, br	1425s	1216s	1395s	——	3122s, br	1451s	1558w, br	0.953
(**4**)	1682s, br	1600vw, sh		1177s, br					1539w, br	
	1654s, br			1153s, br					761s	
2-TU-Cu-2HQ	1692m	1638s	1428s	1202m	1396w	——	3124w, sh	1449w	1559w	0.807
(**5**)	1654s	1601m		1171w					1543w	
				1153w					756s	
2-TU-Mn-2HQ	1701m	1637s	1428s	1214s	1396m	——	3126w, sh	1469m	1559s	0.794
(**6**)	1684m	1601m		1175w					758s	
	1654s			1154w						
2-TU	1700s	1628m	1421s	1214s	1394m	3510br	3086br	1450m	1560s	——
	1684s			1176s			3048br		761s	
				1158s						
2HQ	1652s, br	1599s, br	——	1213s	1381s	——	3255w, sh	1428s	1554s	——
				1154m					759vs	
				1135s						
8HQ	——	1580m	——	1286s	1381s	3145br	——	1410s	——	——

Note: 2-TU = 2-thiouracil, 2HQ = 2-hydroxyquinoline, 8HQ = 8-hydroxyquinoline, br = broad, m = medium, s = strong, sh = sharp, vs = very strong, vw = very weak and w = weak.

Table 4.2 Antioxidant activities of 2-thiouracil-hydroxyquinolines metal complexes (**1**-**6**) and ligands.

Compound[a]	Radical scavenging activity (IC_{50}, μM)	Superoxide scavenging activity (IC_{50}, μM)
2-TU-Ni-8HQ (**1**)	171.31	15.73
2-TU-Cu-8HQ (**2**)	388.56	10.06
2-TU-Mn-8HQ (**3**)	ND	5.04
2-TU-Ni-2HQ (**4**)	ND	69.07
2-TU-Cu-2HQ (**5**)	194.25	1.81
2-TU-Mn-2HQ (**6**)	ND	516.56
2TU	ND	ND
2HQ	ND	ND
8HQ	1113.75	91.83

[a] Vitamin E was used as a control for DPPH assay displaying IC_{50} = 1.40 μM, [b]superoxide dismutase (SOD) from bovine erythrocytes was used as a control for SOD assay showing IC_{50} = 0.021 μM. Complexes **3**, **4**, **6** and ligands (i.e., 2TU and 2HQ) exhibited RSA <50% at 300 μg/mL (24.56%, 34.92%, 21.68%, 33.00% and 10.10%, respectively). The 2TU and 2HQ showed SOD activity <50% at 300 μg/mL (28.70% and 25.19%, respectively). ND = not determined.

Table 4.3 Antimicrobial activity of 2-thiouracil-hydroxyquinolines metal complexes (**1**-**6**) and ligands.

Compound	MIC (μM)[a]	Microorganism[b]
2-TU-Ni-8HQ (**1**)	701.35	*S. aureus* ATCC 29213, *S. aureus* ATCC 25923, *E. faecalis* ATCC 29212, *E. faecalis* ATCC 33186,
		M. luteus ATCC 10240, *B. subtilis* ATCC 6633, *C. diphtheriae* NCTC 10356, *B. cereus, C. fluendii*
	350.67	*S. epidermidis* ATCC 12228, *P. shigelloides*
2-TU-Cu-8HQ (**2**)	757.70	*S. putrefaciens* ATCC 8071, *M. morganii*
	378.85	*E. coli* ATCC 25922, *S. macesens* ATCC 8100, *S. typhimurium* ATCC 13311,*C. fluendii*
	189.43	*S. cerevisiae* ATCC 2601, *A. hydrophila*
	94.71	*S. aureus* ATCC 25923, *E. faecalis* ATCC 29212, *E. faecalis* ATCC 33186, *M. luteus* ATCC 10240,
		C. diphtheriae NCTC 10356, *B. cereus, L. monocytogenes*
	47.36	*S. aureus* ATCC 29213, *B. subtilis* ATCC 6633,
	23.68	*S. epidermidis* ATCC 12228, *P. shigelloides*
2-TU-Mn-8HQ (**3**)	708.64	*E. coli* ATCC 25922, *P. stutzeri* ATCC 17587, *S. putrefaciens* ATCC 8071,
		A. xylosoxidans ATCC 27061, *M. luteus* ATCC 10240, *C. fluendii*
	354.32	*S. dysenteriae*
	88.56	*S. cerevisiae* ATCC 2601
	44.29	*E. faecalis* ATCC 29212, *E. faecalis* ATCC 33186, *B. subtilis* ATCC 6633,
		C. diphtheriae NCTC 10356, *B. cereus, L. monocytogenes*
	22.15	*S. aureus* ATCC 29213, *S. aureus* ATCC 25923, *S. epidermidis* ATCC 12228

Table 4.3 Antimicrobial activity of 2-thiouracil-hydroxyquinolines metal complexes (**1**-**6**) and ligands (cont.)

Compound	MIC (μM)[a]	Microorganism[b]
	≤11.07	*P. shigelloides*
2-TU-Ni-2HQ (**4**)	Inactive	-
2-TU-Cu-2HQ (**5**)	Inactive	-
2-TU-Mn-2HQ (**6**)	Inactive	-
2-TU	1997.62	*M. luteus* ATCC 10240
2HQ	Inactive	-
8HQ	1763.60	*P. aeruginosa* ATCC 15442
	440.90	*K. pneumoniae* ATCC 700603, *S. choleraesuis* ATCC 10708*, M. morgamii*
	220.45	*E. coli* ATCC 25922, *S. macesens* ATCC 8100, *S. typhimurium* ATCC 13311, *P. stutzeri* ATCC 17587, *S. putrefaciens* ATCC 8071, *A. xylosoxidans* ATCC 27061, *S. enteridis*, *C. fluendii*
	110.22	*A. hydrophila*
	55.11	*M. lutens* ATCC 10240
	≤27.56	*S. aureus* ATCC 29213, *S. aureus* ATCC 25923, S. *epidermidis* ATCC 12228, *E. faecalis* ATCC 29212, *E. faecalis* ATCC 33186, *B. subtilis* ATCC 6633, C*. diphtheriae* NCTC 10356, *S. cerevisiae* ATCC 2601, *C. albicans* ATCC 90028, *S. dysenteriae, B. cereus*, *P. shigelloides, L. monocytogenes*

[a]MIC : Minimum inhibitory concentration is the lowest concentration of a compound to inhibit growth of microorganisms. [b]Ampicillin at 26.93 μM was used as a control of antimicrobial testing system that showed growth inhibiton against *S. typhimurium* ATCC 13311, *P. stutzeri* ATCC 17587, *C. diphtheriae* NCTC 10356, *S. aureus* ATCC 29213, *S. aureus* ATCC 25923, *S. epidermidis* ATCC 12228, *M. luteus* ATCC 10240, *B. subtilis* ATCC 6633, *L. monocytogenes* and *P. shigelloides.*

CHAPTER V
ANTIOXIDANT AND CYTOTOXIC ACTIVITIES OF COPPER COMPLEXES OF SULFONAMIDE ANALOGS

5.1 Abstract

Copper (Cu) complexes (**7**-**16**) of 4-substituted (NO_2, OCH_3, CH_3 and Cl) benzenesulfonamide of anthranilic acid were synthesized and determined for antioxidant, antimicrobial and cytotoxic activities. The Cu complexes **7**-**16** exhibited antioxidant activity with IC_{50} of 0.062-0.152 μM and cytotoxic activity against MOLT-3 cell lines with IC_{50} of 21.60-28.92 μM. Particularly, complex **10** (sulfonamides with NO_2 and Cl groups) showed the strongest SOD activity as IC_{50} of 0.062 μM, whereas complex **16** (sulfonamide with Cl group) displayed the best cytotoxicity as IC_{50} of 21.60 μM against MOLT-3 cell lines. Furthermore, the function groups of Cu-sulfonamide complexes such as NO_2 and Cl have influence for their biological activities interacting with target which displayed good bioactive compounds. The finding reveals novel Cu-sulfonamide complexes with a potential compounds for further development for medicinal applications.

5.2 Introduction

Free radicals are defined as unstable molecules having unpaired electron (68, 95). It has been associated with development of various diseases such as cancer, diabetes mellitus, cardiovascular disease, aging and neurodegenerative diseases (67). Antioxidant systems in human are used to protect free radicals that occur inside the body including enzymatic system such as superoxide dismutase (SOD), catalase and glutathione peroxidase, and non-enzymatic system from supplemental nutrition (69, 96). Furthermore, transition metal ions (i.e., manganese (Mn), cobalt (Co), nickel (Ni), copper (Cu) and zinc (Zn)) are essential elements to help catalytic reaction working with enzymes/protein as call as metalloprotein such as found in SOD enzyme (2, 97). The development and discovery of novel compounds has been interested as used as treatment and prevention of progression of free radical-related diseases. Based on correlation between metal ions with enzyme, the mimic compound coordinated with transition metal ions have been synthesized for exerting interesting pharmacological activities. Particularly, mimic compounds (SOD-mimic) using

metal ions with ligands having atoms coordination which has been synthesized of metal complexes displaying a variety of biological activities. Interestingly, Copper is considered as an essential element of several endogenous antioxidant enzymes, therefore, using transition copper ions have been attractive target metal ion (98). Cu complexes of nicotinic with aromatic carboxylic acids (i.e., phthalic, salicylic and anthranilic acids) have been shown of antioxidant (SOD) and antimicrobial activities (7) as well as Cu complexes with pyridine derivatives (i.e., nicotinic acid, 2-hydroxypyridine, 2-aminopyridine and picolinic acid) (8). Furthermore, nicotinic acid-copper complex prevent gastric congestion (99), reduce lipids, control levels of liver enzymes and lipid peroxidation (100), and nicotine-copper complexes showed SOD-like antioxidant properties for Alzheimer's disease (101).

Sulfonamide is an important pharmacophore found in many drugs and bioactive compounds. Its derivatives exhibited various biological activities such as antimicrobial (50), anticancer (51) and antiviral (52) properties. Considering the sulfonamide structure containing aromatic ring, sulphonamide ($-SO_2NH_2$) and functional groups (R). It is interesting to structural modification as use as the ligand to form metal complexes having pharmacological properties. Sulfonamide derivatives were used as a ligand to coordinate with metal ions (i.e., moononuclear complexes of 5-chloro-2-hydroxybenzylidene)aminobenzenesulfonamides with various metal ions (Co, Cu, Zn, Ni and Mn) (53) and Cu complexes of *N*-substituted sulfonamides (54)). It has found that metal complexes of sulfonamide derivatives exhibited biological activities such as anti-*Trypanosoma cruzi* activity (53), DNA cleavage and cytotoxic activities (54).

Anthranilic acid is a scaffold to be attracted great interest which was synthesized and displayed anticancer (102), antioxidant (103) and antimicrobial activities (104). Furthermore, 4-substitueted benzenesulfonamide of anthranilic acid were synthesized and exhibited antifungal, antioxidant and anticancer activities (105).

Therefore, this present study aims to synthesize of copper complexes (**7-16**) of 4-substitueted benzenesulfonamide of anthranilic acid (ligands 1-4) and determine their biological activities including antioxidant, antimicrobial and cytotoxic activities. In addition, structure-activity relationship has been provided to insight into influence of function groups in their activities.

5.3 Materials and methods

5.3.1 General

Infrared (IR) spectra were obtained on a Perkin Elmer System 2000 FTIR. Mass spectra were recorded on a Finnigan INCOS50 and a Bruker Daltonics (Micro TOF).

Magnetic moment was performed on a Magnetic Susceptibility Balance, Mark 1, Serial 15257, Sherwood Scientific, Cambridge, UK. Melting points were determined on an Electrothermal melting point apparatus and are uncorrected. Chemicals and reagents were analytical grade included RPMI-1640 (Rosewell Park Memorial Institute medium from Gibco and Hyclone laboratories, USA; MTT (3(4,5-dimethylthiazol-2-yl)-2,5-diphenyltetrazolium bromide), XTT (2,3-bis-(2-methoxy-4-nitro-5-sulfophenyl)-2H-tetrazolium-5-carboxanilide salt), HEPES (*N*-2-hydroxyethylpiperazine-*N*′-2-ethanesulfonic acid), nitroblue tetrazolium (NBT) salt, L-methionine, riboflavin, Triton-100, superoxide dismutase (SOD) from bovine erythrocytes, DMSO (dimethyl sulfoxide, 99.9%), ampicillin, ciprofloxacin, tetracycline, L-glutamine, penicillin, streptomycin, sodium pyruvate and glucose from Sigma, USA; Müeller Hinton Broth and Müeller Hinton Agar from Becton Dickinson, USA and sodium chloride from Merck, German. from Sigma, USA; Ham's/F12 (Nutrient mixture F-12), DMEM (Dulbecco's Modified Eagle's Medium) and FBS (fetal bovine serum) from Hyclone laboratories, USA and gentamicin sulfate from Government Pharmaceutical Organization, Thailand.

5.3.2 Synthesis of copper-sulfonamide complexes (7-16)

The 4-substitueted benzenesulfonamide of anthranilic acid (ligands 1-4: l1-l4) were synthesized by Doungsoongnuen et al. (105) which functional groups (R = NO_2, OCH_3, CH_3 and Cl) were substituted on benzenesulfonamides at position 4 (Figure 5.1). It was used as ligands for coordinated with copper (Cu). Cu complexes of sulfonamide ligands (l1 – l4) were further synthesized. The solid products were collected by filtration and dried at room temperature.

A solution of metal salts (1 mmol) dissolved in methanol (2 mL) was added dropwise to the solution of ligands (1 mmol) in 70°C methanol (30 mL) and then heated for 45 min. A solution of ligands (1 mmol) in methanol (2 mL) was added dropwise to the reaction mixture and further heated for 1 h. The precipitated solid was collected by filtration, washed 4-5 times with cold methanol and dried *in vacuo* at room temperature. Complexes **7-16** were produced from 1 mmol of ligands (l1-l4) and 1 mmol of $Cu(OAc)_2 \cdot H_2O$. Chemical structures and characterization of Cu complexes were determined using IR, ^{1}H NMR and mass spectra and magnetic moment.

5.3.3 Biological activities

Metal complexes (**7**-**16**) were determined for their biological activities composed of antioxidant, antimicrobial and cytotoxic activities.

5.3.3.1 Antioxidant activity

The transition metal complexes were evaluated for their antioxidant activity using 2 superoxide dismutase (SOD) assays (81). The SOD assay was performed by mixed 1 mL of solution (27 mL of HEPES buffer (50 mM, pH 7.8), 1.5 mL of L-methionine (30 mg/mL), 1 mL of nitro blue tetrazolium (NBT, 1.41 mg/mL) and 0.75 mL of Triton X-100 (1 wt%)) to 0.45 mL solution of a tested compound to a final concentration of 300 µg/mL. The reaction was initiated by adding10 µL of riboflavin (44 µg/mL) and was excited under a Philips Classic Tone lamp (60 W) in a light box for 7 min. The absorbance at 550 nm was measured of the photoreduction of NBT using UV–Vis spectrophotometer and the percentage of SOD activity will be calculated using equation (1).

$$\%\text{Inhibition} = \left(1 - \frac{Abs._{sample}}{Abs._{control}}\right) \times 100 \quad (1)$$

where $Abs._{control}$ is the absorbance of the control reaction, and $Abs._{sample}$ is the absorbance of the tested compound. Superoxide dismutase (SOD) from bovine erythrocytes was used as a control.

In addition, IC_{50} (50% inhibition concentration of radical and superoxide-scavenging activities) was performed in which tested complexes at 300 µg/mL displayed antioxidant activities more than 50% inhibition.

5.3.3.2 Antimicrobial activity

The metal complexes were determined of antimicrobial activity using agar dilution method (82). The compounds were individually dissolved in DMSO. The two-fold dilution was performed using Muller Hinton (MH) broth which was transferred to MH agar solution to obtain the final concentrations of 256 to 4 mg/mL. In addition, the MH Broth, DMSO, ampicillin, ciprofloxacin and tetracycline drugs were used as the control. Microorganisms were cultured in MH broth at 37°C for 24 h and diluted with 0.9% normal saline solution to adjust the cell density of 1×10^{8} CFU/mL compared to 0.5 McFarland standards. Then, microorganisms were inoculated onto each plate of tested compound with various concentrations using a multipoint inoculators and further

incubated at 37°C for 24-48 h. The inhibition of microbial cell growth as well as the minimum inhibitory concentration (MIC as the lowest concentration to inhibit the growth of microorganisms) of the compounds was determined. Twenty-seven strains of microorganisms composed of reference strain and clinical isolates as following: **gram positive bacteria**: *Staphylococcus aureus* ATCC 29213, *Staphylococcus aureus* ATCC 25923, *Staphylococcus epidermidis* ATCC 12228, *Enterococcus faecalis* ATCC 29212, *Enterococcus faecalis* ATCC 33186, *Micrococcus luteus* ATCC 10240, *Corynebacterium diphtheriae* NCTC 10356, *Bacillus subtilis* ATCC 6633, *Streptococcus pyogenes*, *Listeria monocytogenes*, *Bacillus* cereus; **gram negative bacteria**: *Escherichia coli* ATCC 25922*, Klebsiella pneumoniae* ATCC 700603, *Serratia macescens* ATCC 8100, *Salmonella typhimurium* ATCC 13311, *Shewanella putrefaciens* ATCC 8071, *Achromobacter xylosoxidans* ATCC 2706, *Pseudomonas aeruginosa* ATCC 15442, *Pseudomonas stutzeri* ATCC 17587, *Shigella dysenteriae*, *Salmonella enteritidis*, *Morganella morganii*, *Aeromonas hydrophila*, *Citrobacter freundii*, *Plesiomonas shigelloides* and **diploid fungus (yeast)**: *Candida albicans* ATCC 90028, *Saccharomyces cerevisiae* ATCC 2601.

5.3.3.3 Cytotoxicity

Cytotoxicity of the metal complexes (**7**-**16**) was determined against four human cancer cell lines composed of hepatocellular carcinoma (HepG2), cholangiocarcinoma (HuCCA-1), lung carcinoma (A549) and T-lymphoblast (MOLT-3, acute lymphoblastic leukemia) cell lines. The cancer cells including HuCCA-1 and A549 cells were grown in Hamm's/F12 medium containing L-glutamine (2 mM) supplemented with 100 U/mL penicillin-streptomycin and FBS (10%); MOLT-3 cells were grown in RPMI-1640 medium containing L-glutamine (2 mM), 100 U/mL penicillin-streptomycin, sodium pyruvate, glucose and 10% FBS; and HepG2 cells were grown in DMEM medium containing 100 U/ mL penicillin-streptomycin and 10% FBS. The assay was performed using the cell lines suspended in RPMI-1640 containing 10% FBS, which contained a density of 5×10^{3}-2×10^{4} cells per well in a 96-well plate (Costar No. 3599, USA). The cells were then incubated at 37^{o}C under a humidified atmosphere with 95% air and 5% CO_2 for 24 h. The tested compound and controls was added to the desired final concentrations. The plates were incubated for 48 h. Cell viability was determined by staining with MTT for adherent cell (A549, HuCCA-1 and HepG2 cells) [38-39], and with XTT [40] assay for suspended cell (MOLT-3 cells). The plates were read on a micro-plate reader (Molecular Devices, USA) and the absorbance was measured at 550

nm. Furthermore, the IC_{50} values of the compound or drug concentration that provided 50% cell growth inhibition were performed. Doxorubicin and/or etoposide were used as reference drugs (4, 106).

5.4 Results and discussion

5.4.1 Chemistry

The Cu complexes structures (**7-16**) were synthesized and IR spectra of the complexes were analyzed. It was shown (Table 5.1) that the Cu-sulfonamide complexes were successfully synthesized which compared to their ligands (l1-l4). The chemical structures of ligands and complexes (**7-16**) were displayed in Figure 5.1. In addition, characteristics of Cu-sulfonamide complexes (**7-16**) composed of %yield and melting point of the complexes were shown in Table 5.2

5.4.2 Antioxidant activity

The metal complexes **7-16** were determined of antioxidant activity using SOD assays. It was found (Table 5.3) that all metal complexes (**7-16**) exhibited antioxidant activity in IC_{50} range of 0.062-0.152 μM. Complex **10** showed the strongest SOD activity (IC_{50} of 0.062 μM) compared with other complexes. Considering complexes **7-16** having 4-substitued benzenesulfonamide of NO_2, OCH_3, CH_3 and Cl. It was observed that form coordinated with the same ligands showed low SOD activity than with different ligands, for example, complex **10** contained ligand 1 (NO_2) and ligand 4 (Cl) with IC_{50} of 0.062 μM and complex **7** consisted of ligand 1 (NO_2) and ligand 1 (NO_2) with IC_{50} of 0.152 μM as well as in complexes **8** (IC_{50} of 0.074 μM) and **9** (IC_{50} of 0.076 μM). This phenomenon displayed the fashion in the ligands 2, 3 and 4 which used to coordinate with Cu ion such as complexes **11, 14** and **16** having low antioxidant activity of IC_{50} as 0.076, 0.104 and 0.121 μM compared with other complexes **12**, **13** and **15** having IC_{50} of 0.077, 0.075 and 0.077 μM, respectively, coordinated using different ligands. It was implied that ligand with different functional groups in metal complexes have effect for antioxidant activity. The ligands (l1-l4) reported weak antioxidant activity which ligands 2 and 4 have 15.7% of SOD activity at 300 μg/mL, respectively whereas ligands 1 and 3 were no activity (7, 8). This activity also depended on the asymmetric charge localization in the complexes. It was observed that high asymmetric charge exhibited high SOD activity (22). Furthermore, Cu complexes displayed high antioxidant (SOD) activity (5, 7, 8).

In addition, anthranilic acid was used as a ligand for coordination with Cu and nicotinic acid. This complexes displayed good SOD activity in IC_{50} of 47.49 μM whereas free antranilic acid has IC_{50} >236.25 μM (8). This evidence was also found that Cu complexes of benzenesulfonamide of anthranilic acid exhibited good antioxidant activity than its free ligands.

5.4.3 Antimicrobial activity

The Cu-sulfonamide complexes (**7**-**16**) were investigated of antimicrobial activity using agar dilution method. The results showed that all metal complexes had no antimicrobial activity. Previous studied, sulfonamide ligands showed antimicrobial activity against *C. albicans* ATCC 90028 (25-50 %) at 4 μg/mL (105). It was found that these effects may be depended on functional groups and position substituent on benzenesulfonamide. However, metal complexes using ligands (l1-l4) were inactive.

5.4.4 Cytotoxic activity

The Cu-sulfonamide complexes (**7**-**16**) were determined of cytotoxic activity against four cancer cell lines using MTT and XTT assays. It was found that compounds **7**-**16** displayed cytotoxic activity for MOLT-3 cells, whereas had no activity for HepG2, HuCCA-1 and A549 as shown in Table 5.4. Interestingly, complex **16** (l4-l4) exhibited the strongest cytotoxicity (IC_{50} of 21.60 μM) than other complexes (IC_{50} range of 23.31-28.92 μM), on the other hand, free ligand displayed low cytotoxic activity than its complexes (Table 5.4). Although, free ligand 1 with NO_2 substituted at 4-position on benzenesulfonamide has been reported of highest cytotoxicity (Table 5.4) than free ligands 2 (OCH_3), 3 (CH_3) and 4 (Cl), but Cu complexes with these ligands displayed good cytotoxic activity than free ligand (Table 5.4). Interestingly, ligand 2 with OCH_3 has been reported as inactive compounds (105), after used as ligand coordinated with Cu, the complexes (**8** and **11**-**13**) showed cytotoxic activity against MOLT-3 cells. Both free ligands and its complexes exhibited selectively MOLT-3 cells. In addition, it has found that Cu complex (5Nu-Cu-8HQ) exerted most potent cytotoxic activity than other metal complexes (5).

In summary, copper-sulfonamide complexes (**7**-**16**) were synthesized and determined of antioxidant, antimicrobial and cytotoxic activities. All complexes displayed antioxidant and cytotoxic properties. Interestingly, complex **10** (coordinated with l1 (NO_2) and l4 (Cl) and Cu ion) exhibited the strongest SOD activity with IC_{50} of 0.062 μM and complex **16** (coordinated with l4 (Cl) showed the best cytotoxic activity with IC_{50} of 21.60 μM. Furthermore, the effect of biological activities was depended on functional groups that substituted on benzenesulfonamide of anthranilic acid. This finding demonstrated that Cu-sulfonamide complexes exhibited SOD-like activity and cytotoxic activity, and could be potential for further development as medicinal compounds.

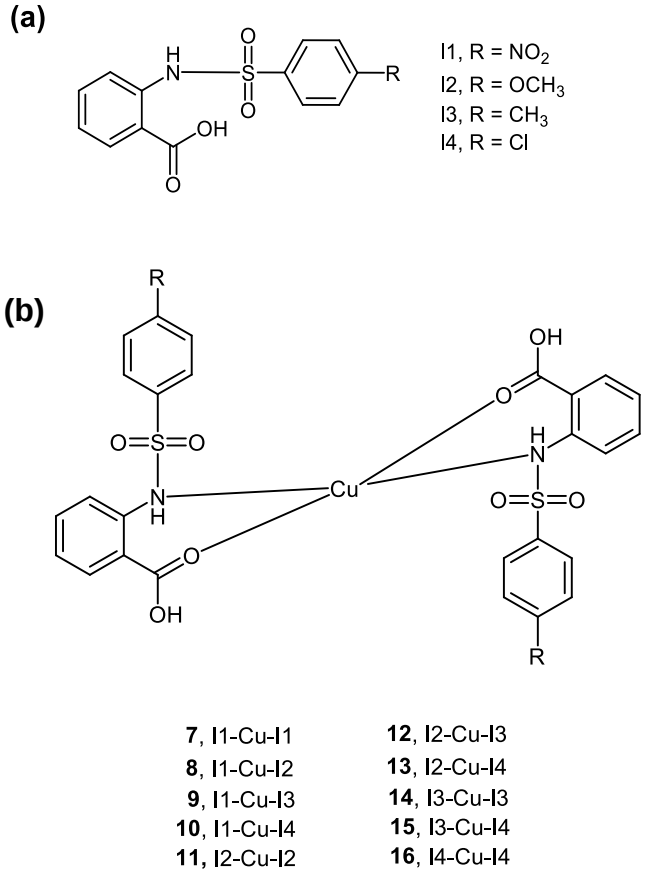

7, I1-Cu-I1
8, I1-Cu-I2
9, I1-Cu-I3
10, I1-Cu-I4
11, I2-Cu-I2
12, I2-Cu-I3
13, I2-Cu-I4
14, I3-Cu-I3
15, I3-Cu-I4
16, I4-Cu-I4

Figure 5.1. Chemical structures of ligands (a) and Cu-sulfonamide complexes (**7**-**16**) (b)

Table 5.1 IR spectra (cm^{-1}) and μ_{eff} (B.M) of copper complexes of sulfonamide analogs (**7**-**16**).

Compound	νO-H	νC-O	νSO_2	νNO_2	νN-H	νC-N	νS-N	νC=O	δO-H	δN-H	μ_{eff}
SA01-Cu-SA01 (**7**)	3475m, br	1091m, sh	1314m 1164vs	1531s 1394vs	—	1276s	945s	—	1394s, sh	—	0.82
SA01-Cu-SA02 (**8**)	3448s, br	1093s 1024w	1161s	1534s 1350s	—	1274m	938s, br	—	1396vs	—	0.80
SA01-Cu-SA03 (**9**)	3449s, br	1091s	1163vs	1534s 1350s	—	1274m	941m, br	—	1396vs	—	0.80
SA01-Cu-SA04 (**10**)	3450s, br	1093s	1161vs	1534s 1350s	—	1274s	941m, br	—	1396vs	—	0.84
SA02-Cu-SA02 (**11**)	3471m, br	1096s 1025m	1330m, br	—	—	1264s	931s, br	—	1397s	—	0.79
SA02-Cu-SA03 (**12**)	3449s, br	1093m 1024vw	1156s	—	—	1267m	934w, br	—	1396s	—	0.54
SA02-Cu-SA04 (**13**)	3449m, br	1093s 1024w	1332w 1156vs	—	—	1274s	938m, br	—	1396vs	—	0.82
SA03-Cu-SA03 (**14**)	3554s, sh 3493m, sh	1090s	1331m 1169s	—	—	1268s	927s	—	1394vs	—	0.93
SA03-Cu-SA04 (**15**)	3448s, br	1094s	1334m 1158vs	—	3181w, br	1275s	936s, br	—	1396vs	—	0.82
SA04-Cu-SA04 (**16**)	3465m, br	1095s	1335m 1159s	—	—	1279s	937s, br	—	1396vs	—	0.69
SA01	3449m, br	1086s	1318m 1162vs	1531vs 1349s	3196m, sh	1264s	926s	1665s	1393m, sh	1582m 758s	—
SA02	3492m, br	1092s 1022s	1344m 1160s	—	3202s, sh	1261s	926s	1678s	1389s	1581s 754s	—
SA03	3449w, br	1089s	1342s 1162s	—	3201	1258s	922s	1675s	1389m	1585m 754s	—
SA04	3442w, br	1093s	1342s 1164s	—	3188w, sh	1261m	929s	1662s	1380m	1585s 753s	—

Note: br = broad, m = medium, s = strong, sh = sharp, vs = very strong, vw = very weak and w = weak.

Table 5.2 Characteristics of Cu-sulfonamide complexes (**7**-**16**).

Compound	%Yield	mp (°C)
SA01-Cu-SA01 (**7**)	86	270-275
SA01-Cu-SA02 (**8**)	47	270-275
SA01-Cu-SA03 (**9**)	40	270-275
SA01-Cu-SA04 (**10**)	55	265-270
SA02-Cu-SA02 (**11**)	57	265-272
SA02-Cu-SA03 (**12**)	5	272-276
SA02-Cu-SA04 (**13**)	21	270-275
SA03-Cu-SA03 (**14**)	40	270-275
SA03-Cu-SA04 (**15**)	14	270-282
SA04-Cu-SA04 (**16**)	43	270-275

Table 5.3 Antioxidant activity (SOD) of Cu-sulfonamide complexes (**7**-**16**).

Compound[a]	SOD (IC_{50}, μM)[b]
SA01-Cu-SA01 (**7**)	0.152
SA01-Cu-SA02 (**8**)	0.074
SA01-Cu-SA03 (**9**)	0.076
SA01-Cu-SA04 (**10**)	0.062
SA02-Cu-SA02 (**11**)	0.076
SA02-Cu-SA03 (**12**)	0.077
SA02-Cu-SA04 (**13**)	0.075
SA03-Cu-SA03 (**14**)	0.104
SA03-Cu-SA04 (**15**)	0.077
SA04-Cu-SA04 (**16**)	0.121

[a]SA01 and SA04 showed antioxidant activity of 15.7% and 6.07%SOD, respectively at 300 μg/mL. SA02 and SA04 were no antioxidant activity at 300 μg/mL (105).

[b]Superoxide dismutase (SOD) from bovine erythrocytes was used as a control in SOD assay (IC_{50} = 0.013 μM).

Table 5.4 Cytotoxic activity of Cu-sulfonamide complexes (**7**-**16**).

Compound	IC_{50} (μM)[a]			
	MOLT-3	HuCCA-1	A549	HepG2
SA01-Cu-SA01 (**7**)	25.43±1.02	Inactive	Inactive	Inactive
SA01-Cu-SA02 (**8**)	25.84±0.33	Inactive	Inactive	Inactive
SA01-Cu-SA03 (**9**)	27.62±0.68	Inactive	Inactive	Inactive
SA01-Cu-SA04 (**10**)	27.11±1.23	Inactive	Inactive	Inactive
SA02-Cu-SA02 (**11**)	28.64±0.40	Inactive	Inactive	Inactive
SA02-Cu-SA03 (**12**)	28.92±0.62	Inactive	Inactive	Inactive
SA02-Cu-SA04 (**13**)	26.21±1.13	Inactive	Inactive	Inactive
SA03-Cu-SA03 (**14**)	26.08±1.13	Inactive	Inactive	Inactive
SA03-Cu-SA04 (**15**)	23.31±18.00	Inactive	Inactive	Inactive
SA04-Cu-SA04 (**16**)	21.60±1.79	Inactive	Inactive	Inactive
SA01[b]	48.74±2.17	Inactive	Inactive	Inactive
SA02[b]	Inactive	Inactive	Inactive	Inactive
SA03[b]	112.86±6.01	Inactive	Inactive	Inactive
SA04[b]	108.94±6.61	Inactive	Inactive	Inactive
Etoposide	0.04±0.01	-	-	26.62±1.95
Doxorubicin	-	0.42±0.15	0.24±0.15	0.98±0.11

[a] The assay was performed in triplicate; doxorubicin and/or etoposide was used as reference drugs.

[b] from (105).

MOLT-3: acute lymphoblastic leukemia cell line, HuCCA-1: human cholangiocarcinoma cancer cell, A549: human lung carcinoma cell line and HepG2: human hepatocellular carcinoma cell line.

CHAPTER VI

TOWARDS THE DESIGN OF 3-AMINOPYRAZOLE PHARMACOPHORE OF PYRAZOLOPYRIDINE DERIVATIVES AS A NEW ANTIOXIDANTS

6.1 Abstract

Free radicals and oxidants can cause oxidative damage to physiologically important biomolecules that subsequently leads to the development of a wide range of chronic and degenerative diseases such as aging, cancer, cardiovascular and neurodegenerative diseases. Antioxidants have been shown to be instrumental in counteracting the deleterious effects of these reactive oxygen species. Herein, a series of 20 pyrazolopyridine derivatives with antioxidant activity were utilized for constructing a quantitative structure-activity relationship (QSAR) model as to unravel the origins of the antioxidant activity. Quantum chemical and molecular descriptors were used to quantitate the physicochemical properties of investigated compounds. Significant descriptors as identified by stepwise regression analysis consisted of Mor11m, Mor25v, JGI5, H8p, GATS5p and GVWAI-50. Statistical parameters suggested that the constructed QSAR models were robust with Q^2 = 0.9370 and *RMSE* =4.7414 as evaluated via leave-one-out cross-validation (LOO-CV. The mechanistic basis of the antioxidant activity as deduced from significant descriptors was rationalized. Particularly, compounds with the highest antioxidant activity required compounds to have the highest mean topological charge index of order 5 (JGI5) and Geary autocorrelation–lag 5/weighted by atomic polarizabilities (GATS5p) but necessitated low 3D-MoRSE-signal 25/weighted by atomic van der Waals volumes (Mor25v). Such properties are well corroborated by the 3-aminopyrazole pharmacophore from investigated compounds. Molecular insights unraveled herein is anticipated to be useful as guidelines for further rational design of novel pyrazole analogs with potent antioxidant activity.

6.2 Introduction

Oxidative stress causes deleterious effects to the body induced by an imbalance of free radicals in relation to enzymatic and non-enzymatic antioxidant systems (13). This condition leads to oxidation that subsequently damages biomolecules (e.g., DNA, proteins, lipids and membranes), and give rise to physiological changes that eventually accelerate cell death. Free radicals are a risk factor associated with the development of various diseases such as aging,

cancer, diabetes mellitus, cardiovascular and neurodegenerative diseases (13). Therefore, antioxidant compounds have drawn considerable attention as free radical scavengers. This had attracted considerable interests in screening for the discovery of novel antioxidants either from medicinal plants or by synthesis as to obtain novel bioactive compounds with promising therapeutic potential (65). Particularly, the synthesis of new compounds with various pharmacological activities has been achieved by chemical structural modification of pharmacophoric nucleus (65, 66). Interestingly, pyridine (i.e. a six-membered ring of five carbon atoms and one nitrogen atom) is a chemical moiety found in living organisms (55). It has been used as a core structure for the synthesis of new compounds with pharmacological properties (25, 56-58). Furthermore, pyrazole is a five-membered ring of three carbon atoms and two nitrogen atoms, which has been considerable used as core structure for the drug design (59-61). Therefore, a fused ring of pyridine and pyrazole gave rise to the pyrazolopyridine scaffold, which was shown to exert various biological activities such as antimicrobial (62), anticancer (63) and kinase inhibitory (64) properties. Previously, synthesized pyrazolopyridine derivatives with antioxidant activity were reported (107). Most of the compounds were derived from 3-aminopyrazolopyridine.

Computational drug design have been immensely useful in the discovery, design and development of potentially interesting compounds by investigating their biological or chemical properties *in silico* (65, 66). Particularly, quantitative structure-activity relationship (QSAR) has been widely used to generate predictive models as well as provide insights on the contribution of molecular features in governing their biological activities. Therefore, this study makes use of QSAR modeling to correlate physicochemical properties derived from the chemical structure with the antioxidant activity of pyrazolopyridine derivatives (1-20, Fig.6.1). Contributing factors governing the antioxidant activity was dissected by scrutinizing the significant descriptors derived from the QSAR model.

6.3 Materials and methods

6.3.1 Data set

A data set of 20 pyrazolopyridine derivatives (**1-20**) and their antioxidant activities were obtained from the work of Gouda (107)**.** Briefly, the antioxidant activity was evaluated using the 2,2´-azino-bis-3-ethylbenzthiazoline-6-sulphonic acid (ABTS) assay.

6.3.2 Descriptors calculation

The structures of all compounds were drawn in GaussView version 3.09 (108). Geometry optimization was performed using Gaussian 09 Revision A.02 (109) initially at the

semi-empirical AM1 level followed by full optimization with no symmetry constraint at the density functional theory (DFT) level using the Becke's three-parameter Lee–Yang–Parr functional and with the 6–31g(d) basis set. Quantum chemical descriptors were obtained from the resulting low-energy conformers. The quantum chemical descriptors composed of total energy (E_T), highest occupied molecular orbital (E_{HOMO}), lowest unoccupied molecular orbital (E_{LUMO}), energy gap of the HOMO and LUMO state (E_{HOMO}–E_{LUMO}), total dipole moment (μ) of the molecule, electron affinity (EA, calculated from -E_{LUMO}), ionization potential (IP, calculated from $-E_{HOMO}$), mulliken electronegativity (χ), hardness (η), softness (S), electrophilicity (ω), electrophilicity index (ω_i) and mean absolute charge (Q_m) (110). Furthermore, an additional set of 3,224 molecular descriptors was calculated from Dragon software, version 5.5 (111). This large set of descriptors can be classified into 22 categories including 48 constitutional descriptors, 119 topological descriptors, 47 walk and path counts, 33 connectivity indices, 47 information indices, 96 2D autocorrelation, 107 edge adjacency indices, 64 burden eigenvalues, 21 topological charge indices, 44 eigenvalue-based indices, 41 randic molecular profiles, 74 geometrical descriptors, 150 RDF descriptors, 160 3D-MoRSE descriptors, 99 WHIM descriptors, 197 GETAWAY descriptors, 154 functional group counts, 120 atom-centered fragments, 14 charge descriptors, 29 molecular properties, 780 2D binary fingerprints and 780 2D frequency fingerprints. In addition, a subset of important descriptors was deduced by stepwise multiple linear regression using SPSS statistics 18.0 (SPSS Inc., USA). The cutoff was assigned to be $|r| \geq 0.8$ for determining high correlation between the descriptors.

6.3.3 Data sampling

The pyrazolopyridine derivatives were selected for the training and testing sets. The training set comprising of all compound was used to construct the QSAR model. On the other hand, the testing set was performed using the leave-one-out cross-validation (LOO-CV) method. The LOO-CV was performed by leaving out one sample from the data set and used as the testing set while the remaining N - 1 samples were used as the training set. This process was repeated iteratively until each sample of the data set was used as the testing set (106).

6.3.4 Multiple linear regression

Multiple linear regression (MLR) was used to generate QSAR model as summarized in equation (1):

$$Y = B_0 + \sum B_n X_n \quad (1)$$

where Y is the % inhibition of pyrazolopyridine derivatives, B_0 is the intercept and B_n is the regression coefficients of the descriptors X_n. MLR was performed using the Waikato Environment for Knowledge Analysis (Weka), version 3.4.5. (112).

6.3.5 Statistical analysis

To evaluate the QSAR model, the statistical parameters included squared correlation coefficient (R^2), crossed validated (Q^2), which corresponded to the degree of correlation between the predicted and experimental values, and root mean square error (RMSE) which was used to measure the predictive error of the model and *F*-ratio (113).

6.4 Results and Discussion

6.4.1 Descriptors calculation and feature selection

The antioxidant activity of the pyrazolopyridine derivatives (**1**-**20**, Fig. 1) was investigated using the ABTS assay (107). The compounds exhibited activity in the range of 14.41-86.94 % inhibition (at 1 mg/mL) as shown in Table 6.1.

A data set of the compounds with antioxidant property was employed in the QSAR development. Quantum chemical and molecular descriptors were generated using Gaussian and Dragon softwares, respectively, as mentioned in materials and methods. Such quantum chemical and molecular descriptors have been successfully used to construct various QSAR studies such as antioxidant (25, 114), antimicrobial (115), anticancer (106) and anti-inflammatory (116) activities. Sets of molecular descriptors were expressed in quantitatively describing the physicochemical properties of the investigated set of compounds. In addition, the descriptors generating by the softwares displayed a number of representative structural features, therefore, nonsignificant descriptors were eliminated. In doing so, the feature selection was performed to select the descriptors that correlated with their antioxidant activities. The original molecular descriptors generated from the Dragon software contained 3,224 molecular descriptors, which were subjected to initial removal of multi-collinear and of the redundant descriptors of 1,713 descriptors. The remaining 1,511 descriptors were further combined with 13 quantum chemical descriptors to obtain a set of 1,524 descriptors that were used as independent variables, while the antioxidant activity (%inhibition) was used as the dependent variable, and the significant descriptors were selected using the stepwise approach. The obtained descriptors with their values were then used for developing the QSAR model using MLR in WEKA software, version

3.4.5 (112) as shown in Table 6.1, and the definition of descriptors was described in Table 6.2. The intercorrelation matrix between descriptors was performed using Pearson's correlation in a pairwise manner to determine correlation coefficient of each descriptor as presented in Table 6.3. It was found that each descriptor was independent from other descriptors as observed by low correlation coefficient. The correlation coefficients between descriptors were less than 0.8 (the cutoff was assigned to be $|r| \geq 0.8$). Therefore, the six important descriptors (Table 6.2), composing molecular properties (GVWAI-50), topological charge indices (GVWAI-50), 3D-MoRSE descriptors (Mor11m and Mor25v), GETAWAY descriptors (H8p) and 2D autocorrelation (GATS5p), were employed to construct the QSAR model for predicting the antioxidant activity of pyrazolopyridines derivatives.

6.4.2 QSAR modeling of antioxidant activity

The six descriptors were used to generate a multiparametric regression using MLR method implemented in Weka software, version 3.4.5 (112). The linear regression derived from the QSAR model is shown in equation (2):

$$\%\text{Inhibition} = 1746.2843(\text{JGI5}) + 30.6893(\text{GVWAI-50}) + 28.1446(\text{Mor11m}) + 183.5802(\text{H8p}) - 45.5842(\text{Mor25v}) + 27.2051(\text{GAT5p}) - 73.3343 \quad (2)$$

n = 20, R^2 = 0.9765, RMSE_{Tr} = 2.8864, Q^2 = 0.9370, $\text{RMSE}_{\text{LOO-CV}}$ = 4.7414, R^2 - Q^2 = 0.0395, F-ratio = 32.22

To evaluate the quality of regression model, an internal validation of the QSAR model was performed using LOO-CV method (117, 118) as the testing set. From the Eq. (2) the results of predictive performance model for training and LOO-CV sets for predicting antioxidant activity exhibited statistically good values as observed from the correlation coefficient with more than 0.9 (0.9765 and 0.9370 for the training and the LOO-CV set, respectively), and low RMSE values with 2.8864 and 4.7414 for the training and the LOO-CV sets, respectively. The constructed model displayed R^2 >0.6 and Q^2>0.5, which implied the good performance (113). Furthermore, the model provided good predictability R^2 - Q^2 value of 0.0395 (not exceed 0.3) (119), and the reliable F-ratio was shown to be 32.22. The plot of experimental and predicted activities based on the Eq. (2) is shown in Figure 6.2, and the predicted activity values are outlined in Table 6.1. It was found that the model has good correlation between the experimental and the predicted activities as observed by statistical quality results as shown in the Eq. (2). Although value of RMSE was high number (4.7414), but its correlation coefficient

showed high number of R^2 (0.9765) and Q^2 (0.9370) for training and LOO-CV sets, respectively. However, the RMSE was found to be high value with high correlation coefficient, which has been demonstrated as potential models for QSAR developments (25, 58, 120).

6.4.3 Structure-activity relationship

The MLR equation, Eq. (2), showed the important descriptors involved in the antioxidant activity including 3D-MoRSE-signal 11/weighted by atomic masses (Mor11m), 3D-MoRSE-signal 25/weighted by atomic van der Waals volumes (Mor25v), mean topological charge index of order 5 (JGI5), H autocorrelation of lag 8/weighted by atomic polarizabilities (H8p), Geary autocorrelation–lag 5/weighted by atomic polarizabilities (GATS5p), and Ghose-Viswanadhan-Wendoloski drug-like index at 50% (GVWAI-50) as shown in Tables 6.1 and 6.2. The relative important descriptors in Eq. (2) displayed the following order of significance, JGI5 > H8p > GVWAI-50 > Mor11m > GAT5p > Mor25v, as observed by the coefficient values of 1746.2843, 183.5802, 30.6893, 28.1446, 27.2051, -45.5842, respectively. The positive coefficient values of JGI5, H8p, GVWAI-50, Mor11m and GAT5p in Eq. (2) indicated that the increase of descriptor values correlated with the increased activity as a positive effect. On the other hand, Mor25v had the negative coefficient value indicating the increasing activity with the decreasing value of this descriptor as a negative effect.

The investigated compounds (**1**-**20**) had a common pyrazolopyridine ring substituted with amino (NH2) group at 3-position (**1**, **8**, **9**, **14**, **18**) or with various condensed rings at 2,3-position on the pyrazole ring making the compounds as tricyclic derivatives including pyridine-pyrazole-imidazole (**2**, **3**, **4**-**7**), pyridine-pyrazole-pyrimidine (**10**-**13**, **15**-**17**, **19**), and pyridine-pyrazole-benzodiazepine (**20**). Considering the antioxidant activity of the compounds **1**-**20**, it was found that the most compounds with high JGI5, H8p and GATS5p values, but with low value of Mor25v exhibited high activity as observed in the experimental and predicted activities (Table 6.1). Particularly, 3-amino compound (**1**) with the highest antioxidant activity (86.94%) had the highest mean topological charge index of order 5 (JGI5 = 0.066) and Geary autocorrelation–lag 5/weighted by atomic polarizabilities (GATS5p = 1.375) as the positive effect, but relatively with the lowest 3D-MoRSE-signal 25/weighted by atomic van der Waals volumes (Mor25v = 0.164) as the negative effect. Such descriptor properties of compound 1 could be possibly due to the NH moiety of pyrazole ring, and 3-NH2 as electron releasing group substituted on the pyrazole ring that participated in the electron delocalization and giving rise to ionic charges resonant forms (**1a** and **1b**, respectively, Figure 6.3) in exerting the antioxidant activity by scavenging the radical cation of the ABTS. It should be noted that

compound **1** is the smallest molecular size that correlated to the low value of 3D-MoRSE-signal 25/weighted by atomic van der Waals volumes (Mor25v = 0.164).

When the 3-NH_2 group of compound **1** was converted to electron withdrawing amide group (compound **18**), a remarkable reduced antioxidant activity (35.74%, Table 6.1) was noted as correlated to the reduced values of JGI5 (0.041) and GATS5p (1.193) compared with compound **1**. The results suggested that the pyrazolopyridine with 3-NH_2 group (**1**) is required for the highest antioxidant activity.

The investigated tricyclic scaffolds constitute a variety of substituents and/or fused aryl or heteroaryl rings. Tricyclic pyridine-pyrazole-imidazole (**2** and **3**), resulting from 3-NH_2 group ring closure of compound **1**, displayed lower antioxidant activity than that of the parent compound **1**. However, compound **3** had higher activity (74.29%) than compound **2** (33.31%), in which high values of H8p (0.123) and Mor11m (0.788) but relatively low Mor25v (0.422) were observed for compound **3**. The highest H8p value of compound **3** could be due to the polarizabilities of electron withdrawing CN group of the compound that is capable of interacting with the radical cation of the ABTS.

Apart from the parent compound **1**, compounds with relatively high antioxidant activity (>50% inhibition) were noted for compounds **3**, **5**-**6** (**3>5>6**) showing high values of JGI5 (0.037-0.04), GATS5p (0.830-1.198) and H8p (0.05-0.123).

Among the antioxidant quinone derivatives (**4**-**7** in which **5>6>4>7**), hydroxy-1,4-naphthoquinone **5** had the highest antioxidant activity (64.25%) with high GATS5p (1.198). It might be due to the polarizabilities of OH group on the 1,4-naphthoquinone **5** which provided the high value of GATS5p in governing the high activity compared with the bromo-1,4-naphthoquinone (**4**). In case of 1,4-quinone (**6**) containing diOH groups on the quinone ring, its reduced activity (53.81%) with reduced GATS5p (0.830) and H8p (0.050) were observed comparing with hydroxy-1,4-naphthoquinone (**5**). Remarkably, diacetoxy-1,4-quinone (**7**) displayed lower activity (14.41%) with lower JGI5 (0.036) and H8p (0.029) compared with diOH-1,4-quinone (**6**). It was suggested that 1,4-naphthoquinone (**5**) with *ortho*-OH group is an appropriate moiety condensing with the tricyclic pyridinepyrazolimidazole core scaffold. This might contribute to the H-bonding and lipophilic properties of the hydroxy-1,4-naphthoquinone (**5**) in exerting its antioxidant activity. It should be noted that diacetoxy-1,4-quinone (**7**) with the lowest Mor25v (0.169) had the lowest antioxidant activity compared with compounds **4**-**6** (**5>6>4>7**). This observed effect could be presumed that Mor25v is the last order of relative important chemical descriptors as previously mentioned.

Other compounds (**8**-**20**) with low antioxidant activity (<50% inhibition) mostly had low values of JGI5 (0.025-0.042) and GATS5p (0.838-1.155), but high Mor25v (0.134-0.685) compared with the most active compound **1** (JGI5 = 0.066, GATS5p = 1.375, Mor25v = 0.164), and with the moderately active compounds **3**, **5** and **6** (53.81-74.29% inhibition, JGI5 = 0.037-0.041, GATS5p = 0.830-1.198, Mor25v = 0.196-0.422).

Notably, high Mor25v values of compounds **8**-**20** (except for **18**) could be possibly due to their more complexed ring structures leading to bulky molecules. The antioxidant activity of **8**-**20** and values of these chemical descriptors showed quite good correlation. Compounds **1**-**20** had H8p values in a range of 0.004-0.123 in which compound **3**, the second ranked antioxidant, had the highest H8p (0.123) value. Relatively high H8p values of 0.113 and 0.108 were also noted for compounds **9** and **4**, respectively. This could be due to a diverse range of chemical structures affecting their molecular influence matrices in governing the antioxidant activity

Apparently, the compound (**1**) with the highest antioxidant activity had the important 3-aminopyrazole pharmacophore that well correlated to certain chemical descriptors with high topological charge index and atomic polarizabilities, but with low atomic van der Waals volumes. In this regard, the properties of such descriptors could assist in searching and designing novel antioxidants by modification of the 3-NH_2 group as other electron releasing groups, and the ring structure of compound (**1**) as other heterocyclic rings. Possible structurally modified derivatives of **1** could be displayed, for example, **1A** resulting from a replacement of 3-NH_2 group by other electron donating groups (OH, OR, SH), **1B** resulting from the replacement of pyridine ring by pyrimidine ring, and **1C** resulting from the substitution of phenyl ring with electron withdrawing groups on the pyridine ring as shown in Fig. 6.4.

In summary, the underlying basis of the antioxidant activity of pyrazolopyridines was explored by scrutinizing important descriptors obtained from QSAR model constructed using MLR. It was found that a set of physicochemical parameters comprising of 3D-MoRSE-signal 11/weighted by atomic masses (Mor11m), 3D-MoRSE-signal 25/weighted by atomic van der Waals volumes (Mor25v), mean topological charge index of order 5 (JGI5), H autocorrelation of lag 8/weighted by atomic polarizabilities (H8p), Geary autocorrelation–lag 5/weighted by atomic polarizabilities (GATS5p), and Ghose-Viswanadhan-Wendoloski drug-like index at 50% (GVWAI-50) were important for the antioxidant activity. The compounds with the highest antioxidant activity also had high JGI5 and GATS5p with low Mor25v as noted for the 3-aminopyrazole pharmacophore (**1**). Interestingly, the highest H8p value was noted for the second-ranked antioxidant (**3**). Such high atomic polarizabilities (H8p) may be due to the effect

of the electron-withdrawing CN group and this can be used as a guideline for the rational design of new antioxidants. The results revealed the importance of pharmacophore **1** as a lead compound for further development as potent antioxidants. Structurally modified derivatives of **1** as shown in Fig. 6.4 is proposed as putative compounds (**1A** – **1C**) that may exert promising antioxidant activity.

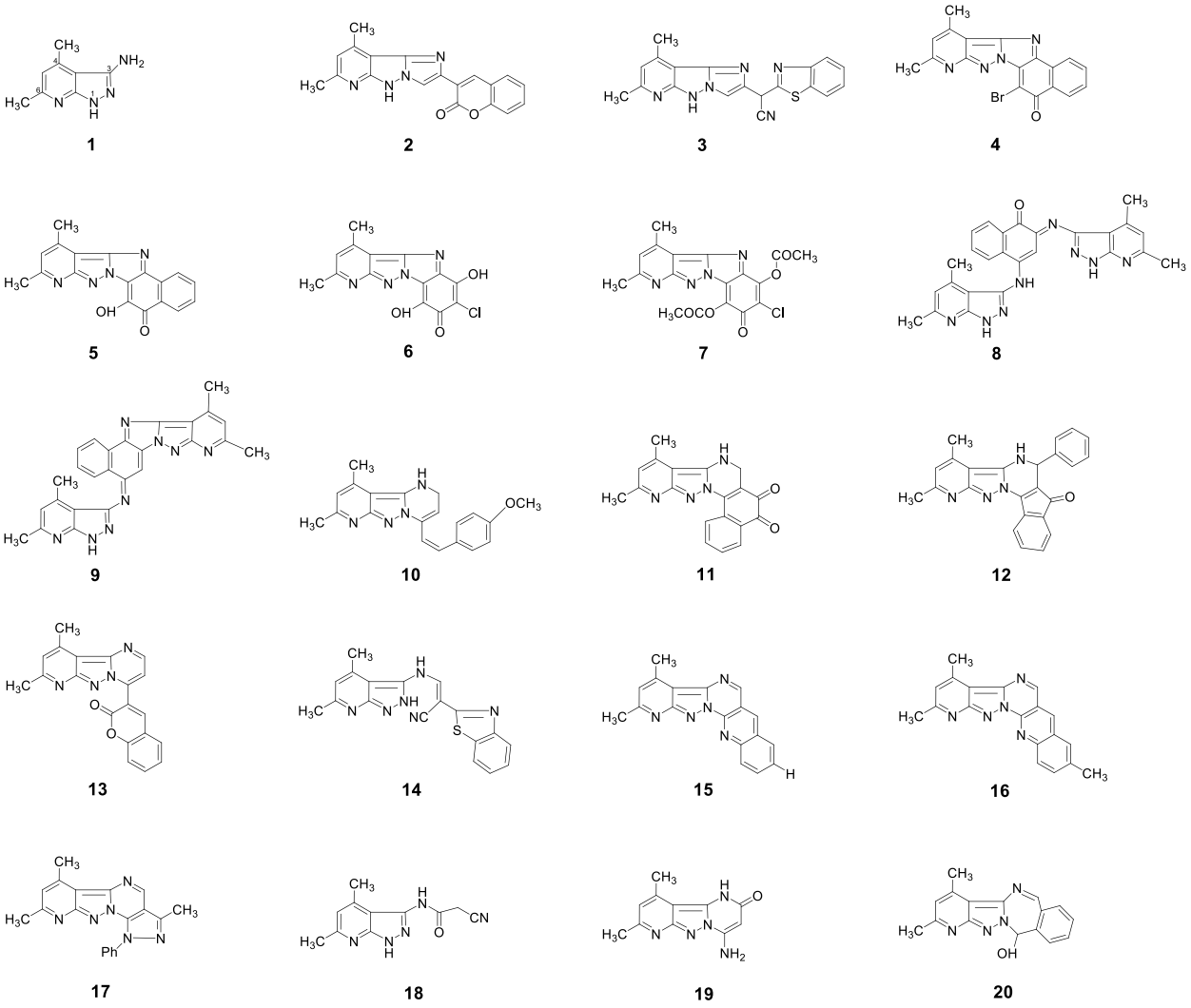

Figure 6.1. Molecular structures of pyrazolopyridine derivatives **1**-**20**.

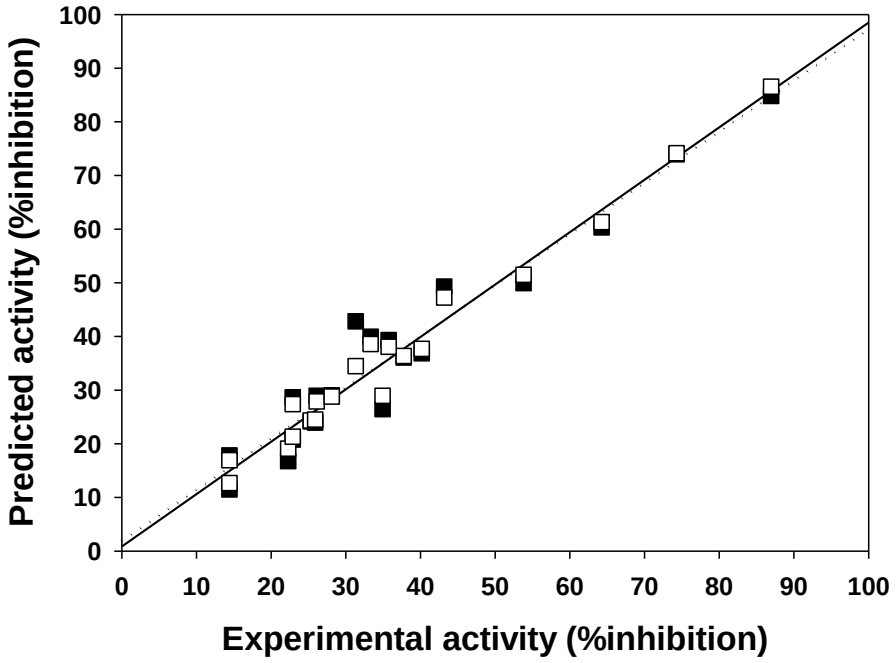

Figure 6.2. Plot of the experimental and predicted activities for the training set (□; regression line is represented as solid line), and the leave-one-out cross-validated set (■; regression line is represented as dotted line).

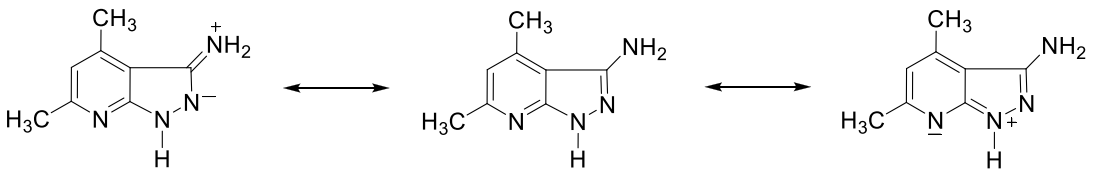

Figure 6.3. Charge distribution of compound **1**.

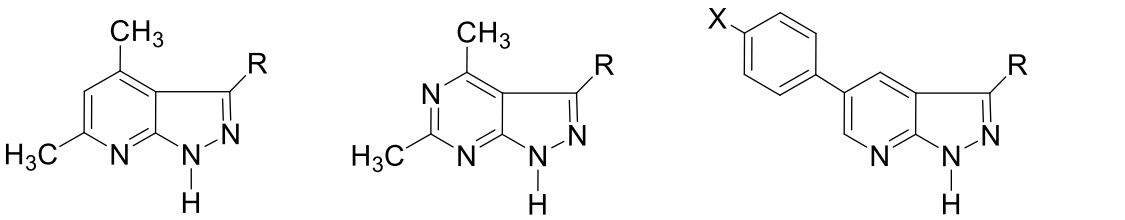

Figure 6.4. Possible structurally modified derivatives (**1A-1C**).

Table 6.1. Antioxidant activity and significant descriptors of pyrazolopyridine derivatives.

Compound	JGI5	GVWAI-50	Mor11m	H8p	Mor25v	GATS5p	Inhibition (%)	
							Exp.	Pred.
1	0.066	0	0.477	0.007	0.164	1.375	86.94	84.84
2	0.035	1	0.455	0.029	0.573	1.033	33.31	39.96
3	0.037	1	0.788	0.123	0.422	0.98	74.29	73.96
4	0.038	1	-0.760	0.108	0.349	1.038	31.32	42.84
5	0.038	1	0.280	0.075	0.365	1.198	64.25	60.33
6	0.041	1	-0.010	0.050	0.196	0.830	53.81	49.93
7	0.036	0	-0.021	0.029	0.169	0.960	14.41	17.83
8	0.027	0	1.300	0.091	0.644	1.108	26.10	28.96
9	0.029	0	0.855	0.113	0.685	1.037	22.28	16.77
10	0.029	1	1.053	0.019	0.652	0.967	40.16	36.87
11	0.029	1	0.206	0.013	0.306	0.977	28.11	29.03
12	0.03	0	0.888	0.059	0.644	1.155	14.41	11.51
13	0.026	1	0.554	0.035	0.618	1.189	34.93	26.47
14	0.025	1	0.712	0.029	0.611	0.838	22.89	20.78
15	0.026	1	0.443	0.033	0.569	1.066	25.30	24.17
16	0.027	1	0.515	0.054	0.508	1.125	37.75	36.08
17	0.026	1	0.915	0.023	0.696	0.970	22.89	20.78
18	0.041	0	0.283	0.030	0.134	1.193	35.74	39.33
19	0.042	0	0.328	0.004	0.285	1.012	25.90	23.94
20	0.028	1	0.700	0.046	0.350	1.059	43.17	49.28

Exp.; Experimental activity, Pred.; Predicted activity.

Table 6.2. Description of important descriptors for constructing the QSAR model.

Descriptors	Type	Description
JGI5	Topological charge indices	Mean topological charge index of order 5
GVWAI-50	Molecular properties	Ghose-Viswanadhan-Wendoloski drug-like index at 50%
Mor11m	3D-MoRSE descriptors	3D-MoRSE-signal 11/weighted by atomic masses
Mor25v	3D-MoRSE descriptors	3D-MoRSE-signal 25/weighted by atomic van der Waals volumes
H8p	GETAWAY descriptors	H autocorrelation of lag 8/weighted by atomic polarizabilities
GATS5p	2D autocorrelations	Geary autocorrelation –lag 5/weighted by atomic polarizabilities

Table 6.3. Intercorrelation matrix of significant descriptors.

Descriptors	JGI5	GVWAI-50	Mor11m	H8p	Mor25v	GATS5p
JGI5	1					
GVWAI-50	-0.388	1				
Mor11m	-0.366	-0.148	1			
H8p	-0.161	0.02	0.012	1		
Mor25v	-0.705	0.223	0.656	0.22	1	
GATS5p	0.449	-0.378	0.072	-0.028	-0.136	1

CHAPTER VI

CONCLUSION AND FURTURE PERSPECTIVE

Drug design and development have been focused on this study to gear towards finding novel compounds for biological activities. A variety of novel metal complexes (**1**-**16**) were synthesized including 2-thiouracil (2TU) and 8-hydroxyquinoline/2-hydroxyquinoline (8HQ/2HQ) transition metals (Ni, Cu, Mn) complexes (**1**-**6**), and Cu complexes (**7**-**16**) of 4-substituted (NO_2, OCH_3, CH_3 and Cl) benzenesulfonamide of anthranilic acid. These metal complexes were investigated for their biological activities i.e, antioxidant, antimicrobial and anticancer activities. The metal complexes **1**-**6** displayed SOD activity, particularly, complex **5** (2TU-Cu-2HQ) exhibited the highest SOD activity (IC_{50} of 1.81 μM). Furthermore, complex **3** (2TU-Mn-8HQ) displayed effective antimicrobial activity with the minimal inhibitory concentration (MIC) in range of 11.07-708.64 μM against microorganisms (i.e., gram-positive bacteria, gram negative bacteria and diploid fungus) **(Appendix A)**. In addition, the Cu complexes **7**-**16** elicited antioxidant (SOD) activity, and cytotoxic effect against MOLT-3 cell lines. The complex **10** (sulfonamides with NO_2 and Cl groups) exhibited the strongest SOD activity with IC_{50} of 0.062 μM, and complex **16** (sulfonamide with Cl group) had the best cytotoxicity against MOLT-3 cell lines with IC_{50} of 21.60 μM **(Appendix B)**. In addition, a data set of 20 pyrazolopyridine derivatives with antioxidant activity was studied to develop QSAR model. The obtained significant variables including Mor11m, Mor25v, JGI5, H8p, GATS5p and GVWAI-50 were used for generating predictive model. The statistical results displayed good predictive performance of Q^2 = 0.9370 and RMSE =4.7414 for internal validation (LOO-CV set). Interestingly, the highest antioxidant activity required the compound with the highest JGI5 and GATS5p but with low Mor25v which related to 3-aminopyrazole pharmacophore of the compound **(Appendix C)**. Pyridine and pyrimidine as privileged scaffolds with attractive anticancer activity have been reported **(Appendix D)**. The body of knowledge is benefit for the design and development of novel bioactive pyridine and pyrimidine-based compounds. For further study, the metal complexes (**1**-**16**) will be studied to obtain informative significant descriptors for understanding the influence of chemical structural features involved in their biological properties via computational approaches. The outcome of this study could be benefit for drug discovery and development as well as medicinal applications.

REFERENCES

1. Abreu IA, Cabelli DE. Superoxide dismutases-a review of the metal-associated mechanistic variations. Biochim Biophys Acta. 2010;1804(2):263-74.
2. Perry JJP, Shin DS, Getzoff ED, Tainer JA. The structural biochemistry of the superoxide dismutases. Biochim Biophys Acta. 2010;1804:245-62.
3. Sheng Y, Abreu IA, Cabelli DE, Maroney MJ, Miller AF, Teixeira M, et al. Superoxide dismutases and superoxide reductases. Chem Rev. 2014;114(7):3854-918.
4. Pingaew R, Worachartcheewan A, Prachayasittikul V, Prachayasittikul S, Ruchirawat S, Prachayasittikul V. Transition metal complexes of 8-aminoquinoline-5-substituted uracils with antioxidative and cytotoxic activities. Lett Drug Des Discov. 2013;10:859-64.
5. Prachayasittikul S, Worachartcheewan A, Pingaew R, Suksrichavalit T, Isarankura-Na-Ayudhya C, Ruchirawat S, et al. Metal complexes of uracil derivatives with cytotoxicity and superoxide scavenging activity. Lett Drug Des Discov. 2012;9:282-7.
6. Sharma D. Kumarm P, Narasimhan B. Synthesis and antibacterial evaluation of Cu(II) and Zn(II) complexes of the β-lactum antibiotic, cefdinir. Med Chem Res. 2012;21(6):796-803.
7. Suksrichavalit T, Prachayasittikul S, Nantasenamat C, Isarankura-Na-Ayudhya C, Prachayasittikul V. Copper complexes of pyridine derivatives with superoxide scavenging and antimicrobial activities. Eur J Med Chem. 2009;44(8):3259-65.
8. Suksrichavalit T, Prachayasittikul S, Piacham T, Isarankura-Na-Ayudhya C, Nantasenamat C, Prachayasittikul V. Copper complexes of nicotinic-aromatic carboxylic acids as superoxide dismutase mimetics. Molecules. 2008;13(12):3040-56.
9. Rehman W, Hassan Z, Rashid U, Rahim F, Abid O.U.R, Waseem M. Synthesis, characterization antibacterial and antifungal activity of some transition metal complexes. Med Chem Res. 2014;23(5):2207-11.
10. Prachayasittikul V, Prachayasittikul S, Ruchirawat S, Prachayasittikul V. 8-Hydroxyquinolines: a review of their metal chelating properties and medicinal applications. Drug Des Devel Ther. 2013;4:1157-78.
11. Biesalski HK. Free radical theory of aging. Curr Opin Clin Nutr Metab Care. 2002;5(1):5-10.
12. Devasagayam TP, Tilak JC, Boloor KK, Sane KS, Ghaskadbi SS, Lele RD. Free radicals and antioxidants in human health: current status and future prospects. J Assoc Physicians India. 2004;52:794-804.

13. Valko M, Leibfritz D, Moncol J, Cronin MT, Mazur M, Telser J. Free radicals and antioxidants in normal physiological functions and human disease. Int J Biochem Cell Biol. 2007;39(1):44-84.
14. Devasagayam TP, Sainis KB. Immune system and antioxidants, especially those derived from Indian medicinal plants. Indian J Exp Biol. 2002;40(6):639-55.
15. Winyard PG, Moody CJ, Jacob C. Oxidative activation of antioxidant defence. Trends in Biochemical Sciences. 2005;30(8):453-61.
16. Leslie JB, Raffa RB, Taylor JB, Tabor A, Muniz E, Nalamachu S, et al. Essential oxygen oil for treatment of sport-related injuries. Am J Sports Med. 2013;1(1):7-12.
17. Livingstone DJ, Davis AM. Drug design strategies: Quantitative approaches. Cambridge, UK: RSC Publishing; 2012.
18. Rick Ng. Drugs from discovery to approval. Wiley-Blackwell. New Jersey, USA: Hoboken; 2009.
19. Guengerich FP. Cytochrome P450s and other enzymes in drug metabolism and toxicity. Aaps J. 2006;8(1):E101-11.
20. Prachayasittikul S, Suphapong S, Worachartcheewan A, Lawung R, Ruchirawat S, Prachayasittikul V. Bioactive metabolites from *Spilanthes acmella* Murr. Molecules. 2009;14(2):850-67.
21. Prachayasittikul S, Buraparuangsang P, Worachartcheewan A, Isarankura-Na-Ayudhya C, Ruchirawat S, Prachayasittikul V. Antimicrobial and antioxidative activities of bioactive constituents from *Hydnophytum formicarum* Jack. Molecules. 2008;13(4):904-21.
22. Prachayasittikul S, Worachartcheewan A, Yainoy S, Lomchoey N, Kittiphatcharin P, Ruchirawat S, et al. Antioxidant and antimicrobial activities of *Saraca thaipingensis* Cantley ex Prain. Asian Pac J Trop Biomed. 2012;2(2):S796-S9.
23. Ravikumar YS, Mahadevan KM, Kumaraswamy MN, Vaidya VP, Manjunatha H, Kumar V, et al. Antioxidant, cytotoxic and genotoxic evaluation of alcoholic extract of *Polyalthia cerasoides* (Roxb.) Bedd. Environ Toxicol Pharmacol. 2008;26(2):142-6.
24. Ragasa CY, De Luna RD, Hofilena JG. Antimicrobial terpenoids from *Pterocarpus indicus*. Nat Prod Res. 2005;19(4):305-9.
25. Worachartcheewan A, Nantasenamat C, Owasirikul W, Monnor T, Naruepantawart O, Janyapaisarn S, et al. Insights into antioxidant activity of 1-adamantylthiopyridine analogs using multiple linear regression. Eur J Med Chem. 2014;73:258-64.
26. Prachayasittikul S, Worachartcheewan A, Nantasenamat C, Chinworrungsee M, Sornsongkhram N, Ruchirawat S, et al. Synthesis and structure-activity relationship of

2-thiopyrimidine-4-one analogs as antimicrobial and anticancer agents. Eur J Med Chem. 2011;46(2):738-42.

27. Mavrova AT, Wesselinova D, Tsenov JA, Lubenov LA. Synthesis and antiproliferative activity of some new thieno[2,3-*d*]pyrimidin-4(3*H*)-ones containing 1,2,4-triazole and 1,3,4-thiadiazole moiety. Eur J Med Chem. 2014;86:676-83.
28. Pingaew R, Worachartcheewan A, Nantasenamat C, Prachayasittikul S, Ruchirawat S, Prachayasittikul V. Synthesis, cytotoxicity and QSAR study of *N*-tosyl-1,2,3,4-tetrahydroisoquinoline derivatives. Arch Pharm Res. 2013;36(9):1066-77.
29. Prachayasittikul V, Pingaew R, Nantasenamat C, Prachayasittikul S, Ruchirawat S, Prachayasittikul V. Investigation of aromatase inhibitory activity of metal complexes of 8-hydroxyquinoline and uracil derivatives. Drug Des Devel Ther. 2014;8:1089-96.
30. Aslan G, Onal Z. Novel metal complexes, their spectrophotometric and QSAR studies. Med Chem Res. 2014;23(5):2596-607.
31. Gimadieva AR, Myshkin VA, Mustafin AG, Chernyschenko YN, Fattakhov A, Abdrakhmanov IB, et al. 5-amino-6-methyluracil is a promising pyrimidine antioxidant. Dokl Biol Sci. 2013;448:7-9.
32. Mohamed MS, Youns MM, Ahmed NM. Synthesis, antimicrobial, antioxidant activities of novel 6-aryl-5-cyano thiouracil derivatives. Eur J Med Chem. 2013;69:591-600.
33. Prachayasittikul S, Sornsongkhram N, Pingaew R, Worachartcheewan A, Ruchirawat S, Prachayasittikul V. Synthesis of *N*-substituted 5-iodouracils as antimicrobial and anticancer agents. Molecules. 2009;14(8):2768-79.
34. Maruyama T, Demizu Y, Kozai S, Witvrouw M, Pannecouque C, Balzarini J, et al. Antiviral activity of 3-(3,5-dimethylbenzyl)uracil derivatives against HIV-1 and HCMV. Nucleo Nucleot Nucl. 2007;26(10-12):1553-8.
35. Bardagí JI, Rossi RA. Advances in the Synthesis of 5- and 6-Substituted Uracil Derivatives. Org Prep Proced Int. 2009;41:479-514.
36. Zenker N. Thyroid function and thyroid drugs. In: Principles of Medicinal Chemistry. Foye, W.O., editor, 3rd ed.: Lea & Febiger: Philadelphia, London,1990, pp. 603-621.
37. Boncel S, Gondela A, Walczak K. Micheal-type addition as a convenient method for regiselective N-alkylation of ambident uracils. Synthesis. 2010;10:1573-89.
38. del Carmen Núñeza M, Entrena A, Rodríguez-Serrano F, Marchal JA, Aránega A, Gallo MA, et al. Synthesis of novel 1-(2,3-dihydro-5*H*-4,1-benzoxathiepin-3-yl)-uracil and -thymine, and their corresponding *S*-oxidized derivatives Tetrahedron. 2005;61:10363-9.
39. De Clercq E. Antiviral drugs in current clinical use. J Clin Virol. 2004;30(2):115-33.

40. Tanaka H, Takashima H, Ubasawa M, Sekiya K, Nitta I, Baba M, et al. Synthesis and antiviral activity of deoxy analogs of 1-[(2-hydroxyethoxy)methyl]-6-(phenylthio)thymine (HEPT) as potent and selective anti-HIV-1 agents. J Med Chem. 1992;35:4713-9.
41. Choi HJ, Yu ST, Lee KI, Choi JK, Chang BY, Kim SY, et al. 6-trifluoromethyl-2-thiouracil possesses anti-Toxoplasma gondii effect in vitro and in vivo with low hepatotoxicity. Exp Parasitol. 2014;143:24-9.
42. Fabrissin S, de Nardo M, Nisi C, Morasca L, Dolfini E, Franchi G. Synthesis and anticancer activity of 5-diethylaminomethyl derivatives and nitrogen mustards of uracil and 2-thiouracils. J Med Chem 1976;19:639-42.
43. Kamalakannan P, Venkappayya D, Balasubramanian T. A new antimetabolite, 5-morpholinomethyl-2-thiouracil—spectral properties, thermal profiles, antibacterial, antifungal and antitumour studies of some of its metal chelates. J Chem Soc, Dalton Trans. 2002:3381-91.
44. Motawia MS, Abdel-Megied AES, Pedersen EB, Nielsen CM, Ebbesen P. Synthesis of 5-alkoxymethyl derivatives of 3'-amino-2',3'-dideoxyuridine and evaluation of their activity against HIV and cancer. Acta Chem Scand. 1992;46:77-81.
45. Mitscher LA. Bacterial topoisomerase inhibitors: quinolone and pyridone antibacterial agents. Chem Rev. 2005;105(2):559-92.
46. Xia Y, Yang ZY, Xia P, Bastow KF, Nakanishi Y, Nampoothiri P, et al. Antitumor agents. Part 226: synthesis and cytotoxicity of 2-phenyl-4-quinolone acetic acids and their esters. Bioorg Med Chem Lett. 2003;13(17):2891-3.
47. Lucero B, Gomes CR, Frugulhetti IC, Faro LV, Alvarenga L, de Souza MC, et al. Synthesis and anti-HSV-1 activity of quinolonic acyclovir analogues. Bioorg Med Chem Lett. 2006;16(4):1010-3.
48. Srisung S, Prachayasittikul S, Suksrichavalit T, Ruchirawat S, Prachayasittikul V. Antimicrobial activity of 8-hydroxyquinoline and transition metal complexes. Int J Pharm. 2013;9:170-5.
49. Patel MN, Parmar PA, Gandhi DS. Third generation fluoroquinolones antibacterial drug based mixed-ligand Cu(II) complexes: structure, antibacterial activity, superoxide dismutase activity and DNA-interaction approach. J Enzyme Inhib Med Chem. 2011;26(2):188-97.
50. Genc Y, Ozkanca R, Bekdemir Y. Antimicrobial activity of some sulfonamide derivatives on clinical isolates of *Staphylococus aureus*. Ann Clin Microbiol Antimicrob. 2008;7(17):17.

51. Hwang YJ, Park SM, Yim CB, Im C. Cytotoxic Activity and Quantitative Structure Activity Relationships of Arylpropyl Sulfonamides. Korean J Physiol Pharmacol. 2013;17(3):237-43.

52. Loh B, Vozzolo L, Mok BJ, Lee CC, Fitzmaurice RJ, Caddick S, et al. Inhibition of HIV-1 Replication by Isoxazolidine and Isoxazole Sulfonamides. Chem Biol Drug Des. 2010;75(5):461-74.

53. Chohan ZH, Hernandes MZ, Sensato FR, Moreira DR, Pereira VR, Neves JK, et al. Sulfonamide-metal complexes endowed with potent anti-*Trypanosoma cruzi* activity. J Enzyme Inhib Med Chem. 2014;29(2):230-6.

54. Garcia-Gimenez JL, Hernandez-Gil J, Martinez-Ruiz A, Castineiras A, Liu-Gonzalez M, Pallardo FV, et al. DNA binding, nuclease activity, DNA photocleavage and cytotoxic properties of Cu(II) complexes of *N*-substituted sulfonamides. J Inorg Biochem. 2013;121:167-78.

55. Kaiser JP, Feng Y, Bollag JM. Microbial metabolism of pyridine, quinoline, acridine, and their derivatives under aerobic and anaerobic conditions. Microbiol Rev. 1996;60(3):483-98.

56. Al-Omar MA, Youssef KM, El-Sherbeny MA, Awadalla SAA, El-Subbagh HI. Synthesis and in vitro antioxidant activity of some new fused pyridine analogs. Arch Pharm Chem Life Sci. 2005;338:175-80.

57. Amr AG, Mohamed AM, Mohamed SF, Abdel-Hafez NA, Hammam Ael F. Anticancer activities of some newly synthesized pyridine, pyrane, and pyrimidine derivatives. Bioorg Med Chem. 2006;14(16):5481-8.

58. Worachartcheewan A, Prachayasittikul S, Pingaew R, Nantasenamat C, Tantimongcolwat T, Ruchirawat S, et al. Antioxidant, cytotoxicity, and QSAR study of 1-adamantylthio derivatives of 3-picoline and phenylpyridines. Med Chem Res. 2012;21:3514-22.

59. Cai J, Liu L, Chen J, Cao M, Ji M. Design, synthesis, and bioactivity of pyrazole acid derivatives as endothelin receptor antagonists. Med Chem. 2013;9(8):1113-22.

60. Kumar H, Saini D, Jain S, Jain N. Pyrazole scaffold: a remarkable tool in the development of anticancer agents. Eur J Med Chem. 2013;70:248-58.

61. Wu J, Shi Q, Chen Z, He M, Jin L, Hu D. Synthesis and bioactivity of pyrazole acyl thiourea derivatives. Molecules. 2012;17(5):5139-50.

62. Abu-Melha S. Synthesis and antimicrobial activity of some new heterocycles incorporating the pyrazolopyridine moiety. Arch Pharm (Weinheim). 2013;346(12):912-21.

63. Gudmundsson KS, Johns BA, Allen SH. Pyrazolopyridines with potent activity against herpesviruses: effects of C5 substituents on antiviral activity. Bioorg Med Chem Lett. 2008;18(3):1157-61.

64. Deng X, N SG. Pyrazolopyridines as inhibitors of the kinase LRRK2: a patent evaluation (WO2011141756). Expert Opin Ther Pat. 2012;22(6):709-13.

65. Prachayasittikul V, Worachartcheewan A, Shoombuatong W, Songtawee N, Simeon S, Prachayasittikul V, et al. Computer-Aided Drug Design of Bioactive Natural Products. Curr Top Med Chem. 2015;15(18):1780-800.

66. Nantasenamat C, Prachayasittikul V. Maximizing computational tools for successful drug discovery. Expert Opin Drug Discov. 2015;10(4):321-9.

67. Pham-Huy LA, He H, Pham-Huy C. Free radicals, antioxidants in disease and health. Int J Biomed Sci. 2008;4(2):89-96.

68. Lobo V, Patil A, Phatak A, Chandra N. Free radicals, antioxidants and functional foods: Impact on human health. Pharmacogn Rev. 2010;4(8):118-26.

69. Birben E, Sahiner UM, Sackesen C, Erzurum S, Kalayci O. Oxidative stress and antioxidant defense. World Allergy Organ J. 2012;5(1):9-19.

70. Bardagí JI, Rossi RA. Advances in the synthesis of 5- and 6-substituted uracil derivatives. Org Prep Proced Int. 2009;41:479-514.

71. Boncel S, Gondela A, Walczak K. Michael-type addition as a convenient method for regioselective *N*-alkylation of ambident uracils. Synthesis. 2010;10:1573-89.

72. del Carmen Núñez M, Entrena A, Rodríguez-Serrano F, Marchal JA, Aránega A, Gallo MÁ, et al. Synthesis of novel 1-(2,3-dihydro-5H-4,1-benzoxathiepin-3-yl)-uracil and -thymine, and their corresponding *S*-oxidized derivatives. Tetrahedron. 2006;61:10363-9.

73. De Clercq E. Antiviral drugs in current clinical use. J Clin Virol. 2004;30(2):115-33.

74. Fathalla OA, Zaghary WA, Radwan HH, Awad SM, Mohamed MS. Synthesis of new 2-thiouracil-5-sulfonamide derivatives with biological activity. Archives of Pharmacal Research. 2002;25(3):258-69.

75. Fabrissin S, de Nardo M, Nisi C, Morasca L, Dolfini E, Franchi G. Synthesis and anticancer activity of 5-diethylaminomethyl derivatives and nitrogen mustards of uracil and 2-thiouracils. J Med Chem. 1976;19(5):639-42.

76. Kamalakannan P, Venkappayya D, Balasubramanian T. A new antimetabolite, 5-morpholinomethyl-2-thiouracil-spectral properties, thermal profiles, antibacterial, antifungal and antitumour studies of some of its metal chelates. J Chem Soc, Dalton Trans. 2002;17: 3381-91.

77. Motawia MS, Abdel-Megied AE, Pedersen EB, Nielsen CM, Ebbesen P. Synthesis of 5-alkoxymethyl derivatives of 3'-amino-2',3'-dideoxyuridine and evaluation of their activity against HIV and cancer. Acta Chem Scand. 1992;46(1):77-81.

78. Oliveri V, Vecchio G. 8-Hydroxyquinolines in medicinal chemistry: A structural perspective. Eur J Med Chem. 2016;120:252-74.

79. Song Y, Xu H, Chen W, Zhan P, Liu X. 8-hydroxyquinoline: a prilegde structure with a broad-ranging pharmacological potential. Med Chem Comm 2015;6:61-74.

80. Prachayasittikul S, Wongsawatkul O, Worachartcheewan A, Nantasenamat C, Ruchirawat S, Prachayasittikul V. Elucidating the structure-activity relationships of the vasorelaxation and antioxidation properties of thionicotinic acid derivatives. Molecules. 2010;15(1):198-214.

81. Piacham T, Isarankura Na Ayudhya C, Prachayasittikul V, Bulow L, Ye L. A polymer supported manganese catalyst useful as a superoxide dismutase mimic. Chem Commun (Camb). 2003(11):1254-5.

82. Baron EJ, Peterson LR, Finegold SM. Methods for testing antimicrobial effectiveness. In: Bailey and Scott's diagnostic microbiology, 9th ed.: St. Louis: Mosby-Year Book, Inc., 1994, pp. 168-193.

83. Shepherd RE, Zhang S, Lin FT, Kortes RA. Influence of the 5-substituent of uracils and uridines on .eta.2 coordination of RuII(hedta)-at the C-5-C-6 bonds. Inor Chem. 1992;31:1457-62.

84. Al-Masoudi NA, Saleh BA, Karim NA, Issa AY, Pannecouque C. Synthesis and anti-HIV activity of new 2-thiolumazine and 2-thiouracil metal complexes. Heteroatom Chem. 2011;22(1):44-50.

85. Yamanari K, Kida M, Fuyuhiro A, Kita M, Kaizaki S. Cobalt(III) promoted ligand fusion reactions of thiobarbituric acid and 4,6-diamino-2-thiouracil (or 4-amino-2-thiouracil). Inorg Chim Acta. 2002;332:115-22.

86. Romero MA, Sánchez MP, Quirós M, Sánchez F, Salas JM, Moreno MN, et al. Transition metal complexes of 6-amino 2-thiouracil; crystal structure of bis(6-amino-2-thiouracilato)aquazinc(II) dihydrate. Can J Chem. 1993;71:29-33.

87. Cherdtrakulkiat R, Boonpangrak S, Sinthupoom N, Prachayasittikul S, Ruchirawat S, Prachayasittikul V. Derivatives (halogen, nitro and amino) of 8-hydroxyquinoline with highly potent antimicrobial and antioxidant activities. Biochem Biophys Rep. 2016;6:135-41.

88. Shaikh S, Fatima J, Shakil S, Rizvi SM, Kamal MA. Antibiotic resistance and extended spectrum beta-lactamases: Types, epidemiology and treatment. Saudi J Biol Sci. 2015;22(1):90-101.

89. Taylor PK, Yeung AT, Hancock RE. Antibiotic resistance in Pseudomonas aeruginosa biofilms: towards the development of novel anti-biofilm therapies. J Biotechnol. 2014;191:121-30.

90. Ahmad S, Abulhamd A. Phenotypic and molecular characterization of nosocomial K. pneumoniae isolates by ribotyping. Adv Med Sci. 2015;60(1):69-75.

91. Lerner A, Adler A, Abu-Hanna J, Cohen Percia S, Kazma Matalon M, Carmeli Y. Spread of KPC-producing carbapenem-resistant Enterobacteriaceae: the importance of super-spreaders and rectal KPC concentration. Clin Microbiol Infect. 2015;21(5):470.e1-7.

92. Shah AA, Hasan F, Ahmed S, Hameed A. Extended-spectrum beta-lactamases (ESbLs): characterization, epidemiology and detection. Crit Rev Microbiol. 2004;30(1):25-32.

93. Colak A, Terzi U, Col M, Karaoglu SA, Karabocek S, Kucukdumlu A, et al. DNA binding, antioxidant and antimicrobial activities of homo- and heteronuclear copper(II) and nickel(II) complexes with new oxime-type ligands. Eur J Med Chem. 2010;45(11):5169-75.

94. Anjaneyulu Y, Rao RP, Swamy RY, Eknath A, Rao KN. In vitro antimicrobial-activity studies on the mixed ligand complexes of Hg(II) with 8-hydroxyquinoline and salicylic acids. Proceedings of the Indian Academy of Sciences - Chemical Sciences. 1982;91(2):157-63.

95. Knight JA. Review: Free radicals, antioxidants, and the immune system. Ann Clin Lab Sci. 2000;30(2):145-58.

96. Nimse SB, Pal D. Free radicals, natural antioxidants, and their reaction mechanisms. RSC Adv. 2015;5:27986–8006.

97. Miller AF. Superoxide dismutases: active sites that save, but a protein that kills. Curr Opin Chem Biol. 2004;8(2):162-8.

98. Valko M, Rhodes CJ, Moncol J, Izakovic M, Mazur M. Free radicals, metals and antioxidants in oxidative stress-induced cancer. Chem Biol Interact. 2006;160(1):1-40.

99. el-Saadani MA, Nassar AY, Abou el-Ela SH, Metwally TH, Nafady AM. The protective effect of copper complexes against gastric mucosal ulcer in rats. Biochem Pharmacol. 1993;46(6):1011-8.

100. Salama RH, Nassar AY, Nafady AA, Mohamed HH. A novel therapeutic drug (copper nicotinic acid complex) for non-alcoholic fatty liver. Liver Int. 2007;27(4):454-64.

101. Shen L, Zhang H-Y, Ji H-F. Computational note on the SOD-like antioxidant potential of nicotine–copper(II) complexes. J Mol Struc-THEOCHEM. 2007;817:161–2.

102. Congiu C, Cocco MT, Lilliu V, Onnis V. New potential anticancer agents based on the anthranilic acid scaffold: synthesis and evaluation of biological activity. J Med Chem. 2005;48(26):8245-52.

103. Lee-Manion AM, Price RK, Strain JJ, Dimberg LH, Sunnerheim K, Welch RW. In vitro antioxidant activity and antigenotoxic effects of avenanthramides and related compounds. J Agric Food Chem. 2009;57(22):10619-24.

104. Kar A, Gugnani HC, Madumere UA. Synthesis and antimicrobial activity of some anthranilic acid derivatives. Pharmazie. 1980;35(8):466-8.

105. Doungsoongnuen S, Worachartcheewan A, Pingaew R, Suksrichavalit T, Prachayasittikul S, Ruchirawat S, et al. Investigation on biological activities of anthranilic acid sulfonamide analogs. EXCLI J. 2011;10:155-61.

106. Prachayasittikul V, Pingaew R, Worachartcheewan A, Nantasenamat C, Prachayasittikul S, Ruchirawat S, et al. Synthesis, anticancer activity and QSAR study of 1,4-naphthoquinone derivatives. Eur J Med Chem. 2014;84:247-63.

107. Gouda MA. Synthesis and antioxidant evaluation of some new pyrazolopyridine derivatives. Arch Pharm (Weinheim). 2012;345(2):155-62.

108. Dennington II R, Keith T, Millam J, Eppinnett K, Hovell WL, Gilliland R. GaussView, Version 3.09; Semichem, Inc.: Shawnee Mission, KS, USA, 2003.

109. Frisch MJ, Trucks GW, Schlegel HB, Scuseria GE, Robb MA, Cheeseman JR, Scalmani G, Barone V, Mennucci B, Petersson GA, Nakatsuji H, Caricato M, Li X, Hratchian HP, Izmaylov AF, Bloino J, Zheng G, Sonnenberg JL, Hada M, Ehara M, Toyota K, Fukuda R, Hasegawa J, Ishida M, Nakajima T, Honda Y, Kitao O, Nakai H, Vreven T, Montgomery JA, Peralta JE, Ogliaro F, Bearpark M, Heyd JJ, Brothers E, Kudin KN, Staroverov VN, Kobayashi R, Normand J, Raghavachari K, Rendell A, Burant JC, Iyengar SS, Tomasi J, Cossi M, Rega N, Millam JM, Klene M, Knox JE, Cross JB, Bakken V, Adamo C, Jaramillo J, Gomperts R, Stratmann RE, Yazyev O, Austin AJ, Cammi R, Pomelli C, Ochterski JW, Martin RL, Morokuma K, Zakrzewski VG, Voth GA, Salvador P, Dannenberg JJ, Dapprich S, Daniels AD, Farkas Ö, Foresman JB, Ortiz JV, Cioslowski J, Fox DJ. Gaussian 09, Revision A.02. Gaussian, Inc., Wallingford, 2009.

110. Worachartcheewan A, Nantasenamat C, Isarankura-Na-Ayudhya C, Prachayasittikul S, Prachayasittikul V. Predicting the free radical scavenging activity of curcumin derivatives. . Chemometr Intell Lab Syst. 2011;109:207-16.

111. Talete srl. DRAGON for Windows (Software for Molecular Descriptor Calculations), version 5.5, Milano, Italy, 2007.

112. Witten IH, Frank E, Hall MA. Data Mining: Practical Machine Learning Tools and Techniques, 3rd ed.: Morgan Kaufmann, San Francisco, 2011.

113. Nantasenamat C, Isarankura-Na-Ayudhya C, Prachayasittikul V. Advances in computational methods to predict the biological activity of compounds. Expert Opin Drug Discov. 2010;5(7):633-54.

114. Amic D, Davidovic-Amic D, Beslo D, Rastija V, Lucic B, Trinajstic N. SAR and QSAR of the antioxidant activity of flavonoids. Curr Med Chem. 2007;14(7):827-45.

115. Alam MS, Ahmed JU, Lee DU. Synthesis, antibacterial, antioxidant activity and QSAR studies of novel 2-arylidenehydrazinyl-4-arylthiazole analogues. Chem Pharm Bull (Tokyo). 2014;62(12):1259-68.

116. Hanna MM. New pyrimido[5,4-e]pyrrolo[1,2-c]pyrimidines: synthesis, 2D-QSAR, anti-inflammatory, analgesic and ulcerogenicity studies. Eur J Med Chem. 2012;55:12-22.

117. Deodhar MN, Khopade PL, Varat MG. Sulfonamide based β-carbonic anhydrase inhibitors: 2D QSAR study. ISRN Med Chem. 2013;2013:1-8.

118. Abdel-Hamid MK, Abdel-Hafez AA, El-Koussi NA, Mahfouz NM. Quantitative structure-activity relationship (QSAR) studies on a series of 1,3,4-thiadiazole-2-thione derivatives as tumor-associated carbonic anhydrase IX inhibitors. J Enzyme Inhib Med Chem. 2009;24(3):722-9.

119. Eriksson L, Johansson E. Multivariate design and modeling in QSAR Chemometr Intell Lab Syst 1996;34:1-19.

120. Branham ML, Ross EA, Govender T. Predictive models for maximum recommended therapeutic dose of antiretroviral drugs. Comput Math Methods Med. 2012;2012:469769.

APPENDIX

1. **Worachartcheewan A***, Pingaew R, Lekcharoen D, Prachayasittikul S, Ruchirawat S, Prachayasittikul V. Synthesis, antioxidant and antimicrobial activities of metal complexes of 2-thiouracil-hydroxyquinoline derivatives. Letter in Drug Design & Discovery. 2017. **(Submission). (Appendix A)**
2. **Worachartcheewan A*,** Pingaew R, Doungsoongnuen S, Prachayasittikul S, Ruchirawat S, Prachayasittikul V. Antioxidant and cytotoxic activities of copper complexes of sulfonamide analogs. 2017. **(Manuscript in Preparation). (Appendix B)**
3. **Worachartcheewan A***, Nantasenamat C, Prachayasittikul S, Aiemsaard A, Prachayasittikul V. Towards the design of 3-aminopyrazole pharmacophore of pyrazolopyridine derivatives as novel antioxidants. Medicinal Chemistry Research. 2017. **(Accepted Manuscript) (Appendix C)**
4. Prachayasittikul S, Pingaew R, **Worachartcheewan A**, Sinthupoom N, Prachayasittikul V, Ruchirawat S, Prachayasittikul V. Roles of pyridine and pyrimidine derivatives as privileged scaffolds in anticancer agents. Mini-Reviews in Medicinal Chemistry. 2017;17(10):869-901. **(Appendix D)**

Send Orders for Reprints to reprints@benthamscience.ae

Letters in Drug Design & Discovery, **2017**, *14*, **000-000**

Synthesis, antioxidant and antimicrobial activities of metal complexes of 2-thiouracil-hydroxyquinoline derivatives

Apilak Worachartcheewan[a,b,c,*], Ratchanok Pingaew[d], Decha Lekcharoen[d], Supaluk Prachayasittikul[c,*], Somsak Ruchirawat[e,f] and Virapong Prachayasittikul[g]

[a]*Department of Community Medical Technology, Faculty of Medical Technology, Mahidol University, Bangkok 10700, Thailand;* [b]*Department of Clinical Chemistry, Faculty of Medical Technology, Mahidol University, Bangkok 10700, Thailand;* [c]*Center of Data Mining and Biomedical Informatics, Faculty of Medical Technology, Mahidol University, Bangkok 10700, Thailand;* [d]*Department of Chemistry, Faculty of Science, Srinakharinwirot University, Bangkok 10110, Thailand;* [e]*Laboratory of Medicinal Chemistry, Chulabhorn Research Institute, and Program in Chemical Biology, Chulabhorn Graduate Institute, Bangkok 10210, Thailand;* [f]*Center of Excellence on Environmental Health and Toxicology, Commission on Higher Education (CHE), Ministry of Education, Thailand;* [g]*Department of Clinical Microbiology and Applied Technology, Faculty of Medical Technology, Mahidol University, Bangkok 10700, Thailand*

*Address correspondence to these author at the Department of Community Medical Technology, Faculty of Medical Technology, Mahidol University, Bangkok 10700, Thailand; Tel: +662-441-4371 ext. 2720; Fax: +662-441-4380; email: apilak.woa@mahidol.ac.th and the Center of Data Mining and Biomedical Informatics, Faculty of Medical Technology, Mahidol University, Bangkok 10700, Thailand; Tel: +662-441-4371 ext. 2720; Fax: +662-441-4380; email: supaluk@g.swu.ac.th

Abstract: ***Introduction:*** Metal ions are cofactors found in antioxidant enzymes such as superoxide dismutase (SOD), and are essential in catalytic mechanisms for scavenging the free radicals. Therefore, synthetic compounds containing metal ions coordination are designed for SOD mimic and other biological activities.

Objective: To synthesize metal metals (Ni, Cu, Mn) complexes of mixed ligands of 2-thiouracil (2TU) with 8-hydroxyquinoline (8HQ) (**1**-**3**) and with 2-hydroxyquinoline (2HQ) (**4**-**6**) and determined for antioxidant and antimicrobial activities.

Results: The metal complexes **1**-**6** elicited SOD activity with IC_{50} of 1.81-516.56 µM, particularly, complex **5** (2TU-Cu-2HQ) showed the highest SOD activity with IC_{50} of 1.81 µM. In addition, complexes **1** (2TU-Ni-8HQ), **5** and **2** (2TU-Cu-8HQ) displayed radical scavenging activity (RSA) with IC_{50} of 171.31, 194.25 and 388.56 µM, respectively, whereas the complexes **3**, **4** and **6** were shown to be inactive. Furthermore, the metal complex **3** (2TU-Mn-8HQ) exhibited good antimicrobial activity with the minimal inhibitory concentration (MIC) range of 11.07-708.64 µM against gram-positive and gram negative bacteria as well as diploid fungus, followed by metal complexes **2** (MIC of 23.68-757.70 µM) and **1** (MIC of 350.67-701.35 µM). Interestingly, the similar mixed ligands with different metal ions of complexes **1** (Ni), **2** (Cu) and **3** (Mn), the complex **3** has the highest SOD (IC_{50} = 5.04 µM) and antimicrobial activities, but Cu complex (**5**) of 2TU and 2HQ showed the highest SOD, RSA and antimicrobial activities than Ni (**4**) and Mn (**6**) complexes.

Conclusion: This finding reveals novel transition metal complexes with a potential for further development as medicinal compounds.

Keywords: 2-thiouracil, 2- and 8-hydroxyquinolines, metal complex, antioxidants, antimicrobials

1. INTRODUCTION

Free radicals are a risk factor of various diseases such as diabetes mellitus, cancer as well as cardiovascular and neurodegenerative diseases [1-2]. Biological molecules in the body such as lipid, protein and deoxyribonucleic acid (DNA) can be damaged by the free radicals. The endogenous defense mechanisms against the free radicals can be overcomed by antioxidant enzymes i.e., superoxide dismutase (SOD), catalase and glutathione peroxidase. In addition, antioxidant compounds can be obtained from external sources i.e., supplement and dietary vitamins A, C and E [3-4]. However, an excess of the free radicals in the body can cause undesirable effects leading to physiological changes and eventually to clinical symptoms and diseases [1-2]. Therefore, antioxidant compounds can be recommended to reduce/neutralize the overload of free radicals for preventing a progression of the diseases. Interestingly, the SOD is an essential enzyme for catalyzing the dismutation of superoxide anion into oxygen and hydrogen peroxide. Considering the SOD structure, it composes of transition

XXX-XXX/14 $58.00+.00

metal ions such as manganese (Mn) found in mitochondria, zinc (Zn) and copper (Cu) found in cytosol, iron (Fe) and nickel (Ni) found in bacteria [5-7]. These metal ions are important cofactors for exerting the SOD activity, and are essential for catalytic mechanisms. Therefore, synthetic compounds containing metal ion coordination are attractive for designing SOD-like activity as well as other pharmacological activities.

Uracil is a heterocyclic compound acting as a nucleobase found in nucleic acid. The uracil and its derivatives were reported to display biological activities i.e., antioxidant [8], antimicrobial [9], anticancer [10] and antiviral [11] properties. Uracils possessing halogen substituents [12] were reported to exhibit interesting bioactivities i.e., 5-fluorouracil as anticancer drug [13] and antimetabolites [14] including N1-substituted derivatives of 5-iodouracil and 5-trifluoromethyluracil [15] are antivirals [16]. Furthermore, a series of thiouracil derivatives have been shown to exhibit diverse bioactivities such as antioxidant, antimicrobial and anticancer activities [17-19]. It is noted that substituted uracils play a vital role in many metabolic processes [20-22]. Therefore, considerable interest has been drawn to use uracils (constitutes two oxygen (O) and two nitrogen (N) atoms) as ligands for the synthesis of various transition metal complexes [23-24].

Quinoline is a bicyclic compound with a variety of pharmacological properties such as antibacterial [25], anticancer [26] and antiviral [27] activities. Quinoline derivatives, for example, 8-hydroxyquinoline (8HQ) exhibited various bioactivities such as fungicidal, antibacterial and anticancer activities [28-30]. The 8HQ is a ligand bearing O and N electron donor atoms with metal chelating effect [28]. It is found in natural products, therapeutics/compounds and chelating agents [28]. It has been reported to display strong antioxidant, cytotoxic and antimicrobial activities [23, 31]. In addition, 2-hydroxyquinoline (2HQ) is an isomeric from of 8HQ that can form coordinated bond with metal ions. Synthetic fluoroquinolones mixed-ligands Cu (II) complexes were reported to display antimicrobial, antioxidant and DNA cleavage activities [32]. Furthermore, metal complexes of 8HQ with 5-iodouracil/5-nitrouracil exhibited cytotoxic, antimicrobial, antioxidant and aromatase inhibitory activities [23, 24, 31].

To search for novel uracil-quinoline metal complxes, therefore, 2-thiouracil (2TU) and hydroxyquinoline (HQ) including 8HQ and 2HQ were used as potential ligands for the synthesis of metal complexes. Herein, the synthesis of mixed ligands (2TU-8HQ/2HQ) transition metals (Ni, Cu, Mn) complexes as well as antimicrobial and antioxidant activities have been reported.

2. MATERIALS AND METHOD

2.1. General

Infrared (IR) spectra were obtained on a Perkin Elmer System 2000 FTIR. Mass spectra were recorded on a Finnigan INCOS50 and a Bruker Daltonics (Micro TOF). Magnetic moment was performed on a Magnetic Susceptibility Balance, Mark 1, Serial 15257, Sherwood Scientific, Cambridge, UK. Melting points were determined on an Electrothermal melting point apparatus and are uncorrected. Reagents for assays included HEPES (*N*-2-hydroxyethylpiperazine-*N*′-2-ethanesulfonic acid), vitamin E, DPPH (2,2-diphenyl-1-picrylhydrazyl), nitroblue tetrazolium (NBT) salt, L-methionine, riboflavin, Triton-100, superoxide dismutase (SOD) from bovine erythrocytes, DMSO (dimethyl sulfoxide, 99.9%) and ampicillin from Sigma, USA; Müeller Hinton Broth and Müeller Hinton Agar from Becton Dickinson, USA and sodium chloride from Merck, German. Solvents were analytical grades.

2.2. Synthesis of 2-thiouracil and 8-hydroxyquinoline/2-hydroxyquinoline metal complexes

A solution of metal salts (1 mmol) dissolved in methanol (2 mL) was added dropwise to the solution of 2-thiouracil (1 mmol) in 70°C methanol (30 mL) and then heated for 45 min. A solution of 8HQ/2HQ (1 mmol) in methanol (2 mL) was added dropwise to the reaction mixture and further heated for 1 h. The precipitated solid was collected by filtration, washed 4-5 times with cold methanol and dried *in vacuo* at room temperature.

Complexes **1**-**3** were separately synthesized from 1 mmol of 2TU (128.2 mg) and 8HQ (145.2 mg) and 1 mmol of metal salts; $Ni(OAc)_2{\cdot}4H_2O$ (248.9 mg) for **1**, $Cu(OAc)_2{\cdot}H_2O$ (199.8 mg) for **2** and $MnCl_2{\cdot}4H_2O$ (198.1 mg) for **3**.

Complexes **4**-**6** were obtained from 1 mmol of 2TU (128.2 mg) and 2HQ (145.2 mg) and 1 mmol of $Ni(OAc)_2{\cdot}4H_2O$ for **4**, of $Cu(OAc)_2{\cdot}H_2O$ for **5** and of $MnCl_2{\cdot}4H_2O$ for **6**. Yield and m.p. of the complexes are summarized: **1** as light yellow-green powder ($C_{13}H_{12}N_3NiO_4S$, MW 365.01 g/mol), 226.0 mg (61.9%), m.p. 282-284°C, **2** as dark green powder ($C_{13}H_{12}CuN_3O_2S$, MW 337.86 g/mol), 123.2 mg (36.9%), m.p.> 350°C, **3** as pale yellow powder ($C_{13}H_{12}MnN_3O_4S$, MW 361.25 g/mol), 120.4 mg (33.31%), m.p. 296-300°C, **4** as light yellow-green powder ($C_{13}H_{12}N_3NiO_2S$, MW 333.01 g/mol), 251.8 mg (75.6%), m.p. 230-234°C, **5** as light green powder ($C_{13}H_{12}CuN_3O_2S$, MW 337.86 g/mol), 181.8 mg (53.8%), m.p. 284-288°C, **6** as pale yellow powder ($C_{13}H_{12}MnN_3O_2S$, MW 329.26 g/mol), 130.2 mg (39.5%), m.p. 286-290°C.

2.3. Antioxidant activity

Antioxidant activities of metal complexes (**1**-**6**) and ligands were evaluated using 1,1-diphenyl-2-picrylhydrazyl (DPPH) and superoxide dismutase (SOD) assays.

DPPH is a stable purple color compound, which reacted with antioxidants to give light-yellow color product of 1,1-diphenyl-2-picrylhydrazine. Briefly, the reaction was performed by adding 1 mL solution of DPPH in methanol (0.1 mM) to the tested compounds (dissolved in DMSO) with the final concentration of 300 μg/mL. The reaction was incubated in a dark room for 30 min, and the absorbance was measured at 517 nm using UV-Visible spectrophotometer (UV-1610, Shimadzu). The percentage of antioxidant or radical scavenging activity (RSA) was calculated [33] using equation (1):

$$\text{RSA (\%)} = \left[1 - \frac{Abs._{sample}}{Abs._{control}}\right] \times 100 \quad (1)$$

where $Abs._{control}$ is the absorbance of the control reaction, and $Abs._{sample}$ is the absorbance of the tested compound. Vitamin E was used as a control and methanol was used as a blank reaction.

SOD activity was determined using SOD assay by measuring nitro blue tetrazolium (NBT) reduction [34]. The stock solution (1 mL) containing 27 mL of HEPES buffer (50 mM, pH 7.8), 1.5 mL of L-methionine (30 mg/mL), 1 mL of NBT (1.41 mg/mL) and 750 µL of Triton X-100 (1 %wt) was added to the solution of metal complexes (**1**-**6**) dissolved in DMSO. The reaction was initially started by adding10 µL of riboflavin (44 mg/mL) to the tested compounds with final concentration of 300 µg/mL, and followed by illumination under a Philips Classic Tone lamp (60 W) in a light box for 7 min. The absorbance of the reaction was measured at 550 nm using UV-Vis spectrophotometer that measured the inhibition of photoreduction of NBT. The percentage of SOD activity was calculated using Eq. (1). The SOD enzyme from bovine erythrocytes was used as a control and DMSO solvent was used as a blank reaction.

The 50% inhibition concentration (IC_{50}) was calculated in case of compounds displayed antioxidant (RSA and SOD) activities greater than 50% at 300 µg/mL. It was calculated by plotting %RSA or %SOD activity against metal complexes concentrations.

2.4. Antimicrobial activity

Antimicrobial activity testing of metal complexes (**1**-**6**) and ligands was investigated by the agar dilution method [35]. In parallel, Müeller Hinton Broth (MHB), DMSO and ampicillin drug were used as the control in this study. The solution of tested compounds was then transferred to the Müeller Hinton Agar (MHA) solution with final concentrations of 4-256 µg/mL. The microorganisms were cultured in MHB at 37°C overnight, and then were diluted with 0.9% normal saline for adjusting the density of microorganism as 1×10^8 cell/mL compared to 0.5 McFarland standards. The microorganisms were inoculated onto the agar plates containing various concentrations of the tested compounds, and incubated at 37°C for 24-48 h. The minimum inhibitory concentration (MIC) of the compounds was determined as the lowest concentration to inhibit the growth of microorganisms. Twenty-seven microorganisms (reference strains and clinical isolates) were used for the assay including **Gram negative bacteria**; *Escherichia coli* ATCC 25922, *Klebsiella pneumoniae* ATCC 700603, *Serratia marcescens* ATCC 8100, *Salmonella typhimurium* ATCC 13311, *Salmonella choleraesuis* ATCC 10708, *Pseudomonas aeruginosa* ATCC 15442, *Pseudomonas stutzeri* ATCC 17587, *Shewanella putrefaciens* ATCC 8071, *Achromobacter xylosoxidans* ATCC 27061, and clinical strains: *Shigella dysenteriae*, *Salmonella enteritidis*, *Morganella morganii*, *Aeromonas hydrophila*, *Citrobacter freundii* and *Plesiomonas shigelloides*, **Gram positive bacteria**; *Staphylococcus aureus* ATCC 29213, *Staphylococcus aureus* ATCC 25923, *Staphylococcus epidermidis* ATCC 12228, *Enterococcus faecalis* ATCC 29212, *Enterococcus faecalis* ATCC 33186, *Micrococcus luteus* ATCC 10240, *Corynebacterium diphtheriae* NCTC 10356, *Bacillus subtilis* ATCC 6633, and clinical strains: *Bacillus cereus* and *Listeria monocytogenes*, and **diploid fungus** (yeast); *Candida albicans* ATCC 90028 and *Saccharomyces cerevisiae* ATCC 2601.

3. RESULTS AND DISCUSSION

3.1. Chemistry

Metal complexes **1**-**6** (Fig. 1) were synthesized using 1:1:1 molar ratio of 2TU:M:8HQ (2HQ) in which M = Ni (**1** and **4**), Cu (**2** and **5**) and Mn (**3** and **6**). These complexes appeared as pale yellow-green to dark green powder.

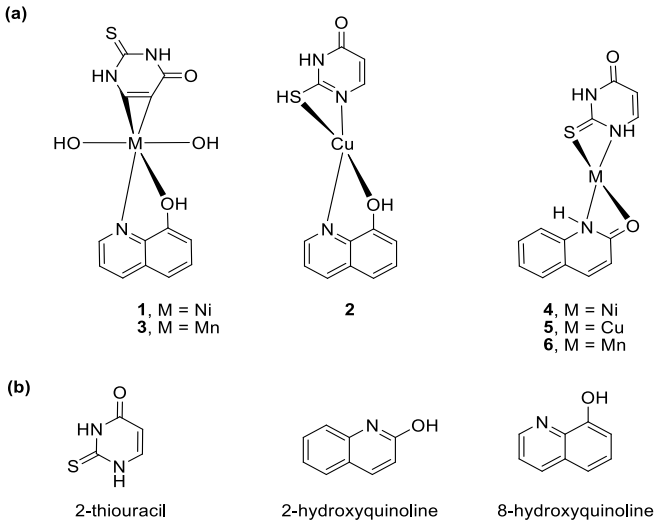

Fig. (1). Chemical structures of 2-thiouracil-hydroxyquinolines metal complexes **1**-**6** (a) and ligands (b).

IR spectra (Table 1) of 2TU-8HQ metal complexes **1** (Ni) and **3**(Mn) showed absorptions (cm^{-1}) of CO at 1701-1702 and 1686, of C=S at 1422-1424, of C=N at 1629 and 1572-1578, of C–N at 1388 and 1368-1374, of C–O at 1281-1285, 1213-1214 and 1108-1111. These absorptions of compounds **1** and **3** remained the same as the absorptions of 2TU free ligand, except for the stretchings of C-N and C-O at 1388 and 1281-1285 were shifted from 1381 and 1286 of 8HQ, respectively. This suggested that metal centered atoms (Ni and Mn) coordinated with C5,6 double bond π donor of 2TU, together with electron donor ring N atom and OH group of 8HQ. It was again confirmed by the absence of OH bending (δOH) at 1410 of 8HQ. However, NH bending of 2TU remained the same as the δNH of 2TU free ligand. Magnetic moments of metal complexes **1** and **3** were 2.70 and 3.40 B.M., respectively. It was suggested that metal complexes **1** and **3** were formed as octahedral geometry using bidentate ligands (2TU and 8HQ) and two water molecules as shown by broad OH stretchings at 3358 and 3400.

Such π electron donor coordination was reported for metal complexes of uracils such as 5-iodouracil-8HQ/8-aminoquinoline metal (Mn, Cu, Ni) complexes [23, 36] and Ru complexes of 5-substituted (X) uracils, X = F, Cl, Br, I and H [37].

Copper complex of 2TU-8HQ (**2**) showed the absorptions of CO at 1693, of C=N at 1625 and 1575, of C–N at 1386 and 1375, and of NH at 3178 as well as the weak bending δNH at 1527. These absorptions of Cu-complex (**2**) were shifted compared with the free ligands (2TU and 8HQ). Apparently, only one strong CO of 2TU moiety was noted at 1693. In addition, C=S of complex **2** was not observed. These suggested that Cu-complex **2** was resulted from the coordination of 2TU through N1, S2 (as thiol form), and 8HQ using ring N-atom and 8OH group. This N1, S2 coordination complex was described for 2-thiolumazine Cu-complex [38]. The complex **2** had μ_{eff} value of 1.315 B.M., which was suggested as a square planar geometry.

Metal complexes (**4**-**6**) displayed the stretching absorptions of CO at 1701, 1962, 1682-1684 and 1654, of C=N at 1628, 1637-1638 and 1600-1601, of C=S at 1425-1428, of C–N at 1395-1396, and NH at 3122-3126. These absorptions were shifted from the free ligands (2TU and 2HQ), suggesting that metal complexes **4**-**6** were formed through the coordinations of 2TU using thione (C=S) and NH electron donors, and of 2HQ using amino keto form of 2-quinolinol. Metal complex formation via amino thione electron donors was previously reported for 6-hydroxy-2-thiouracil (thiobarbituric acid) [39] and 6-amino-2-thiouracil [40]. In addition, the amino keto form involved in metal complexation was previously described for 2-pyridinol metal complex [41]. Magnetic moments of complexes **4**-**6** were 0.953, 0.807 and 0.794, respectively. The results suggested that Ni (**4**), Cu (**5**) and Mn (**6**) complexes were formed as a square planar geometry. Based on the literature, metal complexes **1**-**6** have not been reported. Antimicrobial and antioxidants activities of these compounds (**1**-**6**) were investigated.

Table 1. IR spectra (cm^{-1}) and μ_{eff} (B.M) of 2-thiouracil-hydroxyquinolines metal complexes (**1**-**6**).

Compound	νC=O	νC=N	νC=S	νC-O	νC-N	νOH	νNH	δOH	δNH	μ_{eff}
2-TU-Ni-8HQ (**1**)	1701s 1686s	1629vw 1578s	1424s	1285m 1214s 1111s	1388m 1374s	3358s,br	3196br 3087sh, br	1470s	1560m, br 745s	2.70
2-TU-Cu-8HQ (**2**)	1693s	1625m 1575m	—	1280m 1113s	1386s 1375s	—	3178w, br	1464s	1527w 741m	1.315
2-TU-Mn-8HQ (**3**)	1702s 1686s	1629w 1572s	1422s	1281w 1213s 1108m	1388s 1368w	3400br	3192sh, br 3135sh, br	1466s	1562s 743m	3.40
2-TU-Ni-2HQ (**4**)	1701s, br 1682s, br 1654s, br	1628s, br 1600vw, sh	1425s	1216s 1177s, br 1153s, br	1395s	—	3122s, br	1451s	1558w, br 1539w, br 761s	0.953
2-TU-Cu-2HQ (**5**)	1692m 1654s	1638s 1601m	1428s	1202m 1171w 1153w	1396w	—	3124w, sh	1449w	1559w 1543w 756s	0.807
2-TU-Mn-2HQ (**6**)	1701m 1684m 1654s	1637s 1601m	1428s	1214s 1175w 1154w	1396m	—	3126w, sh	1469m	1559s 758s	0.794
2-TU	1700s 1684s	1628m	1421s	1214s 1176s 1158s	1394m	3510br	3086br 3048br	1450m	1560s 761s	—
2HQ	1652s, br	1599s, br	—	1213s 1154m 1135s	1381s	—	3255w, sh	1428s	1554s 759vs	—
8HQ	—	1580m	—	1286s	1381s	3145br	—	1410s	—	—

Note: 2-TU = 2-thiouracil, 2HQ = 2-hydroxyquinoline, 8HQ = 8-hydroxyquinoline, br = broad, m = medium, s = strong, sh = sharp, vs = very strong, vw = very weak and w = weak.

3.2 Antioxidative activity

The metal complexes **1**-**6** and ligands (2TU, 2HQ and 8HQ) were investigated for their antioxidative activities using DPPH and SOD assays in term of radical-and superoxide-scavenging activities. The results (Table **2**) showed that compounds **1, 2**, **5** and 8HQ displayed the radical scavenging activity (RSA) with IC_{50} of 171.31, 388.56, 194.25 and 1113.75 μM, respectively, whereas compounds **3**, **4**, **6**, 2TU and 2HQ exhibited RSA <50% (24.56%, 34.92%, 21.68%, 33.00% and 10.10%, respectively) at 300 μg/mL. Compounds **1** (IC_{50} = 171.31 μM) and **5** (IC_{50} = 194.25 μM) showed stronger RSA than compound **2** (IC_{50} = 388.56 μM) and free ligands such as 8HQ (IC_{50} = 1113.75 μg/mL).

SOD activity of the metal complexes (**1**-**6**) was determined using NBT reduction. Most complexes (Table 2) exhibited good SOD activity with IC_{50} range of 1.81-69.07 μM, except for Mn complex (**6**, IC_{50} = 516.56 μM). Interestingly, Cu complex **5** afforded the strongest SOD activity with IC_{50} of 1.81μM followed by **3**>**2**>**1**>**4**>**6** with IC_{50} = 5.04, 10.06, 15.73, 69.07 and 516.56 μM, respectively. In a series of 2TU-8HQ metal complexes (**1**-**3**), Mn complex **3** (IC_{50} = 5.04 μM) displayed the strongest SOD activity. However, Cu complex (**5**, IC_{50} = 1.81 μM) of 2TU-2HQ was shown to be the most active antioxidant

compared with the other tested compounds. In addition, 8HQ showed SOD activity with IC_{50} of 91.83 µM, but other ligands including 2TU (28.70%) and 2HQ (25.19%) displayed weak activity <50% at 300 µg/mL. The results indicated that types of ligands and metal ions for metal coordination played roles in antioxidant activities.

Table 2. Antioxidant activities of 2-thiouracil-hydroxyquinolines metal complexes (**1**-**6**) and ligands.

Compound[a]	Radical scavenging activity (IC_{50}, µM)	Superoxide scavenging activity (IC_{50}, µM)
2-TU-Ni-8HQ (**1**)	171.31	15.73
2-TU-Cu-8HQ (**2**)	388.56	10.06
2-TU-Mn-8HQ (**3**)	ND	5.04
2-TU-Ni-2HQ (**4**)	ND	69.07
2-TU-Cu-2HQ (**5**)	194.25	1.81
2-TU-Mn-2HQ (**6**)	ND	516.56
2TU	ND	ND
2HQ	ND	ND
8HQ	1113.75	91.83

[a] Vitamin E was used as a control for DPPH assay displaying IC_{50} = 1.40 µM, [b]superoxide dismutase (SOD) from bovine erythrocytes was used as a control for SOD assay showing IC_{50} = 0.021 µM. Complexes **3**, **4**, **6** and ligands (i.e., 2TU and 2HQ) exhibited RSA <50% at 300 µg/mL (24.56%, 34.92%, 21.68%, 33.00% and 10.10%, respectively). The 2TU and 2HQ showed SOD activity <50% at 300 µg/mL (28.70% and 25.19%, respectively). ND = not determined.

3.3 Antimicrobial activity

The antimicrobial activity of metal complexes (**1**-**6**) was performed using the agar dilution method against 27 strains of microorganisms. The results (Table 3) showed that compounds **1**-**3** exerted antimicrobial activity, whereas complexes **4**-**6** were inactive compounds. Complex **1** (Ni) displayed antimicrobial activity against gram positive bacteria: *S. aureus* ATCC 29213, *S. aureus* ATCC 25923, *E. faecalis* ATCC 29212, *E. faecalis* ATCC 33186, *M. luteus* ATCC 10240, *B. subtilis* ATCC 6633, *C. diphtheriae* NCTC 10356, and *B. cereus* as well as gram negative bacteria: *C. fluendii* with MIC of 701.35 µM. At lower MIC (350.67 µM), *S. epidermidis* ATCC 12228 and *P. shigelloides* were inhibited. Interestingly, complexes **2** (Cu) and **3** (Mn) showed better antimicrobial property with a range of MIC values 23.68-757.70 µM and 11.07-708.64 µM, respectively. Compound **2** showed antigrowth activity with MIC of 757.70 µM against gram negative bacteria: *S. putrefaciens* ATCC 8071 and *M. morganii*, with MIC of 378.85 µM against *E. coli* ATCC 25922, *S. macesens* ATCC 8100, *S. typhimurium* ATCC 13311, and *C. fluendii*, with MIC of 189.43 µM for *S. cerevisiae* ATCC 2601 and *A. hydrophila*, with MIC of 94.71 µM against *S. aureus* ATCC 25923, *E. faecalis* ATCC 29212, *E. faecalis* ATCC 33186, *M. luteus* ATCC 10240, *C. diphtheriae* NCTC 10356, *B. cereus* and *L. monocytogenes*, with MIC of 47.36 µM against *S. aureus* ATCC 29213 and *B. subtilis* ATCC 6633, and with MIC of 23.68 µM against *S. epidermidis* ATCC 12228 and *P. shigelloides*. Complex **3** (Mn) showed activity against *E. coli* ATCC 25922, *P. stutzeri* ATCC 17587, *S. putrefaciens* ATCC 8071, *A. xylosoxidans* ATCC 27061, *M. luteus* ATCC 10240 and *C. fluendii* with MIC of 708.64 µM, against *S. dysenteriae* with MIC of 354.32 µM, against *S. cerevisiae* ATCC 2601 with MIC of 88.56 µM, against *E. faecalis* ATCC 29212, *E. faecalis* ATCC 33186, *B. subtilis* ATCC 6633, *C. diphtheriae* NCTC 10356, *B. cereus* and *L. monocytogenes* with MIC of 44.29 µM, against *S. aureus* ATCC 29213, *S. aureus* ATCC 25923 and *S. epidermidis* ATCC 12228 with MIC of 22.15 µM, and against *P. shigelloides* with MIC of ≤11.07 µM. In addition, the free ligands (2TU, 8HQ and 2HQ) were also investigated for growth inhibition. It was shown that 2HQ had no activity against the tested microorganisms, but 2TU inhibited only *M. luteus* ATCC 10240 with MIC = 1997.62 µM. However, 8HQ showed antimicrobial activity (MIC = ≤27.56-1763.60 µM) against gram positive and gram negative bacteria as well as dipoid fungi [31, 42]. Particularly, the resistant gram positive bacteria such as *S. aureus* ATCC 29213 and *S. aureus* ATCC 25923 displayed the activity with MIC ≤27.56 µM. At higher MIC value (220.45 µM), *E. coli* ATCC 25922, *S. typhimurium* ATCC 13311, *P. stutzeri* ATCC 17587 and *C. fluendii* were inhibited by 8HQ. In addition, 8HQ also showed antigrowth activity against *K. pneumoniae* ATCC 700603 (MIC = 440.90 µM) and *P. aeruginosa* ATCC 15442 (MIC = 1763.60 µM). Moreover, *P. shigelloides* was inhibited by 8HQ with the lowest MIC (≤27.56 µM). It should be noted that Cu complex **2** (MIC = 23.68 µM against *S. epidermidis* ATCC 12228 and *P. shigelloides*), and Mn complex **3** (MIC = 22.15 µM against *S. aureus* ATCC 29213, *S. aurues* ATCC 25923 and *S. epidermidis* ATCC 12228, MIC ≤11.07 µM against *P. shigelloides*) exerted better activity than the reference drug, ampicillin (MIC = 26.93 µM). Furthermore, all active compounds (**1**-**3** and 8HQ) expressed higher growth inhibition against gram positive bacteria than gram negative bacteria. Notably, it was found that 2TU-8HQ metal complexes (**1**-**3**) showed better antimicrobial activity than 2TU- 2HQ metal complexes (**4**-**6**). Particularly, compounds

2 (Cu) and **3** (Mn) displayed higher activity than compound **1** (Ni). In case of 2TU-2HQ metal complexes (**4**-**6**), all compounds exhibited no antimicrobial activity. In addition, the DMSO solvent was determined in parallel with the tested compounds, but no antimicrobial activity was observed.

Table 3 Antimicrobial activity of 2-thiouracil-hydroxyquinolines metal complexes (**1**-**6**) and ligands.

Compound	MIC (μM)[a]	Microorganism[b]
2-TU-Ni-8HQ (**1**)	701.35	*S. aureus* ATCC 29213, *S. aureus* ATCC 25923, *E. faecalis* ATCC 29212, *E. faecalis* ATCC 33186, *M. luteus* ATCC 10240, *B. subtilis* ATCC 6633, *C. diphtheriae* NCTC 10356, *B. cereus, C. fluendii*
	350.67	*S. epidermidis* ATCC 12228, *P. shigelloides*
2-TU-Cu-8HQ (**2**)	757.70	*S. putrefaciens* ATCC 8071, *M. morganii*
	378.85	*E. coli* ATCC 25922, *S. macesens* ATCC 8100, *S. typhimurium* ATCC 13311, *C. fluendii*
	189.43	*S. cerevisiae* ATCC 2601, *A. hydrophila*
	94.71	*S. aureus* ATCC 25923, *E. faecalis* ATCC 29212, *E. faecalis* ATCC 33186, *M. luteus* ATCC 10240, *C. diphtheriae* NCTC 10356, *B. cereus, L. monocytogenes*
	47.36	*S. aureus* ATCC 29213, *B. subtilis* ATCC 6633,
	23.68	*S. epidermidis* ATCC 12228, *P. shigelloides*
2-TU-Mn-8HQ (**3**)	708.64	*E. coli* ATCC 25922, *P. stutzeri* ATCC 17587, *S. putrefaciens* ATCC 8071, *A. xylosoxidans* ATCC 27061, *M. luteus* ATCC 10240, *C. fluendii*
	354.32	*S. dysenteriae*
	88.56	*S. cerevisiae* ATCC 2601
	44.29	*E. faecalis* ATCC 29212, *E. faecalis* ATCC 33186, *B. subtilis* ATCC 6633, *C. diphtheriae* NCTC 10356, *B. cereus, L. monocytogenes*
	22.15	*S. aureus* ATCC 29213, *S. aureus* ATCC 25923, *S. epidermidis* ATCC 12228
	≤11.07	*P. shigelloides*
2-TU-Ni-2HQ (**4**)	Inactive	-
2-TU-Cu-2HQ (**5**)	Inactive	-
2-TU-Mn-2HQ (**6**)	Inactive	-
2-TU	1997.62	*M. luteus* ATCC 10240
2HQ	Inactive	-
8HQ	1763.60	*P. aeruginosa* ATCC 15442
	440.90	*K. pneumoniae* ATCC 700603, *S. choleraesuis* ATCC 10708, *M. morgamii*
	220.45	*E. coli* ATCC 25922, *S. macesens* ATCC 8100, *S. typhimurium* ATCC 13311, *P. stutzeri* ATCC 17587, *S. putrefaciens* ATCC 8071, *A. xylosoxidans* ATCC 27061, *S. enteridis, C. fluendii*
	110.22	*A. hydrophila*
	55.11	*M. lutens* ATCC 10240
	≤27.56	*S. aureus* ATCC 29213, *S. aureus* ATCC 25923, S. *epidermidis* ATCC 12228, *E. faecalis* ATCC 29212, *E. faecalis* ATCC 33186, *B. subtilis* ATCC 6633, C. *diphtheriae* NCTC 10356, *S. cerevisiae* ATCC 2601, *C. albicans* ATCC 90028, *S. dysenteriae, B. cereus, P. shigelloides, L. monocytogenes*

[a]MIC : Minimum inhibitory concentration is the lowest concentration of a compound to inhibit growth of microorganisms. [b]Ampicillin at 26.93 μM was used as a control of antimicrobial testing system that showed growth inhibiton against *S. typhimurium* ATCC 13311, *P. stutzeri* ATCC 17587, *C. diphtheriae* NCTC 10356, *S. aureus* ATCC 29213, *S. aureus* ATCC 25923, *S. epidermidis* ATCC 12228, *M. luteus* ATCC 10240, *B. subtilis* ATCC 6633, *L. monocytogenes* and *P. shigelloides.*

An increase of antibiotic resistance in bacteria, causing either community-acquired infections or hospital-acquired infections, is a major health problem worldwide. Particularly, an attention has been focused on the multiple resistant pathogen i.e., *E. coli*, *K. pneumoniae* and

methicillin-resistant *Staphylococcus aureus* (MRSA) [31, 43].

Currently, *P. aeruginosa* which is the common cause of nosocomial infection has been reported to generate multidrug resistance because of its biofilm synthesis [44]. *K. pneumoniae* was found to be a causative agent of pneumonia, and a pathogen of septicemia in patients [45]. The spread of *K. pneumoniae* carbapenemase (KPC) emerged in many countries has been reported [46].

There are many drug-resistant strains found in gram positive bacteria such as MRSA, vancomycin-resistant Enterococci (VRE) and penicillin-resistant *S. pneumoniae* (PRSP), and in gram negative bacteria i.e., extended spectrum β-lactamase (ESBL), AmpC β-lactamase and carbapenemase-producing Enterobacteriaceae (CPE) [42]. ESBLs are enzymes capable of hydrolysing penicillins, broad spectrum cephalosporin and monobactams, and are generally derived from TEM and SHV-type enzymes [47]. ESBL producing organisms are *K. pneumoniae*, *P. aeruginosa*, *E. coli*, *P. stutzeri*, *S. typhimurium* and *C. fruendii* [43, 47].

Interestingly, 2TU-8HQ metal complexes (**1**-**3**) exerted the activity against resistant gram positive (*S. aureus*) and gram negative ESBL (*E. coli*, *S. typhimurium*, *P. stutzeri* and *C. fluendii*) bacteria. The higher activity against gram positive bacteria was noted for Mn (**3**) complex, and against gram negative bacteria was noted for Cu (**2**) complex. The results implied the potential of Cu (**2**) and Mn (**3**) complexes as antimicrobials for resistant *S. aureus* and ESBL producing organisms, respectively. On the other hand, the strongest antioxidant (SOD) activity was noted for 2TU-2HQ Cu complex (**5**) with IC_{50} of 1.81 µM.

The strongest SOD activity was noted for metal complex of 2TU-2HQ ligands compared with 2TU-8HQ metal complexes. It could be suggested that an inductive effect of both ligands, 2TU (4-oxo function) and 2HQ (2-oxo moiety), can withdraw electrons from the Cu centered atom (compound **5**) and facilitate the superoxide scavenging activity [23]. In case of 2TU-8HQ, the inductive effect was resulted from one ligand (2TU) using 4-oxo group (compounds **1** and **3**), and using 2-thioimine moiety conjugated with α, β-unsaturated keto (compound **2**) as the superoxide scavenger. Metal complexes with the same ligands, but different metal ions would provide the compounds with different bioactivity [48] as seen for compounds **1**-**3** (**3**>**2**>**1**) and compounds **4**-**6** (**5**>**4**>**6**). In a series of 2TU-8HQ (**1**-**3**), Mn complex (**3**) afforded the strongest SOD activity (IC_{50} = 5.04 µM), whereas 2TU-2HQ Mn complex (**6**) displayed the lowest SOD activity (IC_{50} = 516.56 µM). Besides the property of ligands, metal centered atom also played important role in bioactivities of metal complexes [23]. Cu is essential for SOD activity [49], therefore, an incorporation of Cu into the ligand structures (2TU and 2HQ) increased the SOD activity as observed for Cu complex **5**. This is due to the change in oxidation state of Cu atom modulated through its coordination with metal chelating ligands [41].

However, dissociation of the metal complexes (**1**-**6**) could give rise to 1:1 charged complexes, $(8HQ\text{-}M)^+$ and $(2HQ\text{-}M)^+$, and free ligand (2TU) [50]. The charged complexes ($(8HQ\text{-}M)^+$ and $(2HQ\text{-}M)^+$) became toxic entity by interacting and blocking the metal binding sites on enzymes that involved in the pteridine biosynthesis [50]. This can account for antimicrobial activity of complexes **1**-**3** compared with complexes **4**-**6**. It is possibly due to $(8HQ\text{-}M)^+$ of metal complexes **1**-**3** bearing 8HQ with the antimicrobial effect. Inversely, 2HQ was inactive compound, thus, metal complexes **4**-**6** exerted no antimicrobial activity.

CONCLUSION

Novel metal (Ni, Cu, Mn) complexes of 2TU-8HQ (**1**-**3**) and 2TU-2HQ (**4**-**6**) were synthesized and investigated for antimicrobial and antioxidant (DPPH and SOD) activities. These metal complexes contanined 2TU as a common ligand, but different 8HQ or 2HQ ligands. These metal complexes exerted SOD activity, particularly, Cu complex **5** bearing 2HQ displayed the strongest SOD activity with IC_{50} of 1.81 µM. The Mn complex **3** bearing 8HQ exhibited good antimicrobial activity against gram-positive and gram negative bacteria as well as diploid fungus with MIC of 11.07-708.64 µM. This finding revealed the novel bioactive mixed ligand transition metal complexes with SOD-mimic and antimicrobial activities, and has a potential for further development as medicinal compounds.

LIST OF ABBREVIATIONS

2HQ	=	2-Hydroxyquinoline
2TU	=	2-Thiouracil
8HQ	=	8-Hydroxyquinoline
MIC	=	minimum inhibitory concentration
RSA	=	Radical scavenging activity
SOD	=	Superoxide dismutase

CONFLICT OF INTEREST

The authors confirm that this article content has no conflict of interest.

ACKNOWLEDGEMENTS

AW gratefully acknowledges the research grant supported by the Thailand Research Fund (Grant No. TRG5880143) and this project is partially supported by the Office of the Higher Education Commission and Mahidol University under the National Research Universities Initiative.

REFERENCES

[1] Pham-Huy, L.A.; He, H.; Pham-Huy, C. Free radicals, antioxidants in disease and health. *Int. J. Biomed. Sci.*, **2008**, *4*, 89-96.

[2] Lobo, V.; Patil, A.; Phatak, A.; Chandra, N. Free radicals, antioxidants and functional foods: Impact on human health. *Pharmacogn. Rev.*, **2010**, *4*, 118-126.

[3] Winyard, P.G.; Moody, C.J.; Jacob, C. Oxidative activation of antioxidant defence, *Trends Biochem. Sci.*, **2005**, *30*, 453-461.

[4] Birben, E.; Sahinerm, U.M.; Sackesen, C.; Erzurum, S.; Kalayci, O. Oxidative stress and antioxidant defense. *World Allergy Organ. J.*, **2012**, *5*, 9-19.

[5] Abreu, I.A.; Cabelli, D.E. Superoxide dismutases-a review of the metal-associated mechanistic variations. *Biochim. Biophys. Acta.*, **2010**, *1804*, 263-274.

[6] Sheng, Y.; Abreu, I.A.; Cabelli, D.E.; Maroney, M.J.; Miller, A.-F.; Teixeira, M.; Valentine, J.S. Superoxide dismutases and superoxide reductases. *Chem. Rev.*, **2014**, *114*, 3854-3918.

[7] Perry, J.J.P.; Shin, D.S.; Getzoff, E.D.; Tainer, J.A. The structural biochemistry of the superoxide dismutases. *Biochim. Biophys. Acta.*, **2010**, *1804*:, 245-262.

[8] Gimadieva, A.R.; Myshkin, V.A.; Mustafin, A.G.; Chernyschenko, Y.N.; Fattakhov, A.; Abdrakhmanov, I.B.; Tolstikov, G.A. 5-Amino-6-methyluracil is a promising pyrimidine antioxidant. *Dokl. Biol. Sci.*, **2013**, *448*, 7-9.

[9] Mohamed, M.S.; Youns, M.M.; Ahmed, N.M. Synthesis, antimicrobial, antioxidant activities of novel 6-aryl-5-cyano thiouracil derivatives, *Eur. J. Med. Chem.*, **2013**, *69*, 591-600.

[10] Prachayasittikul, S.; Sornsongkhram, N.; Pingaew, R.; Worachartcheewan, A.; Ruchirawat, S.; Prachayasittikul, V. Synthesis of *N*-substituted 5-iodouracils as antimicrobial and anticancer agents, *Molecules*, **2009**, *14*, 2768-2779.

[11] Maruyama, T.; Demizu, Y.; Kozai, S.; Witvrouw, M.; Pannecouque, C.; Balzarini, J.; Snoecks, R.; Andrei, G.; De Clercq, E. Antiviral activity of 3-(3,5-dimethylbenzyl)uracil derivatives against HIV-1 and HCMV. *Nucleo. Nucleot. Nucl.*, **2007**, *26*, 1553-1558.

[12] Bardagí, J.I.; Rossi, R.A. Advances in the synthesis of 5- and 6-substituted uracil derivatives. *Org. Prep. Proced. Int.*, **2009**, *41*, 479-514.

[13] Zenker, N. *Thyroid function and thyroid drugs. In: Principles of Medicinal Chemistry*. Foye, W.O., editor, 3rd ed.; Lea & Febiger: Philadelphia, London, **1990**, pp.603-621.

[14] Boncel, S.; Gondela, A.; Walczak, K. Michael-type addition as a convenient method for regioselective *N*-alkylation of ambident uracils. *Synthesis*, **2010**, *10*, 1573-1589.

[15] del Carmen Núñeza, M.; Entrena, A.; Rodríguez-Serrano, F.; Marchal, J.A.; Aránega, A.; Gallo, M.A.; Espinosa, A.; Campos, J.M. Synthesis of novel 1-(2,3-dihydro-5*H*-4,1-benzoxathiepin-3-yl)-uracil and -thymine, and their corresponding S-oxidized derivatives. *Tetrahedron*, **2005**, *61*, 10363-10369.

[16] De Clercq, E. Antiviral drugs in current clinical use. *J. Clin. Virol.*, **2004**, *30*, 115-133.

[17] Prachayasittikul, S.; Worachartcheewan, A.; Nantasenamat, C.; Chinworrungsee, M.; Sornsongkhram, N.; Ruchirawat, S.; Prachayasittikul, V. Synthesis and structure-activity relationship of 2-thiopyrimidine-4-one analogs as antimicrobial and anticancer agents. *Eur. J. Med. Chem.*, **2011**, *46*, 738-742.

[18] Fathalla, O.A.; A. Zaghary, W.A.; Radwan, H. H.; Awad, S.M., Mohamed, M.S. Synthesis of new 2-thiouracil-5-sulfonamide derivatives with biological activity. *Arch. Pharm. Res.*, **2002**, *25*, 258-269.

[19] Choi, H.J.; Yu, S.T.; Lee, K.I.; Choi, J.K.; Chang, B.Y.; Kim, S.Y.; Ko, M.H.; Song, H.O.; Park, H. 6-Trifluoromethyl-2-thiouracil possesses anti-*Toxoplasma gondii* effect in vitro and in vivo with low hepatotoxicity. *Exp. Parasitol.*, **2014**, *143*, 24-29.

[20] Fabrissin, S.; de Nardo, M.; Nisi, C.; Morasca, L.; Dolfini, E.; Franchi, G. Synthesis and anticancer activity of 5-diethylaminomethyl derivatives and nitrogen mustards of uracil and 2-thiouracils. *J. Med. Chem.*, **1976**, *19*, 639-642.

[21] Kamalakannan, P.; Venkappayya, D.; Balasubramanian, T. A new antimetabolite, 5-morpholinomethyl-2-thiouracil-spectral properties, thermal profiles, antibacterial, antifungal and antitumour studies of some of its metal chelates. *J. Chem. Soc., Dalton. Trans.*, **2002**, *17*, 3381-3391.

[22] Motawia, M.S.; Abdel-Megied, A.E.S.; Pedersen, E.B.; Nielsen, C.M.; Ebbesen, P. Synthesis of 5-alkoxymethyl derivatives of 3'-amino-2',3'-dideoxyuridine and evaluation of their activity against HIV and cancer. *Acta Chem. Scand.*, **1992**, *46*, 77-81.

[23] Prachayasittikul, S.; Worachartcheewan, A.; Pingaew, R.; Suksrichavalit, T.; Isarankura-Na-Ayudhya, C.; Ruchirawat, S.; Prachayasittikul, V. Metal complexes of uracil derivatives with cytotoxicity and superoxide scavenging activity. *Lett. Drug Des. Discov.*, **2012**, *9*, 282-287.

[24] Prachayasittikul, V.; Pingaew, R.; Nantasenamat, C.; Prachayasittikul, S.; Ruchirawat, S.; Prachayasittikul, V. Investigation of aromatase inhibitory activity of metal complexes of 8-hydroxyquinoline and uracil derivatives. *Drug Des. Devel. Ther.*, **2014**, *8*, 1089-1096.

[25] Mitscher, L.A. Bacterial topoisomerase inhibitors: quinolone and pyridone antibacterial agents. *Chem. Rev.*, **2005**, *105*, 559-592.

[26] Xia, Y.; Yang, Z.Y.; Xia, P.; Bastow, K.F.; Nakanishi, Y.; Nampoothiri, P.; Hamel, E.; Brossi, A.; Lee, K.H. Antitumor agents. Part 226: synthesis and cytotoxicity of 2-phenyl-4-quinolone acetic acids and their esters. *Bioorg. Med. Chem. Lett.*, **2003**, *13*, 2891-2893.

[27] Lucero, B.; Gomes, C.R.; Frugulhetti, I.C.; Faro, L.V.; Alvarenga, L.; de Souza, M.C.; de Souza, T.M.; Ferreira, V.F. Synthesis and anti-HSV-1 activity of quinolonic acyclovir analogues. *Bioorg. Med. Chem. Lett.*, **2006**, *16*, 1010-1013.

[28] Prachayasittikul, V.; Prachayasittikul, S.; Ruchirawat, S.; Prachayasittikul ,V. 8-Hydroxyquinolines: a review of their metal chelating properties and medicinal applications. *Drug Des. Devel. Ther.*, **2013**, *4*, 1157-1178.

[29] Oliveri, V.; Vecchio, G. 8-Hydroxyquinolines in medicinal chemistry: a structural perspective. *Eur. J. Med. Chem.*, **2016**, *120*, 252-274.

[30] Song, Y.; Xu, H.; Chen, W.; Zhan, P.; Liu, X. 8-hydroxyquinoline: a prilegde structure with a broad-ranging pharmacological potential. *Med. Chem. Comm.*, **2015**, *6*, 61-74.

[31] Srisung, S.; Prachayasittikul, S.; Suksrichavalit, T.; Ruchirawat, S.; Prachayasittikul, V. Antimicrobial activity of 8-hydroxyquinoline and transition metal complexes. *Int. J. Pharm.*, **2013**, *9*, 170-175.

[32] Patel, M.N.; Parmar, P.A.; Gandhi, D.S. Third generation fluoroquinolones antibacterial drug based mixed-ligand Cu(II) complexes: structure, antibacterial activity, superoxide dismutase activity and DNA-interaction approach. *J. Enzyme Inhib. Med. Chem.*, **2011**, *26*, 188-197.

[33] Prachayasittikul, S.; Wongsawatkul, O.; Worachartcheewan, A.; Nantasenamat, C.; Ruchirawat, S.; Prachayasittikul, V. Elucidating the structure-activity relationships of the vasorelaxation and antioxidation properties of thionicotinic acid derivatives. *Molecules*, **2010**, *15*, 198-214.

[34] Piacham, T.; Isarankura-Na-Ayudhya, C.; Prachayasittikul, V.; Bülow, L.; Ye, L. A polymer supported manganese catalyst useful as a superoxide dismutase mimic. *Chem. Commun.*, **2003**, *11*, 1254-125.

[35] Baron, E.J.; Peterson, L.R.; Finegold, S.M. *Methods for testing antimicrobial effectiveness. In: Bailey and Scott's diagnostic microbiology*, 9th ed.; St. Louis: Mosby-Year Book, Inc., **1994**, pp. 168-193.

[36] Pingaew, R.; Worachartcheewan, A.; Prachayasittikul, V.; Prachayasittikul, S.; Ruchirawat, S.; Prachayasittikul, V. Transition metal complexes of 8-aminoquinoline-5-substituted uracils with antioxidative and cytotoxic activities. *Lett. Drug Des. Discov.*, **2013**, *10*, 859-864.

[37] Shepherd, R.E.; Zhang, S.; Lin, F.-T.; Kortes, R.A. Influence of the 5-substituent of uracils and uridines on η^2 coordination of RuII(hedta)$^-$at the C-5-C-6 bonds. *Inor. Chem.*, **1992**, *31*, 1457-1462.

[38] Al-Masoudi, NA, Saleh BA, Abdul Karim N, Issa AY, Pannecouque C. Synthesis and anti-HIV activity of new 2-thiolumazine and 2-thiouracil metal complexes. *Heteroatom Chem.*, **2011**, *22*, 44-50.

[39] Yamanari, K.; Kida, M.; Fuyuhiro, A.; Kita, M.; Kaizaki, S. Cobalt(III) promoted ligand fusion reactions of thiobarbituric acid and 4,6-diamino-2-thiouracil (or 4-amino-2-thiouracil). *Inorg. Chim. Acta.*, **2002**, *332*, 115-122.

[40] Angustias Romero, M.; Purificación Sánchez, M.; Quirós, M.; Sánchez, F.; Salas, J. M.; Moreno, M.N.; Faure, R. Transition metal complexes of 6-amino 2-thiouracil; crystal structure of bis(6-amino-2-thiouracilato)aquazinc(II) dihydrate. *Can. J. Chem.*, **1993**, *71*, 29-33.

[41] Suksrichavalit, T.; Prachayasittikul, S.; Nantasenamat, C.; Isarankura-Na-Ayudhya, C.; Prachayasittikul, V. Copper complexes of pyridine derivatives with superoxide scavenging and antimicrobial activities. *Eur. J. Med. Chem.*, **2009**, *44*, 3259-3265.

[42] Cherdtrakulkiat, R.; Boonpangrak, S.; Sinthupoom, N.; Prachayasittikul, S.; Ruchirawat, S.; Prachayasittikul, V. Derivatives (halogen, nitro and amino) of 8-hydroxyquinoline with highly potent antimicrobial and antioxidant activities. *Biochem. Biophys. Rep.*, **2016**, *6*, 135-141.

[43] Shaikh, S.; Fatima, J.; Shakil, S.; Rizvi, S.M.; Kamal, M.A. Antibiotic resistance and extended spectrum beta-lactamases: types, epidemiology and treatment. *Saudi J. Biol. Sci.*, **2015**, *22*, 90-101.

[44] Taylor, P.K.; Yeung, A.T.; Hancock, R.E. Antibiotic resistance in *Pseudomonas aeruginosa* biofilms: towards the development of novel anti-biofilm therapies. *J. Biotechnol.*, **2014**, *191*, 121-30.

[45] Ahmad, S.; Abulhamd, A. Phenotypic and molecular characterization of nosocomial *K. pneumoniae* isolates by ribotyping. *Adv. Med. Sci.*, **2015**, *60*, 69-75.

[46] Lerner, A.; Adler, A.; Abu-Hanna, J.; Cohen Percia, S.; Kazma Matalon, M.; Carmeli, Y. Spread of KPC-producing carbapenem-resistant Enterobacteriaceae: the importance of super-spreaders and rectal KPC concentration. *Clin. Microbiol. Infect.*, **2015**, *21*, 470.e1–470.e7.

[47] Shah, A.A.; Hasan, F.; Ahmed, S.; Hameed, A. Extended-spectrum beta-lactamases (ESbLs): characterization, epidemiology and detection. *Crit. Rev. Microbiol.*, **2004**, *30*, 25-32.

[48] Colak, A.; Terzi, Ü.; Col, M.; Karaoglu, Ş.A.; Karaböcek, S.; Küçükdumlu, A.; Ayaz, F.A. DNA binding, antioxidant and antimicrobial activities of homo- and heteronuclear copper(II) and nickel(II) complexes with new oxime-type ligands. *Eur. J. Med. Chem.*, **2010**, *45*, 5169-5175.

[49] Suksrichavalit, T.; Prachayasittikul, S.; Piacham, T.; Isarankura-Na-Ayudhya, C.; Nantasenamat, C.; Prachayasittikul V. Copper complexes of nicotinic-aromatic carboxylic acids as superoxide dismutase mimetics. *Molecules*, **2008**, *13*, 3040-3056.

[50] Anjaneyulu, Y.; Rao, R.P.; Swamy, R.Y.; Eknath, A.; Rao Narasimha, K. In vitro antimicrobial activity studies on the mixed ligand complexes of Hg(II) with 8-hydroxyquinoline and salicylic acids. *Proc. Indian Acad. Sci. (Chem. Sci.)*, **1982**, *91*, 157-163.

Received: XX XX, 2017 Revised: XX XX, 2017 Accepted: XX XX, 2017

Antioxidant and cytotoxic activities of copper complexes of sulfonamide analogs

Apilak Worachartcheewan[1,2,3,*], Ratchanok Pingaew[4], Sutanun Doungsoongnuen[4], Supaluk Prachayasittikul[3], Somsak Ruchirawat [5,6], Virapong Prachayasittikul

[1]Department of Community Medical Technology, Faculty of Medical Technology, Mahidol University, Bangkok 10700, Thailand

[2]Department of Clinical Chemistry, Faculty of Medical Technology, Mahidol University, Bangkok 10700, Thailand

[3]Center of Data Mining and Biomedical Informatics, Faculty of Medical Technology, Mahidol University, Bangkok 10700, Thailand

[4]Department of Chemistry, Faculty of Science, Srinakharinwirot University, Bangkok 10110, Thailand

[5]Laboratory of Medicinal Chemistry, Chulabhorn Research Institute, and Program in Chemical Biology, Chulabhorn Graduate Institute, Bangkok 10210, Thailand

[6]Center of Excellence on Environmental Health and Toxicology, Commission on Higher Education (CHE), Ministry of Education, Thailand

[7]Department of Clinical Microbiology and Applied Technology, Faculty of Medical Technology, Mahidol University, Bangkok 10700, Thailand

✉ apilak.woa@mahidol.ac.th; Tel: +662-441-4371 ext. 2720; Fax: +662-441-4380

Abstract: Copper (Cu) complexes (**1**-**10**) of 4-substituted benzenesulfonamide (NO_2, OCH_3, CH_3 and Cl) of anthranilic acid were synthesized and determined for antioxidant, antimicrobial and cytotoxic activities. The Cu complexes **1**-**10** exhibited antioxidant activity with IC_{50} of 0.062-0.152 µM and cytotoxic activity against MOLT-3 cell lines with IC_{50} of 21.60-28.92 µM. Particularly, complex **4** (sulfonamides with NO_2 and Cl groups) showed the strongest SOD activity as IC_{50} of 0.062 µM, whereas complex **10** (sulfonamide with Cl group) displayed the best cytotoxicity as IC_{50} of 21.60 µM against MOLT-3 cell lines. Furthermore, the function groups of Cu-sulfonamide complexes such as NO_2 and Cl have influence for their biological activities interacting with target which displayed good bioactive compounds. The finding reveals novel Cu-sulfonamide complexes with a potential compounds for further development for medicinal applications.

Keywords: metal complex, copper, sulfonamide, cytotoxicity, antioxidants,

Introduction

Free radicals are defined as unstable molecules having unpaired electron (1,2). It has been associated with development of various diseases such as cancer, diabetes mellitus, cardiovascular disease, aging and neurodegenerative diseases (3). Antioxidant systems in human are used to protect free radicals that occur inside the body including enzymatic system such as superoxide dismutase (SOD), catalase and glutathione peroxidase, and non-enzymatic system from supplemental nutrition (4,5). Furthermore, transition metal ions (i.e., manganese (Mn), cobalt (Co), nickel (Ni), copper (Cu) and zinc (Zn)) are essential elements to help catalytic reaction working with enzymes/protein as call as metalloprotein such as found in SOD enzyme (6,7). The development and discovery of novel compounds has been interested as used as treatment and prevention of progression of free radical-related diseases. Based on correlation between metal ions with enzyme, the mimic compound coordinated with transition metal ions have been synthesized for exerting interesting pharmacological activities. Particularly, mimic compounds (SOD-mimic) using metal ions with ligands having atoms coordination which has been synthesized of metal complexes displaying a variety of biological activities. Interestingly, Copper is considered as an essential element of several endogenous antioxidant enzymes, therefore, using transition copper ions have been attractive target metal ion (8). Cu complexes of nicotinic with aromatic carboxylic acids (i.e., phthalic, salicylic and anthranilic acids) have been shown of antioxidant (SOD) and antimicrobial activities (9) as well as Cu complexes with pyridine derivatives (i.e., nicotinic acid, 2-hydroxypyridine, 2-aminopyridine and picolinic acid) (10). Furthermore, nicotinic acid-copper complex prevent gastric congestion (11), reduce lipids, control levels of liver enzymes and lipid peroxidation (12), and nicotine-copper complexes showed SOD-like antioxidant properties for Alzheimer's disease (13).

Sulfonamide is an important pharmacophore found in many drugs and bioactive compounds. Its derivatives exhibited various biological activities such as antimicrobial (14), anticancer (15) and antiviral (16) properties. Considering the sulfonamide structure containing aromatic ring, sulphonamide ($-SO_2NH_2$) and functional groups (R). It is interesting to structural modification as use as the ligand to form metal complexes having pharmacological properties. Sulfonamide derivatives were used as a ligand to coordinate with metal ions (i.e., moononuclear complexes of 5-chloro-2-hydroxybenzylidene)aminobenzenesulfonamides with various metal ions (Co, Cu, Zn, Ni and Mn) (17) and Cu complexes of *N*-substituted sulfonamides (18)). It has found that metal complexes of sulfonamide derivatives exhibited biological activities such as anti-*Trypanosoma cruzi* activity (17), DNA cleavage and cytotoxic activities (18).

Anthranilic acid is a scaffold to be attracted great interest which was synthesized and displayed anticancer (19), antioxidant (20) and antimicrobial activities (21). Furthermore, 4-substitueted benzenesulfonamide of anthranilic acid were synthesized and exhibited antifungal, antioxidant and anticancer activities (22).

Therefore, this present study aims to synthesize of copper complexes (**1**-**10**) of 4-substitueted benzenesulfonamide of anthranilic acid (ligands 1-4) and determine their biological activities including antioxidant, antimicrobial and cytotoxic activities. In addition, structure-activity relationship has been provided to insight into influence of function groups in their activities.

Materials and methods

General

Infrared (IR) spectra were obtained on a Perkin Elmer System 2000 FTIR. Mass spectra were recorded on a Finnigan INCOS50 and a Bruker Daltonics (Micro TOF). Magnetic

moment was performed on a Magnetic Susceptibility Balance, Mark 1, Serial 15257, Sherwood Scientific, Cambridge, UK. Melting points were determined on an Electrothermal melting point apparatus and are uncorrected. Chemicals and reagents were analytical grade included RPMI-1640 (Rosewell Park Memorial Institute medium from Gibco and Hyclone laboratories, USA; MTT (3(4,5-dimethylthiazol-2-yl)-2,5-diphenyltetrazolium bromide), XTT (2,3-bis-(2-methoxy-4-nitro-5-sulfophenyl)-2H-tetrazolium-5-carboxanilide salt), HEPES (*N*-2-hydroxyethylpiperazine-*N*′-2-ethanesulfonic acid), nitroblue tetrazolium (NBT) salt, L-methionine, riboflavin, Triton-100, superoxide dismutase (SOD) from bovine erythrocytes, DMSO (dimethyl sulfoxide, 99.9%), ampicillin, ciprofloxacin, tetracycline, L-glutamine, penicillin, streptomycin, sodium pyruvate and glucose from Sigma, USA; Müeller Hinton Broth and Müeller Hinton Agar from Becton Dickinson, USA and sodium chloride from Merck, German. from Sigma, USA; Ham's/F12 (Nutrient mixture F-12), DMEM (Dulbecco's Modified Eagle's Medium) and FBS (fetal bovine serum) from Hyclone laboratories, USA and gentamicin sulfate from Government Pharmaceutical Organization, Thailand.

Synthesis of copper-sulfonamide complexes (1-10)

The 4-substitueted benzenesulfonamide of anthranilic acid (ligands 1-4: l1-l4) were synthesized by Doungsoongnuen et al. (22) which functional groups (R = NO_2, OCH_3, CH_3 and Cl) were substituted on benzenesulfonamides at position 4 (Figure 1). It was used as ligands for coordinated with copper (Cu). Cu complexes of sulfonamide ligands (l1 – l4) were further synthesized. The solid products were collected by filtration and dried at room temperature.

A solution of metal salts (1 mmol) dissolved in methanol (2 mL) was added dropwise to the solution of ligands (1 mmol) in 70°C methanol (30 mL) and then heated for 45 min. A

solution of ligands (1 mmol) in methanol (2 mL) was added dropwise to the reaction mixture and further heated for 1 h. The precipitated solid was collected by filtration, washed 4-5 times with cold methanol and dried *in vacuo* at room temperature. Complexes **7**-**16** were produced from 1 mmol of ligands (l1-l4) and 1 mmol of $Cu(OAc)_2 \cdot H_2O$. Chemical structures and characterization of Cu complexes were determined using IR, ^1H NMR and mass spectra and magnetic moment.

Biological activities

Metal complexes (**1**-**10**) were determined for their biological activities composed of antioxidant, antimicrobial and cytotoxic activities.

Antioxidant activity

The transition metal complexes were evaluated for their antioxidant activity using 2 superoxide dismutase (SOD) assays (23). The SOD assay was performed by mixed 1 mL of solution (27 mL of HEPES buffer (50 mM, pH 7.8), 1.5 mL of L-methionine (30 mg/mL), 1 mL of nitro blue tetrazolium (NBT, 1.41 mg/mL) and 0.75 mL of Triton X-100 (1 wt%)) to 0.45 mL solution of a tested compound to a final concentration of 300 µg/mL. The reaction was initiated by adding10 µL of riboflavin (44 µg/mL) and was excited under a Philips Classic Tone lamp (60 W) in a light box for 7 min. The absorbance at 550 nm was measured of the photoreduction of NBT using UV–Vis spectrophotometer and the percentage of SOD activity will be calculated using equation (1).

$$\%\text{Inhibition} = \left(1 - \frac{Abs._{sample}}{Abs._{control}}\right) \times 100 \quad (1)$$

where $Abs._{control}$ is the absorbance of the control reaction, and $Abs._{sample}$ is the absorbance of the tested compound. Superoxide dismutase (SOD) from bovine erythrocytes was used as a control.

In addition, IC_{50} (50% inhibition concentration of radical and superoxide-scavenging activities) was performed in which tested complexes at 300 µg/mL displayed antioxidant activities more than 50% inhibition.

Antimicrobial activity

The metal complexes were determined of antimicrobial activity using agar dilution method (24). The compounds were individually dissolved in DMSO. The two-fold dilution was performed using Muller Hinton (MH) broth which was transferred to MH agar solution to obtain the final concentrations of 256 to 4 mg/mL. In addition, the MH Broth, DMSO, ampicillin, ciprofloxacin and tetracycline drugs were used as the control. Microorganisms were cultured in MH broth at 37°C for 24 h and diluted with 0.9% normal saline solution to adjust the cell density of 1×10^8 CFU/mL compared to 0.5 McFarland standards. Then, microorganisms were inoculated onto each plate of tested compound with various concentrations using a multipoint inoculators and further incubated at 37°C for 24-48 h. The inhibition of microbial cell growth as well as the minimum inhibitory concentration (MIC as the lowest concentration to inhibit the growth of microorganisms) of the compounds was determined. Twenty-seven strains of microorganisms composed of reference strain and clinical isolates as following: **gram positive bacteria**: *Staphylococcus aureus* ATCC 29213, *Staphylococcus aureus* ATCC 25923, *Staphylococcus epidermidis* ATCC 12228, *Enterococcus faecalis* ATCC 29212, *Enterococcus faecalis* ATCC 33186, *Micrococcus luteus* ATCC 10240, *Corynebacterium diphtheriae* NCTC 10356, *Bacillus subtilis* ATCC 6633, *Streptococcus pyogenes*, *Listeria monocytogenes*, *Bacillus* cereus; **gram negative**

bacteria: *Escherichia coli* ATCC 25922, *Klebsiella pneumoniae* ATCC 700603, *Serratia macescens* ATCC 8100, *Salmonella typhimurium* ATCC 13311, *Shewanella putrefaciens* ATCC 8071, *Achromobacter xylosoxidans* ATCC 2706, *Pseudomonas aeruginosa* ATCC 15442, *Pseudomonas stutzeri* ATCC 17587, *Shigella dysenteriae*, *Salmonella enteritidis*, *Morganella morganii*, *Aeromonas hydrophila*, *Citrobacter freundii*, *Plesiomonas shigelloides* and **diploid fungus (yeast)**: *Candida albicans* ATCC 90028, *Saccharomyces cerevisiae* ATCC 2601.

Cytotoxicity

Cytotoxicity of the metal complexes (**1**-**10**) was determined against four human cancer cell lines composed of hepatocellular carcinoma (HepG2), cholangiocarcinoma (HuCCA-1), lung carcinoma (A549) and T-lymphoblast (MOLT-3, acute lymphoblastic leukemia) cell lines. The cancer cells including HuCCA-1 and A549 cells were grown in Hamm's/F12 medium containing L-glutamine (2 mM) supplemented with 100 U/mL penicillin-streptomycin and FBS (10%); MOLT-3 cells were grown in RPMI-1640 medium containing L-glutamine (2 mM), 100 U/mL penicillin-streptomycin, sodium pyruvate, glucose and 10% FBS; and HepG2 cells were grown in DMEM medium containing 100 U/ mL penicillin-streptomycin and 10% FBS. The assay was performed using the cell lines suspended in RPMI-1640 containing 10% FBS, which contained a density of 5×10^3-2×10^4 cells per well in a 96-well plate (Costar No. 3599, USA). The cells were then incubated at 37^oC under a humidified atmosphere with 95% air and 5% CO_2 for 24 h. The tested compound and controls was added to the desired final concentrations. The plates were incubated for 48 h. Cell viability was determined by staining with MTT for adherent cell (A549, HuCCA-1 and HepG2 cells) [38-39], and with XTT [40] assay for suspended cell (MOLT-3 cells). The plates were read on a micro-plate reader (Molecular Devices, USA) and the absorbance was measured at 550 nm.

Furthermore, the IC_{50} values of the compound or drug concentration that provided 50% cell growth inhibition were performed. Doxorubicin and/or etoposide were used as reference drugs (25,26).

Results and discussion

Chemistry

The Cu complexes structures (**1-10**) were synthesized and IR spectra of the complexes were analyzed. It was shown (Table 1) that the Cu-sulfonamide complexes were successfully synthesized which compared to their ligands (l1-l4). The chemical structures of ligands and complexes (**7-16**) were displayed in Figure 1. In addition, characteristics of Cu-sulfonamide complexes (**7-16**) composed of %yield and melting point of the complexes were shown in Table 2

Antioxidant activity

The metal complexes **1-10** were determined of antioxidant activity using SOD assays. It was found (Table 3) that all metal complexes (**1-10**) exhibited antioxidant activity in IC_{50} range of 0.062-0.152 µM. Complex **4** showed the strongest SOD activity (IC_{50} of 0.062 µM) compared with other complexes. Considering complexes **1-10** having 4-substitued benzenesulfonamide of NO_2, OCH_3, CH_3 and Cl. It was observed that form coordinated with the same ligands showed low SOD activity than with different ligands, for example, complex **4** contained ligand 1 (NO_2) and ligand 4 (Cl) with IC_{50} of 0.062 µM and complex **1** consisted of ligand 1 (NO_2) and ligand 1 (NO_2) with IC_{50} of 0.152 µM as well as in complexes **2** (IC_{50} of 0.074 µM) and **3** (IC_{50} of 0.076 µM). This phenomenon displayed the fashion in the ligands 2, 3 and 4 which used to coordinate with Cu ion such as complexes **5, 8** and **10** having low antioxidant activity of IC_{50} as 0.076, 0.104 and 0.121 µM compared with other

complexes **6**, **7** and **9** having IC_{50} of 0.077, 0.075 and 0.077 µM, respectively, coordinated using different ligands. It was implied that ligand with different functional groups in metal complexes have effect for antioxidant activity. The ligands (l1-l4) reported weak antioxidant activity which ligands **2** and **4** have 15.7% of SOD activity at 300 µg/mL, respectively whereas ligands **1** and **3** were no activity (9,10). This activity also depended on the asymmetric charge localization in the complexes. It was observed that high asymmetric charge exhibited high SOD activity (22). Furthermore, Cu complexes displayed high antioxidant (SOD) activity (9,10,27).

In addition, anthranilic acid was used as a ligand for coordination with Cu and nicotinic acid. This complexes displayed good SOD activity in IC_{50} of 47.49 µM whereas free antranilic acid has IC_{50} >236.25 µM (10). This evidence was also found that Cu complexes of benzenesulfonamide of anthranilic acid exhibited good antioxidant activity than its free ligands.

Antimicrobial activity

The Cu-sulfonamide complexes (**1-10**) were investigated of antimicrobial activity using agar dilution method. The results showed that all metal complexes had no antimicrobial activity. Previous studied, sulfonamide ligands showed antimicrobial activity against *C. albicans* ATCC 90028 (25-50 %) at 4 µg/mL (22). It was found that these effects may be depended on functional groups and position substituent on benzenesulfonamide. However, metal complexes using ligands (l1-l4) were inactive.

Cytotoxic activity

The Cu-sulfonamide complexes (**1-10**) were determined of cytotoxic activity against four cancer cell lines using MTT and XTT assays. It was found that compounds **1-10**

displayed cytotoxic activity for MOLT-3 cells, whereas had no activity for HepG2, HuCCA-1 and A549 as shown in Table 4. Interestingly, complex **10** (l4-l4) exhibited the strongest cytotoxicity (IC_{50} of 21.60 µM) than other complexes (IC_{50} range of 23.31-28.92 µM), on the other hand, free ligand displayed low cytotoxic activity than its complexes (Table 4). Although, free ligand 1 with NO_2 substituted at 4-position on benzenesulfonamide has been reported of highest cytotoxicity (Table 4) than free ligands 2 (OCH_3), 3 (CH_3) and 4 (Cl), but Cu complexes with these ligands displayed good cytotoxic activity than free ligand (Table 4). Interestingly, ligand 2 with OCH_3 has been reported as inactive compounds (22), after used as ligand coordinated with Cu, the complexes (**2** and **5-7**) showed cytotoxic activity against MOLT-3 cells. Both free ligands and its complexes exhibited selectively MOLT-3 cells. In addition, it has found that Cu complex (5Nu-Cu-8HQ) exerted most potent cytotoxic activity than other metal complexes (27).

Conclusion

Copper-sulfonamide complexes (**1**-**10**) were synthesized and determined of antioxidant, antimicrobial and cytotoxic activities. All complexes displayed antioxidant and cytotoxic properties. Interestingly, complex **4** (coordinated with l1 (NO_2) and l4 (Cl) and Cu ion) exhibited the strongest SOD activity with IC_{50} of 0.062 µM and complex **10** (coordinated with l4 (Cl) showed the best cytotoxic activity with IC_{50} of 21.60 µM. Furthermore, the effect of biological activities was depended on functional groups that substituted on benzenesulfonamide of anthranilic acid. This finding demonstrated that Cu-sulfonamide complexes exhibited SOD-like activity and cytotoxic activity, and could be potential for further development as medicinal compounds.

Acknowledgements

AW gratefully acknowledges the research grant supported by the Thailand Research Fund (Grant No. TRG5880143) and partially supported by the Office of the Higher Education Commission and Mahidol University under the National Research Universities Initiative.

References

1. Lobo V, Patil A, Phatak A, Chandra N. Free radicals, antioxidants and functional foods: Impact on human health. Pharmacogn Rev. 2010;4(8):118-126.
2. Knight JA. Review: free radicals, antioxidants, and the immune system. Ann Clin Lab Sci. 2000;30(2):145-58.
3. Pham-Huy LA, He H, Pham-Huy C. Free radicals, antioxidants in disease and health. Int J Biomed Sci. 2008;4(2):89-96.
4. Nimse SB, Pal D. Free radicals, natural antioxidants, and their reaction mechanisms. RSC Adv., 2015; 5:27986–28006.
5. Birben E, Sahiner UM, Sackesen C, Erzurum S, Kalayci O. Oxidative stress and antioxidant defense. World Allergy Organ J. 2012;5(1):9-19.
6. Miller A-F. Superoxide dismutases: active sites that save, but a protein that kills. Curr Opin Chem Biol. 2004, 8:162–168.
7. Perry JJP, Shin DS, Getzoff ED, Tainer JA. The structural biochemistry of the superoxide dismutases. Biochim Bbiophys Acta. 2010;1804(2):245-262.
8. Valko M, Rhodes CJ, Moncol J, Izakovic M, Mazur M. Free radicals, metals and antioxidants in oxidative stress-induced cancer. Chem Biol Interact. 2006;160(1):1-40.
9. Suksrichavalit T, Prachayasittikul S, Nantasenamat C, Isarankura-Na-Ayudhya C, Prachayasittikul V. Copper complexes of pyridine derivatives with superoxide scavenging and antimicrobial activities. Eur J Med Chem. 2009;44(8):3259-3265.

10. Suksrichavalit T, Prachayasittikul S, Piacham T, Isarankura-Na-Ayudhya C, Nantasenamat C, Prachayasittikul V. Copper complexes of nicotinic-aromatic carboxylic acids as superoxide dismutase mimetics. Molecules. 2008;13(12):3040-30
11. el-Saadani MA, Nassar AY, Abou el-Ela SH, Metwally TH, Nafady AM. The protective effect of copper complexes against gastric mucosal ulcer in rats. Biochem Pharmacol. 1993;46(6):1011-1018.
12. Salama RH, Nassar AY, Nafady AA, Mohamed HH. A novel therapeutic drug (copper nicotinic acid complex) for non-alcoholic fatty liver. Liver Int. 2007;27(4):454-464.
13. Shen L, Zhang H-Y, Ji H-F. Computational note on the SOD-like antioxidant potential of nicotine–copper(II) complexes. J Mol Struc-THEOCHEM. 2007;817:161–162.
14. Genc Y, Ozkanca R, Bekdemir Y. Antimicrobial activity of some sulfonamide derivatives on clinical isolates of *Staphylococus aureus*, Ann Clin Microbiol Antimicrob. 2008;7:17-22.
15. Hwang YJ, Park SM, Yim CB, Im C. Cytotoxic activity and quantitative structure activity relationships of arylpropyl sulfonamides. Korean J Physiol Pharmacol. 2013;17:237-243.
16. Loh B, Vozzolo L, Mok BJ, Lee CC, Fitzmaurice RJ, Caddick S, Fassati A. Inhibition of HIV-1 replication by isoxazolidine and isoxazole sulfonamides. Chem Biol Drug Des. 2010;75:461-474.
17. Chohan ZH, Hernandes MZ, Sensato FR, Moreira DR, Pereira VR, Neves JK, de Oliveira AP, de Oliveira BC, Leite AC. Sulfonamide-metal complexes endowed with potent anti-*Trypanosoma cruzi* activity. J Enzyme Inhib Med Chem. 2014;29:230-6.

18. García-Giménez JL, Hernández-Gil J, Martínez-Ruíz A, Castiñeiras A, Liu-González M, Pallardó FV, Borrás J, Alzuet Piña G. DNA binding, nuclease activity, DNA photocleavage and cytotoxic properties of Cu(II) complexes of N-substituted sulfonamides. J Inorg Biochem. 2013;121:167-78.
19. Congiu C, Cocco MT, Lilliu V, Onnis V. New potential anticancer agents based on the anthranilic acid scaffold: synthesis and evaluation of biological activity. J Med Chem. 2005;48:8245-52.
20. Lee-Manion AM1, Price RK, Strain JJ, Dimberg LH, Sunnerheim K, Welch RW. In vitro antioxidant activity and antigenotoxic effects of avenanthramides and related compounds. J Agric Food Chem. 2009;57(22):10619-24.
21. Kar A, Gugnani HC, Madumere UA. Synthesis and antimicrobial activity of some anthranilic acid derivatives. Pharmazie. 1980;35(8):466-8.
22. Doungsoongnuen S, Worachartcheewan A, Pingaew R, Suksrichavalit T, Prachayasittikul S, Ruchirawat S, Prachayasittikul V. Investigation on biological activities of anthranilic acid sulfonamide analogs. EXCLI J. 2011;10:155-161.
23. Piacham T, Isarankura Na Ayudhya C, Prachayasittikul V, Bülow L, Ye L. A polymer supported manganese catalyst useful as a superoxide dismutase mimic. Chem Commun (Camb). 2003;(11):1254-5.
24. Baron EJ, Peterson LR, Finegold SM. Methods for testing antimicrobial effectiveness. In: Bailey and Scott's diagnostic microbiology, 9th ed.; St. Louis: Mosby-Year Book, Inc., 1994, pp. 168-193.
25. Pingaew R, Worachartcheewan A, Prachayasittikul V, Prachayasittikul S, Ruchirawat S, Prachayasittikul V. Transition metal complexes of 8-aminoquinoline-5-substituted uracils with antioxidative and cytotoxic activities. Lett Drug Des Discov. 2013;10:859-864.

26. Prachayasittikul V, Pingaew R, Worachartcheewan A, Nantasenamat C, Prachayasittikul S, Ruchirawat S, Prachayasittikul V. Synthesis, anticancer activity and QSAR study of 1,4-naphthoquinone derivatives. Eur J Med Chem. 2014;84:247-263.
27. Prachayasittikul S, Worachartcheewan A, Pingaew R, Suksrichavalit T, Isarankura-Na-Ayudhya C, Ruchirawat S, Prachayasittikul V. Metal complexes of uracil derivatives with cytotoxicity and superoxide scavenging activity. Lett Drug Des Discov. 2012;9:282-287.

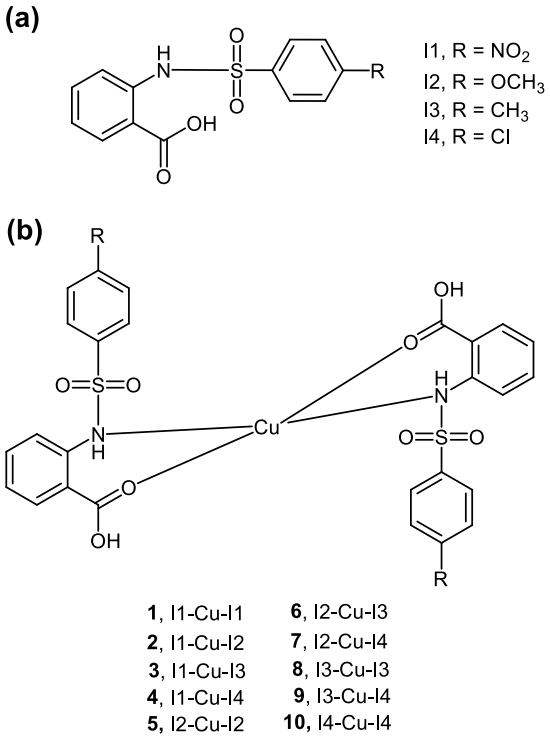

Figure 1 Chemical structures of ligands (a) and Cu-sulfonamide complexes (**1**-**10**) (b)

Table 1. IR spectra (cm^{-1}) and μ_{eff} (B.M) of copper complexes of sulfonamide analogs (**1-10**).

Compound	νO-H	νC-O	νSO_2	νNO_2	νN-H	νC-N	νS-N	νC=O	δO-H	δN-H	μ_{eff}
SA01-Cu-SA01 (**1**)	3475m, br	1091m, sh	1314m 1164vs	1531s 1394vs	—	1276s	945s	—	1394s, sh	—	0.82
SA01-Cu-SA02 (**2**)	3448s, br	1093s 1024w	1161s	1534s 1350s	—	1274m	938s, br	—	1396vs	—	0.80
SA01-Cu-SA03 (**3**)	3449s, br	1091s	1163vs	1534s 1350s	—	1274m	941m, br	—	1396vs	—	0.80
SA01-Cu-SA04 (**4**)	3450s, br	1093s	1161vs	1534s 1350s	—	1274s	941m, br	—	1396vs	—	0.84
SA02-Cu-SA02 (**5**)	3471m, br	1096s 1025m	1330m, br	—	—	1264s	931s, br	—	1397s	—	0.79
SA02-Cu-SA03 (**6**)	3449s, br	1093m 1024vw	1156s	—	—	1267m	934w, br	—	1396s	—	0.54
SA02-Cu-SA04 (**7**)	3449m, br	1093s 1024w	1332w 1156vs	—	—	1274s	938m, br	—	1396vs	—	0.82
SA03-Cu-SA03 (**8**)	3554s, sh 3493m, sh	1090s	1331m 1169s	—	—	1268s	927s	—	1394vs	—	0.93
SA03-Cu-SA04 (**9**)	3448s, br	1094s	1334m 1158vs	—	3181w, br	1275s	936s, br	—	1396vs	—	0.82
SA04-Cu-SA04 (**10**)	3465m, br	1095s	1335m 1159s	—	—	1279s	937s, br	—	1396vs	—	0.69
SA01	3449m, br	1086s	1318m 1162vs	1531vs 1349s	3196m, sh	1264s	926s	1665s	1393m, sh	1582m 758s	—
SA02	3492m, br	1092s 1022s	1344m 1160s	—	3202s, sh	1261s	926s	1678s	1389s	1581s 754s	—
SA03	3449w, br	1089s	1342s 1162s	—	3201	1258s	922s	1675s	1389m	1585m 754s	—
SA04	3442w, br	1093s	1342s 1164s	—	3188w, sh	1261m	929s	1662s	1380m	1585s 753s	—

Note: br = broad, m = medium, s = strong, sh = sharp, vs = very strong, vw = very weak and w = weak.

Table 2. Characteristics of Cu-sulfonamide complexes (**1**-**10**).

Compound	%Yield	mp (°C)
SA01-Cu-SA01 (**1**)	86	270-275
SA01-Cu-SA02 (**2**)	47	270-275
SA01-Cu-SA03 (**3**)	40	270-275
SA01-Cu-SA04 (**4**)	55	265-270
SA02-Cu-SA02 (**5**)	57	265-272
SA02-Cu-SA03 (**6**)	5	272-276
SA02-Cu-SA04 (**7**)	21	270-275
SA03-Cu-SA03 (**8**)	40	270-275
SA03-Cu-SA04 (**9**)	14	270-282
SA04-Cu-SA04 (**10**)	43	270-275

Table 3. Antioxidant activity (SOD) of Cu-sulfonamide complexes (**1-10**).

Compound[a]	SOD (IC_{50}, μM)[b]
SA01-Cu-SA01 (**1**)	0.152
SA01-Cu-SA02 (**2**)	0.074
SA01-Cu-SA03 (**3**)	0.076
SA01-Cu-SA04 (**4**)	0.062
SA02-Cu-SA02 (**5**)	0.076
SA02-Cu-SA03 (**6**)	0.077
SA02-Cu-SA04 (**7**)	0.075
SA03-Cu-SA03 (**8**)	0.104
SA03-Cu-SA04 (**9**)	0.077
SA04-Cu-SA04 (**10**)	0.121

[a]SA01 and SA04 showed antioxidant activity of 15.7% and 6.07%SOD, respectively at 300 μg/mL. SA02 and SA04 were no antioxidant activity at 300 μg/mL (Ref).

[b]Superoxide dismutase (SOD) from bovine erythrocytes was used as a control in SOD assay (IC_{50} = 0.013 μM).

Table 4. Cytotoxic activity of Cu-sulfonamide complexes (**1**-**10**).

Compound	IC_{50} (μM)[a]			
	MOLT-3	HuCCA-1	A549	HepG2
SA01-Cu-SA01 (**1**)	25.43±1.02	Inactive	Inactive	Inactive
SA01-Cu-SA02 (**2**)	25.84±0.33	Inactive	Inactive	Inactive
SA01-Cu-SA03 (**3**)	27.62±0.68	Inactive	Inactive	Inactive
SA01-Cu-SA04 (**4**)	27.11±1.23	Inactive	Inactive	Inactive
SA02-Cu-SA02 (**5**)	28.64±0.40	Inactive	Inactive	Inactive
SA02-Cu-SA03 (**6**)	28.92±0.62	Inactive	Inactive	Inactive
SA02-Cu-SA04 (**7**)	26.21±1.13	Inactive	Inactive	Inactive
SA03-Cu-SA03 (**8**)	26.08±1.13	Inactive	Inactive	Inactive
SA03-Cu-SA04 (**9**)	23.31±18.00	Inactive	Inactive	Inactive
SA04-Cu-SA04 (**10**)	21.60±1.79	Inactive	Inactive	Inactive
SA01[b]	48.74±2.17	Inactive	Inactive	Inactive
SA02[b]	Inactive	Inactive	Inactive	Inactive
SA03[b]	112.86±6.01	Inactive	Inactive	Inactive
SA04[b]	108.94±6.61	Inactive	Inactive	Inactive
Etoposide	0.04±0.01	-	-	26.62±1.95
Doxorubicin	-	0.42±0.15	0.24±0.15	0.98±0.11

[a] The assay was performed in triplicate; doxorubicin and/or etoposide was used as reference drugs.
[b] from (22).
MOLT-3: acute lymphoblastic leukemia cell line, HuCCA-1: human cholangiocarcinoma cancer cell, A549: human lung carcinoma cell line and HepG2: human hepatocellular carcinoma cell line.

Towards the design of 3-aminopyrazole pharmacophore of pyrazolopyridine derivatives as novel antioxidants

Apilak Worachartcheewan[1,2,3] • Chanin Nantasenamat[3] • Supaluk Prachayasittikul[3] • Anyaporn Aiemsaard[1] • Virapong Prachayasittikul[4]

✉ Apilak Worachartcheewan
apilak.woa@mahidol.ac.th
✉ Virapong Prachayasittikul
virapong.pra@mahidol.ac.th

[1]Department of Community Medical Technology, Faculty of Medical Technology, Mahidol University, Bangkok 10700, Thailand
[2]Department of Clinical Chemistry, Faculty of Medical Technology, Mahidol University, Bangkok 10700, Thailand
[3]Center of Data Mining and Biomedical Informatics, Faculty of Medical Technology, Mahidol University, Bangkok 10700, Thailand
[4]Department of Clinical Microbiology and Applied Technology, Faculty of Medical Technology, Mahidol University, Bangkok 10700, Thailand

Abstract

Free radicals and oxidants can cause oxidative damage to physiologically important biomolecules that subsequently leads to the development of a wide range of chronic and degenerative diseases such as aging, cancer, cardiovascular and neurodegenerative diseases. Antioxidants have been shown to be instrumental in counteracting the deleterious effects of these reactive oxygen species. Herein, a series of 20 pyrazolopyridine derivatives with antioxidant activity were utilized for constructing a quantitative structure-activity relationship (QSAR) model as to unravel the origins of the antioxidant activity. Quantum chemical and molecular descriptors were used to quantitate the physicochemical properties of investigated compounds. Significant descriptors as identified by stepwise regression analysis consisted of Mor11m, Mor25v, JGI5, H8p, GATS5p and GVWAI-50. Statistical parameters suggested that the constructed QSAR models were robust with Q^2 = 0.9370 and *RMSE* =4.7414 as evaluated via leave-one-out cross-validation (LOO-CV. The mechanistic basis of the antioxidant activity as deduced from significant descriptors was rationalized. Particularly, compounds with the highest antioxidant activity required compounds to have the highest mean topological charge index of order 5 (JGI5) and Geary autocorrelation–lag 5/weighted by atomic polarizabilities (GATS5p) but necessitated low 3D-MoRSE-signal 25/weighted by atomic van der Waals volumes (Mor25v). Such properties are well corroborated by the 3-aminopyrazole pharmacophore from investigated compounds. Molecular insights unraveled herein is anticipated to be useful as guidelines for further rational design of novel pyrazole analogs with potent antioxidant activity.

***Keywords*:** pyrazolopyridine; antioxidant activity; oxidative stress; QSAR; multiple linear regression; data mining

Introduction

Oxidative stress causes deleterious effects to the body induced by an imbalance of free radicals in relation to enzymatic and non-enzymatic antioxidant systems (Valko et al., 2007). This condition leads to oxidation that subsequently damages biomolecules (e.g., DNA, proteins, lipids and membranes), and give rise to physiological changes that eventually accelerate cell death. Free radicals are a risk factor associated with the development of various diseases such as aging, cancer, diabetes mellitus, cardiovascular and neurodegenerative diseases (Valko et al., 2007). Therefore, antioxidant compounds have drawn considerable attention as free radical scavengers. This had attracted considerable interests in screening for the discovery of novel antioxidants either from medicinal plants or by synthesis as to obtain novel bioactive compounds with promising therapeutic potential (Prachayasittikul et al., 2015). Particularly, the synthesis of new compounds with various pharmacological activities has been achieved by chemical structural modification of pharmacophoric nucleus (Nantasenamat et al., 2015; Prachayasittikul et al., 2015). Interestingly, pyridine (i.e. a six-membered ring of five carbon atoms and one nitrogen atom) is a chemical moiety found in living organisms (Kaiser et al., 1996). It has been used as a core structure for the synthesis of new compounds with pharmacological properties (Al-Omar et al., 2005; Amr et al., 2006; Worachartcheewan et al., 2012, 2014; Prachayasittikul et al., 2016). Furthermore, pyrazole is a five-membered ring of three carbon atoms and two nitrogen atoms, which has been considerable used as core structure for the drug design (Cai et al., 2013; Kumar et al., 2013; Wu et al., 2012). Therefore, a fused ring of pyridine and pyrazole gave rise to the pyrazolopyridine scaffold, which was shown to exert various biological activities such as antimicrobial (Abu-Melha 2013), anticancer (Gudmundsson et al., 2008) and kinase inhibitory (Deng and Gray, 2012) properties. Previously, synthesized pyrazolopyridine derivatives with antioxidant activity were reported (Gouda 2012). Most of the compounds were derived from 3-aminopyrazolopyridine (**1**).

Computational drug design have been immensely useful in the discovery, design and development of potentially interesting compounds by investigating their biological or chemical properties *in silico* (Nantasenamat et al., 2015; Prachayasittikul et al., 2015). Particularly, quantitative structure-activity relationship (QSAR) has been widely used to generate predictive models as well as provide insights on the contribution of molecular features in governing their biological activities. Therefore, this study makes

use of QSAR modeling to correlate physicochemical properties derived from the chemical structure with the antioxidant activity of pyrazolopyridine derivatives (**1**-**20**, Fig.1). Contributing factors governing the antioxidant activity was dissected by scrutinizing the significant descriptors derived from the QSAR model.

Materials and methods

Data set

A data set of 20 pyrazolopyridine derivatives (**1**-**20**) and their antioxidant activities were obtained from the work of Gouda (2012). Briefly, the antioxidant activity was evaluated using the 2,2′-azino-bis-3-ethylbenzthiazoline-6-sulphonic acid (ABTS) assay.

Descriptor calculation

The structures of all compounds were drawn in GaussView version 3.09 (Dennington et al., 2003). Geometry optimization was performed using Gaussian 09 Revision A.02 (Frisch et al., 2004) initially at the semi-empirical AM1 level followed by full optimization with no symmetry constraint at the density functional theory (DFT) level using the Becke's three-parameter Lee–Yang–Parr functional and with the 6–31g(d) basis set. Quantum chemical descriptors were obtained from the resulting low-energy conformers. The quantum chemical descriptors composed of total energy (E_T), highest occupied molecular orbital (E_{HOMO}), lowest unoccupied molecular orbital (E_{LUMO}), energy gap of the HOMO and LUMO state (E_{HOMO}–E_{LUMO}), total dipole moment (μ) of the molecule, electron affinity (EA, calculated from -E_{LUMO}), ionization potential (IP, calculated from $-E_{HOMO}$), mulliken electronegativity (χ), hardness (η), softness (S), electrophilicity (ω), electrophilicity index (ω_i) and mean absolute charge (Q_m) (Worachartcheewan et al., 2011). Furthermore, an additional set of 3,224 molecular descriptors was calculated from Dragon software, version 5.5 (Talete 2007). This large set of descriptors can be classified into 22 categories including 48 constitutional descriptors, 119 topological descriptors, 47 walk and path counts, 33 connectivity indices, 47 information indices, 96 2D autocorrelation, 107 edge

adjacency indices, 64 burden eigenvalues, 21 topological charge indices, 44 eigenvalue-based indices, 41 randic molecular profiles, 74 geometrical descriptors, 150 RDF descriptors, 160 3D-MoRSE descriptors, 99 WHIM descriptors, 197 GETAWAY descriptors, 154 functional group counts, 120 atom-centered fragments, 14 charge descriptors, 29 molecular properties, 780 2D binary fingerprints and 780 2D frequency fingerprints. In addition, a subset of important descriptors was deduced by stepwise multiple linear regression using SPSS statistics 18.0 (SPSS Inc., USA). The cutoff was assigned to be $|r| \geq 0.8$ for determining high correlation between the descriptors.

Data sampling

The pyrazolopyridine derivatives were selected for the training and testing sets. The training set comprising of all compound was used to construct the QSAR model. On the other hand, the testing set was performed using the leave-one-out cross-validation (LOO-CV) method. The LOO-CV was performed by leaving out one sample from the data set and used as the testing set while the remaining N - 1 samples were used as the training set. This process was repeated iteratively until each sample of the data set was used as the testing set (Prachayasittikul et al., 2014).

Multiple linear regression

Multiple linear regression (MLR) was used to generate QSAR model as summarized in equation (1):

$$Y = B_0 + \sum B_n X_n \quad (1)$$

where Y is the % inhibition of pyrazolopyridine derivatives, B_0 is the intercept and B_n is the regression coefficients of the descriptors X_n. MLR was performed using the Waikato Environment for Knowledge Analysis (Weka), version 3.4.5. (Witten et al., 2011).

Statistical analysis

To evaluate the QSAR model, the statistical parameters included squared correlation coefficient (R^2), crossed validated (Q^2), which corresponded to the degree of correlation between the predicted and

experimental values, and root mean square error (*RMSE*) which was used to measure the predictive error of the model and *F*-ratio (Nantasenamat et al., 2010).

Results and Discussion

Descriptor calculation and feature selection

The antioxidant activity of the pyrazolopyridine derivatives (**1**-**20**, Fig. 1) was investigated using the ABTS assay (Gouda 2012). The compounds exhibited activity in the range of 14.41-86.94 % inhibition (at 1 mg/mL) as shown in Table 1.

A data set of the compounds with antioxidant property was employed in the QSAR development. Quantum chemical and molecular descriptors were generated using Gaussian and Dragon softwares, respectively, as mentioned in materials and methods. Such quantum chemical and molecular descriptors have been successfully used to construct various QSAR studies such as antioxidant (Amić et al., 2007; Worachartcheewan et al., 2014), antimicrobial (Alam et al., 2014), anticancer (Prachayasittikul et al., 2014) and anti-inflammatory (Hanna 2012) activities. Sets of molecular descriptors were expressed in quantitatively describing the physicochemical properties of the investigated set of compounds. In addition, the descriptors generating by the softwares displayed a number of representative structural features, therefore, nonsignificant descriptors were eliminated. In doing so, the feature selection was performed to select the descriptors that correlated with their antioxidant activities. The original molecular descriptors generated from the Dragon software contained 3,224 molecular descriptors, which were subjected to initial removal of multi-collinear and of the redundant descriptors of 1,713 descriptors. The remaining 1,511 descriptors were further combined with 13 quantum chemical descriptors to obtain a set of 1,524 descriptors that were used as independent variables, while the antioxidant activity (%inhibition) was used as the dependent variable, and the significant descriptors were selected using the stepwise approach. The obtained descriptors with their values were then used for developing the QSAR model using MLR in WEKA software, version 3.4.5 (Witten et al., 2011) as shown in Table 1, and the definition of descriptors was described in Table 2. The intercorrelation matrix between descriptors was performed using Pearson's correlation in a pairwise manner to determine correlation coefficient of each

descriptor as presented in Table 3. It was found that each descriptor was independent from other descriptors as observed by low correlation coefficient. The correlation coefficients between descriptors were less than 0.8 (the cutoff was assigned to be $|r| \geq 0.8$). Therefore, the six important descriptors (Table 2), composing molecular properties (GVWAI-50), topological charge indices (GVWAI-50), 3D-MoRSE descriptors (Mor11m and Mor25v), GETAWAY descriptors (H8p) and 2D autocorrelation (GATS5p), were employed to construct the QSAR model for predicting the antioxidant activity of pyrazolopyridine derivatives.

QSAR modeling of the antioxidant activity

The six descriptors were used to generate a multiparametric regression using MLR method implemented in Weka software, version 3.4.5 (Witten et al., 2011). The linear regression derived from the QSAR model is shown in equation (2):

$$\%\text{Inhibition} = 1746.2843(\text{JGI5}) + 30.6893(\text{GVWAI-50}) + 28.1446(\text{Mor11m}) + 183.5802(\text{H8p}) - 45.5842(\text{Mor25v}) + 27.2051(\text{GATS5p}) - 73.3343 \quad (2)$$

n = 20, R^2 = 0.9765, $RMSE_{Tr}$ = 2.8864, Q^2 = 0.9370, $RMSE_{LOO\text{-}CV}$ = 4.7414, R^2 - Q^2 = 0.0395, F-ratio = 32.22

To evaluate the quality of regression model, an internal validation of the QSAR model was performed using LOO-CV method (Deodhar et al., 2013; Abdel-Hamid et al., 2009) as the testing set. From the Eq. (2) the results of predictive performance model for training and LOO-CV sets for predicting antioxidant activity exhibited statistically good values as observed from the correlation coefficient with more than 0.9 (0.9765 and 0.9370 for the training and the LOO-CV set, respectively), and low *RMSE* values with 2.8864 and 4.7414 for the training and the LOO-CV sets, respectively. The constructed model displayed R^2 >0.6 and Q^2>0.5, which implied the good performance (Nantasenamat et al., 2010). Furthermore, the model provided good predictability R^2 - Q^2 value of 0.0395 (not exceed 0.3) (Eriksson and Johansson, 1996), and the reliable *F*-ratio was shown to be 32.22. The plot of experimental and predicted activities based on the Eq. (2) is shown in Fig. 2, and the predicted activity values are outlined in Table 1. It was

found that the model has good correlation between the experimental and the predicted activities as observed by statistical quality results as shown in the Eq. (2). Although value of *RMSE* was high number (4.7414), but its correlation coefficient showed high number of R^2 (0.9765) and Q^2 (0.9370) for training and LOO-CV sets, respectively. However, the *RMSE* was found to be high value with high correlation coefficient, which has been demonstrated as potential models for QSAR developments (Branham et al., 2012; Worachartcheewan 2012, 2014).

Structure-activity relationship

The MLR equation, Eq. (2), showed the important descriptors involved in the antioxidant activity including 3D-MoRSE-signal 11/weighted by atomic masses (Mor11m), 3D-MoRSE-signal 25/weighted by atomic van der Waals volumes (Mor25v), mean topological charge index of order 5 (JGI5), H autocorrelation of lag 8/weighted by atomic polarizabilities (H8p), Geary autocorrelation–lag 5/weighted by atomic polarizabilities (GATS5p), and Ghose-Viswanadhan-Wendoloski drug-like index at 50% (GVWAI-50) as shown in Tables 1 and 2. The relative important descriptors in Eq. (2) displayed the following order of significance, JGI5 > H8p > GVWAI-50 > Mor11m > GATS5p > Mor25v, as observed by the coefficient values of 1746.2843, 183.5802, 30.6893, 28.1446, 27.2051, -45.5842, respectively. The positive coefficient values of JGI5, H8p, GVWAI-50, Mor11m and GATS5p in Eq. (2) indicated that the increase of descriptor values correlated with the increased activity as a positive effect. On the other hand, Mor25v had the negative coefficient value indicating the increasing activity with the decreasing value of this descriptor as a negative effect.

The investigated compounds (**1**-**20**) had a common pyrazolopyridine ring substituted with amino (NH_2) group at 3-position (**1**, **8**, **9**, **14**, **18**) or with various condensed rings at 2,3-position on the pyrazole ring making the compounds as tricyclic derivatives including pyridine-pyrazole-imidazole (**2**, **3**, **4**-**7**), pyridine-pyrazole-pyrimidine (**10**-**13**, **15**-**17**, **19**), and pyridine-pyrazole-benzodiazepine (**20**). Considering the antioxidant activity of compounds **1**-**20**, it was found that most compounds with high JGI5, H8p and GATS5p values, but with low value of Mor25v exhibited high activity as observed in the experimental and predicted activities (Table 1). Particularly, 3-amino compound (**1**) with the highest antioxidant activity (86.94%) had the highest mean topological charge index of order 5 (JGI5 = 0.066)

and Geary autocorrelation–lag 5/weighted by atomic polarizabilities (GATS5p = 1.375) as the positive effect, but relatively with the lowest 3D-MoRSE-signal 25/weighted by atomic van der Waals volumes (Mor25v = 0.164) as the negative effect. Such descriptor properties of compound **1** could be possibly due to the NH moiety of pyrazole ring, and 3-NH_2 as electron releasing group substituted on the pyrazole ring that participated in the electron delocalization and giving rise to ionic charges resonant forms (**1a** and **1b**, respectively, Fig. 3) in exerting the antioxidant activity by scavenging the radical cation of the ABTS. It should be noted that compound **1** is the smallest molecular size that correlated to the low value of 3D-MoRSE-signal 25/weighted by atomic van der Waals volumes (Mor25v = 0.164).

When the 3-NH_2 group of compound **1** was converted to electron withdrawing amide group (compound **18**), a remarkable reduced antioxidant activity (35.74%, Table 1) was noted as correlated to the reduced values of JGI5 (0.041) and GATS5p (1.193) compared with compound **1**. The results suggested that the pyrazolopyridine with 3-NH_2 group (**1**) is required for the highest antioxidant activity.

The investigated tricyclic scaffolds constitute a variety of substituents and/or fused aryl or heteroaryl rings. Tricyclic pyridine-pyrazole-imidazole (**2** and **3**), resulting from 3-NH_2 group ring closure of compound **1**, displayed lower antioxidant activity than that of the parent compound **1**. However, compound **3** had higher activity (74.29%) than compound **2** (33.31%), in which high values of H8p (0.123) and Mor11m (0.788) but relatively low Mor25v (0.422) were observed for compound **3**. The highest H8p value of compound **3** could be due to the polarizabilities of electron withdrawing CN group of the compound that is capable of interacting with the radical cation of the ABTS.

Apart from the parent compound **1**, compounds with relatively high antioxidant activity (>50% inhibition) were noted for compounds **3**, **5**-**6** (**3**>**5**>**6**) showing high values of JGI5 (0.037-0.04), GATS5p (0.830-1.198) and H8p (0.05-0.123).

Among the antioxidant quinone derivatives (**4**-**7** in which **5**>**6**>**4**>**7**), hydroxy-1,4-naphthoquinone **5** had the highest antioxidant activity (64.25%) with high GATS5p (1.198). It might be due to the polarizabilities of OH group on the 1,4-naphthoquinone **5** which provided the high value of GATS5p in governing the high activity compared with the bromo-1,4-naphthoquinone (**4**). In case of 1,4-quinone (**6**) containing diOH groups on the quinone ring, its reduced activity (53.81%) with reduced GATS5p (0.830) and H8p (0.050) were observed comparing with hydroxy-1,4-naphthoquinone (**5**). Remarkably, diacetoxy-1,4-quinone (**7**) displayed lower activity (14.41%) with lower JGI5 (0.036) and H8p (0.029)

compared with diOH-1,4-quinone (**6**). It was suggested that 1,4-naphthoquinone (**5**) with *ortho*-OH group is an appropriate moiety condensing with the tricyclic pyridinepyrazolimidazole core scaffold. This might contribute to the H-bonding and lipophilic properties of the hydroxy-1,4-naphthoquinone (**5**) in exerting its antioxidant activity. It should be noted that diacetoxy-1,4-quinone (**7**) with the lowest Mor25v (0.169) had the lowest antioxidant activity compared with compounds **4**-**6** (**5**>**6**>**4**>**7**). This observed effect could be presumed that Mor25v is the last order of relative important chemical descriptors as previously mentioned.

Other compounds (**8**-**20**) with low antioxidant activity (<50% inhibition) mostly had low values of JGI5 (0.025-0.042) and GATS5p (0.838-1.155), but high Mor25v (0.134-0.685) compared with the most active compound **1** (JGI5 = 0.066, GATS5p = 1.375, Mor25v = 0.164), and with the moderately active compounds **3**, **5** and **6** (53.81-74.29% inhibition, JGI5 = 0.037-0.041, GATS5p = 0.830-1.198, Mor25v = 0.196-0.422).

Notably, high Mor25v values of compounds **8**-**20** (except for **18**) could be possibly due to their more complexed ring structures leading to bulky molecules. The antioxidant activity of **8**-**20** and values of these chemical descriptors showed quite good correlation. Compounds **1**-**20** had H8p values in a range of 0.004-0.123 in which compound **3**, the second ranked antioxidant, had the highest H8p (0.123) value. Relatively high H8p values of 0.113 and 0.108 were also noted for compounds **9** and **4**, respectively. This could be due to a diverse range of chemical structures affecting their molecular influence matrices in governing the antioxidant activity (Talete 2007).

Apparently, the compound (**1**) with the highest antioxidant activity had the important 3-aminopyrazole pharmacophore that well correlated to certain chemical descriptors with high topological charge index and atomic polarizabilities, but with low atomic van der Waals volumes. In this regard, the properties of such descriptors could assist in searching and designing novel antioxidants by modification of the 3-NH_2 group as other electron releasing groups, and the ring structure of compound (**1**) as other heterocyclic rings. Possible structurally modified derivatives of **1** could be displayed, for example, **1A** resulting from a replacement of 3-NH_2 group by other electron donating groups (OH, OR, SH), **1B** resulting from the replacement of pyridine ring by pyrimidine ring, and **1C** resulting from the substitution of phenyl ring with electron withdrawing groups on the pyridine ring as shown in Fig. 4.

Conclusions

The underlying basis of the antioxidant activity of pyrazolopyridines was explored by scrutinizing important descriptors obtained from QSAR model constructed using MLR. It was found that a set of physicochemical parameters comprising of 3D-MoRSE-signal 11/weighted by atomic masses (Mor11m), 3D-MoRSE-signal 25/weighted by atomic van der Waals volumes (Mor25v), mean topological charge index of order 5 (JGI5), H autocorrelation of lag 8/weighted by atomic polarizabilities (H8p), Geary autocorrelation–lag 5/weighted by atomic polarizabilities (GATS5p), and Ghose-Viswanadhan-Wendoloski drug-like index at 50% (GVWAI-50) were important for the antioxidant activity. The compounds with the highest antioxidant activity also had high JGI5 and GATS5p with low Mor25v as noted for the 3-aminopyrazole pharmacophore (**1**). Interestingly, the highest H8p value was noted for the second-ranked antioxidant (**3**). Such high atomic polarizabilities (H8p) may be due to the effect of the electron-withdrawing CN group and this can be used as a guideline for the rational design of new antioxidants. The results revealed the importance of pharmacophore **1** as a lead compound for further development as potent antioxidants. Structurally modified derivatives of **1** as shown in Fig. 4 is proposed as putative compounds (**1A** – **1C**) that may exert promising antioxidant activity.

Acknowledgements We gratefully acknowledge the support from the Office of the Higher Education Commission, Mahidol University under the National Research Universities Initiative as well as partial support from the Annual Government Grant under Mahidol University (B.E. 2556–2558). AW gratefully acknowledges the research grant supported by the Thailand Research Fund (Grant No. TRG5880143).

Conflict of interest The authors declare that they have no conflict of interest.

References

Abdel-Hamid MK, Abdel-Hafez AA, El-Koussi NA, Mahfouz NM (2009) Quantitative structure-activity relationship (QSAR) studies on a series of 1,3,4-thiadiazole-2-thione derivatives as tumor-associated carbonic anhydrase IX inhibitors. J Enzyme Inhib Med Chem 24:722-729

Abu-Melha S (2013) Synthesis and antimicrobial activity of some new heterocycles incorporating the pyrazolopyridine moiety. Arch Pharm Chem Life Sci 346:912-921

Alam MS, Ahmed JU, Lee DU (2014) Synthesis, antibacterial, antioxidant activity and QSAR studies of novel 2-arylidenehydrazinyl-4-arylthiazole analogues. Chem Pharm Bull 62:1259-1268

Al-Omar MA, Youssef KM, El-Sherbeny MA, Awadalla SA, El-Subbagh HI (2005) Synthesis and in vitro antioxidant activity of some new fused pyridine analogs. Arch Pharm Chem Life Sci. 338:175-180

Amić D, Davidović-Amić D, Beslo D, Rastija V, Lucić B, Trinajstić N (2007) SAR and QSAR of the antioxidant activity of flavonoids. Curr Med Chem 14:827-845

Amr AG, Mohamed AM, Mohamed SF, Abdel-Hafez NA, Hammam Ael-F (2006) Anticancer activities of some newly synthesized pyridine, pyrane, and pyrimidine derivatives. Bioorg Med Chem 14:5481-5488

Branham ML, Ross EA, Govender T. Predictive models for maximum recommended therapeutic dose of antiretroviral drugs. Comput Math Methods Med. 2012;2012:1-9

Cai J, Liu L, Chen J, Cao M, Ji M (2013) Design, synthesis, and bioactivity of pyrazole acid derivatives as endothelin receptor antagonists. Med Chem 9:1113-1122

Deng X, Gray NS (2012) Pyrazolopyridines as inhibitors of the kinase LRRK2: a patent evaluation (WO2011141756). Expert Opin Ther Pat 22:709-713

Dennington II R, Keith T, Millam J, Eppinnett K, Hovell WL, Gilliland R (2003) GaussView, Version 3.09; Semichem, Inc.: Shawnee Mission, KS, USA

Deodhar MN, Khopade PL, Varat MG (2013) Sulfonamide based β-carbonic anhydrase inhibitors: 2D QSAR study. ISRN Med Chem 2013:1-8

Eriksson L, Johansson E (1996) Multivariate design and modeling in QSAR. Chemometr Intell Lab Syst 34:1-19

Frisch MJ, Trucks GW, Schlegel HB, Scuseria GE, Robb MA, Cheeseman JR, Scalmani G, Barone V, Mennucci B, Petersson GA, Nakatsuji H, Caricato M, Li X, Hratchian HP, Izmaylov AF, Bloino J, Zheng G, Sonnenberg JL, Hada M, Ehara M, Toyota K, Fukuda R, Hasegawa J, Ishida M, Nakajima T, Honda Y, Kitao O, Nakai H, Vreven T, Montgomery JA, Peralta JE, Ogliaro F, Bearpark M, Heyd JJ, Brothers E, Kudin KN, Staroverov VN, Kobayashi R, Normand J,

Raghavachari K, Rendell A, Burant JC, Iyengar SS, Tomasi J, Cossi M, Rega N, Millam JM, Klene M, Knox JE, Cross JB, Bakken V, Adamo C, Jaramillo J, Gomperts R, Stratmann RE, Yazyev O, Austin AJ, Cammi R, Pomelli C, Ochterski JW, Martin RL, Morokuma K, Zakrzewski VG, Voth GA, Salvador P, Dannenberg JJ, Dapprich S, Daniels AD, Farkas Ö, Foresman JB, Ortiz JV, Cioslowski J, Fox DJ (2009) Gaussian 09, Revision A.02. Gaussian, Inc., Wallingford

Gouda MA (2012) Synthesis and antioxidant evaluation of some new pyrazolopyridine derivatives. Arch Pharm Chem Life Sci 345:155-162

Gudmundsson KS, Johns BA, Allen SH (2008) Pyrazolopyridines with potent activity against herpesviruses: effects of C5 substituents on antiviral activity. Bioorg Med Chem Lett 18:1157-1161

Hanna MM (2012) New pyrimido[5,4-*e*]pyrrolo[1,2-*c*]pyrimidines: synthesis, 2D-QSAR, anti-inflammatory, analgesic and ulcerogenicity studies. Eur J Med Chem 55:12-22

Kaiser JP, Feng Y, Bollag JM (1996) Microbial metabolism of pyridine, quinoline, acridine, and their derivatives under aerobic and anaerobic conditions. Microbiol Rev 60:483–498

Kumar H, Saini D, Jain S, Jain N (2013) Pyrazole scaffold: a remarkable tool in the development of anticancer agents. Eur J Med Chem 70:248-258

Nantasenamat C, Isarankura-Na-Ayudhya C, Prachayasittikul V (2010) Advances in computational methods to predict the biological activity of compounds. Expert Opin Drug Discov 5:633-654

Nantasenamat C, Prachayasittikul V (2015) Maximizing computational tools for successful drug discovery. Expert Opin Drug Discov 10:321-329

Prachayasittikul V, Pingaew R, Worachartcheewan A, Nantasenamat C, Prachayasittikul S, Ruchirawat S, Prachayasittikul V (2014) Synthesis, anticancer activity and QSAR study of 1,4-naphthoquinone derivatives. Eur J Med Chem 84:247-263

Prachayasittikul V, Worachartcheewan A, Shoombuatong W, Songtawee N, Simeon S, Prachayasittikul V, Nantasenamat C (2015) Computer-aided drug design of bioactive natural products. Curr Top Med Chem 15:1780-1800

Prachayasittikul S, Pingaew R, Worachartcheewan A, Sinthupoom N, Prachayasittikul V, Ruchirawat S, Prachayasittikul V (2016) Roles of pyridine and pyrimidine derivatives as privileged scaffolds in anticancer agents. Mini Rev Med Chem 2016. doi: 10.2174/1389557516666160923125801

Talete srl (2007) DRAGON for Windows (Software for Molecular Descriptor Calculations), version 5.5, Milano, Italy

Valko M, Leibfritz D, Moncol J, Cronin MT, Mazur M, Telser J (2007) Free radicals and antioxidants in normal physiological functions and human disease. Int J Biochem Cell Biol 39:44-84

Witten IH, Frank E, Hall MA (2011) Data mining: practical machine learning tools and techniques, 3rd ed. Morgan Kaufmann, San Francisco

Worachartcheewan A, Nantasenamat C, Isarankura-Na-Ayudhya C, Prachayasittikul S, Prachayasittikul V (2011) Predicting the free radical scavenging activity of curcumin derivatives. Chemometr Intell Lab Syst 109:207-216

Worachartcheewan A, Prachayasittikul S, Pingaew R, Nantasenamat C, Tantimongcolwat T, Ruchirawat S, Prachayasittikul V (2012) Antioxidant, cytotoxicity and QSAR study of 1-adamantylthio derivatives of 3-picoline and phenylpyridines. Med Chem Res 21:3514–3522

Worachartcheewan A, Nantasenamat C, Owasirikul W, Monnor T, Naruepantawart O, Janyapaisarn S, Prachaysittikul S, Prachayasittikul V (2014) Insights into antioxidant activity of 1-adamantylthiopyridine analogs using multiple linear regression. Eur J Med Chem 73:258-264

Wu J, Shi Q, Chen Z, He M, Jin L, Hu D (2012) Synthesis and bioactivity of pyrazole acyl thiourea derivatives. Molecules 17:5139-5150

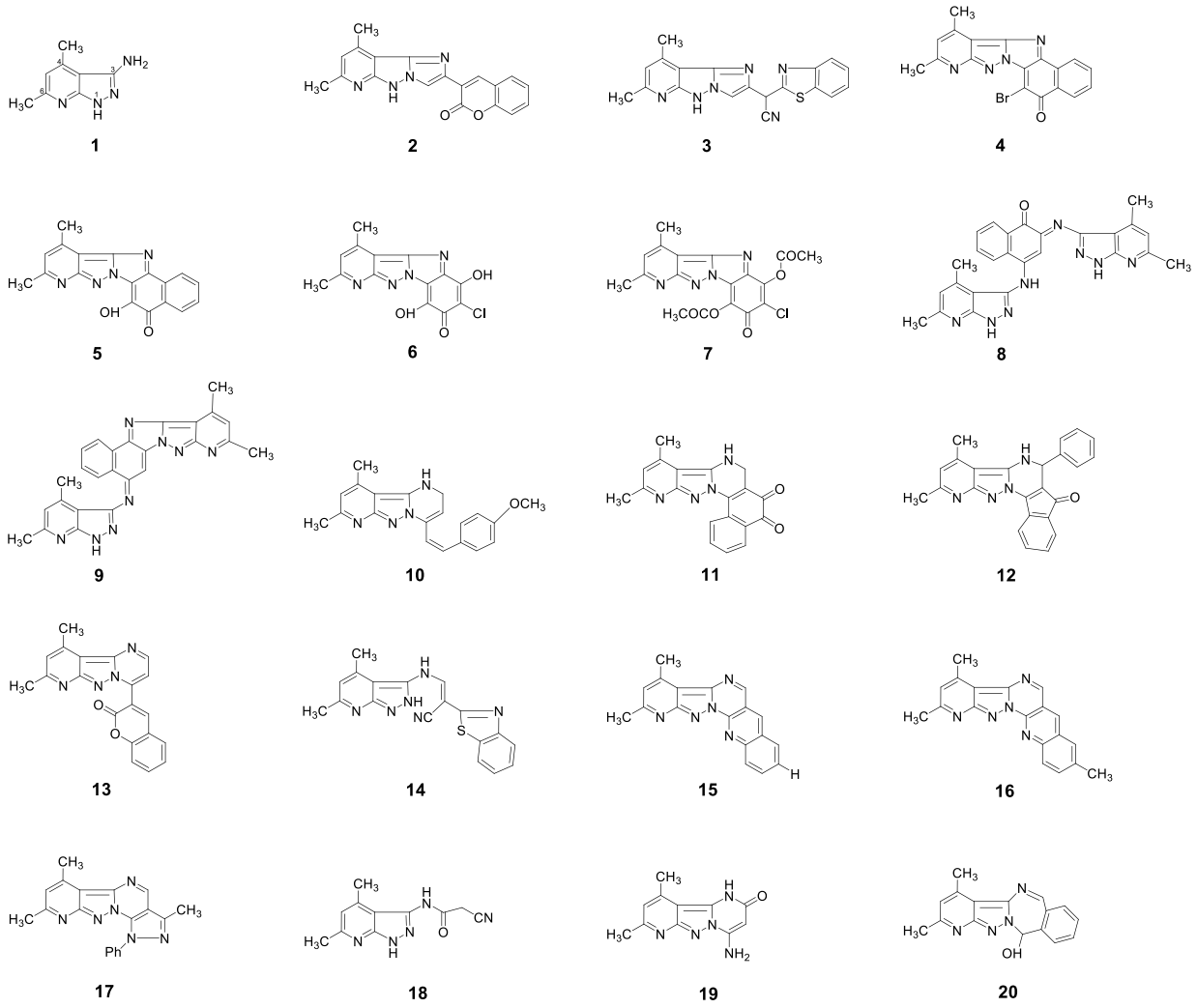

Fig. 1 Molecular structures of pyrazolopyridine derivatives **1**-**20**

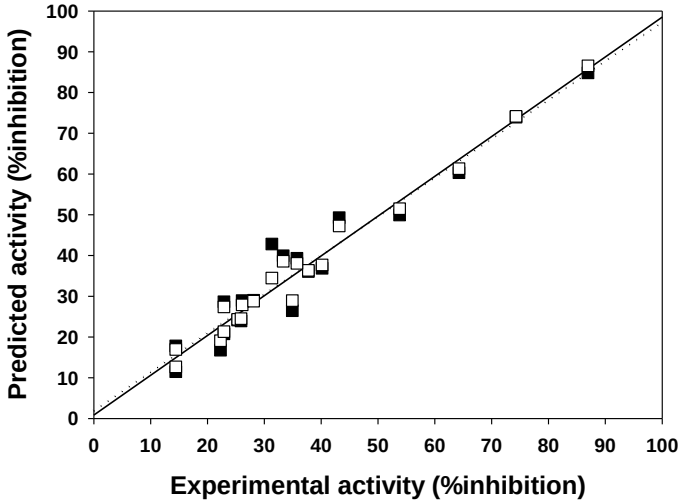

Fig. 2 Plot of the experimental and predicted activities for the training set (□; regression line is represented as solid line), and the leave-one-out cross-validated set (■; regression line is represented as dotted line)

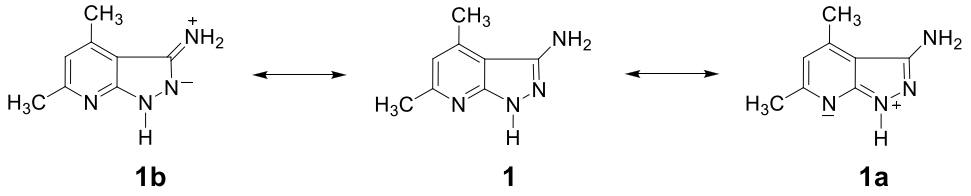

Fig. 3 Charge distribution of compound **1**

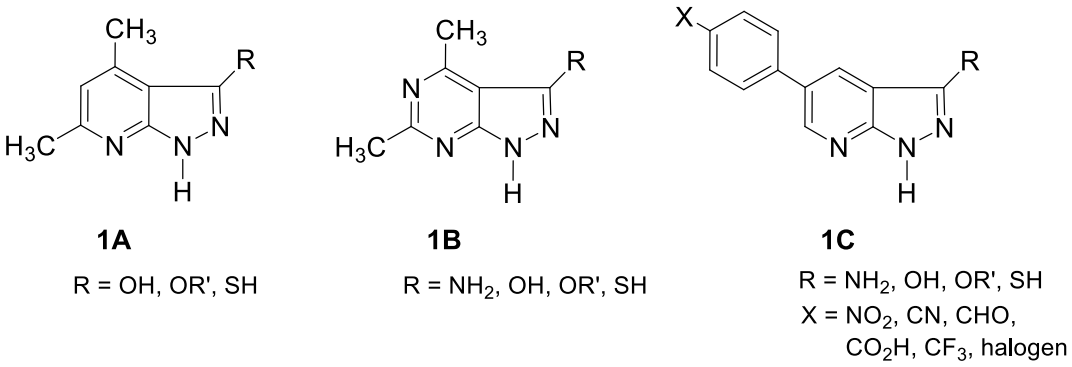

Fig. 4 Possible structurally modified derivatives (**1A-1C**)

Table 1 Antioxidant activity and significant descriptors of pyrazolopyridine derivatives

Compound	JGI5	GVWAI-50	Mor11m	H8p	Mor25v	GATS5p	Inhibition (%)	
							Exp.	Pred.
1	0.066	0	0.477	0.007	0.164	1.375	86.94	84.84
2	0.035	1	0.455	0.029	0.573	1.033	33.31	39.96
3	0.037	1	0.788	0.123	0.422	0.98	74.29	73.96
4	0.038	1	-0.760	0.108	0.349	1.038	31.32	42.84
5	0.038	1	0.280	0.075	0.365	1.198	64.25	60.33
6	0.041	1	-0.010	0.050	0.196	0.830	53.81	49.93
7	0.036	0	-0.021	0.029	0.169	0.960	14.41	17.83
8	0.027	0	1.300	0.091	0.644	1.108	26.10	28.96
9	0.029	0	0.855	0.113	0.685	1.037	22.28	16.77
10	0.029	1	1.053	0.019	0.652	0.967	40.16	36.87
11	0.029	1	0.206	0.013	0.306	0.977	28.11	29.03
12	0.030	0	0.888	0.059	0.644	1.155	14.41	11.51
13	0.026	1	0.554	0.035	0.618	1.189	34.93	26.47
14	0.025	1	0.712	0.029	0.611	0.838	22.89	20.78
15	0.026	1	0.443	0.033	0.569	1.066	25.30	24.17
16	0.027	1	0.515	0.054	0.508	1.125	37.75	36.08
17	0.026	1	0.915	0.023	0.696	0.970	22.89	20.78
18	0.041	0	0.283	0.030	0.134	1.193	35.74	39.33
19	0.042	0	0.328	0.004	0.285	1.012	25.90	23.94
20	0.028	1	0.700	0.046	0.350	1.059	43.17	49.28

Exp.; Experimental activity, Pred.; Predicted activity.

Table 2 Description of important descriptors for constructing the QSAR model

Descriptors	**Type**	**Description**
JGI5	Topological charge indices	Mean topological charge index of order 5
GVWAI-50	Molecular properties	Ghose-Viswanadhan-Wendoloski drug-like index at 50%
Mor11m	3D-MoRSE descriptors	3D-MoRSE-signal 11/weighted by atomic masses
Mor25v	3D-MoRSE descriptors	3D-MoRSE-signal 25/weighted by atomic van der Waals volumes
H8p	GETAWAY descriptors	H autocorrelation of lag 8/weighted by atomic polarizabilities
GATS5p	2D autocorrelation descriptors	Geary autocorrelation –lag 5/weighted by atomic polarizabilities

Table 3 Intercorrelation matrix of significant descriptors

Descriptors	JGI5	GVWAI-50	Mor11m	H8p	Mor25v	GATS5p
JGI5	1					
GVWAI-50	-0.388	1				
Mor11m	-0.366	-0.148	1			
H8p	-0.161	0.02	0.012	1		
Mor25v	-0.705	0.223	0.656	0.22	1	
GATS5p	0.449	-0.378	0.072	-0.028	-0.136	1

Send Orders for Reprints to reprints@benthamscience.ae

Mini-Reviews in Medicinal Chemistry, 2017, *17*, 000-000

REVIEW ARTICLE

Roles of Pyridine and Pyrimidine Derivatives as Privileged Scaffolds in Anticancer Agents[§]

Supaluk Prachayasittikul[1,*], Ratchanok Pingaew[2], Apilak Worachartcheewan[1,3,4], Nujarin Sinthupoom[5], Veda Prachayasittikul[1], Somsak Ruchirawat[6,7] and Virapong Prachayasittikul[5]

[1]*Center of Data Mining and Biomedical Informatics, Faculty of Medical Technology, Mahidol University, Bangkok 10700, Thailand;* [2]*Department of Chemistry, Faculty of Science, Srinakharinwirot University, Bangkok 10110, Thailand;* [3]*Department of Clinical Chemistry, Faculty of Medical Technology, Mahidol University, Bangkok 10700, Thailand;* [4]*Department of Community Medical Technology, Faculty of Medical Technology, Mahidol University, Bangkok 10700, Thailand;* [5]*Department of Clinical Microbiology and Applied Technology, Faculty of Medical Technology, Mahidol University, Bangkok 10700, Thailand;* [6]*Laboratory of Medicinal Chemistry, Chulabhorn Research Institute, and Program in Chemical Biology, Chulabhorn Graduate Institute, Bangkok 10210, Thailand;* [7]*Center of Excellence on Environmental Health and Toxicology, Commission on Higher Education (CHE), Ministry of Education, Thailand*

ARTICLE HISTORY

Received: February 29, 2016
Revised: July 22, 2016
Accepted: September 20, 2016

DOI:
10.2174/1389557516666160923125801

Abstract: Cancer has been considered to be a global health concern due to the impact of disease on the quality of life. The continual increase of cancer cases as well as the resistance of cancer cells to the existing drugs have driven the search for novel anticancer drugs with better potency and selectivity, improved pharmacokinetic profiles, and minimum toxicities. Pyridine and pyrimidine are presented in natural products and genetic materials. These pyridine/pyrimidine core structures have been noted for their roles in many biological processes as well as in cancer pathogenesis, which make such compounds become attractive scaffolds for discovery of novel drugs. In the recent years, pyridine- and pyrimidine-based anticancer drugs have been developed based on structural modification of these core structures (*i.e.*, substitution with moieties and rings, conjugation with other compounds, and coordination with metal ions). Detailed discussion is provided in this review to highlight the potential of these small molecules as privileged scaffolds with attractive properties and biological activities for the search of novel anticancer agents.

Keywords: Anticancer agents, cancer, fused-pyridine/pyrimidine, metal-based pyridine/pyrimidine, pyridine, pyrimidine.

1. INTRODUCTION

In the recent years, the trend of global health situation has been directed towards non-communicable diseases including cancers [1]. Cancer is a chronic disease in which its sequelae affect long-term quality of life [2]. Cancer has been reported by the World Health Organization (WHO) as one of the Global Burden of Diseases [3]. New cases are estimated to be continuously increasing, and cancers are predicted to be one of the main causes of death in the next decades [4, 5]. Hence, the continuous search for novel anticancer agents is essential, and is a global impact issue.

For decades, great attention has been focused on the search for novel anticancer drugs due to impacts of the disease on human life. Many classes of novel anticancer agents, acting at various therapeutic targets *via* several mechanisms of action, have been discovered. However, some of the compounds do not fall into any types of the classical classification system [6]. In this regard, anticancer drugs have been reclassified based on their mechanisms of action [7], and their therapeutic targets [8].

1.1. Classification of Anticancer Drugs Based on Mechanism of Action

Regarding the mechanism of action, anticancer drugs are classified into many types *i.e.*, alkylating agents, antimetabolites, cytotoxic antibiotics, spindle poisons and topoisomerase

*Address correspondence to this author at the Center of Data Mining and Biomedical Informatics, Faculty of Medical Technology, Mahidol University, Bangkok 10700, Thailand; Tel: 662-441-4376; Fax: 662-441-4380; E-mail: supaluk@g.swu.ac.th

[§]*This invited review article is dedicated to Professor Ludwig Bauer, Professor Emeritus, Department of Medicinal Chemistry and Pharmacognosy, College of Pharmacy, University of Illinois at Chicago, Chicago, Illinois, 60680, USA*

1389-5575/17 $58.00+.00

Table 1. Classification of anticancer drugs based on mechanism of action.

Type	Mechanism of Action	Example Drug
Alkylating agents [7]	Form crosslinks (adducts) with cancer DNA	Nitrogen mustards, nitrosoureas, tetrazines, oxazaphosphorenes, aziridines, alkyl alkanes sulphonates, procarbazines, platinum agents, cytotoxic antibiotics (actinomycin D, mitomycin C)
Antimetabolites [7]	Compete with natural substances to bind with receptors or enzymes and/or incorporate into DNA/RNA of cancer	Folic acid antagonist (methotrexate) pyrimidine analogues (5-fluorouracil, cytarabine, gemcitabine), purine analogs (6-mercaptopurine, thioguanine)
Spindle poisons [7]	Inhibit mitosis *via* binding to tubulin	Vinca alkaloids (vinblastine), toxoids (paclitaxel)
Topoisomerase inhibitors [7, 11]	Inhibit topoisomerase I Inhibit topoisomerase II	Camptothecin, topotecan, rubitecan, irinotecan, belotecan, anthracyclines (doxorubicin, etoposide)
Antiangiogenic agents [9]	Inhibit growth of endothelial cell	Thalidomide, endostatin, combretastatin A4
	Block angiogenesis signaling	Antibodies against VEGF (bevacizumab), antibodies against EGFR (cetuximab, panitumumab), tyrosine kinase inhibitor (erlotinib), mTOR inhibitor (rapamycin)
	Block break down of extracellular matrix	MMPs inhibitors
Vasculogenic mimicry inhibitors [12-19]	Inhibit vasculogenic mimicry formation	Galunisertib, fasudil, ginsenoside Rg3, incarvine, norcantharidin, hinokitiol, doxycycline, curcumin
Inhibitors of signaling intermediates	Inhibit PI3K/Akt/mTOR Pathway [20, 21]	GSK690693, afuresertib, uprosertib, ipatasertib, MK-2206, triciribine phosphate, BEZ-235, everolimus
	Inhibit tyrosine kinases [9, 22]	Sunitinib, sorafenib, pazopanib, sutent, gefitinib, erlotinib, imatinib, semaxinib
	Inhibit Ras/Raf/MEK/ERK pathway [20]	R115777, MEK162, selumetinib, trametinib, vemurafenib
	Inhibit hedgehog signaling pathway [10, 23, 24]	Cyclopamine, saridegib, vismodegib, arsenic trioxide, robotnikinin, NVP-LDE225
Proteasome inhibitors [9, 25]	Inhibit proteasome function leading to cancer cell apoptosis	Bortezomib, carfilzomib, isazomib, delanzomib, marizomib
HSP90 inhibitors [10, 26]	Inhibit heat shock protein HSP90	Geldanamycin, ganetespib, 17-AAG, NVP-AUY922, valproic acid, herbimycin A, radicicol
Epigenetic modifiers	Inhibit histone deacetylase [27, 28]	Vorinostat, entinostat, depsipeptide, valproic acid, benzamides, romidepsin
	Inhibit DNA methyltransferase [29, 30]	Cytidine analogs (azacytidine, decitabine,zebularine), hydralazine, procaine, RG108, epigallocatechin gallate (EGCG)

inhibitors, antiangiogenetic agents [9], and vasculogenic mimicry inhibitors (Table **1**). Drugs targeting other therapeutic targets such as signaling intermediates, protein folding, proteasome function, and epigenetic modifications also are summarized herein [10] (Table **1**).

1.2. Classification of Anticancer Drugs Based on Therapeutic Targets

According to Espinosa *et al.*, anticancer agents are classified by their target sites of action at various levels ranging from cancer cells, endothelium, extracellular matrix, and host cells [8] as provided in Fig. (**1**).

Most of the classical anticancer drugs are cytotoxic agents which have low selectivity towards cancer cells thereby leading to considerable adverse effects (*i.e.*, bone marrow suppression, alopecia, nausea and vomiting). In addition, most of the drugs are mainly active against proliferating cells but do not affect cancer cells in the resting phase [7]. Hence, novel drugs acting at various targets have been continuously developed for improving disease control and prevention. Anticancer drugs of later generations are developed to achieve higher potency and selectivity, better pharmacokinetics as well as minimum toxicity.

Pyridine and pyrimidine are attractive scaffolds for drug design and development. Many currently used anticancer drugs contain these privileged structures. Such anticancer drugs acting at various drug targets were designed and developed. For example, the nucleic acids of genetic materials (DNA and RNA) are pyrimidine and purine derivatives. In this regard, many antimetabolites anticancer drugs have been developed based on mimicking natural substrate to competitively bind with the targets *i.e.*, receptors or enzymes [7].

Anticancer drugs were also developed based on the role of compounds in modulating cancer-related biological pathways. Nicotinamide, an amide form of niacin or vitamin B3, is a pyridine derivative which plays several roles in biological processes [31]. Nicotinamide elicits anticancer effect *via* two main mechanisms, Fig. (**2**). First, nicotinamide serves as a primary substrate for production of poly ADP-ribose polymerase-1 (PARP-1) enzyme [32], which is an essential enzyme requiring for DNA repair and maintenance of

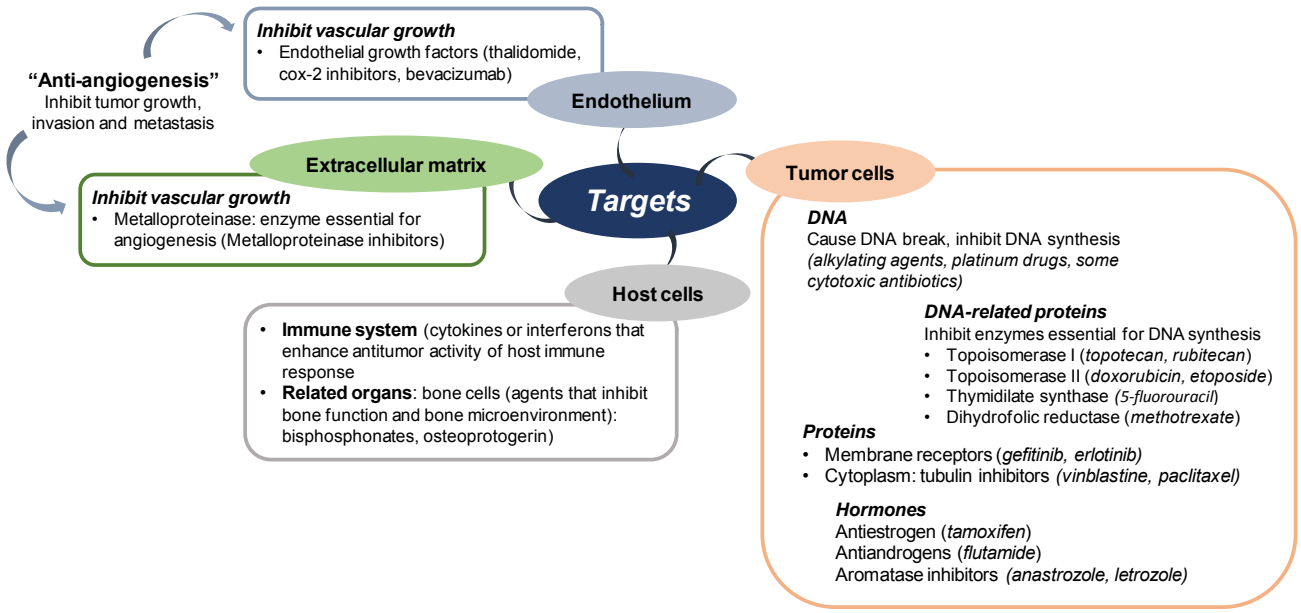

Fig. (1). Classification of anticancer drugs based on therapeutic targets.

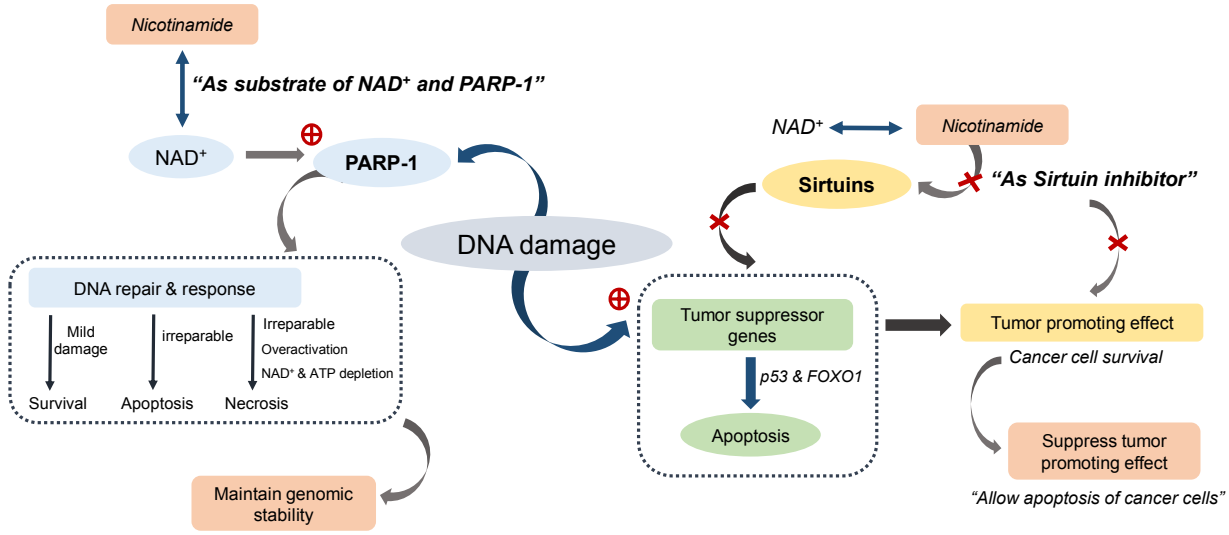

Fig. (2). Anticancer effects of nicotinamide *via* two main roles as PARP-1 substrate and sirtuin inhibitor. PARP-1: poly ADP-ribose polymerase-1 enzyme, NAD^+: nicotinamide adenine dinucleotide.

genomic stability [32]. Second, the nicotinamide is a non-competitive sirtuin inhibitor [33, 34]. Sirtuins are a family of nicotinamide adenine dinucleotide (NAD^+)-dependent deacetylases which play important roles in many biological processes including cell survival and apoptosis [35-37]. Sirtuins deacetylate many classes of protein including tumor suppressor genes [34], and the function of these proteins are inactivated upon deaceylation [38]. Sirtuin overexpression was noted to increase lifespan of many organisms (*i.e.*, yeast, worms and files) whereas inverse effect was observed for its deletion or inhibition [39-41]. In addition, overexpression or upregulation of sirtuins is found in many types of cancer [42]. Sirtuins have been noted for their tumor promoting effects with respect to their abilities to promote survival of cancer cells [43]. The promotion of cancer cell survival is elicited by the deactivation of tumor suppressor genes [43] (*i.e.*, p53 [36] and FOXO1 [44]), Fig. (**2**). In this context, the regulation regarding apoptosis of the cancer cells is altered, thereby promotes their survival and growth. Anticancer mechanism of nicotinamide as sirtuin inhibitor is outlined in Fig. (**2**). As an enzyme, sirtuin utilizes NAD^+ as a substrate for production of nicotinamide, the activity of enzyme is modulated by intracellular levels of NAD^+ and nicotinamide [34]. Therefore, the nicotinamide itself also acts as a non-competitive sirtuin inhibitor [34]. The inhibition of sirtuin by nicotinamide also suppresses tumor promoting effect of the surtuin, thereby, promoting cancer cell apoptosis [35, 43], Fig. (**2**).

Several classes of anticancer agents such as 1,2,3-triazole-based sulfonamide [45], 1,4-naphthoquinone derivatives [46, 47], quinolines [48], coumarins [49], and derivatives of pyridine [49-51] and pyrimidine [52-54] as well as fused pyridines/pyrimidines [55-57] have been developed in the recent years. However, only pyridine- and pyrimidine-based compounds are discussed in this review.

2. PYRIDINES

Pyridine, a simple six membered heterocycle containing one nitrogen (N) atom in the ring, has been found in a variety naturally occurring compounds, and in therapeutics such as niacin (nicotinic acid) and NAD^+ acting as a substrate or cofactor in biological processes [31], Recently, a number of substituted pyridines have been synthesized and reported for their anticancer activities [49-51, 58, 59].

2.1. Monosubstituted Pyridines

Recently, a variety of monosubstituted pyridines with cytotoxic activity was reported, for example, thiosemicarbazone analogs of pyridine (**1**-**2**) were synthesized by a condensation of the corresponding carbonyl compound with thiosemicarbazides [60]. In addition, analogs of quinoline (**3**) and isoquinolines (**4**-**5**) were synthesized [60]. The synthesized compounds (**1**-**5,** Fig. **3**) displayed potent cytotoxicity against four cancer cell lines (HuCCA-1, HepG2, A549 and MOLT-3). Promisingly, the condensed pyridine analog **2** was shown to be the most potent compound with IC_{50} value of 4 ng/mL toward MOLT-3 cell line.

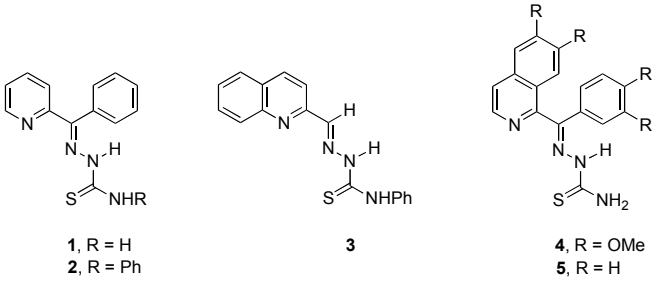

1, R = H
2, R = Ph

3

4, R = OMe
5, R = H

Fig. (3). Chemical structures of thiosemicarbazone analogs of pyridine and condensed pyridines.

It was also reported that coumarin-based hydrazide-hydrazone derivative of monosubstituted pyridine (**6**, Fig. **4**) displayed inhibitory activity against non-small cell lung cancer (NCI-H460) with GI_{50} value of 10 μM in comparison with doxorubicin [49].

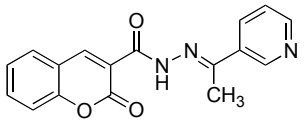

6

Fig. (4). Chemical structure of monosubstituted pyridine containing coumarin.

Moreover, 1,3-disubstituted (thio)urea derivatives of monosubstituted pyridines (**7**-**12**) have been synthesized by treatment of the amines (**13**, **14**) with iso(thio)cyanates (**15**) as shown in Scheme **1** [61]. The obtained compounds (**7**-**12**) exhibited moderate cytotoxic activity against HepG2 and MOLT-3 cancer cell lines.

Recently, the synthesis of a series of 1,4-naphthoquinones (**16**-**19**) tethered by monosubstituted pyridine sulfonamide moieties (Scheme **2**), and evaluation of their bioactivities have been reported by Pingaew *et al.* [46]. The compounds were synthesized by nucleophilic substitution of 2,3-dichloro-1,4-naphthoquinone (**20**) with the appropriate aminobenzene-sulfonamide derivatives (**21**-**24**) in refluxing ethanol. The compounds **16**-**19** displayed a broad spectrum of cytotoxic activities against all of the tested cell lines (HuCCA-1, HepG2, A549, MOLT-3) with IC_{50} range of 1.37-31.37 μM, and exerted stronger anticancer activity against HepG2 cell than that of the etoposide.

Additionally, 1,2,3,4-tetrahydroisoquinoline bearing 3-pyridyl moiety (**25**, Scheme **3**), derived from the Pictet-Spengler reaction of sulfonamide **26** with 3-formylpyridine, exerted cytotoxicity against HuCCA-1, HepG2, A549 and MOLT-3 cancer cell lines with IC_{50} values of 12.42-117.61 μM [62].

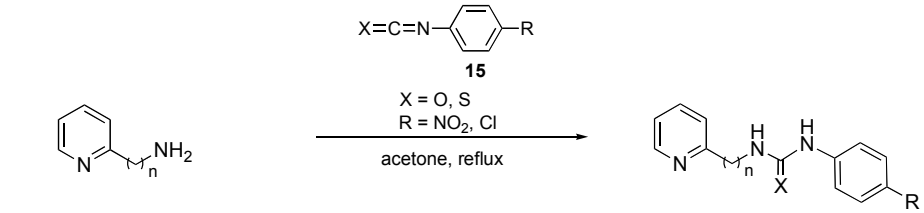

13, 2-pyridylethylamine , n = 2
14, 2-picolylamine , n = 1

7, R = NO_2 , X = S, n = 2
8, R = Cl , X = S, n = 2
9, R = Cl , X = O, n = 2
10, R = NO_2 , X = S, n = 1
11, R = Cl , X = S, n = 1
12, R = Cl , X = O, n = 1

Scheme (1). Synthesis of monosubstituted pyridine derivatives of (thio) ureas.

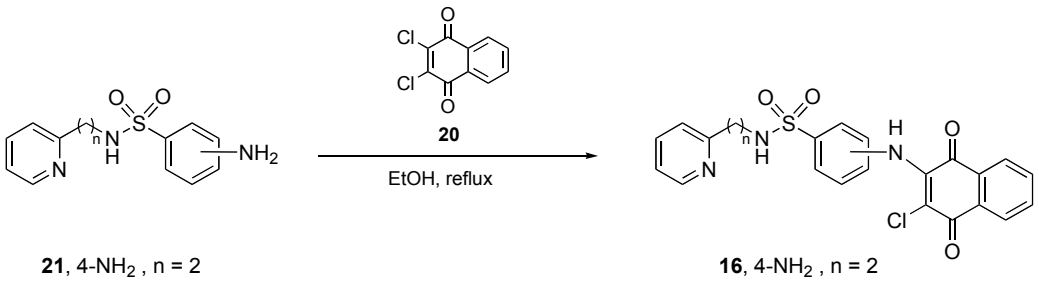

21, 4-NH_2 , n = 2
22, 4-NH_2 , n = 1
23, 3-NH_2 , n = 2
24, 3-NH_2 , n = 1

16, 4-NH_2 , n = 2
17, 4-NH_2 , n = 1
18, 3-NH_2 , n = 2
19, 3-NH_2 , n = 1

Scheme (2). Synthesis of monosubstituted pyridines bearing 1,4-naphthoquinones.

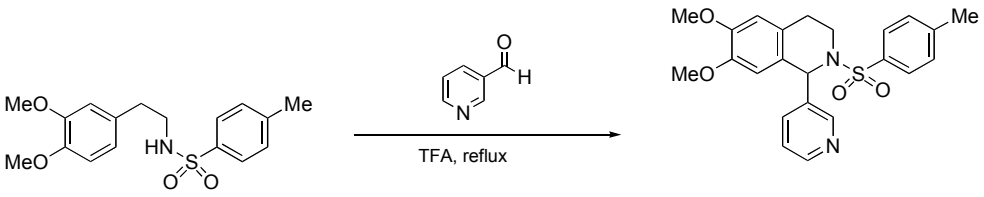

26 **25**

Scheme (3). Synthesis of monosubstituted pyridine analog of 1,2,3,4-tetrahydroisoquinoline.

Breast cancer is one of the leading causes of cancer-related mortality among women worldwide [45]. Aromatase is an enzyme involved in the final step of the estrogen biosynthetic pathway. Therefore, aromatase inhibitors (AIs) have been developed and used as antibreast cancer agent [63]. AIs can be classified into two classes based on their chemical structures including steroidal and nonsteroidal derivatives [45, 63]. Currently, several non-steroidal AIs are in clinical use *i.e.*, anastrozol, letrozole and exemestane [45, 63].

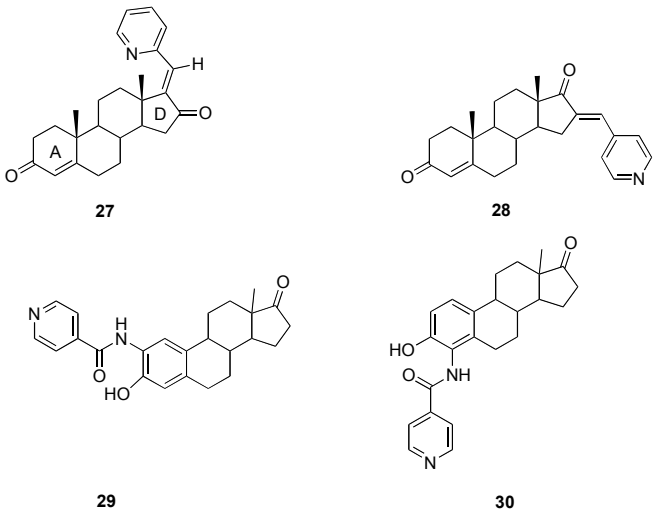

27 **28** **29** **30**

Fig. (5). Chemical structures of monosubstituted pyridines bearing steroidal moieties.

Steroidal AIs bearing pyridine moieties (Fig. **5**) have been reported [63]. For example, 2-picolinylidene substituted at 17-position on ring D of the steroid (**27**) displayed the most effective aromatase inhibitory activity among the tested series. A new series of arylidene derivatives were synthesized and investigated for the activity, 4-pyridyl derivative **28** was shown to be the most potent AI with IC_{50} value of 5.2 μM [63]. In case of pyridyl amides substituted on ring A of the steroid, compounds **29** and **30** exerted potent aromatase inhibitory activity with IC_{50} values of 31 and 28 μM, respectively [63].

For non-steroidal AIs, a number of potent AIs bearing pyridine rings (Fig. **6**) were reported [63]. 4-Pyridyl compound containing tetralone (**31**), and tetraline (**32**) exhibited potent antiaromatse activity. Interestingly, the condensed pyridine derivative (**33**) was shown to be the potent AI (IC_{50} = 0.50 μM).

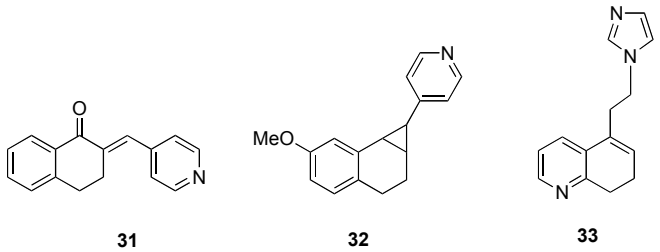

31 **32** **33**

Fig. (6). Chemical structures of 4-pyridyl and condensed pyridine derivatives.

4-Pyridylmethylthio analog of isoflavone (**34**) was reported to be the most potent AI (IC_{50} = 210 μM) in the tested

series. In addition, 3-pyridyl derivative of chroman-4-ones (**35** and **36**) exerted the most potent aromatase inhibitory activity with IC_{50} values of 2.5 and 0.8 μM, respectively [63]. These pyridyl derivatives are shown in Fig. (**7**).

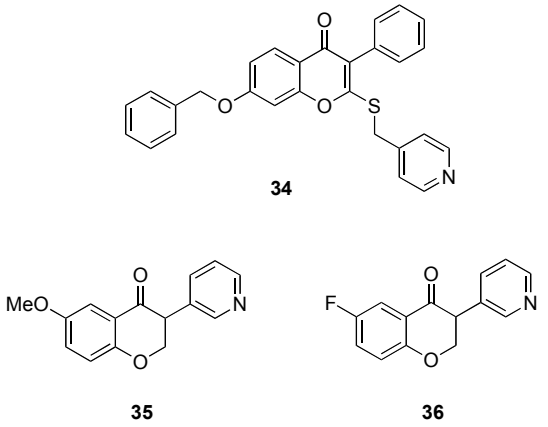

Fig. (7). Chemical structures of pyridyl analogs of isoflavone and chroman-4-ones.

Furthermore, 3,5-dipyridyl-1,2,4-thiadiazole derivatives **37** and **38** (Fig. **8**) were reported to be the potent AIs with IC_{50} values of 0.2 and 0.8 μM, respectively [63].

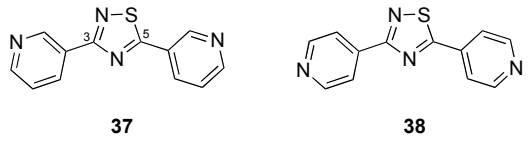

Fig. (8). Chemical structures of 3,5-dipyridyl-1,2,4-thiadiazoles.

Previously, histone deacetylase (HDAC) inhibitors (Fig. **9**) belonging to monosubstituted pyridine derivatives such as MS-275 (**39**) and SB-379278A (**40**) were reported [64].

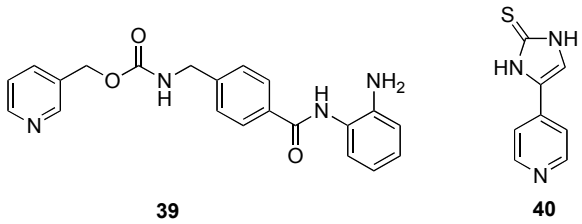

Fig. (9). Chemical structures of monosubstituted pyridines as HDAC inhibitors.

2.2. Disubstituted Pyridines

3-Aminopyridine-2-carboxaldehyde thiosemicarbazone (**41** or 3-AP), 2,3-disubstituted pyridine, was developed for cancer therapy (Triapine®, Vion Pharmaceuticals) [65]. Anticancer activity of 3-AP was resulted from the inhibition of ribonucleotide reductase (RNR) which is a key enzyme required for DNA synthesis [66, 67]. The 3-AP is one of the important RNR inhibitors, used in the treatment of various cancers [68].

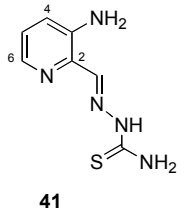

Fig. (10). Chemical structure of 3-aminopyridine thiosemicarbazone.

2,6-Disubstituted pyridine derivative of thiocoumarin **42** (Fig. **11**) exhibited potent antiproliferative activity with GI_{50} value of 2.11 μM against A549 lung cancer cell lines in comparison with paclitaxel [49].

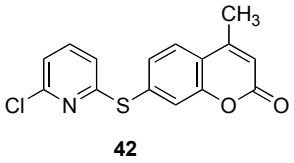

Fig. (11). Chemical structure of disubstituted pyridine analog of thiocoumarin.

Many series of pyridine derivatives as promising new glycogen synthase kinase-3 (GSK-3) inhibitors have been recently reported [50]. For example, 2,4-disubstituted pyridines such as thiazolylpyridine **43** and pyridylpyridine **44** (Fig. **12**) displayed potent GSK-3β inhibitory activity with IC_{50} values of 0.29 nM and 4.4 nM, respectively. Both compounds (**43** and **44**) constitute a common acylaminopyridine core structure. GSK-3, a serine/threonine kinase enzyme, has been implicated in many diseases such as cancer, stroke, diabetes, bipolar disorders and neurodegenerative diseases [69-71].

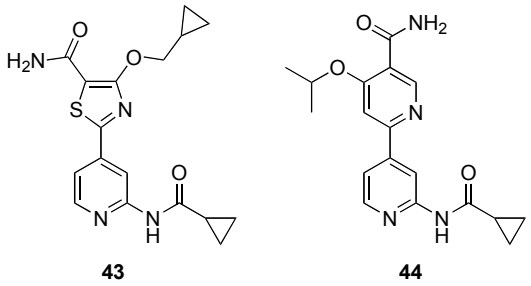

Fig. (12). Chemical structures of disubstituted pyridines as GSK-3 inhibitors.

Previously, 2,4-disubstitited pyridine containing anthranilic acid derivatives (**45-47**, Fig. **13**) were reported to exhibit cytotoxic activity against a panel of human cancer cell lines [72]. It was found that esters **46** and **47** displayed potent activity against MCF-7 cell line with GI_{50} values of 0.28 and 0.16 μM, respectively. On the other hand, carboxylic acid **45** was shown to be an inactive compound.

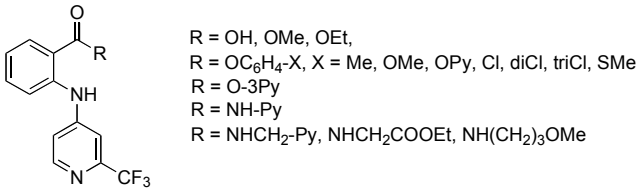

45, R = OH
46, R = OC_6H_4-Cl-*o*
47, R = O-pyridyl-3

Fig. (13). Chemical structures of disubstituted pyridine analogs of anthranilic acids.

Urea derivative of 2,5-disubstituted pyridine **48** was documented to show high antitumor activity *in vivo* (P388 leukemia). The activity of compound **48** arose from the inhibition of tubulin polymerization thereby causing microtubule depolymerization [73]. In addition, acylthiourea derivative of quinoline **49** was reported to be a promising inhibitor of certain types of cell proliferative disorder [74]. Compounds **48** and **49** are shown in Fig. (**14**).

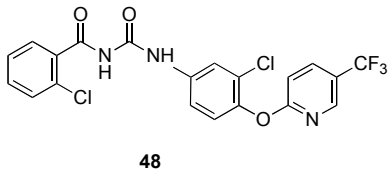

48

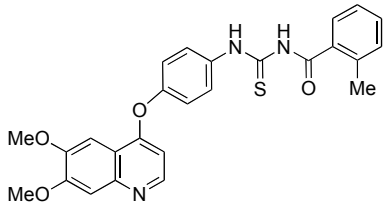

49

Fig. (14). Chemical structures of disubstituted pyridine and condensed pyridine bearing acylurea.

A series of 2,6-diaminopyridine derivatives (**50-57**, Fig. **15**) were synthesized from 2,6-diaminopyridine [75]. The pyridine derivatives (**50-55**) were shown to be the most effective compounds against HepG2 cell line compared with 5-fluorouracil (5-FU) and doxorubicin.

Previously, the opened chain bispyridinium dienes (**58** and **59**, Fig. **16**) were reported to display higher HDAC inhibitory potency than the natural products (cyclostelletamine bispyridinium macrocyclic alkaloid) [64]. The diene **58** is a HDAC subclass IIa-selective inhibitor, and **59** is a HDAC1-selective inhibitor.

Various aminopyridine derivatives were synthesized by the reductive amination of aminopyridine with benzaldehyde. The obtained compounds such as 3,5-disubstituted pyridine **60** (Fig. **17**) exhibited excellent inhibitory activity against many cancer cell lines *i.e.*, A2780, A549 and B16-F1 at < 5 μM; and HT at < 15 μM [76].

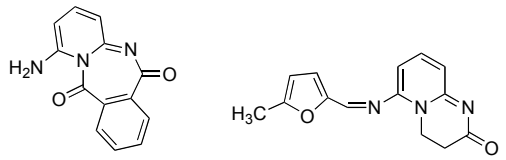

50 **51**

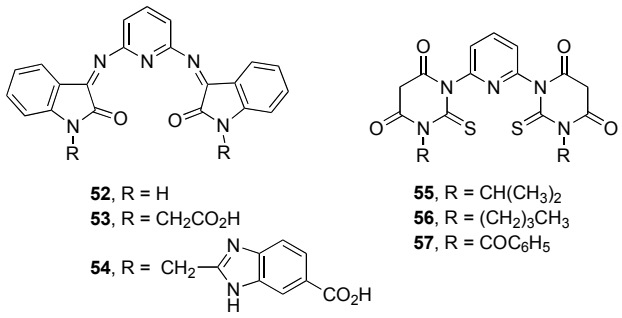

Fig. (15). Chemical structures of 2,6-diaminopyridine derivatives.

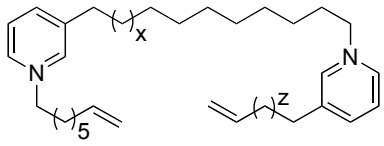

58, X = 3, Z = 2
59, X = 3, Z = 3

Fig. (16). Chemical structures of bispyridinium dienes as HDAC inhibitors.

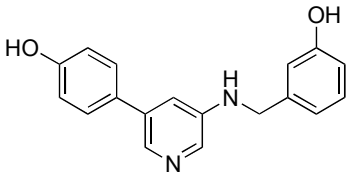

60

Fig. (17). Chemical structure of 3,5-disubstituted pyridine.

A series of disubstituted pyridines bearing 1-adamantylthio (1-AdmS) group at various positions with substitutents (R) at 3-position (**61-67**, Fig. **18**) were synthesized [77, 78] and investigated for their cytotoxic activities against 4 human cancer cell lines (HuCCA-1, HepG2, A549, MOLT-3). It was found that thiopyridine compound **65** exhibited a broad spectrum cytotoxic activity against all of the tested cells. However, compound **61** selectively displayed activity against MOLT-3 cells [79].

In addition, a series of picolines and phenylpyridines containing 1-AdmS group (**68-75**, Fig. **19**) were synthesized [78, 80] and tested for their cytotoxicities [81]. The results showed that compounds **68-75** exerted cytotoxicity against MOLT-3 cell lines. Compound **75** possessed the highest cytotoxicity followed by compound **70** with IC_{50} values of 8.02 and 15.84 μg/mL, respectively.

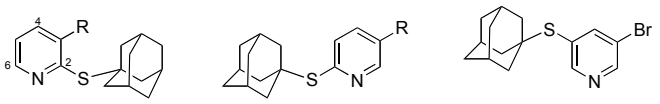

61, R = $N(COCH_3)_2$
62, R = COOH
63, R = $CONH_2$
64, R = CN

65, R = OH
66, R = CN

67

Fig. (18). Chemical structures of disubstituted pyridines bearing 1-AdmS group.

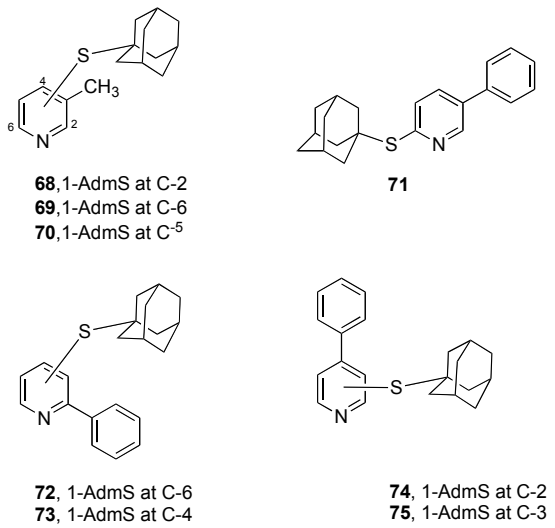

68,1-AdmS at C-2
69,1-AdmS at C-6
70,1-AdmS at C^{-5}

71

72, 1-AdmS at C-6
73, 1-AdmS at C-4

74, 1-AdmS at C-2
75, 1-AdmS at C-3

Fig. (19). Chemical structures of picolines and phenylpyridines containing 1-AdmS group.

2.2. Trisubstituted Pyridines

In recent years, 2,4,6-trisubstituted pyridines have been synthesized and studied for their topoisomerase (Topo) I and II inhibitory activities, and cytotoxicity [51, 58, 59, 82-85]. The substituted groups on pyridine ring are triphenyls (**76**) [82], triheterocyclic rings (**77**) [85]; and a combination of diphenyls and heterocyclic rings (**78**) [58, 59, 83, 84] and (**79**) [51]. However, most of the pyridine derivatives constitute diphenoxy groups at 2, 4-, and 2, 6-positions with heterocyclic rings at either 6- or 4-position (**78** and **79**, respectively). General structures of these trisubstituted pyridines (**76-79**) are shown in Fig. (**20**).

2.2.1. 2,4,6-Triphenyl Pyridines

A series of 2,4,6-triphenyl pyridines (**76**) bearing hydroxyl groups, R^4 and R^6 at ortho- (*o*-), *meta*- (*m*-) or *para*- (*p*-) position were synthesized and investigated for their Topo I and II inhibitory activities, and cytotoxicity against five human cancer cell lines [82]. The results showed that most dihydroxylated pyridine derivatives displayed stronger Topo II inhibitory activity and cytotoxicity compared with those of monohydroxylated 2,4,6-trisubstituted pyridines. Structure-activity relationships (SAR) revealed that significant Topo II activity and cytotoxicity were noted for compounds with OH group at *m*- or *p*-position on the 2-phenyl ring. For example, compounds **80** and **81** (Fig. **21**) displayed Topo II inhibitory activity (at 100 μM) with 96.8 and 100%, respectively.

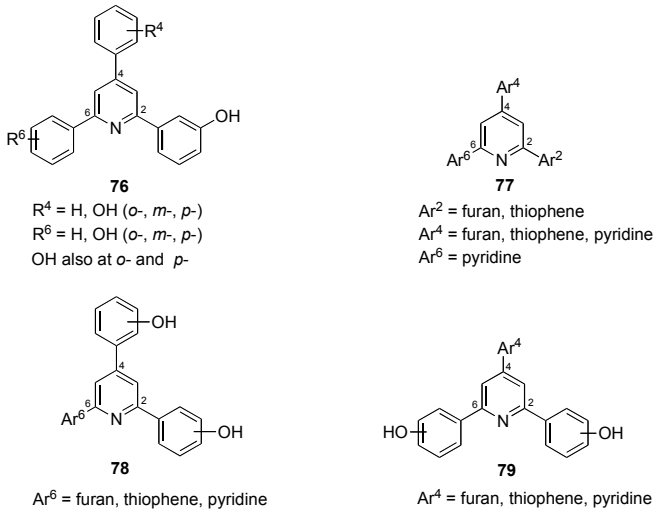

76
R^4 = H, OH (*o*-, *m*-, *p*-)
R^6 = H, OH (*o*-, *m*-, *p*-)
OH also at *o*- and *p*-

77
Ar^2 = furan, thiophene
Ar^4 = furan, thiophene, pyridine
Ar^6 = pyridine

78
Ar^6 = furan, thiophene, pyridine

79
Ar^4 = furan, thiophene, pyridine

Fig. (20). Chemical structures of trisubstituted pyridines.

For cytotoxicity, most of the investigated compounds were effective against HCT-15 and K562 cell lines. Particularly, compounds with OH group at *p*-position on 2-phenyl ring were more favorable than *ortho*- (*o*-) and/or *m*-position as noted for compounds **82-84** (Fig. **21**), which exerted strong cytotoxic activity (HCT-15, IC_{50} range 0.79-0.88 μM) compared with the control drugs, etoposide and adriamycin, IC_{50} = 1.33 and 1.28 μM, respectively [82].

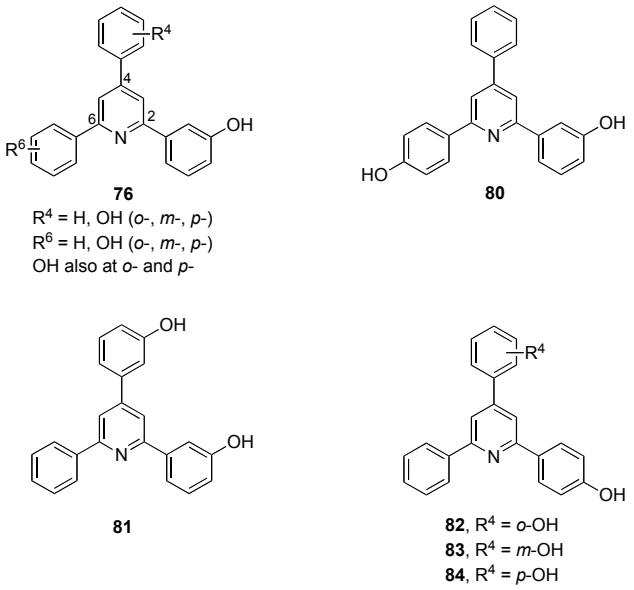

76
R^4 = H, OH (*o*-, *m*-, *p*-)
R^6 = H, OH (*o*-, *m*-, *p*-)
OH also at *o*- and *p*-

80

81

82, R^4 = *o*-OH
83, R^4 = *m*-OH
84, R^4 = *p*-OH

Fig. (21). Chemical structures of 2,4,6-triphenyl pyridines.

2.2.2. 2,4,6-Triheteroaryl Pyridines

Previously, 2,4,6-trisubstituted pyridines (**77**, Fig. **22**) were reported to show significant Topo I or II inhibitory ac-

tivities. Compounds **77** with various Ar groups (Ar^2 = thiophene, Ar^4 = furan, thiophene, Ar^6 = pyridine) exerted considerable cytotoxicity against several human cancer cell lines [85].

Mostly, significant Topo I inhibitors were noted for compounds with thiophene ring at 4-position, for example, compounds **85** and **86**. However, significant Topo II inhibitory activity was observed for compounds bearing pyridine and furan moieties at 4-position such as compounds **87** and **88**.

Considerable cytotoxic activity against four human cancer cell lines (A549, SK-OV-3, SK-MEL-2 and HCT-15), especially on HCT-15, was noted for 2,4-dithiopheneyl pyridines such as compounds **89** and **90** compared with the etoposide. Among these, compound **89** had stronger activity (IC_{50} = 1.72 μM) than that of the etoposide (IC_{50} = 2.43 μM) [85]. The SAR study revealed that 4-pyridyl group substituted at 6-position on the central pyridine ring (Fig. **22**) play a key role in the bioactivity.

2.2.3. 2,6-Diphenyl-4-heteroaryl Pyridines

Recently, a new series of 2,6-diphenyl-4-heteroaryl pyridines containing OH groups at *o*-, *m*- or *p*-position on 2- and 6-phenyl rings (**79**) [51] were synthesized and investigated for Topo I and II inhibitory activities as well as cytotoxic activity against several human cancer cell lines [51]. It was found that compounds with 2-thiopheneyl ring substituted at 4-position on the pyridine core structure (**91**) exhibited strong Topo I inhibitory activity at 100 μM, in which compound **92** (2- and 6-phenyl rings with OH groups at *m*-positions) was shown to be the strongest Topo I inhibitor. However, some of the series compound **91** had stronger activity than that of the control drug, camptothecin. In addition, compound series **91** showed moderate to significant Topo II inhibitory activity. A series compound **94** bearing 3-thiopheneyl ring at 4-position on the pyridine ring exerted stronger Topo II inhibitory activity than the etoposide at 100 μM concentration [51].

Similarly, 2-furanyl substituted at 4-position of trisubstituted pyridines with dihydroxylated phenyls at 2- and 6-positions in a series compound **96** displayed stronger Topo I inhibitory activity compared with the control, camptothecin. Particularly, compounds **97** and **98** showed 100% inhibition at 100 μM [51].

In case of 3-furanyl substituted at 4-position of 2,4,6-trisubstituted pyridine, compound **100** showed significant Topo II inhibitory activity (95% at 100 μM). Moreover, 2- or 3-thiopheneyl substituted at 4-position of trisubstituted pyridines (**92**, **93** and **95**) exerted considerable cytotoxicity against DU 145, HCT-15 and HeLa cells. However, such compounds (**92**, **93** and **95**) displayed much stronger activity (IC_{50} = 0.78 μM) in T47D cell lines compared with the etoposide, IC_{50} = 13.17 μM. In addition, compound **102** was shown to exhibit strong cytotoxicity against all of the four tested cell lines (DU 145, HCT-15, T47D and HeLa) [51]. Chemical structures of pyridines **91**-**102** are shown in Fig. (**23**).

2.2.4. 2,4-Diphenyl-6-aryl/heteroaryl Pyridines

Recently, Karki *et al.* [58] described the synthesis, Topo I and II inhibitory activities, and cytotoxicity against several human cancer cell lines of 2,4-diphenoxy-6-aryl pyridines. Most compounds in series **78** exhibited significant antiproliferative activity against HCT-15 and K562 cell lines, and potent Topo II inhibitory activity comparable to or stronger than the etoposide [58]. Compound **103** was shown to be

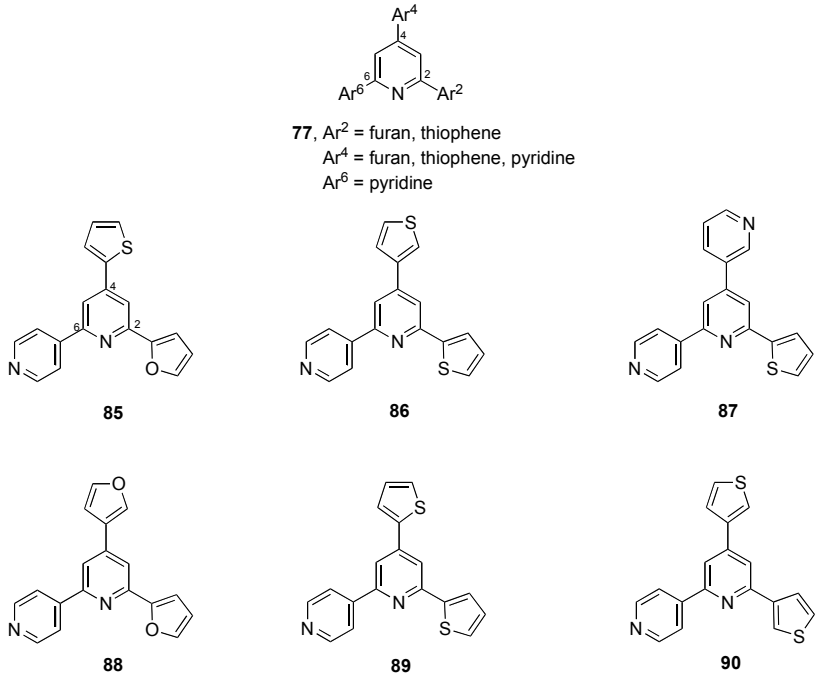

Fig. (22). Chemical structures of 2,4,6-triheteroaryl pyridines.

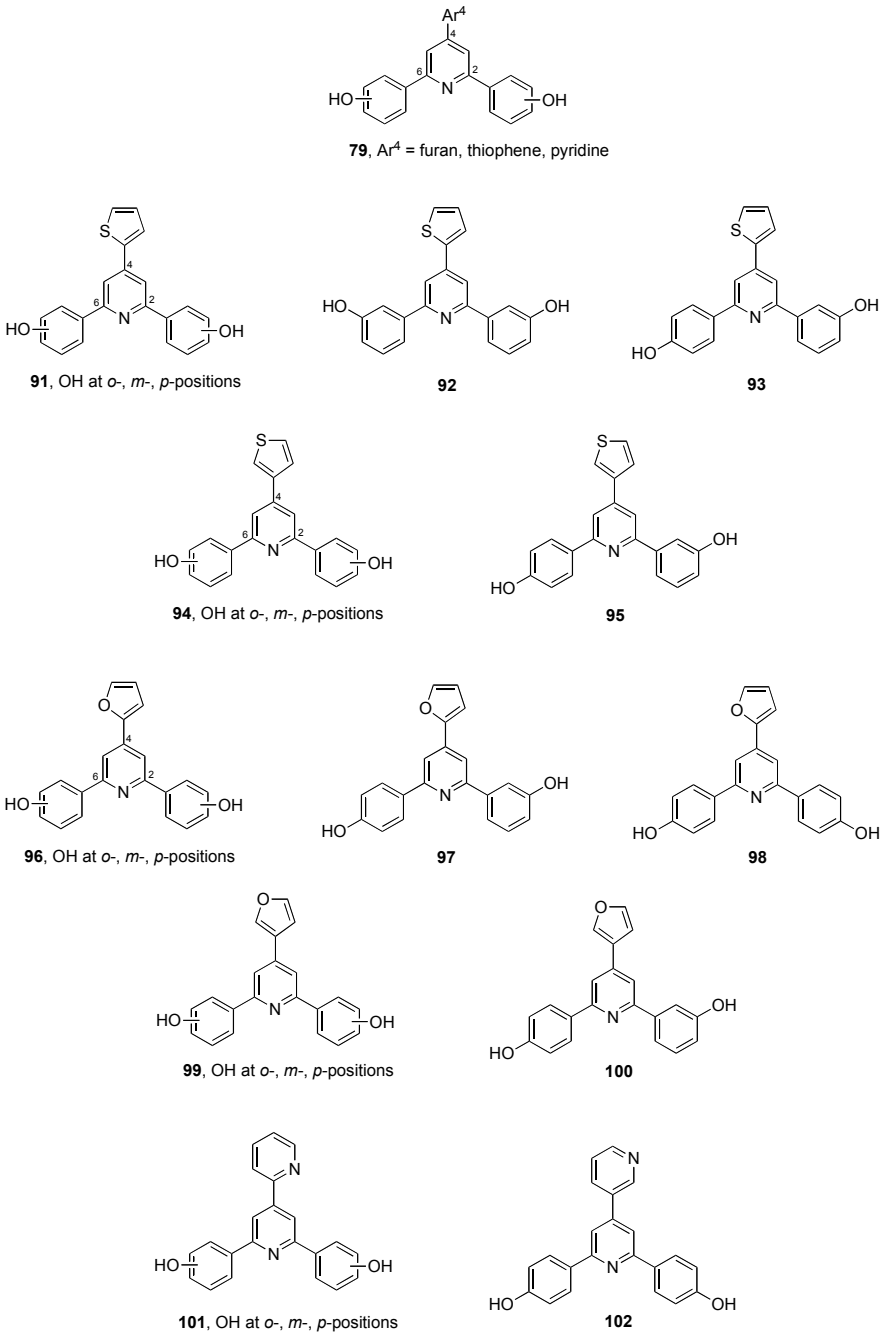

Fig. (23). Chemical structures of 2,6-diphenyl-4-heteroaryl pyridines.

the most potent Topo II inhibitor at low concentration (20 μM), and functioned as a topoisomerase poison like action of the etoposide [58]. Among the tested compounds, compound **104** displayed the strongest Topo II inhibitory activity (98.2 %) at 100 μM concentration. In addition, compound **104** was the most potent cytotoxic agent against HCT-15 with IC_{50} value of 0.08 μM. Pyridine derivatives **103** and **104** are shown in Fig. (**24**).

The structure-activity relationship suggested that 2,4-diphenyl rings with OH groups at *o*-, *m*- or *p*-position displayed the most potent Topo II inhibitory and cytotoxic activities [58].

Previously, the synthesis, Topo I and II inhibitory and cytotoxic activities of a series of forty-five 2,4,6-trisubstituted pyridines were reported by Karki *et al.* [83]. Triphenylpyridine **105** containing OH group at *m*-position of 2,6-diphenyl rings showed the strongest Topo II inhibitory activity (86.5 % at 100 μM and 49.0 % at 20 μM), which is stronger than that of the etoposide. Conversly, compounds **106** and **107** showed significant Topo I inhibitory activity comparable to the activity of camptothecin. It was found that trisubstituted pyridines (**107**-**114**) bearing *p*-OH group (phenoxy) at 2- or 4-position, and various Ar groups on the central pyridine ring displayed significant cytotoxicity in most of the tested cell lines with similar or slightly weaker activity

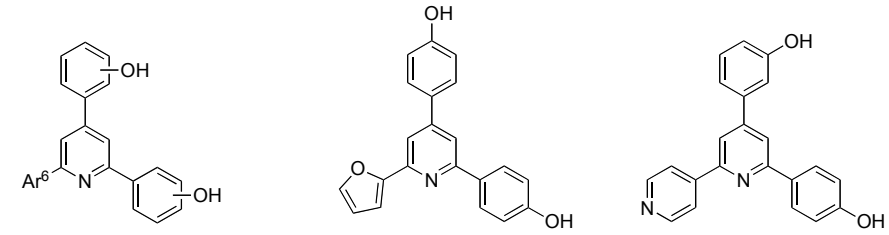

Fig. (24). Chemical structures of 2,4-diphenoxyl-6-heteroaryl pyridines.

than the etoposide [83]. Compounds **105-114** are shown in Fig. (**25**).

Apparently, *p*-OH group on the phenyl ring at 2- or 4-position on the central pyridine ring showed relatively strong cytotoxic activity against several human cancer cell lines. Additionally, the number of OH groups increased the Topo II inhibitory activity in the order of *m* > *p* > *o* [83].

The SAR study revealed that substitution with OH group (s) increased Topo I and II inhibitory activities in the order of *m* > *p* > *o* position. 2-Phenyl ring with OH group at *m*- or *p*-position, and 4-phenyl ring with OH group at *o*-, *m*- or *p*-position displayed the most potent Topo II inhibitory and cytotoxic activities [83].

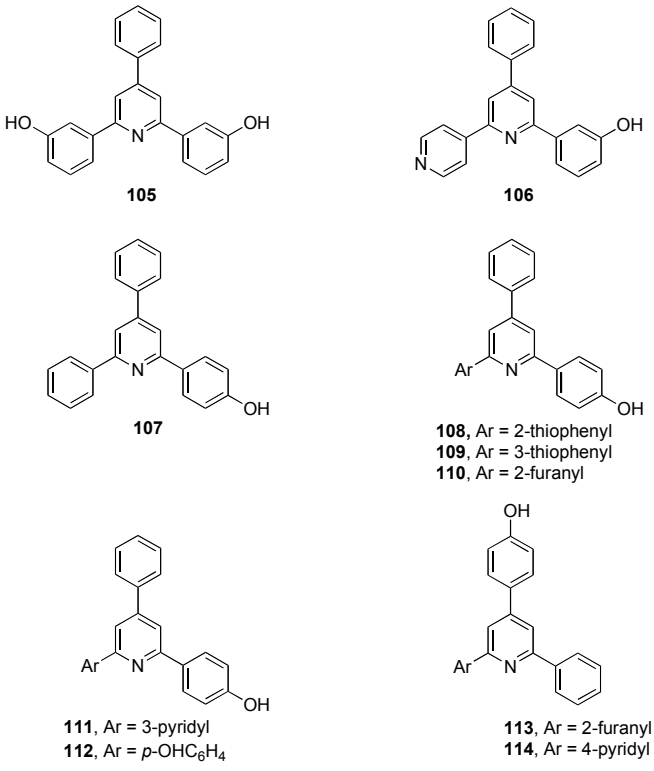

Fig. (25). Chemical structures of 2,4,6-triphenyl pyridines and 2,4-diphenyl-6-heteroaryl pyridines.

It was reported that a series of 2,4-diphenoxyl groups of trisubstituted pyridines containing 2-thiopheneyl group at 6-position (**115**) exerted excellent activity toward Topo II compared with Topo I, in which compound **116** had the highest Topo II inhibitory activity [59]. In addition, the compounds in series **115**, except for compound **116**, exhibited cytotoxic activity against five human cancer cell lines (HCT-15, K 562, DU 145, MCF-7 and HeLa). Particularly, compound **117** displayed the highest cytotoxicity with IC_{50} < 6 μM as well as inhibited cell migration and induced G1 arrest [59]. These compounds (**115-117**) are presented in Fig. (**26**).

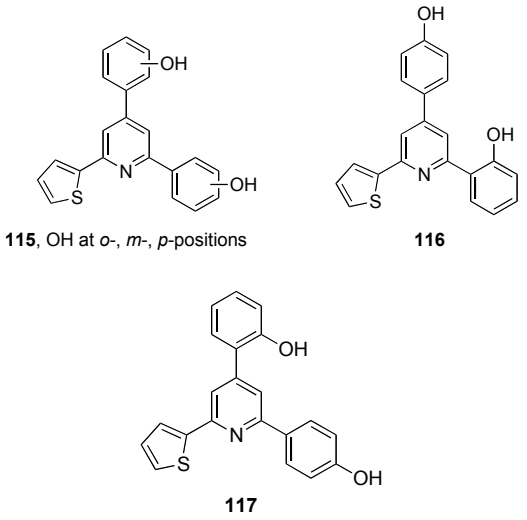

Fig. (26). Chemical structures of 2,4-diphenoxy pyridines bearing 6-thiophenyl moiety.

In case of 2-chlorophenyl-4-phenoxypyridines (Fig. **27**) with 6-aryl (phenyl, thiopheneyl, furanyl, pyridyl) groups (**118**), most of the synthesized compounds showed better Topo II inhibitory activity compared with Topo I [84]. Notably, compounds with *m*-Cl and *m*-OH (**119** and **120**); *p*-Cl and *m*-OH (**121-124**); and *p*-Cl and *p*-OH (**125-128**) groups at 2,4-diphenyl groups, and substituents at 6-position (phenyl, 2- and 3-thiopheneyl, and 2-furanyl) of the central pyridine ring showed stronger Topo II inhibitory activity (at 100 and 200 μM) than that of the etoposide [84].

Additionally, most compounds in the series **118** displayed moderate cytotoxicity with IC_{50} range of 1.48-39 μM against four human cancer cell lines (HEK 293, DU 145, HCT-15, T47D), in which the compound **124** exerted the most significant cytotoxic activity [84].

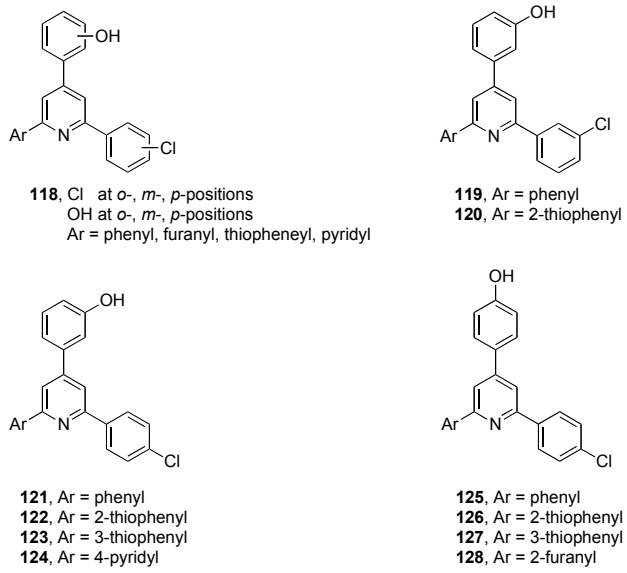

Fig. (27). Chemical structures of 2,4-diphenyl pyridines containing 6-aryl/heteroaryl moieties.

3. PYRIMIDINES

Pyrimidine, a six membered heterocyclic compound bearing two N-atoms in the ring, constitutes an important component of nucleic acid, and it is used as an important pharmacophore for the synthesis of many drugs *i.e.*, anticancer, antiviral and antibacterial agents [86].

3.1. Disubstituted Pyrimidines

3.1.1. 2,4-Disubstituted Pyrimidines

Previously, 2-thiopyrimidine-4-one analogs (**129**-**133**, Fig. **28**) were synthesized and evaluated for their cytotoxic activities against eleven cancer cell lines (KB, HuCCA-1, MDA-MB231, T47D, A549, H69AR, HeLa, HepG2, HCC-S102, HL-60 and P388) [86]. It was found that compounds **129**, **131** and **133** exhibited anticancer activity in which compound **133** was the most potent cytotoxic compound against multidrug-resistant small cell lung cancer (H69AR). This is presumably due to a hydrophobic effect of sterically hindered 1-adamantyl group (1-Adm) that enhances the penetration of compound **133** to the cancer cell.

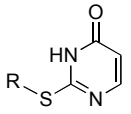

Fig. (28). Chemical structures of 2-thiopyrimidine-4-one analogs.

3.1.2. 2,5-Disubstituted Pyrimidines

A series of 2,5-disubstituted pyrimidines have been synthesized using the Suzuki coupling of 2-substituted benzyloxy-5-bromopyrimidines with various arylboronic acids in the presences of catalytic amount of $PdPCl_2$ $(PPh_3)_2$ with aqueous Na_2CO_3in water at 80ºC. The 2,5-disubstituted pyrimidines **134**-**140** (Fig. **29**) displayed moderate cytotoxic activity against HeLa cell line. Among the tested compounds, compound **135** exhibited more potent anticancer activity than compounds **136**, **139**, **137** and **138**, respectively [87].

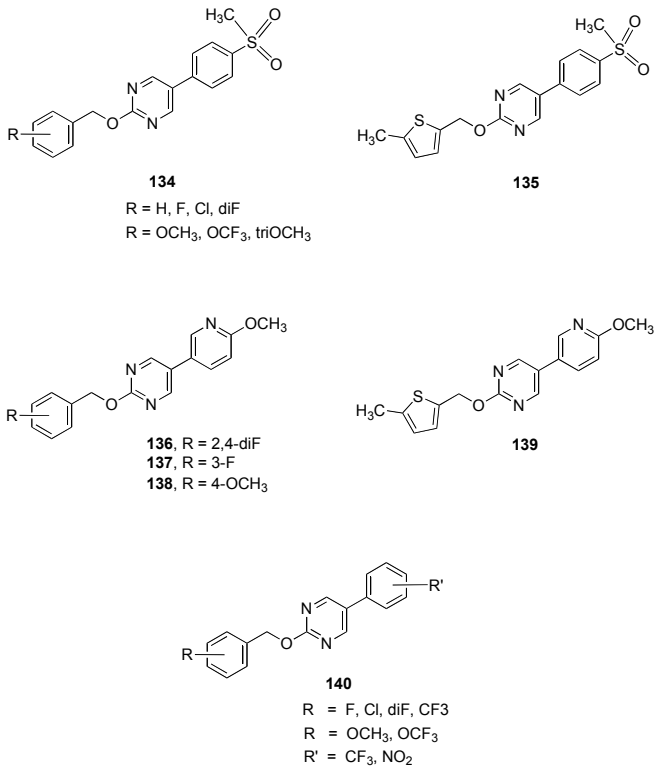

Fig. (29). Chemical structures of 2,5-disubstituted pyrimidines.

Pyrimidine analogs of benzoylureas (Fig. **30**) [73] such as compound **141** showed antitumor activity (orally administration) and is free from cross resistance to any known antitumor agents [88]. Its mode of action was reported to be the inhibition of DNA polymerase. Compound **142** exhibited effective cell growth inhibition of BxPC3 and Hep2 cell lines [89].

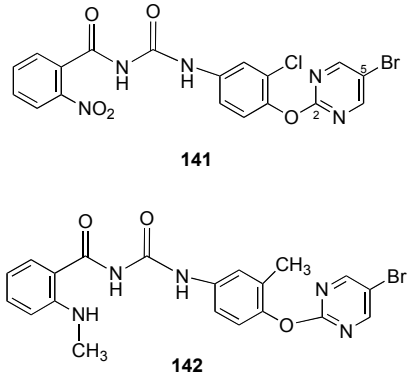

Fig. (30). Chemical structures of pyrimidines bearing benzoylureas.

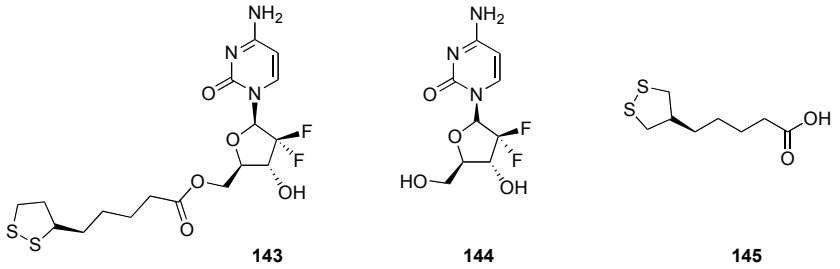

143 **144** **145**

Fig. (31). Chemical structures of trisubstituted pyrimidine containing gemcitabine-lipoic acid linkage.

3.2. Trisubstituted Pyrimidines

3.2.1. 1,2,4-Trisubstituted Pyrimidines

The interlinkage of oxidative stress and cancer has been reported [52]. Recently, molecular hybrid strategy using covalently link two distinct potent moieties into one molecule, is a promising area of drug design [90-95]. For example, 1,2,4-trisubstituted pyrimidine, gemcitabine-5′-*O*-lipoate (**143**) was achieved from an enzymatic regioselective coupling of the chemotherapeutic drug gemcitabine (**144**) which is the first line for cancer therapy, and α-lipoic acid (**145**) which is a potent antioxidant. The hybrid ester **143** was found to be superior to the parent compounds (GEM and LA) against both non-small cell lung cancer and bladder cancer cells [52]. These compounds **143**-**145** are shown in Fig. (**31**).

3.2.2. 2,4,5- and 2,4,6-Trisubstituted Pyrimidines

Aurora kinases, a family of serine/ threonine, have been served as potential therapeutic targets in oncology [96, 97]. The family includes 3 kinase, Aurora kinases A, B and C. It has been known that the expressions of Aurora kinases A and B are elevated in various human cancers, and are associated with poor prognosis [98]. The Aurora kinases play potential roles in regulating cell mitosis and tumorigenesis thereby making them attractive targets for anticancer therapy. Pyrimidine is the important pharmacophore in the Aurora kinases. Therefore, a number of pyrimidine Aurora kinase inhibitors have been developed and introduced to clinical trials, for example, VX-680 (**146**) and ENMD-2076 (**147**) [53] as shown in Fig. (**32**).

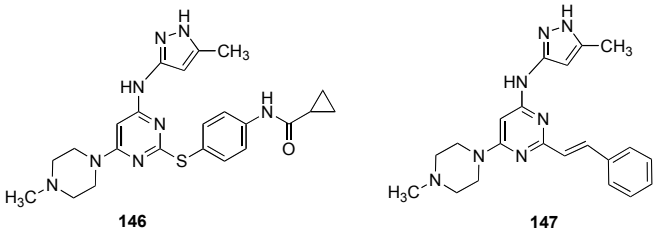

146 **147**

Fig. (32). Chemical structures of trisubstituted pyrimidines as Aurora kinase inhibitors.

Recently, a series of 2,4-diaminopyrimidines substituted with 5-halo (F, Cl, Br) and NO_2 groups (**148**-**151**, Fig. **33**) have been synthesized, and investigated for their antiproliferative activities and Aurora kinase inhibitory activity [53]. Generally, the compounds exhibited more potent cytotoxic activity against tumor cell lines compared with the control drug, VX-680 (**146**). Particularly, compound **150** displayed the highest cytotoxicity against four human cancer cell lines (HeLa, A549, HCT-8 and HepG2) with IC_{50} values of 0.5-4.0 μM. Moreover, the pyrimidine **150** had more than 35-fold more selectivity for Aurora kinase A over Aurora kinase B, and induced G2/M cell cycle arrest in HeLa cells. This series of compounds (**148**-**151**) have the potential for further development as selective Aurora kinase A inhibitors for anticancer activity [53].

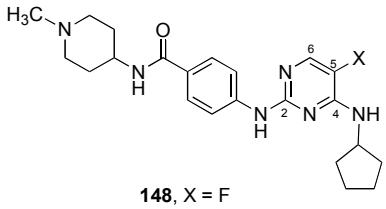

148, X = F
149, X = Cl
150, X = Br
151, X = NO_2

Fig. (33). Chemical structure of 2,4-diaminopyrimidine analogs.

Previously, 2,4,5-trisubstituted pyrimidines (**152** and **153**, Fig. **34**) were reported to be the potent thymidylate synthase inhibitors. Particularly, the compound **153** was shown to be the most potent inhibitor [99].

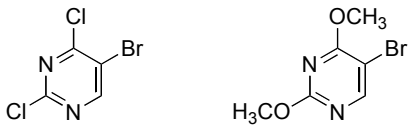

152 **153**

Fig. (34). Chemical structures of 2,4,5-trisubstituted pyrimidines.

However, a large number of pyrimidine-based antimetabolites were reported [100]. 5-Fluorouracil (5-FU, **154**) is one of the well-known antimetabolites, which has been widely used as anticancer drug in the treatment of solid tumors such as colon and breast cancers [101]. Other 5-substituted uracils possess anticancer activity such as tegafur (**155**) and uramustine (**156**) [100]. These uracils (**154**-**156**) are displayed in Fig. (**35**).

It is well known that 5-substituted uracils play a vital role in many metabolic processes [102-104]. Previously,

5-iodouracils substituted (R = nC_4H_9, sC_4H_9, $CH_2C_6H_{11}$, $CH_2C_6H_5$) at N1 or N1 and N3 were achieved through an alkylation reaction of 5-iodouracil [105]. The synthesized compounds (**157** and **158**, Fig. **36**) were reported to show inhibitory activity against many tested cancer cell lines (T47D, KB, HepG2, P388 and HeLa; and HepG2, A549 and HuCCA-1). Notably, the growth of HepG2 cell lines was selectively inhibited by compounds **157** and **158**, in which the N1, N3-disubstituted uracil **158** exhibited the most potent anticancer activity [105].

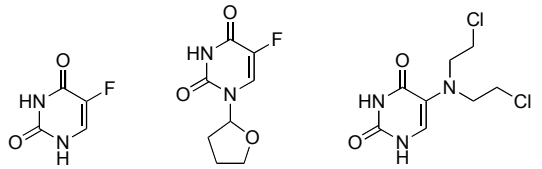

154 **155** **156**

Fig. (35). Chemical structures of 5-substituted uracils.

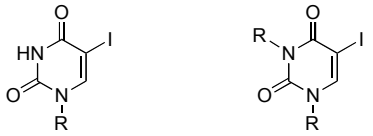

157, R = $CH_2C_6H_{11}$ **158**, R = $CH_2C_6H_{11}$

Fig. (36). Chemical structures of N1 and N1, N3-substituted uracils.

Trisubstituted pyrimidines with various substituents at positions 2-, 4- and 6- were reported to show anticancer activity. For example, 2-amino-4,6-diarylpyrimidine (**159**) [106] displayed anticancer activity against prostate cancer cell line (DU145), and 2-mercapto-4,6-diarylpyrimidines **160** and **161** [107] are active against non-small cell lung cancer (HOP-92). In addition, compound **162** has significant antiproliferative activity against breast cancer cell lines (MCF-7) compared with the reference drug, 5FU [108]. These pyrimidines **159**-**162** are shown in Fig. (**37**).

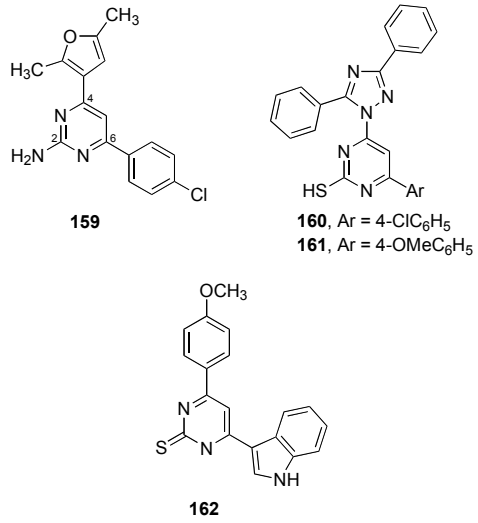

159

160, Ar = 4-ClC_6H_5
161, Ar = 4-$OMeC_6H_5$

162

Fig. (37). Chemical structures of trisubstituted pyrimidines.

Moreover, 2-thio-6-*n*-propylpyrimidine-4-ones **163**-**166** (Fig. **38**) were synthesized and reported to exhibit cytotoxic activity against 11 cancer cell lines [109]. Particularly, compound **165** was shown to be the most potent cytotoxic against multidrug-resistant small cell lung cancer cell lines (H69AR) [109].

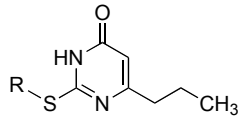

163, R = *n*-C_4H_9 **165**, R = $CH_2C_6H_{11}$
164, R = *s*-C_4H_9 **166**, R = 1-Adm

Fig. (38). Chemical structures of 6-substituted 2-thiouracils.

The selectivity towards killing cancer cells while not affecting normal cells is a crucial goal for chemotherapy [110]. This goal leads to the use of compounds that are capable of differentiating cancer cells into non-proliferating or normal phenotype [110]. HDAC enzyme is well-known to play roles in activating and repressing transcriptions of genes including genes that regulate cell cycle, differentiation and apoptosis [110]. Alterations of HDAC expression, function and binding were noted to determine cellular fate of cancer cells *i.e.*, tumor onset and progression [111, 112]. In this regard, inhibition of HDAC is a strategy to modulate fate of cancer cells by reversing inappropriate HDAC-mediated transcription as well as facilitating expression of differentiation-inducing genes. Such compounds were reported as HDAC inhibitors including trichostatin A (TSA) [113] or suberoylanilide hydroxamic acid (SAHA) [114]. A series of HDAC inhibitors belonging to hydroxamates were reported to display the activity at low nanomolar concentrations. It was found that 2,4,6-trisubstituted pyrimidine analogs of hydroxamates (**167** and **168**, Fig. **39**) exerted more potent activity than the SAHA [110].

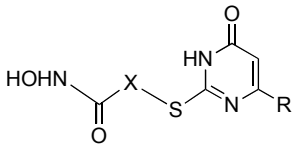

167, R = Bz, X = $(CH_2)_5$
168, R = Ph, X = $(CH_2)_5$

Fig. (39). Chemical structures of thiopyrimidine hydroxamates.

3.3. Tetrasubstituted Pyrimidines

3.3.1. 2,4,5,6-tetrasubstituted Pyrimidines

A number of 2,4,5,6-tetrasubstituted pyrimidines were developed based on the structural modification of 5FU and 5-chlorouracil or 5ClU (which are the first pharmacological active compounds) at positions N1, N3, C5 and C6 [54]. Such tetrasubstituted pyrimidines (Fig. **40**) *i.e.*, 6-amino-5-chlorouracil and 6-amino-5-bromouracil (**169**, X = Cl, Br) were the first thymidine phosphorylase inhibitors (TPI) [54]. However, the compounds were not further developed into

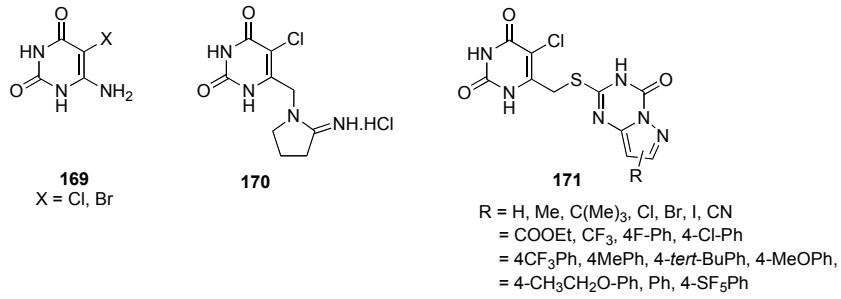

Fig. (40). Chemical structures of uracils bearing 5,6-disubstituents.

drug candidates due to their relatively less favorable IC_{50} values. Previously, 6-[1-(2-iminopyrrolidinyl)methyl analog of 5-ClU (**170**) acting as a very potent TPI was reported [115]. TP (thymidine phosphorylase) is an enzyme that catalyzes the reversible phosphorolysis of pyrimidine nucleoside. In addition, 6-methylthiopyrazolo[1,5-*a*][1,3,5]triazin-4-one analogs of 5ClU (**171**) displayed the inhibition of TP with IC_{50} value as low as 0.36 ± 0.1μM [116].

Recently, various 2,4,5,6-tetrasubstituted pyrimidines such as 2-thio-4-amino-5-cyano-6-arylpyrimidines have been synthesized and investigated for their anticancer activities [117-120]. The synthesized compounds (Fig. **41**) were pyrimidine-urea (thiourea) hybrids. Among a series of tested compounds (**172**), the pyrimidine-thiourea hybrid bearing terminal alkyne moiety **173** was shown to be the most potent (IC_{50}= 0.65 μM) and selective LSDI inhibitor [117]. LSD1 (histone lysine specific demethylase 1) has been reported to be overexpressed in many human cancers and recognized as a promising anticancer drug target. The compound **173** also displayed marked inhibition of cell migration and invasion including significant *in vivo* tumor suppressing and antimetastasis role without significant side effects by oral administration [117].

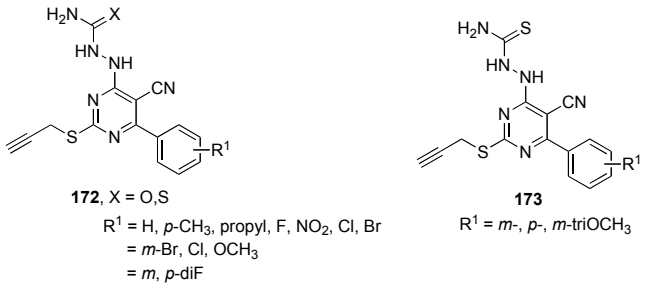

Fig. (41). Chemical structures of pyrimidine-urea (thiourea) hybrids.

A novel series of 1,2,3-triazole-pyrimidine-urea hybrids (**174**), mostly, exhibited moderate to potent activity against all of the cancer cell lines (MGC-803, BE109, MCF-7 and B16-F10). Particularly, compounds **175-177** displayed excellent growth inhibition against B16-F10 with IC_{50} values of 32, 35 and 42 nM, respectively [118]. These pyrimidine analogs (**174-177**) are shown in Fig. (**42**).

In addition, a series of 1,2,3-triazole-pyrimidine hybrids (**178**, Fig. **43**) displayed moderate to good activity against four cancer cell lines, in which the hybrid **179** exerted the most potent and selective anticancer activity against three cancer cell lines (EC-109, MCF-7 and MGC-803), and even more potent than the reference drug (5FU) [119]. Furthermore, the pyrimidine **179** could obviously inhibit the proliferation of EC-109 cancer cells by inducing cell apoptosis and arresting cell cycle at G2/M phase [119].

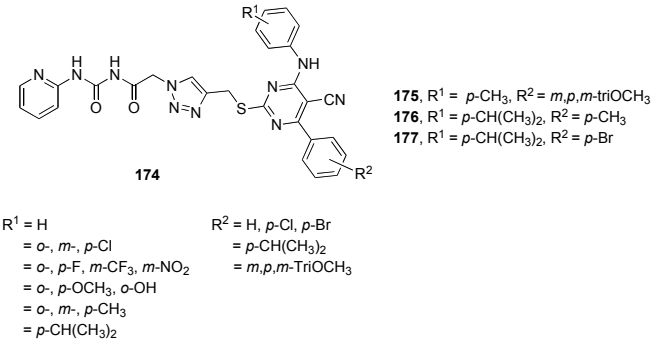

Fig. (42). Chemical structures of triazole-pyrimidine-urea hybrids.

Benzimidazole-pyrimidine derivatives containing 4-substituted-5-cyano-6-phenyl substituents were studied, and 4-phenylhydrazino compound **180** (Fig. **44**) was shown to be one of the most potent compounds against melanoma (G361) and neuroblastoma (NB-1) cell lines [121].

A series of 2-alkylthio-4-substituted (Cl, amino)-5-carbonitrile-6-phenylpyrimidines (**181-187**, Fig. **45**) were investigated for cytotoxic activity using the National Cancer Institute (NCI) 60 cell lines panel assay at 10 μM. The results showed that compounds **183** and **185** exhibited high inhibitory activity against leukemia, whereas compounds **182**, **186** and **187** displayed moderate activity [120].

In case of 4-oxo substitution of 2-thio-5-carbonitrile-6-phenylpyrimidines (**188** and **189**), the analog **188** displayed moderate activity against MOLT-4 leukemia tumor cell line and UO-31 renal cancer cell line, whereas the compound **189** exerted selective activity against leukemia (K-562 and RPMI-8226) and renal cancer (ACHN and UO-31) cell lines at 10 μM concentration [122]. Notably, N3-alkylated compounds **190** and **191** displayed promising anticancer activity against leukemia, non-small cell lung, melanoma and renal cancers [122]. These pyrimidine derivatives are outlined in Fig. (**46**).

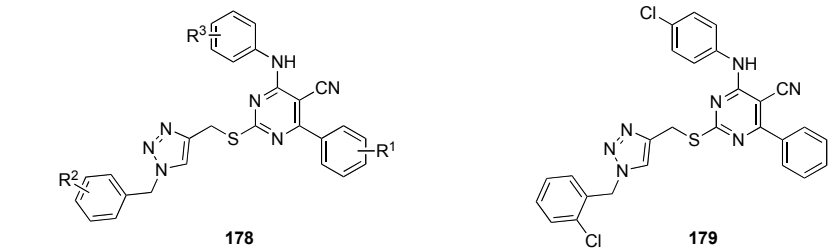

178

179

R^1 = H
= *p*-CH_3
= *p*-$CH(CH_3)_2$
= *p*-Cl, Br
= *m*-, *p*-, *m*-triOCH_3

R^2 = *p*-CH_3
= *o*-, *p*-Cl
= *p*-F

R^3 = H
= *o*-, *m*-, *p*-CH_3
= o-, *p*-F
= *o*-, *m*-, *p*-Cl
= *m*-CF_3, *m*-NO_2
= *o*-, *p*-OCH_3

Fig. (43). Chemical structures of triazole-pyrimidine hybrids.

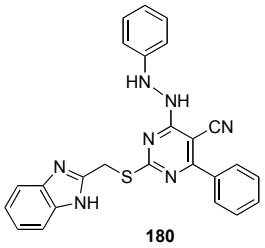

180

Fig. (44). Chemical structure of benzimidazole analog of pyrimidine.

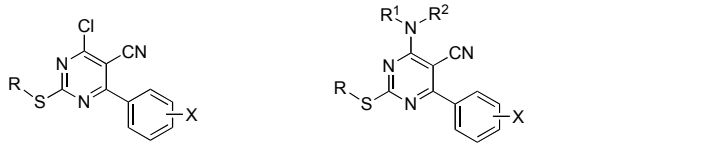

181, R = CH_3; X = 4-Cl
182, R = C_2H_5; X= 3-Br
183, R = $CH(CH_3)_2$; X= 4-F
184, R = $CH(CH_3)_2$; X= 4-Br

185, R = CH_3; X = 4-Cl; NR^1R^2 = sulfamethoxy
186, R = $CH(CH_3)_2$; X= 4-Br; NR^1R^2 = morpholino
187, R = C_2H_5; X= 3-Br; NR^1R^2 = sulfamethoxazole

Fig. (45). Chemical structures of 2,4,5,6-tetrasubstituted pyrimidines.

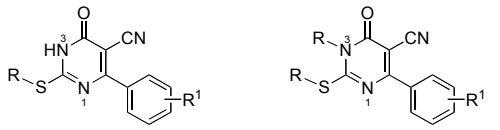

188, R = CH_3, R^1 = 3-Br
189, R = C_2H_5, R^1 = 4-Br

190, R = CH_3, R^1 = 3-Br
191, R = C_2H_5, R^1 = 4-Br

Fig. (46). Chemical structures of 2-thiouracils containing 5,6-disubstituents.

Moreover, a series of 4-oxothiouracilcarbonitrils bearing 6-aryl substituents (**192**) were reported to exhibit growth inhibitory effect against some cancer cell lines, for example, compounds **193** and **194** (Fig. **47**) at 10 μM displayed potent activity against non-small cell lung cancer HOP-92 and leukemia MOLT-4 cell lines, respectively [123].

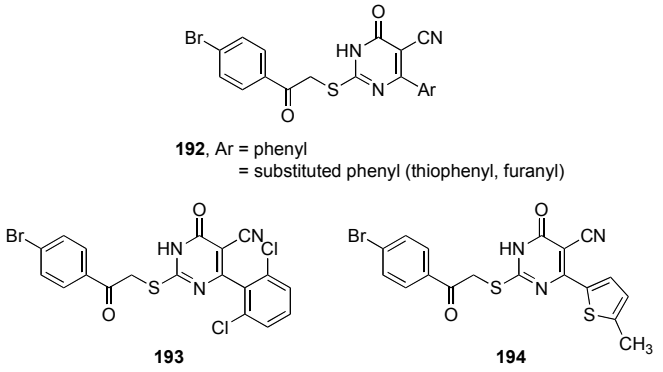

192, Ar = phenyl
= substituted phenyl (thiophenyl, furanyl)

193

194

Fig. (47). Chemical structures of 4-oxothiouracilcarbonitrile bearing 6-aryls.

4. FUSED PYRIMIDINES/PYRIDINES

Pyridine and pyrimidine rings can be fused or condensed with other five or six membered heterocyclic rings (*i.e.*, pyrrole, pyrazole, pyrimidine, imidazole), and even with a phenyl ring. A variety of fused heterocyclic compounds possess anticancer activity has been discussed.

4.1. Pyrrolo-Pyrimidines

Recently, a new series of 5-substituted thiopheneylpyrrolo[2,3-*d*]pyrimidines (**195**-**200**, Fig. **48**) were designed and synthesized as hybrid molecules of the clinically used anticancer drug (pemetrexed or PMX, **201**) and 6-substituted thiopheneyl pyrrolo[2,3-*d*]pyrimidines [56]. Compounds in series **195**-**200** displayed inhibitory activity against KB human tumor cells, in which compounds **198** and **199** had the most potent activity. The compounds **197**-**199** were also shown to be inhibitors of purine nucleotide biosynthesis rather than thymidylate biosynthesis. The antiproliferative effect of compounds **197** and **198** appeared to be due to their dual inhibitions of *β*-glycinamide ribonucleotide formyltransferase (GARFTase) and 5-aminoimidazole-4-carboxamide ribonucleotide formyltransferase [56].

4.2. Pyrazole-Pyrimidines

It is known that pyrazole-pyrimidine derivatives **202** (PP242), **203** (PP30) and **204** (PDE5) have possessed good kinase selectivity profiles as cyclin-dependent kinase (CDK) and ATP-competitive mTORC1/mTORC2 inhibitors [124]. Recently, pyrazole-pyrimidine derivatives (**205** and **206**) have been reported to display cytotoxic activity against SGC-7901,

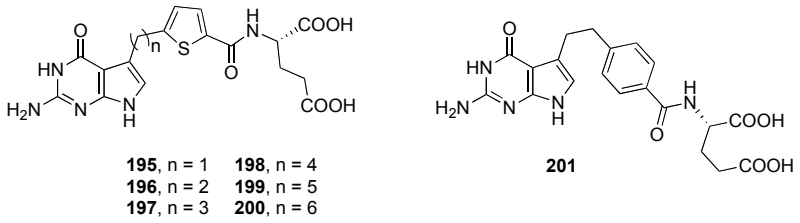

195, n = 1 **198**, n = 4
196, n = 2 **199**, n = 5
197, n = 3 **200**, n = 6

201

Fig. (48). Chemical structures of pyrrolo-pyrimidines.

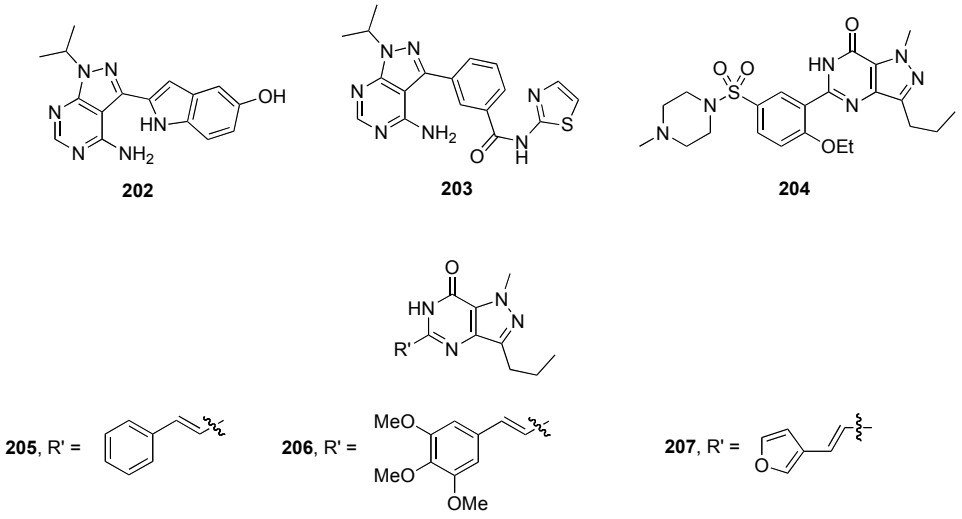

202 **203** **204**

205, R' = **206**, R' = **207**, R' =

Fig. (49). Chemical structures of pyrazole-pyrimidines.

MGC-803 and Bcap-37 cell lines [55]. In addition, compounds **206** and **207** exhibited inhibitory effects against telomerase. The telomerase is an enzyme active in the early stages of life. Such enzyme represents one of the promising targets in drug discovery [125, 126]. Telomere and telomerase have been reported to be closely related to the occurrence and development of gastric cancer [127]. These pyrazole-pyrimidines (**202-207**) are shown in Fig. (**49**).

Previously, a new series of pyrazolo[3,4-*d*]pyrimidines (**208-216**, Fig. **50**) were synthesized and investigated for their antiproliferative activities against human breast adenocarcinoma (MCF-7) cell lines [128]. Most of the investigated compounds showed potent to moderate growth inhibitory activity, particularly, compound **212** displayed superior potency (IC_{50}= 7.60 μM) to the reference drug (cisplatin, IC_{50}= 13.29μM). Moreover, sulfone derivative **213** almost had the same activity as compound **208**. However, compounds **214-216** exhibited lower activity compared with the compounds **209-212**, probably due to lower stability of the pyrazole-sulfone linkage [128]. So far, phenyl pyrazole analog **217** (Fig. **50**) bearing 3-quinolinyl group at 5-position was reported to exert potent cytotoxic activity against MCF-7 cell line [128].

A series of new hydrazone derivatives of pyrazolo[3,4-*d*]pyrimidines (**218-224**, Fig. **51**) were synthesized and studied for their antitumor activities against 60 different human tumor cell lines [129]. It was found that pyrazole-pyrimidine hydrazone **218** displayed the most effective antitumor activity with IC_{50} values of 0.326-4.31 μM towards 57 different cell lines. The activity (GI_{50}) against CCRF-CEM, NCI-H322M and UO-31 cell lines were shown to be 0.326, 0.335 and 0.348 μM, respectively. In addition, substituted pyrazole-pyrimidine (**223**) was reported to exhibit anticancer activity against cervical carcinoma (HeLa53) [130].

4.3. Thienopyrimidines

Thieno[2,3-*d*]pyrimidines were reported to exhibit potent anticancer activity [131-134]. Recently, a series of 17 newly synthesized thienopyrimidines (**225-229**, Fig. **52**) were evaluated for their anticancer activities against 59 different human tumor cell lines, representing leukemia, melanoma and cancers of lung, colon, central nervous system, ovary, kidney, prostate and breast [57]. The results showed that compound **230** displayed a broad spectrum potent anticancer activity against 56 human tumor cell lines with GI_{50} less than 10 μM ranging from 0.495 to 5.57 μM. Moreover, the compound **230** had the marked highest selectivity against two cell lines (T-47D and MDA-MB-468) belonging to breast cancer with GI_{50} values of 0.495 and 5.57 μM, respectively. In addition, compound **230** induced cell cycle arrest at G2/M phase, and also showed accumulation of cells in pre-G1 phase which may result from fragmentation of genetic materials indicating a possible role of apoptosis in compound **230** induced cancer cell death and cytotoxicity [57]. Compound **228** was selective against K-562, SR and MOLT-4 cell lines belonging to leukemia as well as displayed lethal activity

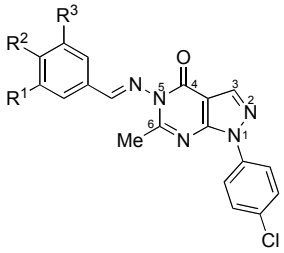

208, $R^1 = R^2 = R^3 = H$
209, $R^1 = H$, $R^2 = OMe$, $R^3 = H$
210, $R^1 = OMe$, $R^2 = OH$, $R^3 = H$
211, $R^1 = OMe$, $R^2 = OMe$, $R^3 = H$
212, $R^1 = R^2 = R^3 = OMe$

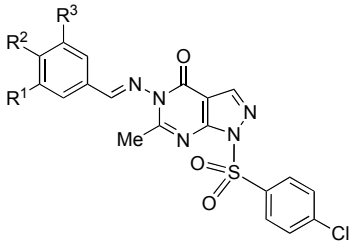

213, $R^1 = R^2 = R^3 = H$
214, $R^1 = H$, $R^2 = OMe$, $R^3 = H$
215, $R^1 = OMe$, $R^2 = OMe$, $R^3 = H$
216, $R^1 = R^2 = R^3 = OMe$

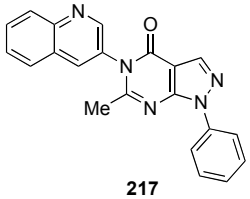

217

Fig. (50). Chemical structures of pyrazolo[3,4-*d*]pyrimidines.

against HOP-92 cell line (non-small cell lung cancer). Additionally, compound **229** exhibited lethal activity to HOP-92 [57].

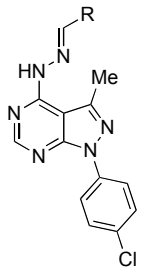

218, R = 2-OH-Ph
219, R = 4-OMe-Ph
220, R = 3-NO_2-Ph

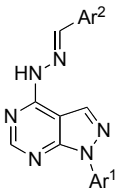

221, $Ar^1 = Ph$, $Ar^2 = Ph$
222, $Ar^1 = Ph$, $Ar^2 = 4$-Cl-Ph
223, $Ar^1 = 4$-Cl-Ph, $Ar^2 = Ph$
224, $Ar^1 = 4$-Cl-Ph, $Ar^2 = 4$-Cl-Ph

Fig. (51). Chemical structures of hydrazone derivatives of pyrazolepyrimidines.

Previously, a series of thienopyrimidine urea analogs were reported as receptor tyrosine kinase inhibitors [73, 135]. For example, compound **231** exhibited potent inhibition of KDR with IC_{50} value of 36 nM. Compounds **232** and **233** bearing *m*-CH_3 (R) group on the phenyl urea moiety displayed better potency of KDR inhibition with IC_{50} values of 6 and 3 nM, respectively. In addition, both urea analogs **232** and **233** had potent antitumor efficacy against the HT 1080 human fibrosarcoma xenograft tumor growth model [73]. In this regard, heterocyclic urea derivatives play an important role in anticancer activity due to their good inhibitory activity against receptor tyrosine kinase, protein tyrosine kinase and NADH oxidase [73]. These thienopyrimidines **231**-**233** are shown in Fig. (**53**).

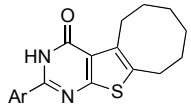

225
Ar = 3-pyridyl, 1-naphthalenyl

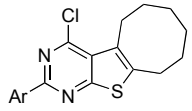

226
Ar = 3-pyridyl, 1-naphthalenyl

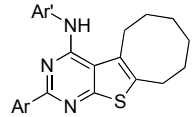

227
Ar = 3-pyridyl, 1-naphthalenyl
Ar' = 2-OMe-Ph, 4-OMe-Ph

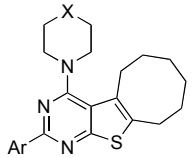

228
X = NMe; Ar = 2-pyridyl

229
X = NMe; Ar = 1-naphthalenyl

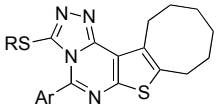

230
R = $CH_2C_6H_5$; Ar = 3-pyridyl

Fig. (52). Chemical structures of thienopyrimidines.

4.4.Quinazolin-4-one Derivatives

Quinazolinone (**234**) is a core structure found in diverse arrays of bioactive natural products [136, 137]. Quinazolines play a key role in medicinal chemistry as promising scaffolds in the search for new bioactive compounds such as anticancer, antimicrobial, anti-inflammatory and antidiabetic [138].

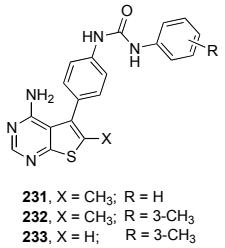

Fig. (53). Chemical structures of urea-thienopyrimidine analogs.

Recently, quinazolin-4-one scaffold linked to oxadiazole (**235**), and to pyrazole (**236**) were synthesized and reported to exhibit anticancer activity (IC_{50} = 23 and 22 nmole/mL, respectively) against human breast cancer cell line (MCF-7) with comparable activity to doxorubicin (IC_{50} = 22 nmole/mL [138]. Moreover, the most active hybrid compounds linked by quinazolin-4-one and thiazolidinone *i.e.*, compounds **237-240** which showed their IC_{50} range of 3-9 nmol/mL [138]. Quinazoline derivatives **234-240** are displayed in Fig. (**54**).

A series of quinazolin-4-one derivatives **241** were designed and synthesized in one step using standard microwave-assisted three components one pot reaction from anthranilic acid, *N*-Boc amino acid and aldehyde as shown in Scheme **4** [139]. The synthesized compounds in series **241** were screened for their bioactivities.

Cytotoxic activity of compounds in series **241** against five cancer cell lines (NCI-H460, A549, DU145, MDA-MB-231, SF-268) revealed that the highly oxygenated substitution pattern of the pendant phenyl ring of compound **241** (R^2 = 4-OH, 3,5-diOMe) play an important role in the activity [139]. The active compounds **242-250** (Fig. **55**) displayed cytotoxic activity with IC_{50} values less than 20 μM in most tested cancer cell lines. Remarkably, the quinazolone derivative **242** showed promising cytotoxic activity [139].

4.5. Pyridopyrimidines

Pyridopyrimidines are fused 6,6-bicyclic heterocyclic compounds containing a pyridine fused to a pyrimidine, and there are four isomeric structures of the pyridopyrimidines (**A**-**D**) as shown in Fig. (**56**).

These compounds (**A**-**D**) are interesting core structures which have found applications in pharmaceutical products such as anticancer, CNS disorders and antiviral therapies [140-142]. Examples of the pyridopyrimidines such as compound **251** (Ku 0063794) was reported to be a potent inhibitor of the mammalian target of rapamycin (mTOR) kinase [140]. This kinase is a central regulator of cell growth and proliferation [143]. In addition, compound **252** (AZD 2014) possessed the best pharmacokinetic parameters and was selected for clinical development [140]. Compounds **251** and **252** are shown in Fig. (**57**).

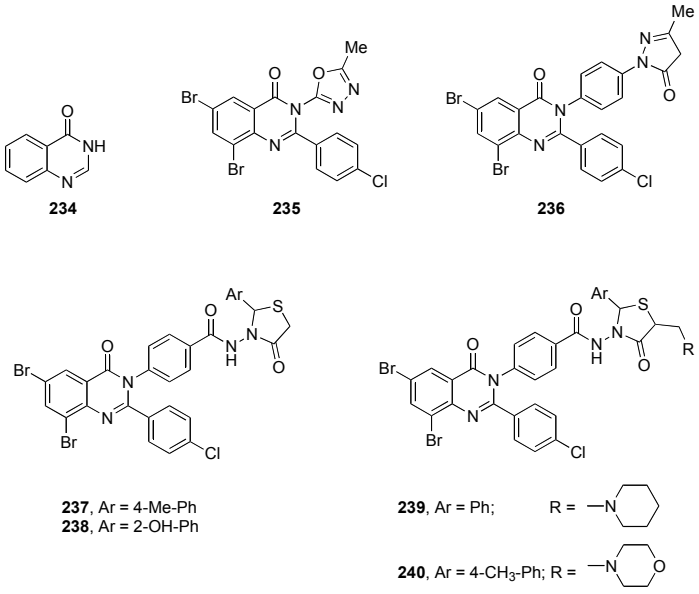

Fig. (54). Chemical structures of quinazolin-4-one derivatives.

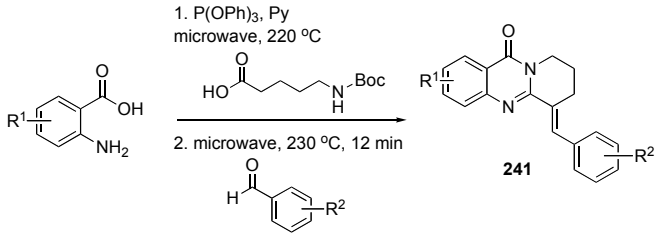

Scheme (4). Synthesis of quinazoline-4-one derivatives.

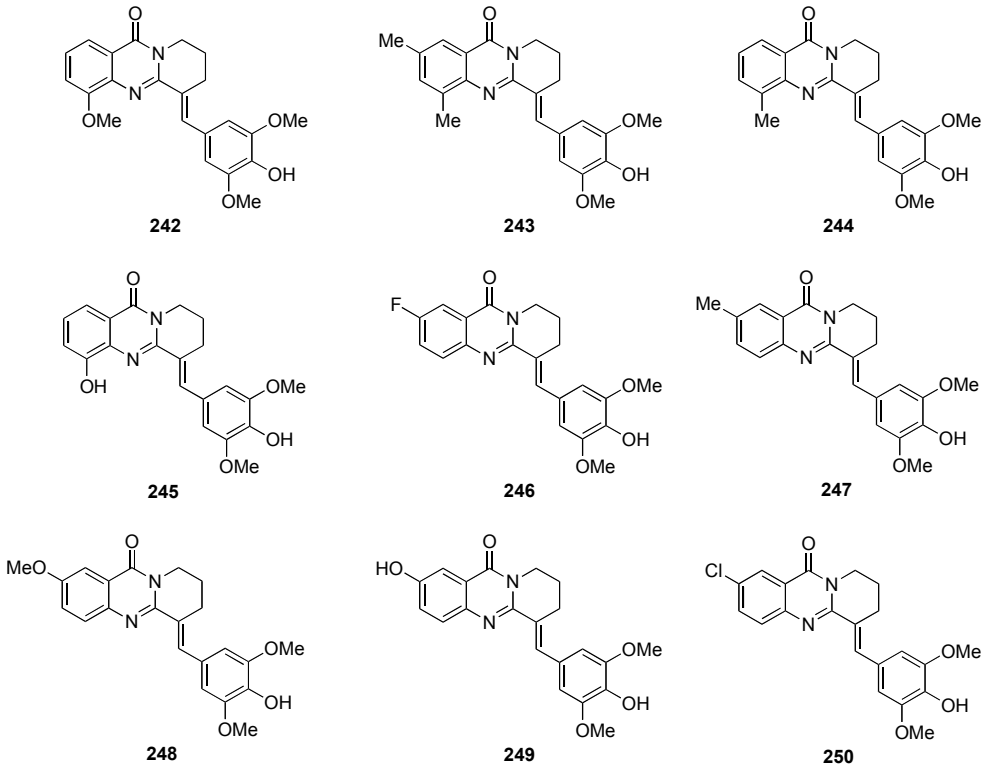

Fig. (55). Chemical structures of quinazolin-4-one bearing phenoxyl moieties.

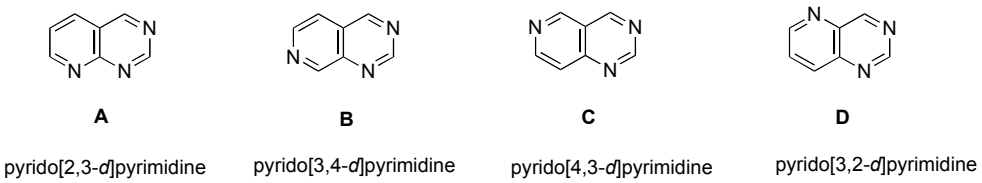

Fig. (56). Chemical structures of pyridopyrimidines.

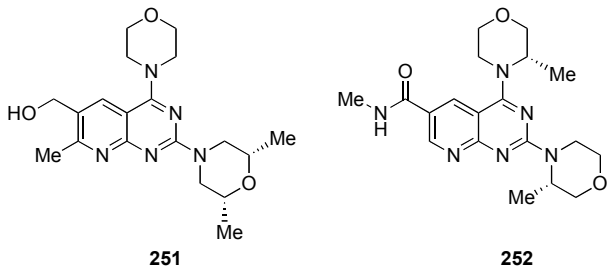

Fig. (57). Chemical structures of pyridopyrimidine bearing diamino groups.

As other kinase inhibitors, compound **253** was reported to be the best inhibitor with nanomolar range of activity against MAP4K4 (mitogen activated protein kinase) [144]. The MAP4K4 is a seronine threonine kinase involved in a variety of signaling pathways. Such inhibition might be beneficial in pathological processes including cancer [140].

The ErbB protein family and epidermal growth factor receptor (EGFR) family are transmembrane receptor tyrosine kinases involved in signal transductions and cellular functions, and are associated with many types of cancer. Thus, inhibitors of the growth factor signaling pathway *via* ErbB2 or EGFR have been designed as potential anticancer drugs [140].

Pyrido[3,4-*d*]pyrimidine scaffold *i.e.*, compounds **254** and **255** as dual ErbB2/EGFR tyrosine kinase inhibitors were studied as potential anticancer agents [145]. However, the pyridopyrimidine ErB2 inhibitor **256** was found to be 200 fold more selective over EGFR kinase [146]. These pyridopyrimidines **253**-**256** are shown in Fig. (**58**).

Among the tested pyrido[4,3-*d*]pyrimidines, compound **257** displayed the most potent cytotoxic activity against KB cell lines (human oral carcinoma), CHE2 cells (human nasopharyngeal carcinoma) and MGC-803 cells (human gastric carcinoma) with IC_{50} values of 0.48, 0.15 and 0.59 μM, respectively [147]. Compound **258**, pyrido[2,3-*d*]pyrimidine-2,4-diamino analog, exhibited good anticancer activity as an apoptosis inducer associated with activating caspase-3 and inducing DNA fragmentation [140]. In addition, compound **259** exerted marked cytotoxic activity against leukemia

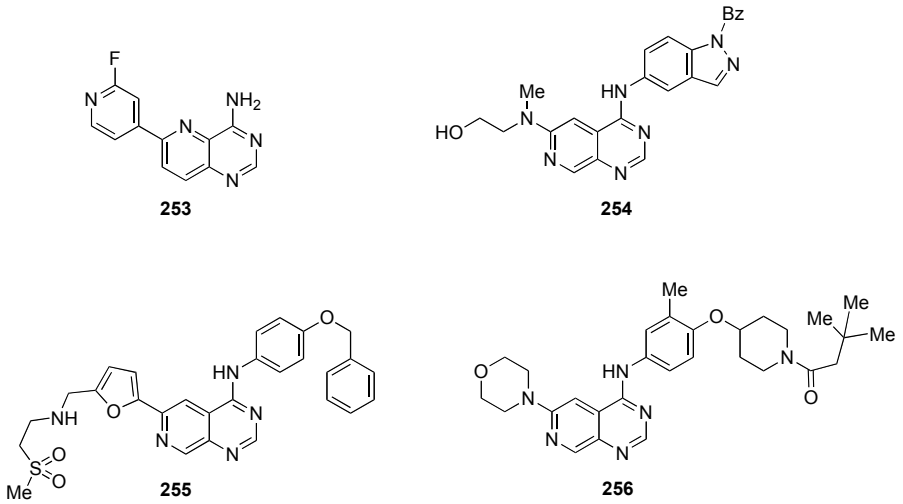

Fig. (58). Chemical structures of aminopyridopyrimidines.

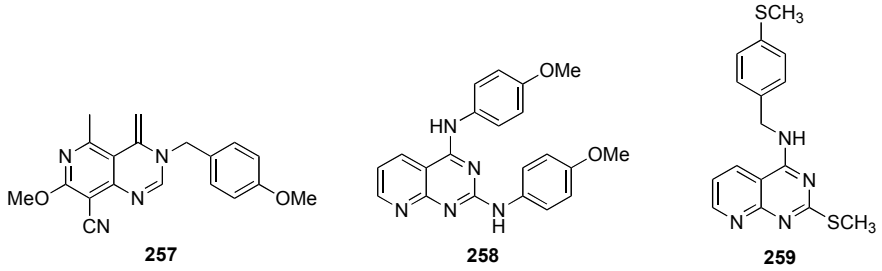

Fig. (59). Chemical structures of pyridopyrimidines bearing amino, methoxy and thio moieties.

CCFF-CEM, colon HT-29, lung HTB-54 and breast MCF-7 cell lines [140]. Compounds **257**-**259** are shown in Fig. (**59**).

4.6. Thiosubstituted Purines

Purines bearing thio moiety have been considered as effective anticancer drugs [148, 149]. Recently, new thiopurines with various thio groups substituted on the pyrimidine ring were synthesized and evaluated for their anticancer activities against three cancer cell lines including glioblastoma SNB-19, melanoma C-32, and human ductal breast epithelial tumor T47D [150]. It was found that pyrrolidino thiopurine **260** was the most potent compound against SBN-19 and C-32 cell lines with comparable activity to cisplatin [150]. Dialkylaminothio derivatives (**261-264**) displayed good activity against SBN-19 cell line with EC_{50} < 10 μg/mL. The azathioprine analogs (**265** and **266**) were more active than the azathioprine against SBN-19 and C-32 cells [150]. Thiopurine derivatives **260**-**266** are shown in Fig. (**60**).

4.7. Imidazopyridines

Nitrogen-bridgehead fused heterocycles bearing an imidazole ring have been shown as a common core structure in bioactive compounds. For example, imidazopyridines (**267**-**269**, Fig. **61**) were shown to be the most active compounds with modest cytotoxic activity against six human cancer cell lines *i.e.*, U251 (glioma), PC-3 (prostate), K-562 (leukemia), HCT-15 (colon), MCF-7 (breast) and SK-LU-1 (lung) [151]. In addition, these compounds (**267**-**269**) displayed significant arrest in G2/M phase, followed by apoptotic cell death in SK-LU-1 cells.

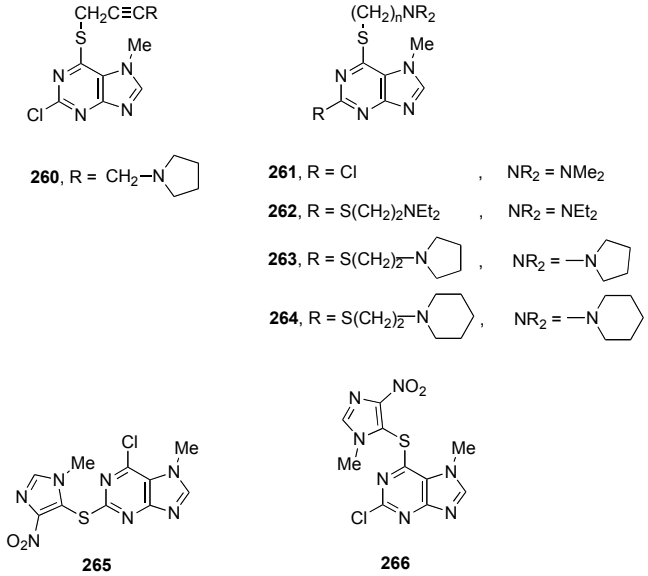

Fig. (60). Chemical structures of thiopurines.

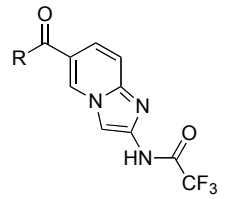

267, R = 3-fluoro-4-methylphenyl
268, R = 2-fluoro-5-methylphenyl
269, R = 1-methyl-1*H*-indol-3-yl

Fig. (61). Chemical structures of imidazopyridine amides.

A series of imidazo[2,1-*b*]pyridine chalcone derivatives (**270**) were synthesized and investigated for their anticancer activities [152]. The results showed that compound **271** exerted promising antiproliferative activity with GI_{50} values less than 1 μM against many tested cancer cell lines such as MCF-7 and DU-145 with GI_{50} values of 0.56 and 0.65 μM, respectively. Interestingly, compound **271** induced G1 cell cycle arrest, down regulation of G1 phase cell cycle regulatory proteins *i.e.*, cyclin D1, E1, and CDK2. Furthermore, compound **271** showed the characteristic features of apoptosis such as enhancement in the levels of p27 and TNFR1 proteins with concomitant down regulation of procaspase-9 [152]. Compounds **270** and **271** are outlined in Fig. (**62**).

270 **271**

R = CF_3, 4-OMe-Ph, 3,4-diOMe-Ph, 4-F-Ph
R = thiopheneyl
R' = 3,4-diOMe-Ph, 3,4,5-triOMe-Ph

Fig. (62). Chemical structures of imidazopyridine chalcone derivatives.

5. PYRIDINE AND PYRIMIDINE METAL COMPLEXES

Metal ions play a very important role in biological processes as well as homeostasis in life [153]. Particularly, transition metal complexes have shown diverse bioactivities *i.e.*, anticancer, antioxidant, antimicrobial and anti-inflammatory activities [154-160]. Generally, molecules bearing electron donor atoms (O, N, S) can act as ligands that are capable of reacting with metal ions to form coordinated compounds. For example, heterocyclic compounds *i.e.*, pyridine, pyrimidine and quinoline including drugs and bioactive compounds [31].

Recently, a series of pincer-type platinum (II) complexes of deprotonated ligands deriving from 1,3-di(2-pyridyl) benzenes **272**-**275** (Fig. **63**) were synthesized and evaluated for their anticancer activities against HeLa cells [161]. It was found that Pt (II) complex **274** exerted high cytotoxicity with IC_{50} value of 0.46 μM. However, the IC_{50} values of compounds **272**-**275** were shown in the range of 0.46-2.45 μM which are 22-fold more potent than cisplatin (IC_{50} = 10 μM).

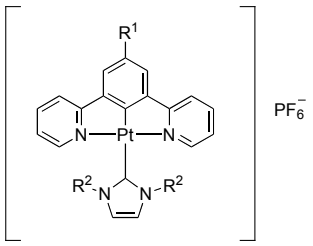

272, R^1 = H , R^2 = nC_4H_9
273, R^1 = H , R^2 = i-C_3H_7
274, R^1 = H , R^2 = cyclohexyl
275, R^1 = CF_3 , R^2 = nC_4H_9

Fig. (63). Chemical structures of pincer-type platinum (II) complexes.

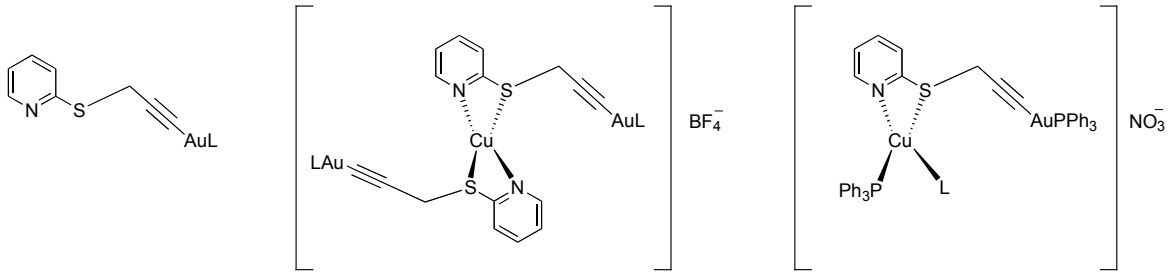

276, L = PTA
277, L = DAPTA
278, L = PPh_3
279, L = TPPTS

280, L = PTA
281, L = DAPTA
282, L = PPh_3
283, L = TPPTS

284, L = PTA
285, L = DAPTA

PTA = 1,3,5-triaza-7-phosphaadamantane
DAPTA = 3,7-diacetyl-1,3,7-triaza-5-phosphabicyclo[3.3.1]nonane
PPh_3 = triphenylphosphine
TPPTS = sodium triphenylphosphane trisulfonate

Fig. (64). Chemical structures of gold (I) and copper (II) complexes of *S*-propagylthiopyridines.

New heteronuclear gold (I) and copper (II) complexes of *S*-propagylthiopyridine **280-285** (Fig. **64**) were synthesized from metalloligand (Au) **276-279**, and investigated for their anticancer activities against human colon cancer cell lines [162]. Most of the thiopyridine metal complexes (**280-285**) exerted more potent cytotoxicity (PD7 and TC7 cancer cell lines) with IC_{50} values of 10^{-4} to 1.17 μM compared with the reference drug, cisplatin [162].

Triphenyltin 2-pyridylthiolate **286** (Fig. **65**) was reported to show antitumor activity against a number of human cancer cells (MCF-7, EVSA-T, WiDr, IGROV, M19MEL and A498) with comparable activity to the control methotrexate and doxorubicin, but with higher activity than that of the carboplatin and cisplatin [163].

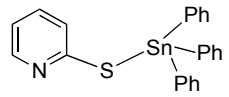

286

Fig. (65). Chemical structure of 2-pyridylthio metal complex.

(Pyrazolylmethyl)pyridine platinum (II), (**287-290**) and gold (III), (**291-296**) complexes (Fig. **66**) were synthesized and investigated for their anticancer activities against HeLa cell [164]. The results showed that platinum complexes **287** and **289** were less active than those with aryl substituents, **288** and **290**. The IC_{50} values of compounds **288** (IC_{50} = 3.849 μM) and **290** (IC_{50} = 8.920 μM) were approximately eight and nineteen times lower than that of the cisplatin. However, the gold (III) complexes (**291-296**) exhibited much lower cytotoxic activity compared with the cisplatin [164].

5-Substituted (CH_3, NO_2, CO_2H, I) uracils were reported to form complexes with metal ions (Cu, Zn, Ni, Mn, Cr, Fe) [165, 166]. Transition metal complexes of mixed ligands such as 5-iodouracil (5Iu)/5-nitrouracil (5Nu)-8-hydroxyquinolines (8HQ) **297-302** (Fig. **67**) have been reported to exert significant cytotoxic activity against four human cancer cell lines (HepG2, A549, HuCCA-1 and MOLT-3) [160]. Notably, the cytotoxicity of these metal complexes **297-302** against HepG2 has been shown to be higher than that of the control drug, etoposide. Copper complex of 5Nu (**301**) is the most potent and promising cytotoxic compound [160]. Moreover, the copper complexes (**298** and **301**) have been reported to be a novel class of aromatase inhibitor, exerting the activity higher than that of the reference drug (ketoconazole) but less active than the letrozole [167].

Instead of 8HQ, 8-aminoquinoline (8AQ) metal complexes of 5Iu and 5Nu (**303-308**, Fig. **68**) were synthesized and investigated for their cytotoxic activities [154]. It was found that nickel complex of 8AQ-5Nu (**308**) displayed cytotoxic activity against MOLT-3 cell line [154].

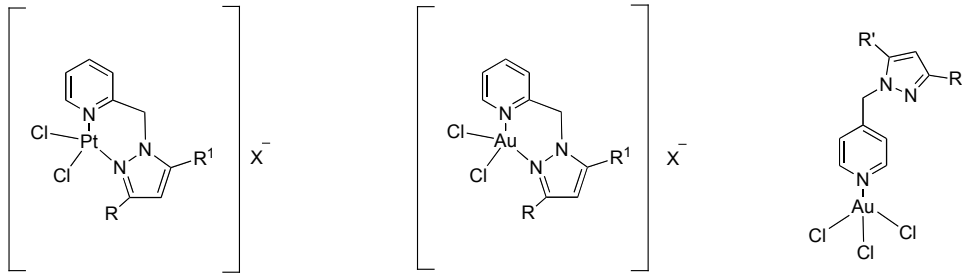

287, R = R^1 = CH_3 , X^- = $[AuCl_4]^-$
288, R = R^1 = C_6H_5 , X^- = Cl^-
289, R = R^1 = *t*Bu , X^- = Cl^-
290, R = $4CH_3$-C_6H_4 , R^1 = H, X^- = $[AuCl_4]^-$

291, R = R^1 = CH_3 , X^- = $[AuCl_4]^-$
292, R = R^1 = C_6H_5 , X^- = Cl^-
293, R = R^1 = *t*Bu , X^- = Cl^-
294, R = $4CH_3$-C_6H_5 , R^1 = H, X^- = $[AuCl_4]^-$

295, R = R' = CH_3
296, R = R' = C_6H_5

Fig. (66). Chemical structures of (pyrazolylmethyl)pyridine metal complexes.

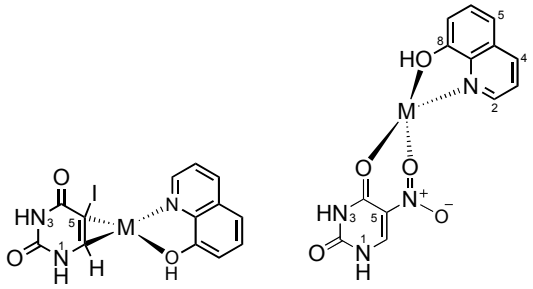

297, M = Mn
298, M = Cu
299, M = Ni

300, M = Mn
301, M = Cu
302, M = Ni

Fig. (67). Chemical structures of uracil-8-hydroxyquinoline metal complexes.

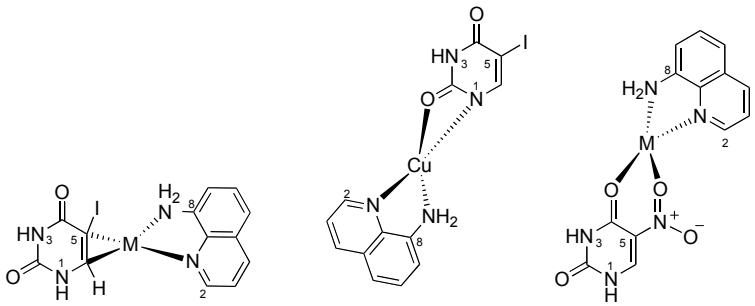

303, M = Mn
304, M = Ni

305

306, M = Mn
307, M = Cu
308 M = Ni

Fig. (68). Chemical structures of uracils-8-aminoquinoline metal complexes.

6. RECENT DRUGS INTRODUCED TO THE MARKET

Pyridine- and pyrimidine-based compounds have been extensively explored for development of new anticancer drugs. Examples of recent drugs, bearing pyridine and pyrimidine pharmacophores, have been introduced to the market as summarized in Table **2** [168-172].

7. LINKAGES OF ANTICANCER AND OTHER BIOLOGICAL ACTIVITIES

Recently, it has been reported that several drugs have a similar mode of treatment may shift the paradigm of drug discovery from one drug-one target-one mechanism to one drug-multiple targets-common mechanism [173]. Various drugs and bioactive compounds *i.e.*, derivatives of quinine, curcumin [173] and 8-hydroxyquinoline [153] have been found to exert anticancer and antimalarial activities. Moreover, some pyridine- and pyrimidine-based compounds have shown such related bioactivities. For example, thiopyridine derivatives (**61**, **65** and **67**, Fig. **18**) displayed anticancer and antimalarial activities [79]. A series of 3-picolyl and phenylpyridines bearing 1-adamantylthio moiety (**68-75**, Fig. **19**) exhibited anticancer and antioxidant activities [81]. Furthermore, pyrimidine metal complexes **297**, **299**, **300** and **302** (Fig. **67**) as well as **308** (Fig. **68**) exerted anticancer and antioxidant activities [154, 160].

Table 2. Pyridine- and pyrimidine-based drugs have been introduced to the market [168-172].

Pyridine and Pyrimidine Drugs	Structure	Type/Indication	Reference
Abiraterone acetate	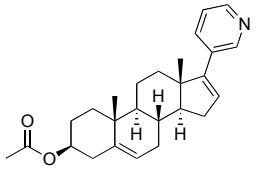	-Treatment of castration resistant prostate cancer	[168]
Avanafil	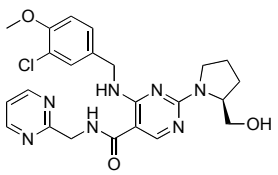	-An oral PDE5 inhibitor -Treatment of erectile dysfunction (ED)	[168]
Axitinib	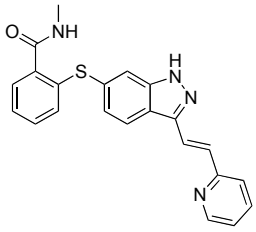	-Treatment of advanced renal cell carcinoma (RCC) (specifically after the failure of other systemic treatments)	[169]

(Table 2) Contd….

Pyridine and Pyrimidine Drugs	Structure	Type/Indication	Reference
Crizotinib	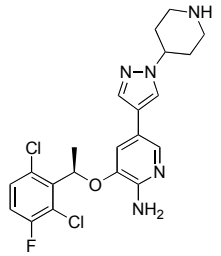	-A potent and selective mesenchymal epithelial transition factor/anaplastic lymphoma kinase (cMET/ALK) inhibitor -Treatment of advanced or metastatic non-small cell lung cancer (NSCLC)	[168]
Dabrafenib mesylate	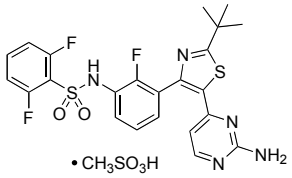	-Treatment of metastatic BRAF-mutant melanoma	[170]
Dexlansoprazole	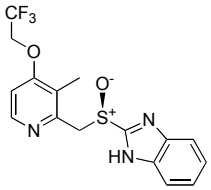	-A dual release formulation of the (R)-isomer of lansoprazol proton pump inhibitor (PPI)	[171]
Edoxaban tosilate	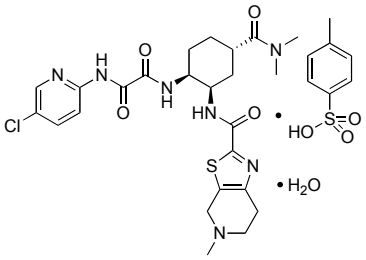	-An orally administered coagulation factor Xa inhibitor -Preventive treatment of venous thromboembolic events (VTE) in patients undergoing total knee arthroplasty, total hip arthroplasty, or hip fracture surgery	[168]
Macitentan	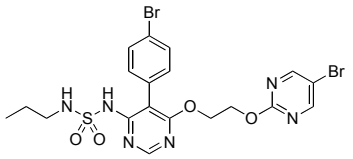	-An endothelin receptor antagonist -Treatment of pulmonary arterial hypertension (PAH)	[170]
Pazopanib hydrochloride	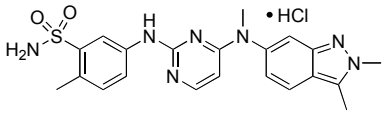	-A potent and selective multi-targeted receptor tyrosine kinase inhibitor of VEGFR-1, VEGFR-2, VEGFR-3, PDGFR-α, PDGFR-β and c-kit -Blocks tumor growth and inhibits angiogenesis	[171]
Perampanel hydrate	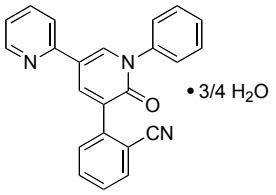	-A selective, non-competitive α-amino-3-hydroxy-5-methyl-4-isoxazolepropionic acid receptor (AMPAR) antagonist -Approved for partial-onset seizures in patients with epilepsy	[169]
Radotinib dihydrochloride	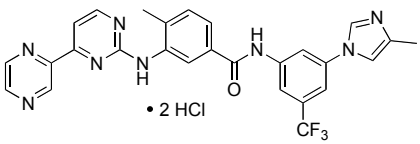	-Treatment of patients with Philadelphia chromosome-positive chronic myeloid leukemia (CML)	[169]

(Table 2) Contd….

Pyridine and Pyrimidine Drugs	Structure	Type/Indication	Reference
Regorafenib hydrate	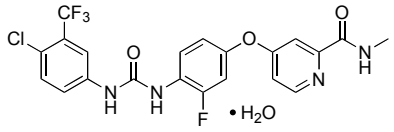	-Treatment of metastatic colorectal cancer and gastro-intestinal stromal tumors	[169]
Rilpivirine hydrochloride	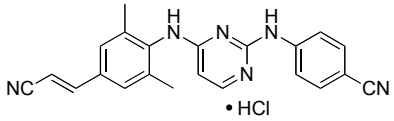	-A non-nucleoside reverse transcriptase inhibitor (NNRTI) -Treatment of HIV-1 infection	[168]
Roflumilast	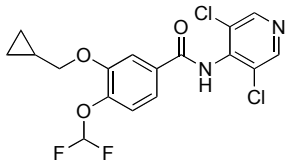	-A selective, long-acting PDE-4 inhibitor -Treatment of inflammatory conditions of the lungs such as asthma and chronic obstructive pulmonary disorder	[172]
Vismodegib	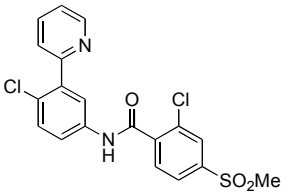	-Treatment of metastatic basal-cell carcinoma (BCC)	[169]
Topiroxostat	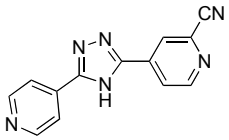	-An orally-administered, non-purine, selective xanthine oxidase (XO) inhibitor -Treatment of hyperuricemia (specifically for patients with gout in Japan)	[170]

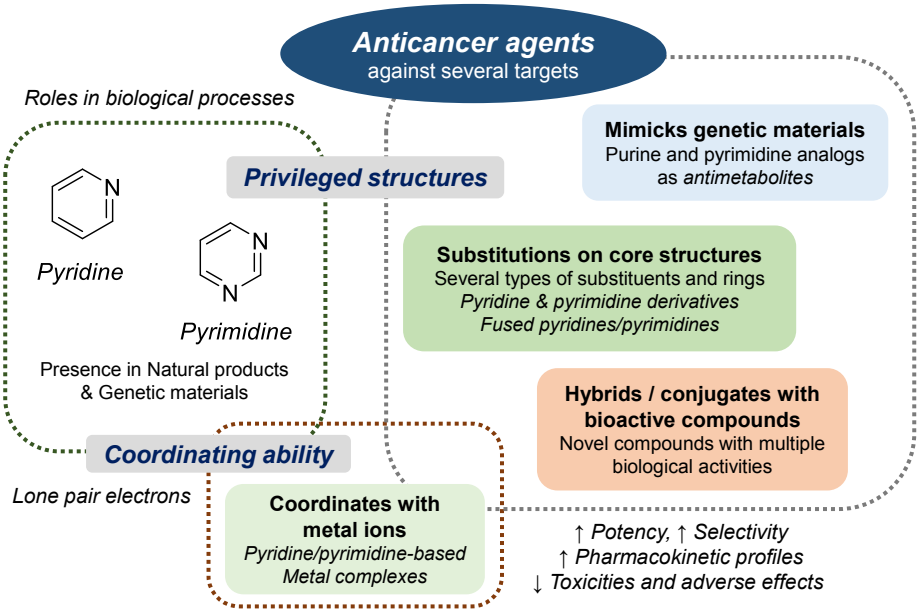

Fig. (69). Development of pyridine/pyrimidine-based anticancer agents.

CONCLUSION

Pyridine and pyrimidine are attractive scaffolds in drug discovery and development due to their roles in biological processes, their diverse biological activities and their coordinating abilities. The summary regarding development of pyridine/pyrimidine-based anticancer agents is provided in Fig. (**69**). As a starting point, strategy of mimicking natural substance was applied for the development of

pyrimidine/purine analogs that exhibited their anticancer activities *via* competing with natural substance to bind with target receptors or enzymes. Later on, the strategy of substitution with various types of moieties and rings on the core structure was employed to obtain a variety of pyridine/pyrimidine derivatives and fused pyridines/ pyrimidines. Regarding trend of polypharmacology, the conjugation of pyridine/pyrimidine core structures with the existing bioactive compounds was conducted to develop novel compounds with multiple medicinal applications. Pyridine and pyrimidine contain lone pair electrons which contribute to their coordinating abilities. In this regard, many pyridine/pyrimidine-based metal complexes were developed as anticancer metal-based agents. It should be noted that these small molecules, pyridine and pyrimidine, are promising scaffolds for the development of anticancer agents against several targets and are noted to be potential pharmacophores for the discovery of novel bioactive compounds for therapeutic applications.

In summary, the most active compounds with their IC_{50} or GI_{50} values are outlined in Table **3**.

FUTURE DIRECTIONS OF PYRIDINE AND PYRIMIDINE SCAFFOLDS

A variety of pyridine and pyrimidine analogs as potential anticancer agents has been disclosed. Based on the reported data, more and new compounds with anticancer and/or related biological activities can be achieved by many aspects. Interestingly, rational design and synthesis of novel bioactive

Table 3. The most active compounds with IC_{50} values and target cell lines.

Type of Compound		IC_{50}	Target Cell Line (or Enzyme)	References
Pyridine	Condensed pyridine (isoquinoline) **4**	4 ng/mL	MOLT-3	[60]
	Condensed pyridine **33**	0.50 μM	Aromatase	[63]
	2,4-Disubstituted pyridines **46** and **47**	[a]0.28 and 0.16 μM	MCF-7	[72]
	2,4,6-Trisubstituted pyridines **82**-**84**	[b]0.79-0.88 μM	HCT-15	[82]
	92, **93**, **95**	[c]0.78 μM	T47D	[51]
	104	[d]0.08 μM	HCT-15	[58]
Pyrimidine	2,4,5-Trisubstituted pyrimidine **150**	0.5-4.0 μM	HeLa, A549, HCT-8 and HepG2	[53]
Fused pyrimidines	Pyrazole-pyrimidine **218**	[a]0.326 μM [a]0.335 μM [a]0.348 μM	CCRF-CEM NCI-H322M UO-31	[129]
	Thienopyrimidines **230**	[a]0.495 μM [a]5.57 μM	T47D MDA-MB-468	[57]
	232, **233**	6.0, 3.0 nM	Tyrosine kinase	[73, 135]
	Quinazoline-4-ones **235**, **236**	[e]23, 22 nmole/mL	MCF-7	[138]
	Quinazoline linked thiazolidinones **237**-**240**	3-9 nmole/mL	MCF-7	[138]
	Pyridopyrimidine **253**	nM range	MAP4K4 (seronine threonine kinase)	[144]
	Imidazopyridine chalcone **271**	[a]0.56, 0.65 μM	MCF-7, DU-145	[152]
Metal complexes	Pincer-type Pt (II) complexes **272**-**275**	[f]0.46-2.45 μM	HeLa	[161]
	274	0.46 μM	HeLa	[161]
	Thiopyridine metal complexes **280**-**285**	[g]10^{-4}-1.17 μM	PD7, TC7	[162]
	Pyrazolylpyridine Pt (II) complexes **288**, **290**	[h]3.847, 8.920 μM	HeLa	[164]

[a]GI_{50} value is presented instead of IC_{50} value.
[b]More active than the reference drugs etoposide (IC_{50} = 1.33 μM) and adriamycin (IC_{50} = 1.28 μM).
[c]More active than etoposide (IC_{50} = 13.17 μM).
[d]Among the tested compounds, **104** was the strongest Topo II inhibitor with 98.2% at 100 μM.
[e]The activity is comparable to doxorubicin (IC_{50} = 22 nmole/mL).
[f]These Pt (II) complexes are 22 folds more potent than cisplatin (IC_{50} = 10 μM).
[g]More active than cisplatin.
[h]Their IC_{50} values are about 18 and 19 times lower than that of cisplatin.

compounds can be performed by computational methods, structural modification and molecular hybrids of the bioactive core scaffolds. Chemical descriptors obtained from the computational methods can give insight into structural features influencing their bioactivities as the quantitative structure-activity relationship (QSAR) for development of promising novel compounds. Furthermore, regarding the drug repositioning, the existing pyridine/pyrimidine drugs (or compounds) for new medicinal usages or for old drugs with new therapeutic values should be explored.

CONFLICT OF INTEREST

The authors confirm that this article content has no conflict of interest.

ACKNOWLEDGEMENTS

This project is supported by Office of the Higher Education Commission and Mahidol University under the National Research Universities Initiative (2559) as well as Mahidol University (B.E. 2556-2558). AW gratefully acknowledges the research grant supported by the Thailand Research Fund (Grant No. TRG5880143).

REFERENCES

[1] World Health Organization. Noncommunicable diseases. http://www.who.int/mediacentre/factsheets/fs355/en/. [Accessed July 15, **2015**].

[2] Vos, T.; Flaxman, A.D.; Naghavi, M.; Lozano, R.; Michaud, C.; Ezzati, M.; Shibuya, K.; Salomon, J.A.; Abdalla, S.; Aboyans, V.; Abraham, J.; Ackerman, I.; Aggarwal, R.; Ahn, S.Y.; Ali, M.K.; AlMazroa, M.A.; Alvarado, M.; Anderson, H.R.; Anderson, L.M.; Andrews, K.G.; Atkinson, C.; Baddour, L.M.; Bahalim, A.N.; Barker-Collo, S.; Barrero, L.H.; Bartels, D.H.; Basáñez, M.-G.; Baxter, A.; Bell, M.L.; Benjamin, E.J.; Bennett, D.; Bernabé, E.; Bhalla, K.; Bhandari, B.; Bikbov, B.; Abdulhak, A.B.; Birbeck, G.; Black, J.A.; Blencowe, H.; Blore, J.D.; Blyth, F.; Bolliger, I.; Bonaventure, A.; Boufous, S.; Bourne, R.; Boussinesq, M.; Braithwaite, T.; Brayne, C.; Bridgett, L.; Brooker, S.; Brooks, P.; Brugha, T.S.; Bryan-Hancock, C.; Bucello, C.; Buchbinder, R.; Buckle, G.; Budke, C.M.; Burch, M.; Burney, P.; Burstein, R.; Calabria, B.; Campbell, B.; Canter, C.E.; Carabin, H.; Carapetis, J.; Carmona, L.; Cella, C.; Charlson, F.; Chen, H.; Cheng, A.T.-A.; Chou, D.; Chugh, S.S.; Coffeng, L.E.; Colan, S.D.; Colquhoun, S.; Colson, K.E.; Condon, J.; Connor, M.D.; Cooper, L.T.; Corriere, M.; Cortinovis, M.; de Vaccaro, K.C.; Couser, W.; Cowie, B.C.; Criqui, M.H.; Cross, M.; Dabhadkar, K.C.; Dahiya, M.; Dahodwala, N.; Damsere-Derry, J.; Danaei, G.; Davis, A.; De Leo, D.; Degenhardt, L.; Dellavalle, R.; Delossantos, A.; Denenberg, J.; Derrett, S.; Des Jarlais, D.C.; Dharmaratne, S.D.; Dherani, M.; Diaz-Torne, C.; Dolk, H.; Dorsey, E.R.; Driscoll, T.; Duber, H.; Ebel, B.; Edmond, K.; Elbaz, A.; Ali, S.E.; Erskine, H.; Erwin, P.J.; Espindola, P.; Ewoigbokhan, S.E.; Farzadfar, F.; Feigin, V.; Felson, D.T.; Ferrari, A.; Ferri, C.P.; Fèvre, E.M.; Finucane, M.M.; Flaxman, S.; Flood, L.; Foreman, K.; Forouzanfar, M.H.; Fowkes, F.G.R.; Franklin, R.; Fransen, M.; Freeman, M.K.; Gabbe, B.J.; Gabriel, S.E.; Gakidou, E.; Ganatra, H.A.; Garcia, B.; Gaspari, F.; Gillum, R.F.; Gmel, G.; Gosselin, R.; Grainger, R.; Groeger, J.; Guillemin, F.; Gunnell, D.; Gupta, R.; Haagsma, J.; Hagan, H.; Halasa, Y.A.; Hall, W.; Haring, D.; Haro, J.M.; Harrison, J.E.; Havmoeller, R.; Hay, R.J.; Higashi, H.; Hill, C.; Hoen, B.; Hoffman, H.; Hotez, P.J.; Hoy, D.; Huang, J.J.; Ibeanusi, S.E.; Jacobsen, K.H.; James, S.L.; Jarvis, D.; Jasrasaria, R.; Jayaraman, S.; Johns, N.; Jonas, J.B.; Karthikeyan, G.; Kassebaum, N.; Kawakami, N.; Keren, A.; Khoo, J.-P.; King, C.H.; Knowlton, L.M.; Kobusingye, O.; Koranteng, A.; Krishnamurthi, R.; Lalloo, R.; Laslett, L.L.; Lathlean, T.; Leasher, J.L.; Lee, Y.Y.; Leigh, J.; Lim, S.S.; Limb, E.; Lin, J.K.; Lipnick, M.; Lipshultz, S.E.; Liu, W.; Loane, M.; Ohno, S.L.; Lyons, R.; Ma, J.; Mabweijano, J.; MacIntyre, M.F.; Malekzadeh, R.; Mallinger, L.; Manivannan, S.; Marcenes, W.; March, L.; Margolis, D.J.; Marks, G.B.; Marks, R.; Matsumori, A.; Matzopoulos, R.; Mayosi, B.M.; McAnulty, J.H.; McDermott, M.M.; McGill, N.; McGrath, J.; Medina-Mora, M.E.; Meltzer, M.; Memish, Z.A.; Mensah, G.A.; Merriman, T.R.; Meyer, A.-C.; Miglioli, V.; Miller, M.; Miller, T.R.; Mitchell, P.B.; Mocumbi, A.O.; Moffitt, T.E.; Mokdad, A.A.; Monasta, L.; Montico, M.; Moradi-Lakeh, M.; Moran, A.; Morawska, L.; Mori, R.; Murdoch, M.E.; Mwaniki, M.K.; Naidoo, K.; Nair, M.N.; Naldi, L.; Narayan, K.M.V.; Nelson, P.K.; Nelson, R.G.; Nevitt, M.C.; Newton, C.R.; Nolte, S.; Norman, P.; Norman, R.; O'Donnell, M.; O'Hanlon, S.; Olives, C.; Omer, S.B.; Ortblad, K.; Osborne, R.; Ozgediz, D.; Page, A.; Pahari, B.; Pandian, J.D.; Rivero, A.P.; Patten, S.B.; Pearce, N.; Padilla, R.P.; Perez-Ruiz, F.; Perico, N.; Pesudovs, K.; Phillips, D.; Phillips, M.R.; Pierce, K.; Pion, S.; Polanczyk, G.V.; Polinder, S.; Pope Iii, C.A.; Popova, S.; Porrini, E.; Pourmalek, F.; Prince, M.; Pullan, R.L.; Ramaiah, K.D.; Ranganathan, D.; Razavi, H.; Regan, M.; Rehm, J.T.; Rein, D.B.; Remuzzi, G.; Richardson, K.; Rivara, F.P.; Roberts, T.; Robinson, C.; De Leòn, F.R.; Ronfani, L.; Room, R.; Rosenfeld, L.C.; Rushton, L.; Sacco, R.L.; Saha, S.; Sampson, U.; Sanchez-Riera, L.; Sanman, E.; Schwebel, D.C.; Scott, J.G.; Segui-Gomez, M.; Shahraz, S.; Shepard, D.S.; Shin, H.; Shivakoti, R.; Silberberg, D.; Singh, D.; Singh, G.M.; Singh, J.A.; Singleton, J.; Sleet, D.A.; Sliwa, K.; Smith, E.; Smith, J.L.; Stapelberg, N.J.C.; Steer, A.; Steiner, T.; Stolk, W.A.; Stovner, L.J.; Sudfeld, C.; Syed, S.; Tamburlini, G.; Tavakkoli, M.; Taylor, H.R.; Taylor, J.A.; Taylor, W.J.; Thomas, B.; Thomson, W.M.; Thurston, G.D.; Tleyjeh, I.M.; Tonelli, M.; Towbin, J.A.; Truelsen, T.; Tsilimbaris, M.K.; Ubeda, C.; Undurraga, E.A.; van der Werf, M.J.; van Os, J.; Vavilala, M.S.; Venketasubramanian, N.; Wang, M.; Wang, W.; Watt, K.; Weatherall, D.J.; Weinstock, M.A.; Weintraub, R.; Weisskopf, M.G.; Weissman, M.M.; White, R.A.; Whiteford, H.; Wiersma, S.T.; Wilkinson, J.D.; Williams, H.C.; Williams, S.R.M.; Witt, E.; Wolfe, F.; Woolf, A.D.; Wulf, S.; Yeh, P.-H.; Zaidi, A.K.M.; Zheng, Z.-J.; Zonies, D.; Lopez, A.D.; Murray, C.J.L. Years lived with disability (YLDs) for 1160 sequelae of 289 diseases and injuries 1990–2010: a systematic analysis for the Global Burden of Disease Study 2010. *Lancet*, **2012**, *380*, 2163-2196.

[3] World Health Organization. The Global burden of disease; 2004 update. *Geneva, World Health Organization* **2008**.

[4] Mathers, C.D.; Loncar, D. Projections of global mortality and burden of disease from 2002 to 2030. *PLoS Med.*, **2006**, *3*, e442.

[5] Soerjomataram, I.; Lortet-Tieulent, J.; Ferlay, J.; Forman, D.; Mathers, C.; Parkin, D.; Bray, F. Estimating and validating disability-adjusted life years at the global level: a methodological framework for cancer. *BMC Med. Res. Methodol.*, **2012**, *12*, 125.

[6] Wu, X.-Z. A new classification system of anticancer drugs – based on cell biological mechanisms. *Med. Hypotheses*, **2006**, *66*, 883-887.

[7] Sarah, P.; David, M., Mechanisms of anticancer drugs, In: *Scott-Brown's Otorhinolaryngology: Head and Neck Surgery 7Ed*; CRC Press, **2008**; Vol. pp. 34-46.

[8] Espinosa, E.; Zamora, P.; Feliu, J.; Gonzalez Baron, M. Classification of anticancer drugs--a new system based on therapeutic targets. *Cancer Treat. Rev.*, **2003**, *29*, 515-523.

[9] Samant, R.S.; Shevde, L.A. Recent advances in anti-angiogenic therapy of cancer. *Oncotarget*, **2011**, *2*, 122-134.

[10] Dobbelstein, M.; Moll, U. Targeting tumour-supportive cellular machineries in anticancer drug development. *Nat. Rev. Drug Discov.*, **2014**, *13*, 179-196.

[11] Pommier, Y.; Leo, E.; Zhang, H.; Marchand, C. DNA topoisomerases and their poisoning by anticancer and antibacterial drugs. *Chemistry & biology*, **2010**, *17*, 421-433.

[12] Chiablaem, K.; Lirdprapamongkol, K.; Keeratichamroen, S.; Surarit, R.; Svasti, J. Curcumin suppresses vasculogenic mimicry capacity of hepatocellular carcinoma cells through STAT3 and PI3K/AKT inhibition. *Anticancer Res.*, **2014**, *34*, 1857-1864.

[13] Guo, J.Q.; Zheng, Q.H.; Chen, H.; Chen, L.; Xu, J.B.; Chen, M.Y.; Lu, D.; Wang, Z.H.; Tong, H.F.; Lin, S. Ginsenoside Rg3 inhibition of vasculogenic mimicry in pancreatic cancer through downregulation of VEcadherin/EphA2/MMP9/MMP2 expression. *Int. J. Oncol.*, **2014**, *45*, 1065-1072.

[14] Meng, J.; Sun, B.; Zhao, X.; Zhang, D.; Zhao, X.; Gu, Q.; Dong, X.; Zhao, N.; Liu, P.; Liu, Y. Doxycycline as an inhibitor of the epithelial-to-mesenchymal transition and vasculogenic mimicry in hepatocellular carcinoma. *Mol. Cancer Ther.*, **2014**, *13*, 3107-3122.

[15] Tu, D.G.; Yu, Y.; Lee, C.H.; Kuo, Y.L.; Lu, Y.C.; Tu, C.W.; Chang, W.W. Hinokitiol inhibits vasculogenic mimicry activity of breast cancer stem/progenitor cells through proteasome-mediated degradation of epidermal growth factor receptor. *Oncol. Lett.*, **2016**, *11*, 2934-2940.

[16] Wang, H.; Sun, W.; Zhang, W.Z.; Ge, C.Y.; Zhang, J.T.; Liu, Z.Y.; Fan, Y.Z. Inhibition of tumor vasculogenic mimicry and prolongation of host survival in highly aggressive gallbladder cancers by norcantharidin *via* blocking the ephrin type a receptor 2/focal adhesion kinase/paxillin signaling pathway. *PLoS One*, **2014**, *9*, e96982.

[17] Xia, Y.; Cai, X.Y.; Fan, J.Q.; Zhang, L.L.; Ren, J.H.; Chen, J.; Li, Z.Y.; Zhang, R.G.; Zhu, F.; Wu, G. Rho kinase inhibitor fasudil suppresses the vasculogenic mimicry of B16 mouse melanoma cells both *in vitro* and *in vivo*. *Mol. Cancer Ther.*, **2015**, *14*, 1582-1590.

[18] Zhang, C.; Chen, W.; Zhang, X.; Huang, B.; Chen, A.; He, Y.; Wang, J.; Li, X. Galunisertib inhibits glioma vasculogenic mimicry formation induced by astrocytes. *Sci. Rep.*, **2016**, *6*, 23056.

[19] Zhang, J.-G.; Zhang, D.-D.; Wu, X.; Wang, Y.-Z.; Gu, S.-Y.; Zhu, G.-H.; Li, X.-Y.; Li, Q.; Liu, G.-L. Incarvine C suppresses proliferation and vasculogenic mimicry of hepatocellular carcinoma cells *via* targeting ROCK inhibition. *BMC Cancer*, **2015**, *15*, 1-12.

[20] Asati, V.; Mahapatra, D.K.; Bharti, S.K. PI3K/Akt/mTOR and Ras/Raf/MEK/ERK signaling pathways inhibitors as anticancer agents: Structural and pharmacological perspectives. *Eur. J. Med. Chem.*, **2016**, *109*, 314-341.

[21] Nitulescu, G.M.; Margina, D.; Juzenas, P.; Peng, Q.; Olaru, O.T.; Saloustros, E.; Fenga, C.; Spandidos, D.; Libra, M.; Tsatsakis, A.M. Akt inhibitors in cancer treatment: The long journey from drug discovery to clinical use (Review). *Int. J. Oncol.*, **2016**, *48*, 869-885.

[22] Arora, A.; Scholar, E.M. Role of tyrosine kinase inhibitors in cancer therapy. *J. Pharmacol. Exp. Ther.*, **2005**, *315*, 971-979.

[23] Kumar, R.M.; Fuchs, B. Hedgehog signaling inhibitors as anti-cancer agents in osteosarcoma. *Cancers*, **2015**, *7*, 784-794.

[24] Trinh, T.N.; McLaughlin, E.A.; Gordon, C.P.; McCluskey, A. Hedgehog signalling pathway inhibitors as cancer suppressing agents. *Med. Chem. Comm.*, **2014**, *5*, 117-133.

[25] Dou, Q.P.; Zonder, J.A. Overview of proteasome inhibitor-based anti-cancer therapies: perspective on bortezomib and second generation proteasome inhibitors versus future generation inhibitors of ubiquitin-proteasome system. *Curr. Cancer Drug Targets*, **2014**, *14*, 517-536.

[26] Soga, S.; Akinaga, S.; Shiotsu, Y. Hsp90 inhibitors as anti-cancer agents, from basic discoveries to clinical development. *Curr. Pharm. Des.*, **2013**, *19*, 366-376.

[27] Ververis, K.; Hiong, A.; Karagiannis, T.C.; Licciardi, P.V. Histone deacetylase inhibitors (HDACIs): multitargeted anticancer agents. *Biologics.*, **2013**, *7*, 47-60.

[28] Walkinshaw, D.R.; Yang, X.J. Histone deacetylase inhibitors as novel anticancer therapeutics. *Curr. Oncol.*, **2008**, *15*, 237-243.

[29] Brueckner, B.; Kuck, D.; Lyko, F. DNA methyltransferase inhibitors for cancer therapy. *Cancer J.*, **2007**, *13*, 17-22.

[30] Gnyszka, A.; Jastrzebski, Z.; Flis, S. DNA methyltransferase inhibitors and their emerging role in epigenetic therapy of cancer. *Anticancer Res.*, **2013**, *33*, 2989-2996.

[31] Sinthupoom, N.; Prachayasittikul, V.; Prachayasittikul, S.; Ruchirawat, S.; Prachayasittikul, V. Nicotinic acid and derivatives as multifunctional pharmacophores for medical applications. *Eur. Food Res. Technol.*, **2015**, *240*, 1-17.

[32] Surjana, D.; Halliday, G.M.; Damian, D.L. Role of nicotinamide in DNA damage, mutagenesis, and DNA repair. *J. Nucleic Acids*, **2010**, *2010*, doi:10.4061/2010/157591.

[33] Audrito, V.; Vaisitti, T.; Rossi, D.; Gottardi, D.; D'Arena, G.; Laurenti, L.; Gaidano, G.; Malavasi, F.; Deaglio, S. Nicotinamide blocks proliferation and induces apoptosis of chronic lymphocytic leukemia cells through activation of the p53/miR-34a/SIRT1 tumor suppressor network. *Cancer Res.*, **2011**, *71*, 4473-4483.

[34] Avalos, J.L.; Bever, K.M.; Wolberger, C. Mechanism of sirtuin inhibition by nicotinamide: altering the NAD^+ cosubstrate specificity of a Sir2 enzyme. *Mol. Cell*, **2005**, *17*, 855-868.

[35] Vaziri, H.; Dessain, S.K.; Eaton, E.N.; Imai, S.I.; Frye, R.A.; Pandita, T.K.; Guarente, L.; Weinberg, R.A. hSIR2(SIRT1) functions as an NAD-dependent p53 deacetylase. *Cell*, **2001**, *107*, 149-159.

[36] Luo, J.; Nikolaev, A.Y.; Imai, S.I.; Chen, D.; Su, F.; Shiloh, A.; Guarente, L.; Gu, W. Negative control of p53 by Sir2α promotes cell survival under stress. *Cell*, **2001**, *107*, 137-148.

[37] Brunet, A.; Sweeney, L.B.; Sturgill, J.F.; Chua, K.F.; Greer, P.L.; Lin, Y.; Tran, H.; Ross, S.E.; Mostoslavsy, R.; Cohen, H.Y.; Hu, L.S.; Cheng, H.L.; Jedrychowski, M.P.; Gygi, S.P.; Sinclair, D.A.; Alt, F.W.; Greenberg, M.E. Stress-dependent regulation of FOXO transcription factors by the SIRT1 deacetylase. *Science*, **2004**, *303*, 2011-2015.

[38] Yi, J.; Luo, J. SIRT1 and p53, effect on cancer, senescence and beyond. *Biochim. Biophys. Acta*, **2010**, *1804*, 1684-1689.

[39] Tissenbaum, H.A.; Guarente, L. Increased dosage of a sir-2 gene extends lifespan in *Caenorhabditis elegans*. *Nature*, **2001**, *410*, 227-230.

[40] Kaeberlein, M.; McVey, M.; Guarente, L. The SIR2/3/4 complex and SIR2 alone promote longevity in *Saccharomyces cerevisiae* by two different mechanisms. *Genes Dev.*, **1999**, *13*, 2570-2580.

[41] Wood, J.G.; Regina, B.; Lavu, S.; Hewitz, K.; Helfand, S.L.; Tatar, M.; Sinclair, D. Sirtuin activators mimic caloric restriction and delay ageing in metazoans. *Nature*, **2004**, *430*, 686-689.

[42] Liu, T.; Liu, P.Y.; Marshall, G.M. The critical role of the class III histone deacetylase SIRT1 in cancer. *Cancer Res.*, **2009**, *69*, 1702-1705.

[43] Hu, J.; Jing, H.; Lin, H. Sirtuin inhibitors as anticancer agents. *Future Med. Chem.*, **2014**, *6*, 945-966.

[44] Yang, Y.; Hou, H.; Haller, E.M.; Nicosia, S.V.; Bai, W. Suppression of FOXO1 activity by FHL2 through SIRT1-mediated deacetylation. *EMBO J.*, **2005**, *24*, 1021-1032.

[45] Pingaew, R.; Prachayasittikul, V.; Mandi, P.; Nantasenamat, C.; Prachayasittikul, S.; Ruchirawat, S.; Prachayasittikul, V. Synthesis and molecular docking of 1,2,3-triazole-based sulfonamides as aromatase inhibitors. *Bioorg. Med. Chem. Lett.*, **2015**, *23*, 3472-3480.

[46] Pingaew, R.; Prachayasittikul, V.; Worachartcheewan, A.; Nantasenamat, C.; Prachayasittikul, S.; Ruchirawat, S.; Prachayasittikul, V. Novel 1,4-naphthoquinone-based sulfonamides: Synthesis, QSAR, anticancer and antimalarial studies. *Eur. J. Med. Chem.*, **2015**, *103*, 446-459.

[47] Prachayasittikul, V.; Pingaew, R.; Worachartcheewan, A.; Nantasenamat, C.; Prachayasittikul, S.; Ruchirawat, S.; Prachayasittikul, V. Synthesis, anticancer activity and QSAR study of 1,4-naphthoquinone derivatives. *Eur. J. Med. Chem.*, **2014**, *84*, 247-263.

[48] Chan-On, W.; Huyen, N.T.B.; Songtawee, N.; Suwanjang, W.; Prachayasittikul, S.; Prachayasittikul, V. Quinoline-based clioquinol and nitroxoline exhibit anticancer activity inducing FoxM1 inhibition in cholangiocarcinoma cells. *Drug Des. Devel. Ther.*, **2015**, *9*, 2033-2047.

[49] Barot, K.; Jain, S.; Kremer, L.; Singh, S.; Ghate, M. Recent advances and therapeutic journey of coumarins: current status and perspectives. *Med. Chem. Res.*, **2015**, *24*, 2771-2798.

[50] Sivaprakasam, P.; Han, X.; Civiello, R.L.; Jacutin-Porte, S.; Kish, K.; Pokross, M.; Lewis, H.A.; Ahmed, N.; Szapiel, N.; Newitt, J.A.; Baldwin, E.T.; Xiao, H.; Krause, C.M.; Park, H.; Nophsker, M.; Lippy, J.S.; Burton, C.R.; Langley, D.R.; Macor, J.E.; Dubowchik, G.M. Discovery of new acylaminopyridines as GSK-3 inhibitors by a structure guided in-depth exploration of chemical space around a pyrrolopyridinone core. *Bioorg. Med. Chem. Lett.*, **2015**, *25*, 1856-1863.

[51] Karki, R.; Song, C.; Kadayat, T.M.; Magar, T.B.; Bist, G.; Shrestha, A.; Na, Y.; Kwon, Y.; Lee, E.S. Topoisomerase I and II inhibitory activity, cytotoxicity, and structure-activity relationship study of dihydroxylated 2,6-diphenyl-4-aryl pyridines. *Bioorg. Med. Chem.*, **2015**, *23*, 3638-3654.

[52] Geromichalou, E.; Sayyad, N.; Kyriakou, E.; Chatzikonstantinou, A.V.; Giannopoulou, E.; Vrbjar, N.; Kalofonos, H.P.; Stamatis, H.; Tzakos, A.G. Regioselective chemical and rapid enzymatic synthesis of a novel redox - antiproliferative molecular hybrid. *Eur. J. Med. Chem.*, **2015**, *96*, 47-57.

[53] Qin, W.W.; Sang, C.Y.; Zhang, L.L.; Wei, W.; Tian, H.Z.; Liu, H.X.; Chen, S.W.; Hui, L. Synthesis and biological evaluation of 2,4-diaminopyrimidines as selective Aurora A kinase inhibitors. *Eur. J. Med. Chem.*, **2015**, *95*, 174-184.

[54] Pałasz, A.; Ciez, D. In search of uracil derivatives as bioactive agents. Uracils and fused uracils: Synthesis, biological activity and applications. *Eur. J. Med. Chem.*, **2015**, *97*, 582-611.

[55] Shi, J.B.; Tang, W.J.; Qi, X.B.; Li, R.; Liu, X.H. Novel pyrazole-5-carboxamide and pyrazole-pyrimidine derivatives: synthesis and anticancer activity. *Eur. J. Med. Chem.*, **2015**, *90*, 889-896.

[56] Wang, Y.; Mitchell-Ryan, S.; Raghavan, S.; George, C.; Orr, S.; Hou, Z.; Matherly, L.H.; Gangjee, A. Novel 5-substituted pyrrolo[2,3-*d*]pyrimidines as dual inhibitors of glycinamide ribonucleotide formyltransferase and 5-aminoimidazole-4-carboxamide ribonucleotide formyltransferase and as potential antitumor agents. *J. Med. Chem.*, **2015**, *58*, 1479-1493.

[57] Kandeel, M.M.; Refaat, H.M.; Kassab, A.E.; Shahin, I.G.; Abdelghany, T.M. Synthesis, anticancer activity and effects on cell cycle profile and apoptosis of novel thieno[2,3-*d*]pyrimidine and thieno[3,2-*e*] triazolo[4,3-*c*]pyrimidine derivatives. *Eur. J. Med. Chem.*, **2015**, *90*, 620-632.

[58] Karki, R.; Park, C.; Jun, K.Y.; Kadayat, T.M.; Lee, E.S.; Kwon, Y. Synthesis and biological activity of 2,4-di-*p*-phenolyl-6-2-furanyl-pyridine as a potent topoisomerase II poison. *Eur. J. Med. Chem.*, **2015**, *90*, 360-378.

[59] Jun, K.Y.; Kwon, H.; Park, S.E.; Lee, E.; Karki, R.; Thapa, P.; Lee, J.H.; Lee, E.S.; Kwon, Y. Discovery of dihydroxylated 2,4-diphenyl-6-thiophen-2-yl-pyridine as a non-intercalative DNA-binding topoisomerase II-specific catalytic inhibitor. *Eur. J. Med. Chem.*, **2014**, *80*, 428-438.

[60] Pingaew, R.; Prachayasittikul, S.; Ruchirawat, S. Synthesis, cytotoxic and antimalarial activities of benzoyl thiosemicarbazone analogs of isoquinoline and related compounds. *Molecules*, **2010**, *15*, 988-996.

[61] Pingaew, R.; Tongraung, P.; Worachartcheewan, A.; Nantasenamat, C.; Prachayasittikul, S.; Ruchirawat, S.; Prachayasittikul, V. Cytotoxicity and QSAR study of (thio)ureas derived from phenylalkylamines and pyridylalkylamines. *Med. Chem. Res.*, **2013**, *22*, 4016-4029.

[62] Pingaew, R.; Worachartcheewan, A.; Nantasenamat, C.; Prachayasittikul, S.; Ruchirawat, S.; Prachayasittikul, V. Synthesis, cytotoxicity and QSAR study of *N*-tosyl-1,2,3,4-tetrahydroisoquinoline derivatives. *Arch. Pharm. Res.*, **2013**, *36*, 1066-1077.

[63] Ahmad, I.; Shagufta. Recent developments in steroidal and nonsteroidal aromatase inhibitors for the chemoprevention of estrogen-dependent breast cancer. *Eur. J. Med. Chem.*, **2015**, *102*, 375-386.

[64] Perez-Balado, C.; Nebbioso, A.; Rodriguez-Grana, P.; Minichiello, A.; Miceli, M.; Altucci, L.; de Lera, A.R. Bispyridinium dienes: histone deacetylase inhibitors with selective activities. *J. Med. Chem.*, **2007**, *50*, 2497-2505.

[65] Jiang, Z.G.; Lebowitz, M.S.; Ghanbari, H.A. Neuroprotective activity of 3-aminopyridine-2-carboxaldehyde thiosemicarbazone (PAN-811), a cancer therapeutic agent. *CNS Drug Rev.*, **2006**, *12*, 77-90.

[66] Cory, J.G.; Sato, A. Regulation of ribonucleotide reductase activity in mammalian cells. *Mol. Cell Biochem.*, **1983**, *53-54*, 257-266.

[67] Thelander, L.; Reichard, P. Reduction of ribonucleotides. *Annu. Rev. Biochem.*, **1979**, *48*, 133-158.

[68] Moorthy, N.S.; Cerqueira, N.M.; Ramos, M.J.; Fernandes, P.A. Development of ribonucleotide reductase inhibitors: a review on structure activity relationships. *Mini Rev. Med. Chem.*, **2013**, *13*, 1862-1872.

[69] Cai, Z.; Zhao, Y.; Zhao, B. Roles of glycogen synthase kinase 3 in Alzheimer's disease. *Curr. Alzheimer Res.*, **2012**, *9*, 864-879.

[70] Piazza, F.; Manni, S.; Semenzato, G. Novel players in multiple myeloma pathogenesis: role of protein kinases CK2 and GSK3. *Leuk. Res.*, **2013**, *37*, 221-227.

[71] Valvezan, A.J.; Klein, P.S. GSK-3 and Wnt signaling in neurogenesis and bipolar disorder *Front. Mol. Neurosci.*, **2012**, *5*, 1-13.

[72] Cocco, M.T.; Congiu, C.; Lilliu, V.; Onnis, V. Synthesis of new *N*-(2-(trifluoromethyl)pyridin-4-yl)anthranilic acid derivatives and their evaluation as anticancer agents. *Bioorg. Med. Chem. Lett.*, **2004**, *14*, 5787-5791.

[73] Li, H.Q.; Lv, P.C.; Yan, T.; Zhu, H.L. Urea derivatives as anticancer agents. *Anticancer Agents Med. Chem.*, **2009**, *9*, 471-480.

[74] Furuta, T.; Sakai, T.; Senga, T.; Osawa, T.; Kubo, K.; Shimizu, T.; Suzuki, R.; Yoshino, T.; Endo, M.; Miwa, A. Identification of potent and selective inhibitors of PDGF receptor autophosphorylation. *J. Med. Chem.*, **2006**, *49*, 2186-2192.

[75] Bassyouni, F.A.; Tawfik, H.A.; Soliman, A.M.; Rehim, M.A. Synthesis and anticancer activity of some new pyridine derivatives. *Res. Chem. Intermed.*, **2012**, *38*, 1291-1310.

[76] Eickhoff, J.E.; Hafenbradl, D.; Schwab, W.; Cotton, M.; Klebl, B.M.; Zech, B.; Mueller, S.; Harris, J.; Savic, V.; Macritchie, J.; Sherborne, B.; Le, J. Pyridinylamines and their prepaprations, pharmaceutical compositions and use for prophylaxis or treatment of various diseases. Patent Number: WO 2006010637. **2006**.

[77] Prachayasittikul, S.; Bauer, L. The deoxydative substitution reactions of nicotinamide and nicotinic acid *N*-oxides by 1-adamantanethiol in acetic anhydride. *J. Heterocycl. Chem.*, **1985**, *22*, 771-775.

[78] Prachayasittikul, S.; Doss, G.; Bauer, L. Deoxydative substitution of pyridine 1-oxides by thiols. Part XX. Reactions of (2, 3, and 4-phenyl)-, 3-acetamido-, 3-bromo-, 3-acetoxy-, 3-ethoxypyridine 1-oxides with 1-adamantanethiol in acetic anhydride. *J. Heterocycl. Chem.*, **1991**, *28*, 1051-1060.

[79] Prachayasittikul, S.; Treeratanapiboon, L.; Ruchirawat, S.; Prachayasittikul, V. Novel activities of 1-adamantylthiopyridines as antibacterials, antimalarials and anticancers. *EXCLI J.*, **2009**, *8*, 121-129.

[80] Prachayasittikul, S.; Kokosa, J.M.; Bauer, L.; Fesik, S.W. Deoxydative substitution of pyridine 1-oxides. 18. Tetrahydropyridines from 3-picoline 1-oxide and *tert*-butyl and 1-adamantyl mercaptan in acetic anhydride. Structural elucidation by long range 2D J(C-H) resolved NMR spectroscopy. *J. Org. Chem.*, **1985**, *50*, 997-1001.

[81] Worachartcheewan, A.; Prachayasittikul, S.; Pingaew, R.; Nantasenamat, C.; Tantimongcolwat, T.; Ruchirawat, S.; Prachayasittikul, V. Antioxidant, cytotoxicity, and QSAR study of 1-adamantylthio derivatives of 3-picoline and phenylpyridines. *Med. Chem. Res.*, **2012**, *21*, 3514-3522.

[82] Karki, R.; Thapa, P.; Yoo, H.Y.; Kadayat, T.M.; Park, P.H.; Na, Y.; Lee, E.; Jeon, K.H.; Cho, W.J.; Choi, H.; Kwon, Y.; Lee, E.S. Dihydroxylated 2,4,6-triphenyl pyridines: synthesis, topoisomerase I and II inhibitory activity, cytotoxicity, and structure-activity relationship study. *Eur. J. Med. Chem.*, **2012**, *49*, 219-228.

[83] Karki, R.; Thapa, P.; Kang, M.J.; Jeong, T.C.; Nam, J.M.; Kim, H.L.; Na, Y.; Cho, W.J.; Kwon, Y.; Lee, E.S. Synthesis, topoisomerase I and II inhibitory activity, cytotoxicity, and structure-activity relationship study of hydroxylated 2,4-diphenyl-6-aryl pyridines. *Bioorg. Med. Chem.*, **2010**, *18*, 3066-3077.

[84] Thapa, P.; Karki, R.; Yun, M.; Kadayat, T.M.; Lee, E.; Kwon, H.B.; Na, Y.; Cho, W.J.; Kim, N.D.; Jeong, B.S.; Kwon, Y.; Lee, E.S. Design, synthesis, and antitumor evaluation of 2,4,6-triaryl pyridines containing chlorophenyl and phenolic moiety. *Eur. J. Med. Chem.*, **2012**, *52*, 123-136.

[85] Basnet, A.; Thapa, P.; Karki, R.; Na, Y.; Jahng, Y.; Jeong, B.S.; Jeong, T.C.; Lee, C.S.; Lee, E.S. 2,4,6-Trisubstituted pyridines: Synthesis, topoisomerase I and II inhibitory activity, cytotoxicity, and structure-activity relationship. *Bioorg. Med. Chem.*, **2007**, *15*, 4351-4359.

[86] Prachayasittikul, S.; Worachartcheewan, A.; Nantasenamat, C.; Chinworrungsee, M.; Sornsongkhram, N.; Ruchirawat, S.; Prachayasittikul, V. Synthesis and structure-activity relationship of 2-thiopyrimidine-4-one analogs as antimicrobial and anticancer agents. *Eur. J. Med. Chem.*, **2011**, *46*, 738-742.

[87] Reddy, O.; Suryanarayana, C.V.; Narayana, K.J.P.; Anuradha, V.; Babu, B.H. Synthesis and cytotoxic evaluation for some new 2,5-disubstituted pyrimidine derivatives for anticancer activity. *Med. Chem. Res.*, **2015**, *24*, 1777-1788.

[88] Fujita, F.; Fujita, M.; Inaba, H.; Sugimoto, T.; Okuyama, Y.; Taguchi, T. Antitumor activity of HO-221, a derivative of benzoylphenylurea against human cancer xenografts in nude mice. *Gan To Kagaku Ryoho.*, **1991**, *18*, 2255-2261.

[89] Gurulingappa, H.; Amador, M.L.; Zhao, M.; Rudek, M.A.; Hidalgo, M.; Khan, S.R. Synthesis and antitumor evaluation of

benzoylphenylurea analogs. *Bioorg. Med. Chem. Lett.*, **2004**, *14*, 2213-2216.

[90] Nepali, K.; Sharma, S.; Sharma, M.; Bedi, P.M.S.; Dhar, K.L. Rational approaches, design strategies, structure activity relationship and mechanistic insights for anticancer hybrids. *Eur. J. Med. Chem.*, **2014**, *77*, 422-487.

[91] Papadopoulou, A.A.; Katsoura, M.H.; Chatzikonstantinou, A.; Kyriakou, E.; Polydera, A.C.; Tzakos, A.G.; Stamatis, H. Enzymatic hybridization of α-lipoic acid with bioactive compounds in ionic solvents. *Bioresour. Technol.*, **2013**, *136*, 41-48.

[92] Karampelas, T.; Argyros, O.; Sayyad, N.; Spyridaki, K.; Pappas, C.; Morgan, K.; Kolios, G.; Millar, R.P.; Liapakis, G.; Tzakos, A.G.; Fokas, D.; Tamvakopoulos, C. GnRH-gemcitabine conjugates for the treatment of androgen-independent prostate cancer: pharmacokinetic enhancements combined with targeted drug delivery. *Bioconjug. Chem.*, **2014**, *25*, 813-823.

[93] Pingaew, R.; Saekee, A.; Mandi, P.; Nantasenamat, C.; Prachayasittikul, S.; Ruchirawat, S.; Prachayasittikul, V. Synthesis, biological evaluation and molecular docking of novel chalcone-coumarin hybrids as anticancer and antimalarial agents. *Eur. J. Med. Chem.*, **2014**, *85*, 65-76.

[94] Janga, S.C.; Tzakos, A. Structure and organization of drug-target networks: Insights from genomic approaches for drug discovery. *Mol. Biosyst.*, **2009**, *5*, 1536-1548.

[95] Bernini, R.; Crisante, F.; Merendino, N.; Molinari, R.; Soldatelli, M.C.; Velotti, F. Synthesis of a novel ester of hydroxytyrosol and *α*-lipoic acid exhibiting an antiproliferative effect on human colon cancer HT-29 cells. *Eur. J. Med. Chem.*, **2011**, *46*, 439-446.

[96] Fu, J.; Bian, M.; Jiang, Q.; Zhang, C. Roles of aurora kinases in mitosis and tumorigenesis. *Mol. Cancer Res.*, **2007**, *5*, 1-10.

[97] Carmena, M.; Earnshaw, W.C. The cellular geography of Aurora kinases. *Nat. Rev. Mol. Cell Biol.*, **2003**, *4*, 842-854.

[98] Landen Jr, C.N.; Lin, Y.G.; Immaneni, A.; Deavers, M.T.; Merritt, W.M.; Spannuth, W.A.; Bodurka, D.C.; Gershenson, D.M.; Brinkley, W.R.; Sood, A.K. Overexpression of the centrosomal protein Aurora-A kinase is associated with poor prognosis in epithelial ovarian cancer patients. *Clin. Cancer Res.*, **2007**, *13*, 4098-4104.

[99] Gopalakrishnan, S.; Vadivel, E.; Sathieshkumar, P.P.; Praba, M.S. Synthesis, molecular docking and ADME prediction of some pyridine and pyrimidine derivatives as anti-colorectal cancer drugs. *J. Chem. Pharm. Res.*, **2010**, *2*, 60-66.

[100] Jain, K.S.; Chitre, T.S.; Miniyar, P.B.; Kathiravan, M.K.; Bendre, V.S.; Veer, V.S.; Shahane, S.R.; Shishoo, C.J. Biological and medicinal significance of pyrimidines. *Current Sci.*, **2006**, *90*, 793-803.

[101] Smith, N.F.; Figg, W.D.; Sparreboom, A. Recent advances in pharmacogenetic approaches to anticancer drug development. *Drug Dev. Res.*, **2004**, *62*, 233-253.

[102] Kamalakannan, P.; Venkappayya, D.; Balasubramanian, T. A new antimetabolite, 5-morpholinomethyl-2-thiouracil—spectral properties, thermal profiles, antibacterial, antifungal and antitumour studies of some of its metal chelates. *J. Chem. Soc., Dalton Trans.*, **2002**, 3381-3391.

[103] Motawia, M.S.; Abdel-Megied, A.E.; Pedersen, E.B.; Nielsen, C.M.; Ebbesen, P. Synthesis of 5-alkoxymethyl derivatives of 3'-amino-2',3'-dideoxyuridine and evaluation of their activity against HIV and cancer. *Acta Chem. Scand.*, **1992**, *46*, 77-81.

[104] Fabrissin, S.; De Nardo, M.; Nisi, C.; Morasca, L.; Dolfini, E.; Franchi, G. Synthesis and anticancer activity of 5-diethylaminomethyl derivatives and nitrogen mustards of uracil and 2-thiouracils. *J. Med. Chem.*, **1976**, *19*, 639-642.

[105] Prachayasittikul, S.; Sornsongkhram, N.; Pingaew, R.; Worachartcheewan, A.; Ruchirawat, S.; Prachayasittikul, V. Synthesis of *N*-substituted 5-iodouracils as antimicrobial and anticancer agents. *Molecules*, **2009**, *14*, 2768-2779.

[106] Arikkatt, S.D.; Mathew V, B.; Joseph, J.; Chandran, M.; Bhat, A.R.; Krishnakumar, K. Pyrimidine derivatives and its biological potential-a review. *Int. J. Org. Bioorg. Chem.*, **2014**, *4*, 1-5.

[107] Khanage, S.G.; Raju, S.A.; Mohite, P.B.; Pandhare, R.B. Synthesis and pharmacological evaluation of some new pyrimidine derivatives containing 1,2,4-triazole. *Adv. Pharm. Bull.*, **2012**, *2*, 213-222.

[108] Nassar, E. Synthesis, (*in vitro*) antitumor and antimicrobial activity of some pyrazoline, pyridine and pyrimidine derivatives linked to indole moiety. *J. Am. Sci.*, **2010**, *6*, 338-347.

[109] Prachayasittikul, S.; Sornsongkhram, N.; Pingaew, R.; Techatanachai, S.; Ruchirawat, S.; Prachayasittikul, V. Synthesis and novel bioactivities of substituted 6-propylthiouracils. *Eur. J. Sci. Res.*, **2009**, *36*, 236-245.

[110] Mai, A.; Massa, S.; Rotili, D.; Pezzi, R.; Bottoni, P.; Scatena, R.; Meraner, J.; Brosch, G. Exploring the connection unit in the HDAC inhibitor pharmacophore model: novel uracil-based hydroxamates. *Bioorg. Med. Chem. Lett.*, **2005**, *15*, 4656-4661.

[111] Jones, P.A.; Baylin, S.B. The fundamental role of epigenetic events in cancer. *Nat. Rev. Genet.*, **2002**, *3*, 415-428.

[112] Mahlknecht, U.; Hoelzer, D. Histone acetylation modifiers in the pathogenesis of malignant disease. *Mol. Med.*, **2000**, *6*, 623-644.

[113] Yoshida, M.; Kijima, M.; Akita, M.; Beppu, T. Potent and specific inhibition of mammalian histone deacetylase both *in vivo* and *in vitro* by trichostatin A. *J. Biol. Chem.*, **1990**, *265*, 17174-17179.

[114] Richon, V.M.; Emiliani, S.; Verdin, E.; Webb, Y.; Breslow, R.; Rifkind, R.A.; Marks, P.A. A class of hybrid polar inducers of transformed cell differentiation inhibits histone deacetylases. *Proc. Natl. Acad. Sci. U.S.A.*, **1998**, *95*, 3003-3007.

[115] Fukushima, M.; Suzuki, N.; Emura, T.; Yano, S.; Kazuno, H.; Tada, Y.; Yamada, Y.; Asao, T. Structure and activity of specific inhibitors of thymidine phosphorylase to potentiate the function of antitumor 2'-deoxyribonucleosides. *Biochem. Pharmacol.*, **2000**, *59*, 1227-1236.

[116] Sun, L.; Li, J.; Bera, H.; Dolzhenko, A.V.; Chiu, G.N.; Chui, W.K. Fragment-based approach to the design of 5-chlorouracil-linked-pyrazolo[1,5-*a*][1,3,5]triazines as thymidine phosphorylase inhibitors. *Eur. J. Med. Chem.*, **2013**, *70*, 400-410.

[117] Ma, L.Y.; Zheng, Y.C.; Wang, S.Q.; Wang, B.; Wang, Z.R.; Pang, L.P.; Zhang, M.; Wang, J.W.; Ding, L.; Li, J.; Wang, C.; Hu, B.; Liu, Y.; Zhang, X.D.; Wang, J.J.; Wang, Z.J.; Zhao, W.; Liu, H.M. Design, synthesis, and structure-activity relationship of novel LSD1 inhibitors based on pyrimidine-thiourea hybrids as potent, orally active antitumor agents. *J. Med. Chem.*, **2015**, *58*, 1705-1716.

[118] Ma, L.Y.; Wang, B.; Pang, L.P.; Zhang, M.; Wang, S.Q.; Zheng, Y.C.; Shao, K.P.; Xue, D.Q.; Liu, H.M. Design and synthesis of novel 1,2,3-triazole-pyrimidine-urea hybrids as potential anticancer agents. *Bioorg. Med. Chem. Lett.*, **2015**, *25*, 1124-1128.

[119] Ma, L.Y.; Pang, L.P.; Wang, B.; Zhang, M.; Hu, B.; Xue, D.Q.; Shao, K.P.; Zhang, B.L.; Liu, Y.; Zhang, E.; Liu, H.M. Design and synthesis of novel 1,2,3-triazole-pyrimidine hybrids as potential anticancer agents. *Eur. J. Med. Chem.*, **2014**, *86*, 368-380.

[120] Taher, A.T.; Helwa, A.A. Synthesis, antitumor and antimicrobial testing of some new thiopyrimidine analogues. *Chem. Pharm. Bull.*, **2012**, *60*, 1305-1313.

[121] Abdel-Mohsen, H.T.; Ragab, F.A.; Ramla, M.M.; El Diwani, H.I. Novel benzimidazole-pyrimidine conjugates as potent antitumor agents. *Eur. J. Med. Chem.*, **2010**, *45*, 2336-2344.

[122] Taher, A.T.; Helwa, A.A. Novel pyrimidinone derivatives: synthesis, antitumor and antimicrobial evaluation. *Chem. Pharm. Bull.*, **2012**, *60*, 521-530.

[123] Taher, A.T.; Abou-Seri, S.M. Synthesis and bioactivity evaluation of new 6-aryl-5-cyano thiouracils as potential antimicrobial and anticancer agents. *Molecules*, **2012**, *17*, 9868-9886.

[124] Zask, A.; Verheijen, J.C.; Curran, K.; Kaplan, J.; Richard, D.J.; Nowak, P.; Malwitz, D.J.; Brooijmans, N.; Bard, J.; Svenson, K.; Lucas, J.; Toral-Barza, L.; Zhang, W.G.; Hollander, I.; Gibbons, J.J.; Abraham, R.T.; Ayral-Kaloustian, S.; Mansour, T.S.; Yu, K. ATP-competitive inhibitors of the mammalian target of rapamycin: design and synthesis of highly potent and selective pyrazolopyrimidines. *J. Med. Chem.*, **2009**, *52*, 5013-5016.

[125] Ding, Z.; Wu, C.J.; Jaskelioff, M.; Ivanova, E.; Kost-Alimova, M.; Protopopov, A.; Chu, G.C.; Wang, G.; Lu, X.; Labrot, E.S.; Hu, J.; Wang, W.; Xiao, Y.; Zhang, H.; Zhang, J.; Gan, B.; Perry, S.R.; Jiang, S.; Li, L.; Horner, J.W.; Wang, Y.A.; Chin, L.; DePinho, R.A. Telomerase reactivation following telomere dysfunction yields murine prostate tumors with bone metastases. *Cell*, **2012**, *148*, 896-907.

[126] Stewart, S.A.; Bertuch, A.A. The role of telomeres and telomerase in cancer research. *Cancer Res.*, **2010**, *70*, 7365-7371.

[127] Gillis, A.J.; Schuller, A.P.; Skordalakes, E. Structure of the *Tribolium castaneum* telomerase catalytic subunit TERT. *Nature*, **2008**, *455*, 633-637.

[128] Hassan, G.S.; Kadry, H.H.; Abou-Seri, S.M.; Ali, M.M.; Mahmoud, A.E. Synthesis and *in vitro* cytotoxic activity of novel pyrazolo[3,4-*d*]pyrimidines and related pyrazole hydrazones toward breast adenocarcinoma MCF-7 cell line. *Bioorg. Med. Chem.*, **2011**, *19*, 6808-6817.

[129] Kandeel, M.M.; Mohamed, L.W.; Abd El Hamid, M.K.; Negmeldin, A.T. Design, synthesis, and antitumor evaluation of novel pyrazolo[3,4-*d*]pyrimidine derivatives. *Sci. Pharm.*, **2012**, *80*, 531-545.

[130] Abd El Razik, H.A.; Wahab, A.E. Synthesis and biological evaluation of some novel fused pyrazolopyrimidines as potential anticancer and antimicrobial agents. *Arch. Pharm. Chem. Life Sci.*, **2011**, *344*, 184-196.

[131] Kandeel, M.M.; Mounir, A.A.; Refaat, H.M.; Kassab, A.E. Synthesis of thieno[2,3-*d*]pyrimidines, thieno[2,3-*d*]triazinones and thieno[2,3-*e*]diazepinones of anticipated anti-cancer activity. *J. Chem. Res.*, **2012**, *36*, 105-110.

[132] Kandeel, M.M.; Mounir, A.A.; Refaat, H.M.; Kassab, A.E. Synthesis of potent anticancer thieno[2,3-*d*]pyrimidine derivatives. *J. Chem. Res.*, **2012**, *36*, 266-275.

[133] Kandeel, M.M.; Mounir, A.A.; Refaat, H.M.; Kassab, A.E. Synthesis of effective anticancer thieno [2,3-*d*] pyrimidine-4-ones and thieno [3,2-*e*]triazolo[4,3-*c*]pyrimidines. *Int. J. Pharm. Pharm. Sci.*, **2012**, *4*, 438-448.

[134] Kassab, A.E.; Gedawy, E.M. Synthesis and anticancer activity of novel 2-pyridyl hexahyrocyclooctathieno[2,3-*d*]pyrimidine derivatives. *Eur. J. Med. Chem.*, **2013**, *63*, 224-230.

[135] Dai, Y.; Guo, Y.; Frey, R.R.; Ji, Z.; Curtin, M.L.; Ahmed, A.A.; Albert, D.H.; Arnold, L.; Arries, S.S.; Barlozzari, T.; Bauch, J.L.; Bouska, J.J.; Bousquet, P.F.; Cunha, G.A.; Glaser, K.B.; Guo, J.; Li, J.; Marcotte, P.A.; Marsh, K.C.; Moskey, M.D.; Pease, L.J.; Stewart, K.D.; Stoll, V.S.; Tapang, P.; Wishart, N.; Davidsen, S.K.; Michaelides, M.R. Thienopyrimidine ureas as novel and potent multitargeted receptor tyrosine kinase inhibitors. *J. Med. Chem.*, **2005**, *48*, 6066-6083.

[136] Horton, D.A.; Bourne, G.T.; Smythe, M.L. The combinatorial synthesis of bicyclic privileged structures or privileged substructures. *Chem. Rev.*, **2003**, *103*, 893-930.

[137] Michael, J.P. Quinoline, quinazoline and acridone alkaloids. *Nat. Prod. Rep.*, **2004**, *21*, 650-668.

[138] Ahmed, M.; Belal, A.; Youns, M. Design, synthesis, molecular modeling and anti-breast cancer activity of novel quinazolin-4-one derivatives linked to thiazolidinone, oxadiazole or pyrazole moieties. *Med. Chem. Res.*, **2015**, *24*, 2993-3007.

[139] Liu, J.F.; Wilson, C.J.; Ye, P.; Sprague, K.; Sargent, K.; Si, Y.; Beletsky, G.; Yohannes, D.; Ng, S.C. Privileged structure-based quinazolinone natural product-templated libraries: identification of novel tubulin polymerization inhibitors. *Bioorg. Med. Chem. Lett.*, **2006**, *16*, 686-690.

[140] Buron, F.; Merour, J.Y.; Akssira, M.; Guillaumet, G.; Routier, S. Recent advances in the chemistry and biology of pyridopyrimidines. *Eur. J. Med. Chem.*, **2015**, *95*, 76-95.

[141] Lunt, E.; Newton, C.C. Pyridodiazines and their benzo derivatives. *Compr. Heterocycl. Chem.*, **1984**, *3*, 199-232.

[142] Sako, M., Product class 19 : pyridopyrimidines In: *Science of synthesis: hetarenes and related ring system: six-membered hetarenes with two identical heteroatoms*; Yamamoto, Y., Ed. Georg Thieme Verlag Stuttgart: New York, **2004**; Vol. *16*, pp. 1155-1267.

[143] Saurat, T.; Buron, F.; Rodrigues, N.; De Tauzia, M.L.; Colliandre, L.; Bourg, S.; Bonnet, P.; Guillaumet, G.; Akssira, M.; Corlu, A.; Guillouzo, C.; Berthier, P.; Rio, P.; Jourdan, M.L.; Bénédetti, H.; Routier, S. Design, synthesis, and biological activity of pyridopyrimidine scaffolds as novel PI3K/mTOR dual inhibitors. *J. Med. Chem.*, **2014**, *57*, 613-631.

[144] Crawford, T.D.; Ndubaku, C.O.; Chen, H.; Boggs, J.W.; Bravo, B.J.; Delatorre, K.; Giannetti, A.M.; Gould, S.E.; Harris, S.F.; Magnuson, S.R.; McNamara, E.; Murray, L.J.; Nonomiya, J.; Sambrone, A.; Schmidt, S.; Smyczek, T.; Stanley, M.; Vitorino, P.; Wang, L.; West, K.; Wu, P.; Ye, W. Discovery of selective 4-amino-pyridopyrimidine inhibitors of MAP4K4 using fragment-based lead identification and optimization. *J. Med. Chem.*, **2014**, *57*, 3484-3493.

[145] Rusnak, D.W.; Affleck, K.; Cockerill, S.G.; Stubberfield, C.; Harris, R.; Page, M.; Smith, K.J.; Guntrip, S.B.; Carter, M.C.; Shaw, R.J.; Jowett, A.; Stables, J.; Topley, P.; Wood, E.R.; Brignola, P.S.; Kadwell, S.H.; Reep, B.R.; Mullin, R.J.; Alligood, K.J.; Keith, B.R.; Crosby, R.M.; Murray, D.M.; Knight, W.B.; Gilmer, T.M.; Lackey, K. The characterization of novel, dual ErbB-2/EGFR, tyrosine kinase inhibitors: potential therapy for cancer. *Cancer Res.*, **2001**, *61*, 7196-7203.

[146] Lippa, B.; Kauffman, G.S.; Arcari, J.; Kwan, T.; Chen, J.; Hungerford, W.; Bhattacharya, S.; Zhao, X.; Williams, C.; Xiao, J.; Pustilnik, L.; Su, C.; Moyer, J.D.; Ma, L.; Campbell, M.; Steyn, S. The discovery of highly selective erbB2 (Her2) inhibitors for the treatment of cancer. *Bioorg. Med. Chem. Lett.*, **2007**, *17*, 3081-3086.

[147] Mo, W.Y.; Liang, Y.J.; Gu, Y.C.; Fu, L.W.; He, H.W. Synthesis and cytotoxicity of 8-cyano-3-substitutedalkyl-5-methyl-4-methylene-7-methoxy-3,4-dihydropyrido[4,3-*d*]pyrimidines. *Bioorg. Med. Chem. Lett.*, **2011**, *21*, 5975-5977.

[148] Relling, M.V.; Gardner, E.E.; Sandborn, W.J.; Schmiegelow, K.; Pui, C.H.; Yee, S.W.; Stein, C.M.; Carrillo, M.; Evans, W.E.; Hicks, J.K.; Schwab, M.; Klein, T.E. Clinical pharmacogenetics implementation consortium guidelines for thiopurine methyltransferase genotype and thiopurine dosing: 2013 update. *Clin. Pharmacol. Ther.*, **2013**, *93*, 324-325.

[149] Rao, P.; Ravindhranath, K.; Kumar, K. Antibacterial activity of novel substituted mercaptopurine derivatives. *Inst. J. Pharm. Biomed. Res.*, **2013**, *4*, 127–131.

[150] Kowalska, A.; Latocha, M.; Pluta, K. Synthesis and anticancer activity of thiosubstituted purines. *Med. Chem. Res.*, **2015**, *24*, 3107-3116.

[151] Martinez-Urbina, M.A.; Zentella, A.; Vilchis-Reyes, M.A.; Guzman, A.; Vargas, O.; Ramirez Apan, M.T.; Ventura Gallegos, J.L.; Diaz, E. 6-Substituted 2-(*N*-trifluoroacetylamino)imidazopyridines induce cell cycle arrest and apoptosis in SK-LU-1 human cancer cell line. *Eur. J. Med. Chem.*, **2010**, *45*, 1211-1219.

[152] Kamal, A.; Reddy, J.S.; Ramaiah, M.J.; Dastagiri, D.; Bharathi, E.V.; Prem Sagar, M.V.; Pushpavalli, S.N.C.V.L.; Ray, P.; Pal-Bhadra, M. Design, synthesis and biological evaluation of imidazopyridine/pyrimidine-chalcone derivatives as potential anticancer agents. *Med. Chem. Commun.*, **2010**, *1*, 355-360.

[153] Prachayasittikul, V.; Prachayasittikul, S.; Ruchirawat, S.; Prachayasittikul, V. 8-Hydroxyquinolines: a review of their metal chelating properties and medicinal applications. *Drug Des. Devel. Ther.*, **2013**, *7*, 1157-1178.

[154] Pingaew, R.; Worachartcheewan, A.; Prachayasittikul, V.; Prachayasittikul, S.; Ruchirawat, S.; Prachayasittikul, V. Transition metal complexes of 8-aminoquinoline-5-substituted uracils with antioxidative and cytotoxic activities. *Lett. Drug Des. Discov.*, **2013**, *10*, 859-864.

[155] Suksrichavalit, T.; Prachayasittikul, S.; Nantasenamat, C.; Isarankura-Na-Ayudhya, C.; Prachayasittikul, V. Copper complexes of pyridine derivatives with superoxide scavenging and antimicrobial activities. *Eur. J. Med. Chem.*, **2009**, *44*, 3259-3265.

[156] Suksrichavalit, T.; Prachayasittikul, S.; Piacham, T.; Isarankura-Na-Ayudhya, C.; Nantasenamat, C.; Prachayasittikul, V. Copper complexes of nicotinic-aromatic carboxylic acids as superoxide dismutase mimetics. *Molecules*, **2008**, *13*, 3040-3056.

[157] Srisung, S.; Suksrichavalit, T.; Prachayasittikul, S.; Ruchirawat, S.; Prachayasittikul, V. Antimicrobial activity of 8-hydroxyquinoline and transition metal complexes. *Int. J. Pharm.*, **2013**, *9*, 170-175.

[158] Rafique, S.; Idrees, M.; Nasim, A.; Akbar, H.; Athar, A. Transition metal complexes as potential therapeutic agents. *Biotechnol. Mol. Biol. Rev.*, **2010**, *5*, 38-45.

[159] Hambley, T.W. Developing new metal-based therapeutics: challenges and opportunities. *Dalton Trans.*, **2007**, 4929-4937.

[160] Prachayasittikul, S.; Worachartcheewan, A.; Pingaew, R.; Suksrichavalit, T.; Isarankura-Na-Ayudhya, C.; Ruchirawat, S.; Prachayasittikul, V. Metal complexes of uracil derivatives with cytotoxicity and superoxide scavenging activity. *Lett. Drug Des. Discov.*, **2012**, *9*, 282-287.

[161] Li, K.; Zou, T.; Chen, Y.; Guan, X.; Che, C.M. Pincer-type platinum(II) complexes containing *N*-heterocyclic carbene (NHC)

ligand: structures, photophysical and anion-binding properties, and anticancer activities. *Chemistry*, **2015**, *21*, 7441-7453.

[162] García-Moreno, E.; Gascón, S.; Rodriguez-Yoldi, M.J.; Cerrada, E.; Laguna, M. S-propargylthiopyridine phosphane derivatives as anticancer agents: characterization and antitumor activity. *Organometallics*, **2013**, *32*, 3710-3720.

[163] Gielen, M.; Bouhdid, A.; Tiekink, E.R.T.; De Vos, D.; Willem, R. Triphenyltin ortho-aminophenyl- and 2-pyridyl-thiolates: Synthesis and *in vitro* antitumour activity. *Met. Based Drugs*, **1996**, *3*, 75-78.

[164] Segapelo, T.V.; Guzei, I.A.; Spencer, L.C.; Zyl, W.E.V.; Darkwa, J. (Pyrazolylmethyl)pyridine platinum(II) and gold(III) complexes: synthesis, structures and evaluation as anticancer agents. *Inorg. Chim. Acta*, **2009**, *362*, 3314-3324.

[165] Singh, U.P.; Singh, B.N.; Ghose, A.K.; Singh, R.K.; Sodhi, A. Synthesis, characterization, and antitumor activity of 5-iodouracil complexes. *J. Inorg. Biochem.*, **1991**, *44*, 277-282.

[166] Singh, V.P.; Singh, S.; Narang, K.K.; Bhattacharya, D. Aluminium(III), chromium(III) and iron(III) complexes with 5-iodouracil and 5-iodouracil-histidine and their antitumour activity. *J. Enzyme Inhib. Med. Chem.*, **2009**, *24*, 105-110.

[167] Prachayasittikul, V.; Pingaew, R.; Nantasenamat, C.; Prachayasittikul, S.; Ruchirawat, S.; Prachayasittikul, V. Investigation of aromatase inhibitory activity of metal complexes of 8-hydroxyquinolineand uracil derivatives. *Drug Des. Devel. Ther.*, **2014**, *8*, 1089-1096.

[168] Ding, H.X.; Liu, K.K.; Sakya, S.M.; Flick, A.C.; O'Donnell, C.J. Synthetic approaches to the 2011 new drugs. *Bioorg. Med. Chem.*, **2013**, *21*, 2795-2825.

[169] Ding, H.X.; Leverett, C.A.; Kyne, R.E., Jr.; Liu, K.K.; Sakya, S.M.; Flick, A.C.; O'Donnell, C.J. Synthetic approaches to the 2012 new drugs. *Bioorg. Med. Chem.*, **2014**, *22*, 2005-2032.

[170] Ding, H.X.; Leverett, C.A.; Kyne, R.E., Jr.; Liu, K.K.; Fink, S.J.; Flick, A.C.; O'Donnell, C.J. Synthetic approaches to the 2013 new drugs. *Bioorg. Med. Chem.*, **2015**, *23*, 1895-1922.

[171] Liu, K.K.; Sakya, S.M.; O'Donnell, C.J.; Flick, A.C.; Li, J. Synthetic approaches to the 2009 new drugs. *Bioorg. Med. Chem.*, **2011**, *19*, 1136-1154.

[172] Liu, K.K.; Sakya, S.M.; O'Donnell, C.J.; Flick, A.C.; Ding, H.X. Synthetic approaches to the 2010 new drugs. *Bioorg. Med. Chem.*, **2012**, *20*, 1155-1174.

[173] Kundu, C.N.; Das, S.; Nayak, A.; Satapathy, S.R.; Das, D.; Siddharth, S. Anti-malarials are anti-cancers and vice versa - one arrow two sparrows. *Acta Trop.*, **2015**, *149*, 113-127.